Ozone-mediated control of food spoilage and food-borne pathogens

A thesis submitted for the degree of Doctor of Philosophy at the University of Oxford

Ashleigh Macdonald

Linacre College

October 2023

Abstract

Post-harvest produce is subject to contamination by pathogens, and this is currently controlled in the food industry by intervention treatments, such as sodium hypochlorite or peracetic acid. Ozone may be a better alternative because it eliminates the requirement for chemical transportation and storage, and unlike sodium hypochlorite, it does not form toxic residues. The aim of this project was to determine if ozone could be used as an alternative treatment to effectively control pathogens on post-harvest produce.

It was identified that ozone treatment changed the native microbiota of post-harvest produce, and these changes might impact the ability of pathogens to survive and proliferate. Some members of the microbiota were more susceptible to ozone than others, which could have been due to a variety of factors. One factor which was hypothesised to aid the tolerance of pathogens to ozone treatment (in addition to sodium hypochlorite and peracetic acid) was the tolerance that pathogens may have evolved against hydrogen peroxide, which they would encounter during host defences. Since hydrogen peroxide, ozone, sodium hypochlorite and peracetic acid are all strong oxidants, they could be tolerated by the same mechanisms in bacteria. Work in this study however identified that although there were similarities in the response of bacteria to hydrogen peroxide and treatments used in the food industry, an increased tolerance to hydrogen peroxide did not necessarily make them more tolerant to treatments. Finally, it was identified that gaseous ozone, but not aqueous ozone, could be as effective as sodium hypochlorite and peracetic acid against pathogens on post-harvest produce. Overall, this project demonstrated that gaseous ozone could be a promising alternative to the treatments which are currently being used in the food industry.

Topics to raise

Anacail Ltd dissolved during the project

Anacail Ltd were originally an industrial partner of the project. They had developed an 'in-pack ozone system' for the food industry, which exposed post-harvest produce to ozone to control for the potential presence of pathogens. This system was intended to be used for work throughout this project, and an internship was planned to be completed at Anacail Ltd, however the company dissolved during the project. This subsequently halted the use of the in-pack ozone system, and the planned internship could no longer be completed. Nevertheless, contact was made with another company which had developed ozone technology to control for pathogens. They supplied their technology for use in this project and an internship was completed there instead.

COVID-19 impacted the original project plan

For this project, the model pathogens which were selected to represent food-borne and plant pathogens respectively were *Salmonella enterica* (*S. enterica*) and *Pseudomonas syringae* pv. tomato (Pst). Work with *S. enterica* was planned to be completed at the Holden lab (formerly at the James Hutton Institute) because they had expertise on *S. enterica*, and they also had the license in place which was required to work with *S. enterica*, since it is a human pathogen. Work with Pst was planned to be completed at the Preston lab (University of Oxford) because they had expertise on this pathogen. Therefore, work for the project was planned to be divided between the Holden lab and the Preston lab.

Lab work for the project began in January 2019 and work was initially completed with *S. enterica* in the Holden lab. In September 2019, I moved to the Preston lab to begin working on Pst and since the Preston lab did not have the required license to work with *S. enterica*, another long-term visit was planned to the Holden lab to continue work on *S. enterica*. However, this planned visit could not be completed due to restrictions in place

caused by COVID-19. Therefore, a non-pathogenic isolate of *E. coli* was used as a proxy for *S. enterica* at the Preston lab, where I remained for the duration of my project. A consequence of this meant that transcriptional fusion fluorescent reporter plasmids, which were generated using genes from *S. enterica*, were placed into *E. coli* for experimental work.

Acknowledgements

I would like to thank my supervisors Gail Preston (University of Oxford) and Nicola Holden (Scotland's Rural College) for their continuous support and guidance throughout my DPhil. I would also like to thank Louise Crozier for her knowledge of the food industry, Hugh Potts for providing his expertise on the in-pack ozone system, and all of the members of the company which supplied the commercial aqueous ozone system for providing their expertise on the system.

I would really like to acknowledge the past and current members of the Preston and Holden lab for creating such a positive, enthusiastic work environment and for their insight into my work. A special thanks goes to William Kay for volunteering his confocal imaging skills, Riccardo Soldan for providing microbiome data analysis guidance, and Nattapong Sanguankiattichai (Tee) for help with making deletion mutants. A special thanks also goes to the lab technicians of the Preston lab (Sarah Rodgers, Caroline O'Brien, Patty Bowman) and Jacqui Marshall who was a previous lab technician in the Holden lab.

I would like to thank the Oxford Statistics Consultancy for their guidance on statistical analysis. Also, I would like to acknowledge Linacre College and the Interdisciplinary Bioscience Doctoral Training Partnership for their support.

A special thanks goes to all of my family and friends (particularly Lee) for all their support and encouragement.

Finally, I would like to thank Biotechnology and Biological Sciences Research Council (BBSRC) for providing the funding for my DPhil. Additionally, I would like to thank the British Society of Plant Pathology (BSPP) and Linacre College for providing further funding to allow for an extension of time due to COVID-19 disruption.

Table of Contents

Chapter 1: Introduction 11

1.1 *E. coli*, *S. enterica*, Pst and tomato as model systems 12

1.2 *E. coli*, *S. enterica* and Pst trigger the oxidative burst in plants 13

1.3 The oxidative burst is cytotoxic 16

1.4 *E. coli*, *S. enterica* and Pst can tolerate the oxidative burst 18

1.5 Ozone as an antimicrobial agent for the food industry 21

1.6 Commercial systems for ozone generation 22

1.7 Ozone has benefits over current food industry treatments 27

1.8 Research aims and rationale 31

Chapter 2: The impact of gaseous ozone treatment on the microbiota of post-harvest produce 34

2.1 Introduction 34

2.1.1 The impact of high gaseous ozone concentrations on whole microbial communities is unknown 34

2.1.2 The tomato calyx and pedicel as a model system 35

2.1.3 The microbiota of the tomato calyx and pedicel is unknown 36

2.1.4 Microbiota changes may occur during post-harvest storage of tomatoes 36

2.1.5 Ozone may induce changes in the microbiota 37

2.1.6 Sequence analysis of the 16S rRNA gene for bacterial community analysis 38

2.1.7 Chapter aims 39

2.2 Materials and methods 39

2.2.1 Bacterial strains and primers 39

2.2.2 Media and growth conditions 40

2.2.3 Tomato cultivation 41

2.2.4 Tomato collection and packing 41

2.2.5 Gaseous ozone treatments 41

2.2.6 Bactericidal action of gaseous ozone on pathogens *in vitro* 42

2.2.7 Impact of gaseous ozone on the tomato calyx and pedicel culturable microbiota 43

2.2.8 Impact of gaseous ozone on the tomato calyx and pedicel bacterial community 44

2.2.9 Presentation and statistical analysis of data 48

2.3 Results 52

2.3.1 Gaseous ozone reduced pathogens *in vitro* 52

2.3.2 Yeasts and moulds on the tomato calyx and pedicel increased over time, and they were reduced by gaseous ozone 57

2.3.3 Gaseous ozone reduced the bacterial DNA library size from the tomato calyx and pedicel 61

2.3.4 The tomato calyx and pedicel bacterial community changed over time, and with ozone treatment 67
2.3.5 Gaseous ozone reduced the bacterial community diversity of the tomato calyx and pedicel 73
2.3.6 Gaseous ozone changed the bacterial community composition of the tomato calyx and pedicel 76
2.3.7 Gaseous ozone caused changes in the abundance of specific ASVs 79
2.4 Discussion 83
2.4.1 Gaseous ozone reduced pathogens *in vitro* 84
2.4.2 Gaseous ozone reduced yeasts and moulds on the tomato calyx and pedicel 85
2.4.3 The tomato calyx and pedicel had a low bacterial abundance 85
2.4.4 Gaseous ozone reduced the bacterial abundance on the tomato calyx and pedicel 86
2.4.5 Proteobacteria/*Pseudomonadaceae*/*Pseudomonas* dominated the tomato calyx and pedicel bacterial community 87
2.4.6 The tomato calyx and pedicel bacterial community changed over time; however, ozone treatment impacted these changes 88
2.4.7 Ozone-induced changes in the native microbiota might impact pathogen survival and proliferation 92
2.4.8 Conclusion 93
Chapter 3: Contribution of the oxidative stress tolerance pathway to ozone, peracetic acid and sodium hypochlorite tolerance in enterics and *P. syringae*..... 95
3.1 Introduction 95
3.1.1 roGFP is a biosensor for the intracellular redox state 95
3.1.2 Transcriptional fusion fluorescent reporters are biosensors for the transcriptional response of genes 98
3.1.3 The role of *oxyR*, *katG*, *soxS*, *soxR*, *ramA* and *lexA* in enterics 99
3.1.4 The role of *oxyR* and catalases in Pst DC3000 treatment tolerance 102
3.1.5 Chapter aims 103
3.2 Methods 104
3.2.1 Antimicrobial chemicals 104
3.2.2 Bacterial strains, plasmids and primers 105
3.2.3 Media and growth conditions 114
3.2.4 Production of transcriptional fusion fluorescent reporters 115
3.2.5 Production of Pst DC3000 Δ*oxyR* and its complemented strain 118
3.2.6 Introduction of pDSK-roGFP and pDSK519 by electrotransformation 121
3.2.7 Treatment effects on bacterial growth and culturability 122
3.2.8 Measurement of the intracellular redox state 124
3.2.9 Measurement of GFP+ transcriptional fusion reporter activity 127
3.2.10 Detection of viable but non-culturable (VBNC) *S. enterica* 129
3.2.11 Presentation and statistical analysis of data 130
3.3 Results 133

3.3.1 Aqueous ozone did not extend the 'apparent' lag growth phase 133
3.3.2 Hydrogen peroxide, peracetic acid and sodium hypochlorite extended the 'apparent' lag growth phase and reduced culturability 135
3.3.3 All treatments except aqueous ozone increased the intracellular redox state of bacteria 139
3.3.4 Oxidative stress tolerance genes were upregulated in response to hydrogen peroxide, peracetic acid and sodium hypochlorite 146
3.3.5 *oxyR* is required for hydrogen peroxide but not peracetic acid or sodium hypochlorite tolerance 153
3.3.6 Catalases are required for hydrogen peroxide and peracetic acid but not sodium hypochlorite tolerance 158
3.4 Discussion 163
3.4.1 Aqueous ozone did not stress bacteria in this study 163
3.4.2 Hydrogen peroxide, peracetic acid and sodium hypochlorite extended the 'apparent' lag growth phase, reduced culturability and increased the intracellular redox state of bacteria 164
3.4.3 Oxidative stress tolerance genes were upregulated in response to hydrogen peroxide, peracetic acid and sodium hypochlorite 166
3.4.4 *oxyR* and catalases were required for hydrogen peroxide but not always peracetic acid or sodium hypochlorite tolerance 170
3.4.5 Conclusion 171
Chapter 4: Bioluminescence imaging to demonstrate the effectiveness of different intervention treatments to control pathogens in the food industry 173
4.1 Introduction 173
4.1.1 *P. viridiflava* and *D. chrysanthemi* as additional model pathogens 174
4.1.2 Concentrations and applications of intervention treatments in the food industry 175
4.1.3 Bioluminescence imaging is a technique for bacterial viability determination 177
4.1.4 The *luxCDABE* operon makes bacteria bioluminescent 179
4.1.5 Chapter aims 181
4.2 Materials and methods 181
4.2.1 Antimicrobial chemicals 181
4.2.2 Bacterial strains, plasmids and primers 181
4.2.3 Media and growth conditions 184
4.2.4 Produce 185
4.2.5 Chromosomal integration of the *luxCDABE* operon by four parental mating conjugation 185
4.2.6 Delivery of the *luxCDABE* operon by the introduction of pIJ11282 186
4.2.7 Bactericidal action of liquid intervention treatments on pathogens *in vitro* 186
4.2.8 Inoculation of bioluminescent pathogens onto produce 187
4.2.9 Delivery of intervention treatments 187
4.2.10 Bioluminescence imaging 189

4.2.11 Bioluminescence imaging for the effectiveness of different intervention treatments 189
4.2.12 Bioluminescence imaging technique validation with colony counts 191
4.2.13 Determining the detection limits for bioluminescent model pathogens 194
4.2.14 Confocal imaging of *E. coli* on the tomato calyx 195
4.2.15 Presentation and statistical analysis of data 195
4.3 Results 196
4.3.1 Peracetic acid, sodium hypochlorite and aqueous ozone reduced model pathogens *in vitro* 196
4.3.2 Bioluminescence imaging can be used to demonstrate the effectiveness of peracetic acid, sodium hypochlorite and aqueous ozone to control pathogens *in planta* 199
4.3.3 Detection limits are variable for bioluminescent model pathogens on LB agar plates 208
4.3.4 Peracetic acid and sodium hypochlorite reduced model pathogens on carrots but not tomatoes, compared to water 210
4.3.5 Bacteria mainly reside on trichomes but also in/around stomata and on the general surface of the tomato calyx 216
4.3.6 Aqueous ozone did not reduce model pathogens on carrots or tomatoes compared to water 220
4.3.7 Gaseous ozone reduced model pathogens on carrots but not tomatoes 223
4.4 Discussion 226
4.4.1 Bioluminescence imaging can be used to demonstrate the effectiveness of peracetic acid, sodium hypochlorite and aqueous ozone to control pathogens *in planta* 226
4.4.2 Intervention treatment effects against pathogens on carrots and tomatoes 229
4.4.3 The tomato calyx provided a protective environment for bacteria against intervention treatments 233
4.4.4 Conclusion 234
Chapter 5: General discussion 235
5.1 Gaseous ozone is a promising alternative treatment for controlling pathogens in the food industry 235
5.2 More work is required to investigate the impact of gaseous ozone on pathogen presence over time 236
5.3 Better treatments are needed to effectively control pathogens on the tomato calyx and pedicel 237
5.4 Aqueous ozone, in the set-up which was used, is not a promising alternative treatment for controlling pathogens in the food industry 238
5.5 Hydrogen peroxide tolerance is not correlated with sodium hypochlorite or peracetic acid tolerance 239
5.5 Conclusion 241
Bibliography 242
Appendices 266
Appendix 1 266

Appendix 2 269
Appendix 3 270
Appendix 4 271
Appendix 5 274
Appendix 6 275
Appendix 7 277
Appendix 8 285
Appendix 9 286
Appendix 10 289
Appendix 11 290
Appendix 12 291
Appendix 13 292
Appendix 14 293
Appendix 15 295

Chapter 1: Introduction

Reactive oxygen species (ROS) are oxygen-containing reactive chemical species which employ a toxic action against micro-organisms by damaging intracellular biomolecules (Mehdy, 1994; Sen and Imlay, 2021). Eukaryotic hosts rapidly release ROS, in a process termed the oxidative burst, as a defence response mechanism when a micro-organism is detected. This is not only to exploit the antimicrobial nature of ROS, but also as part of a signalling cascade which induces further defence response mechanisms (O'Brien *et al.*, 2012). Micro-organisms associated with these hosts have however evolved a strong oxidative stress response to cope with this (Aussel *et al.*, 2011; Dublan *et al.*, 2014; Vassallo *et al.*, 2023).

The antimicrobial nature of ROS has been exploited in the food industry, where systems have been developed to expose post-harvest produce to high concentrations of ROS, primarily in the form of ozone (Sarron *et al*., 2021). This is to control for the presence of contaminants on post-harvest produce, whose survival could have implications. Among these contaminants are food-borne pathogens and toxins from toxin-producing micro-organisms, which are responsible for an estimated 2.4 million cases of food-borne illnesses annually in the UK (Daniel et al., 2020). Also among these contaminants are post-harvest pathogens (plant pathogens which can cause disease in post-harvest produce during transportation, handling, packaging and storage (Youssef *et al.*, 2023)) which cause food spoilage. Ozone has benefits over the intervention treatments which are currently being used for this because it does not form toxic residues (Karaca and Velioglu, 2007); it is generated on-site so eliminates the requirement for the transportation and storage of chemicals (Goodburn and Wallace, 2013), and it may be more cost-effective in the long term (Aslam *et al*., 2020).

The primary aim of this project was to determine if ozone could be used as an alternative treatment to effectively control pathogens on post-harvest produce.

The following sections introduce *Escherichia coli* (*E. coli*), *Salmonella enterica* (*S. enterica*), *Pseudomonas syringae* pv. tomato (Pst) and tomato as model systems, the cytotoxic nature of the oxidative burst, mechanisms that bacteria have evolved to tolerate the oxidative burst, the cytotoxic nature of ozone, commercial systems for ozone generation, and benefits of ozone in the food industry.

1.1 *E. coli*, *S. enterica*, Pst and tomato as model systems

To address the aims of the project, different model systems were selected. This included enteric bacteria: food-borne pathogen *S. enterica* (Hoiseth and Stocker, 1981; Elviss *et al.*, 2009) and a non-pathogenic proxy *E. coli* JHI-5025 (Holden, 2021). The plant pathogen Pst (Cuppels, 1986; Almeida *et al.*, 2009) was also selected. All model pathogens have been associated with food-borne or plant disease outbreaks on *Solanum lycopersicum* (tomato) (Basim *et al.*, 2004; Microbiological Advisory Committee on the Safety of Food, 2005; Shenge *et al.*, 2007; Callejón *et al.*, 2015), so this was the selected model fruit.

Salmonella spp was specifically selected because it is the most common cause of food-borne pathogen outbreaks in the European Union (EU) (European Food Safety Authority; European Centre for Disease Prevention and Control., 2022) so it is important that it is controlled for in the food industry. *S. enterica* can cause acute inflammatory diarrhoea in consumers, and on rare occasions this can progress to invasive non-typhoidal Salmonella disease in susceptible individuals, which is a bloodstream infection (Gordon, 2011; Anderson and Kendall, 2017).

E. coli JHI-5025 (Holden, 2021) is a non-pathogenic enteric which was used as a proxy for a pathogenic enteric. *E. coli* is a relevant model because different types of pathogenic *E. coli* cause food-borne illness in consumers in the form of severe diarrhoeal diseases (U.S. Food and Drug Administration, 2012). For example, Enterohaemorrhagic *E. coli* is one of the most common causal agents of food-borne illness worldwide (U.S. Food and

Drug Administration, 2012), so *E. coli* also requires to be controlled for in the food industry.

Tomatoes were selected as a model fruit because raw tomatoes have been the source of many food-borne outbreaks worldwide (Callejón *et al.*, 2015). *Salmonella* has been the principal cause of this (Callejón *et al.*, 2015) and an outbreak caused by verotoxigenic *E. coli* O157 has previously occurred in the UK (Microbiological Advisory Committee on the Safety of Food, 2005). Therefore, tomatoes which had been colonised by enterics were used as a model system. Also, the ozone treatments which were used in this project did not negatively impact the organoleptic properties of tomatoes which was an important consideration because some fruits and vegetables are more susceptible to ozone damage than others (Horvitz and Cantalejo, 2014; Sarron *et al*., 2021).

Pst is a plant pathogen which can cause bacterial speck on the fruit of susceptible tomato plants, therefore tomatoes which had been colonised by Pst were used as a model system. Bacterial speck is characterised by necrotic lesions and although serious outbreaks of this disease are infrequent (Preston, 2000), they have still been reported to occur (Basim *et al.*, 2004; Shenge *et al.*, 2007). This presents a problem to the food industry because fruit with bacterial speck have a reduced market value (Preston, 2000). Pst DC3000 and Pst T1 were both used as model bacteria for the project because Pst DC3000 is well characterised (Preston, 2000; Xin and He, 2013) and Pst T1 is more virulent against tomatoes than Pst DC3000 (Jones *et al.*, 2015).

1.2 *E. coli*, *S. enterica* and Pst trigger the oxidative burst in plants

For bacteria to become established in plants, they must overcome the plant's natural defences. The plant immune system is triggered when plasma membrane-localised receptor proteins, called pattern recognition receptors (PRRs), detect pathogen associated molecular patterns (PAMPs), which are conserved features common to most micro-organisms (Dodds and Rathjen, 2010). This allows PAMP-triggered immunity (PTI)

to be stimulated, which induces a cascade of signalling events required for the host defence response (Dodds and Rathjen, 2010). Bacteria may however encode effector proteins that can suppress PTI (Wu *et al.*, 2014). Specific effector proteins may be recognised by the host, if it carries an associated resistance (R) gene, to stimulate effector-triggered immunity (ETI) (Wu *et al.*, 2014). ETI provokes further host defence mechanisms so is usually associated with host disease resistance (Wu *et al.*, 2014).

Upon pathogen recognition, one of the plant's earliest responses is the oxidative burst which involves the production of ROS (Torres *et al*., 2006). Pathogens which stimulate ETI provoke a biphasic oxidative burst (figure 1.1) (Lamb and Dixon, 1997; Torres *et al*., 2006; Jwa and Hwang, 2017). Phase I is associated with initial pathogen recognition and is characterised by rapid but weak ROS accumulation (Lamb and Dixon, 1997; Torres *et al*., 2006). The ROS formed are cytotoxic to pathogens and are utilised as signalling molecules to trigger the defence response mechanisms associated with PTI (Jwa and Hwang, 2017). Phase II is characterised by stronger, prolonged ROS accumulation to generate a stronger cytotoxic effect and to provide signalling molecules for the defence response mechanisms associated with ETI (Lamb and Dixon, 1997; Torres *et al*., 2006; Jwa and Hwang, 2017). Pathogens which are detected but successfully evade ETI only stimulate phase I of the oxidative burst (Lamb and Dixon, 1997; Torres *et al*., 2006; Jwa and Hwang, 2017).

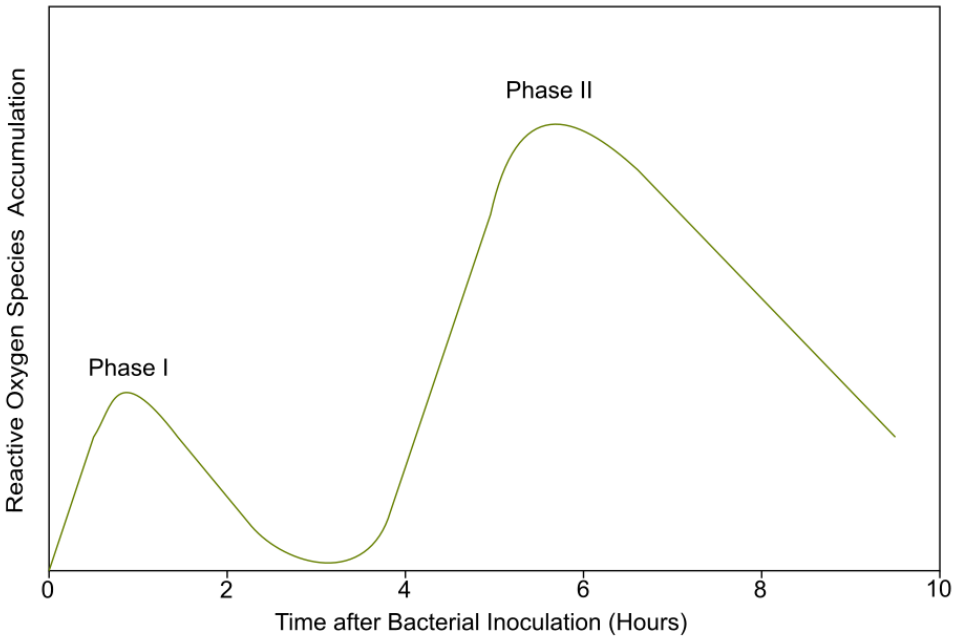


Figure 1.1 adapted from Lamb and Dixon, 1997: Kinetics of the oxidative burst in plant immunity. Reactive oxygen species accumulation in the host, following inoculation with a pathogen which stimulates effector-triggered immunity.

The ability of food-borne pathogens to induce an oxidative burst in a plant host has previously been demonstrated, for example *S. enterica* sv. Typhimurium and *E. coli* could induce a ROS burst in Arabidopsis (Oblessuc *et al*., 2020). A ROS burst in tomato leaves, caused by PAMPs possessed by *S. enterica* sv. Typhimurium has also previously been reported (Meng *et al*., 2013).

PAMPs, which the plant pathogen Pst possesses, have been shown to cause a range of tomato cultivars to produce ROS within 40 minutes, with the quantity produced dependent on the cultivar (Veluchamy *et al.*, 2014; Roberts *et al.*, 2019). Since Pst can cause disease in tomatoes, and has a repertoire of effectors (Wei *et al*., 2018), some tomato cultivars have evolved an R gene to provide associated resistance (Chandra *et al*., 1996). The association of the biphasic oxidative burst with host disease resistance has been demonstrated when Pst, which either had or did not have a particular effector, was used to infect tomatoes with an associated R gene (Chandra *et al*., 1996).

1.3 The oxidative burst is cytotoxic

In plants, the oxidative burst primarily occurs in the apoplast (Torres *et al*., 2006), which comprises intercellular space and cell walls (Farvardin *et al.*, 2020). The major sources of ROS generation during the oxidative burst are membrane-localised nicotinamide adenine dinucleotide phosphate hydrogen (NADPH) oxidases, which generate superoxide ($O_2^{\bullet -}$), and apoplastic peroxidases, which generate hydrogen peroxide (H_2O_2) (Daudi *et al.*, 2012). Superoxide undergoes rapid dismutation to hydrogen peroxide, so in most systems hydrogen peroxide is the major product of the oxidative burst (Lamb and Dixon, 1997; Torres *et al*., 2006).

Both superoxide and hydrogen peroxide are ROS, which is a collective term for oxygen radicals (oxygen species containing one or more unpaired electrons) and oxidising chemical species which are easily converted into them (Bayir, 2005). Their oxidation potentials (tendency of a chemical species to be oxidised by donating electrons) are displayed in table 1.1.

Table 1.1 modified from Epelle *et al*., 2023: Oxidation potentials of oxidants relevant to the project

Oxidant	**Oxidation potential (V)**
Hydroxyl radical ($HO^{\bullet}$)	2.80
Superoxide radical ($O_2^{\bullet -}$)	2.40
Ozone (O_3)	2.07
Hydrogen peroxide (H_2O_2)	1.80
Peracetic acid ($C_2H_4O_3$)	1.76
Hypochlorite ion (OCl^-)	1.70
Hydroperoxyl radical ($HO_2^{\bullet}$)	1.70
Hypochlorous acid (HOCl)	1.49
Chlorine gas (Cl_2)	1.36
Oxygen gas (O_2)	1.23

It is unlikely that superoxide from the apoplast would create cytoplasmic superoxide stress in bacteria because superoxide is negatively charged so does not readily cross bacterial cell membranes (Imlay, 2009; Sen and Imlay, 2021). Also, since it is a free radical, it is short-lived so will generally react where it is produced (Shields *et al*., 2021).

Superoxide can damage the cell surface and periplasm of bacteria, but the specific mechanism of this damage is unknown (Sen and Imlay, 2021). The known targets of superoxide are cytoplasmic iron enzymes, which are also targets of hydrogen peroxide (figure 1.2) (Sen and Imlay, 2021).

Diffusion of hydrogen peroxide across bacterial cell membranes is limited, however it can enter bacterial cells through porins so can easily access the bacterial cell cytoplasm (Bienert *et al*., 2006; Sen and Imlay, 2021). The toxic action of hydrogen peroxide occurs via a Fenton reaction in which hydrogen peroxide reacts with a ferrous ion (Fe^{2+}) to create an extremely reactive hydroxyl radical (HO•) (table 1.1), which can cause irreversible lesions at the site of its formation (Imlay, 2009; Sen and Imlay, 2021). This can result in the deactivation of enzymes with Fe^{2+} in their active site and damage to biomolecules to which Fe^{2+} would be bound to, such as nucleic acids (figure 1.2) (Sen and Imlay, 2021). Hydrogen peroxide can also deactivate dehydratase enzymes that employ a $[4Fe\text{-}4S]^{2+}$ cluster by oxidising a solvent exposed iron atom (figure 1.2) (Sen and Imlay, 2021).

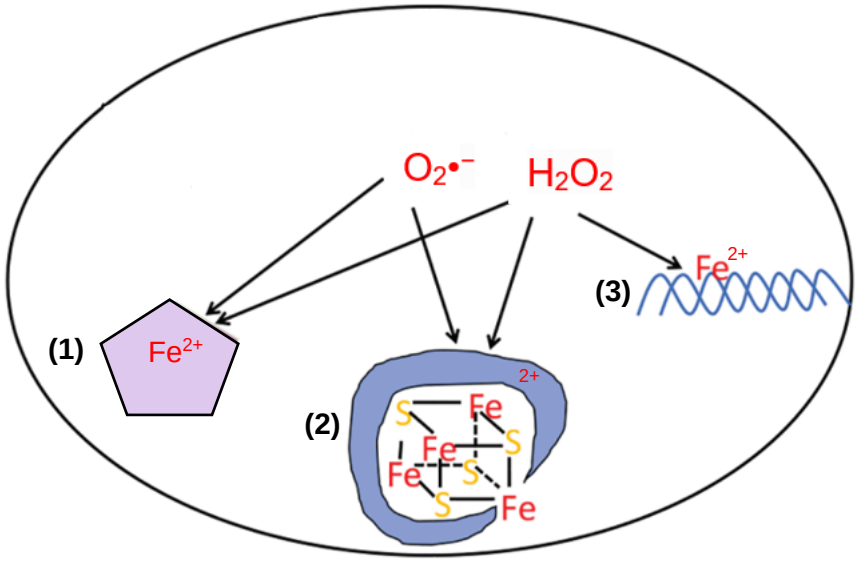


Figure 1.2 adapted from Sen and Imlay, 2021: Intracellular damage to bacteria caused by superoxide and hydrogen peroxide. Superoxide ($O_2^{\bullet -}$) and hydrogen peroxide (H_2O_2) can both deactivate (**1**) enzymes with a ferrous ion (Fe^{2+}) in their active site and (**2**) dehydratase enzymes that employ a $[4Fe\text{-}4S]^{2+}$ cluster. (**3**) Hydrogen peroxide can also damage molecules such as nucleic acids, to which Fe^{2+} would be bound to.

1.4 *E. coli*, *S. enterica* and Pst can tolerate the oxidative burst

E. coli, *S. enterica* and Pst metabolise aerobically, which is associated with the continuous generation of hydrogen peroxide and superoxide due to the autooxidation of non-respiratory flavoproteins (Sen and Imlay, 2021). Hydrogen peroxide and superoxide are generated at potentially lethal doses; however, the presence of scavenging enzymes are adequate defences against these (Imlay, 2009). These include periplasmic and cytoplasmic superoxide dismutases which catalyse superoxide to oxygen and hydrogen peroxide, periplasmic and cytoplasmic catalases which catalyse hydrogen peroxide to water and oxygen, and peroxidases which catalyse hydrogen peroxide to water via an oxidation reaction (Imlay, 2009). During the oxidative burst, bacterial cells are exposed to much greater concentrations of ROS which can overwhelm the basal concentration of these scavenging enzymes, causing oxidative stress (Lamb and Dixon, 1997; Imlay, 2009).

The regulatory response of *E. coli* and *S. enterica* to oxidative stress is primarily mediated by the *oxyR* and *soxRS* regulons, which initiates the transcription of genes required for the activation of resistance mechanisms (Imlay, 2009; Seo *et al.*, 2015) (figure 1.3). Examples of activated resistance mechanisms include an increased concentration of scavenging enzymes (Imlay, 2009; Guo *et al.*, 2012), the repair of DNA and $[4Fe\text{-}4S]^{2+}$ damaged clusters (Imlay, 2009; Romsang *et al.*, 2015), the control of unincorporated iron to minimise the formation of hydroxyl radicals (Imlay, 2009; Butcher *et al.*, 2011), the maintenance of the cellular redox balance (Sen and Imlay, 2021), drug efflux because some drugs are capable of inducing oxidative stress (Vaishampayan and Grohmann, 2021), manganese (Mn^{2+}) importation for use as an alternative to iron by mononuclear enzymes and as a co-factor by some enzymes involved in the ROS response (Sen and Imlay, 2021; Uppalapati and Vazquez-Torres, 2022), zinc (Zn^{2+}) importation for use as a co-factor by some enzymes involved in the ROS response (Seo

et al., 2015), and cell wall synthesis, which could be required to induce structural changes required for ROS protection (Seo *et al.*, 2015) (figure 1.3).

The *oxyR* regulon is also highly conserved in *P. syringae* species, however Pst does not have the *soxRS* regulon (Ishiga and Ichinose, 2015). It has open reading frames encoding protein homologues to FinR and HexR which are transcriptional regulators found to regulate different genes under oxidative stress conditions in *Pseudomonas putida* (Ishiga and Ichinose, 2015). Many of the genes controlled by these regulators belong to the *soxRS* regulon in *S. enterica* (Kim and Park, 2014).

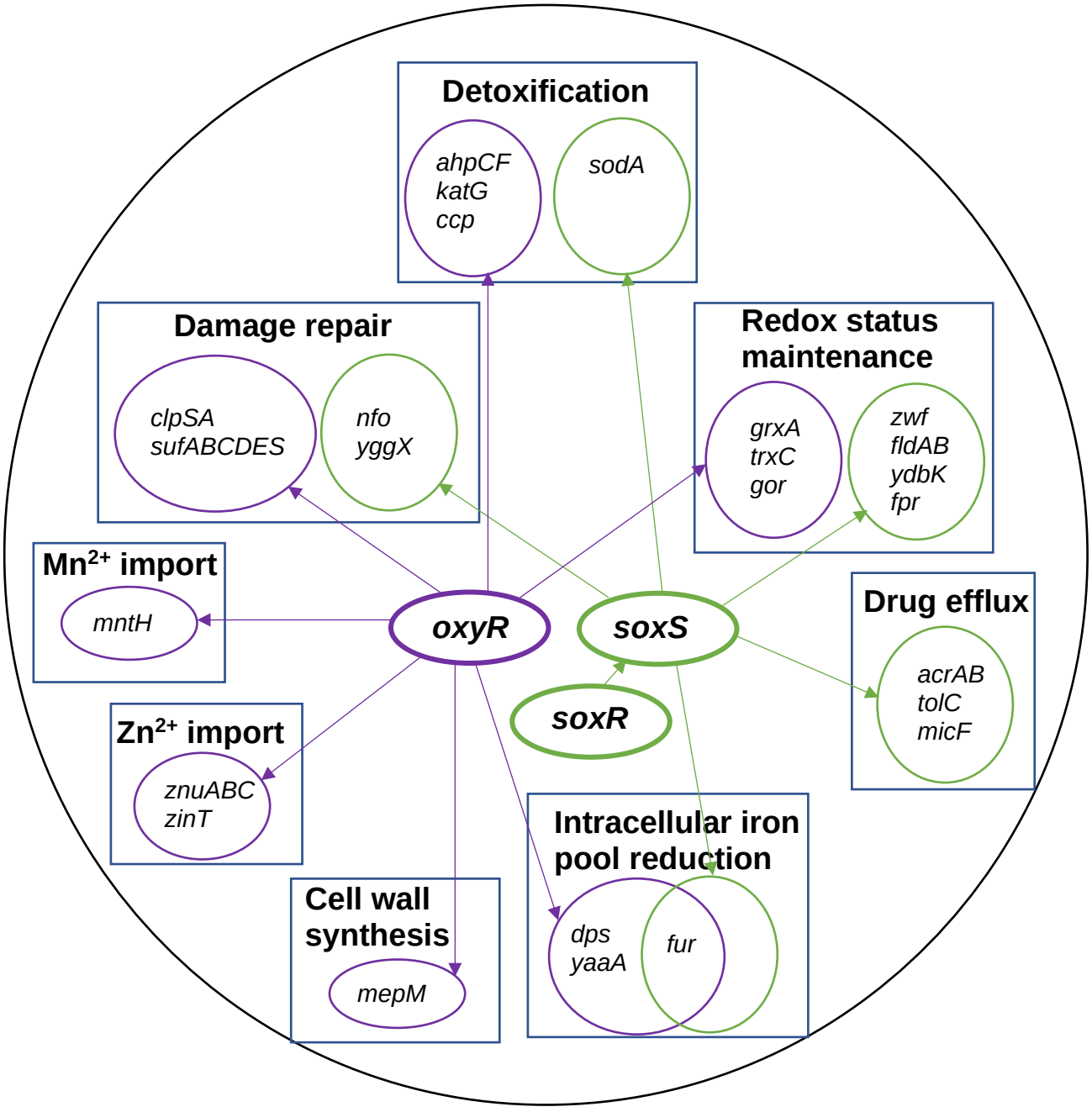


Figure 1.3: A selection of genes activated by the *oxyR* and *soxRS* regulons in *E. coli*. (Imlay, 2009; Seo *et al.*, 2015; Sen and Imlay, 2021).

1.5 Ozone as an antimicrobial agent for the food industry

The antimicrobial nature of ROS has been exploited in the food industry, where systems have been developed to expose post-harvest produce to ROS, primarily in the form of ozone (Sarron *et al*., 2021). Although both gaseous and aqueous forms of ozone are used commercially (Sarron *et al*., 2021), most of our current knowledge of bacterial ozone responses has been obtained using aqueous ozone systems. The damage caused by ozone to bacterial cells is summarised in figure 1.4.

The bacterial cell envelope is the first site of ozone attack in both Gram-positive (Ersoy *et al*., 2019) and Gram-negative bacteria (Scott and Lesher, 1963; Komanapalli and Lau, 1996; Cho *et al.*, 2010; Patil *et al.*, 2011; Zhang *et al.*, 2011, 2015; Ersoy *et al*., 2019) (figure 1.4). Here, ozone oxidises double bonds in unsaturated lipids (Brown *et al*., 2011) (figure 1.4) which cause secondary reactive species, such as aldehydes and hydrogen peroxide to form in the presence of water (Pryor *et al*., 1991). Proteins are also subject to oxidation and different amino acids have different susceptibilities to ozone (Mudd *et al.*, 1969; Sharma and Graham, 2010) (figure 1.4). Cysteine residues are particularly susceptible to ozone oxidation due to the presence of a sulfhydryl group (Komanapalli *et al*., 1997).

Damage to the bacterial cell surface increases cell permeability which causes leakage of intracellular components (Scott and Lesher, 1963; Komanapalli and Lau, 1996; Zhang *et al.*, 2011, 2015; Ersoy *et al*., 2019), and allows ozone to enter the cytoplasm where it can cause further oxidative damage (Komanapalli and Lau, 1996; Komanapalli *et al*., 1997; Cho *et al.*, 2010) (figure 1.4). Ozone can produce breaks in DNA, which if unrepaired can result in DNA breakdown (Hamelin, 1985; Ishizaki *et al.*, 1987) (figure 1.4). Mutagenic effects of ozone have also been reported, however, other studies have failed to observe these effects (Victorin, 1992) (figure 1.4).

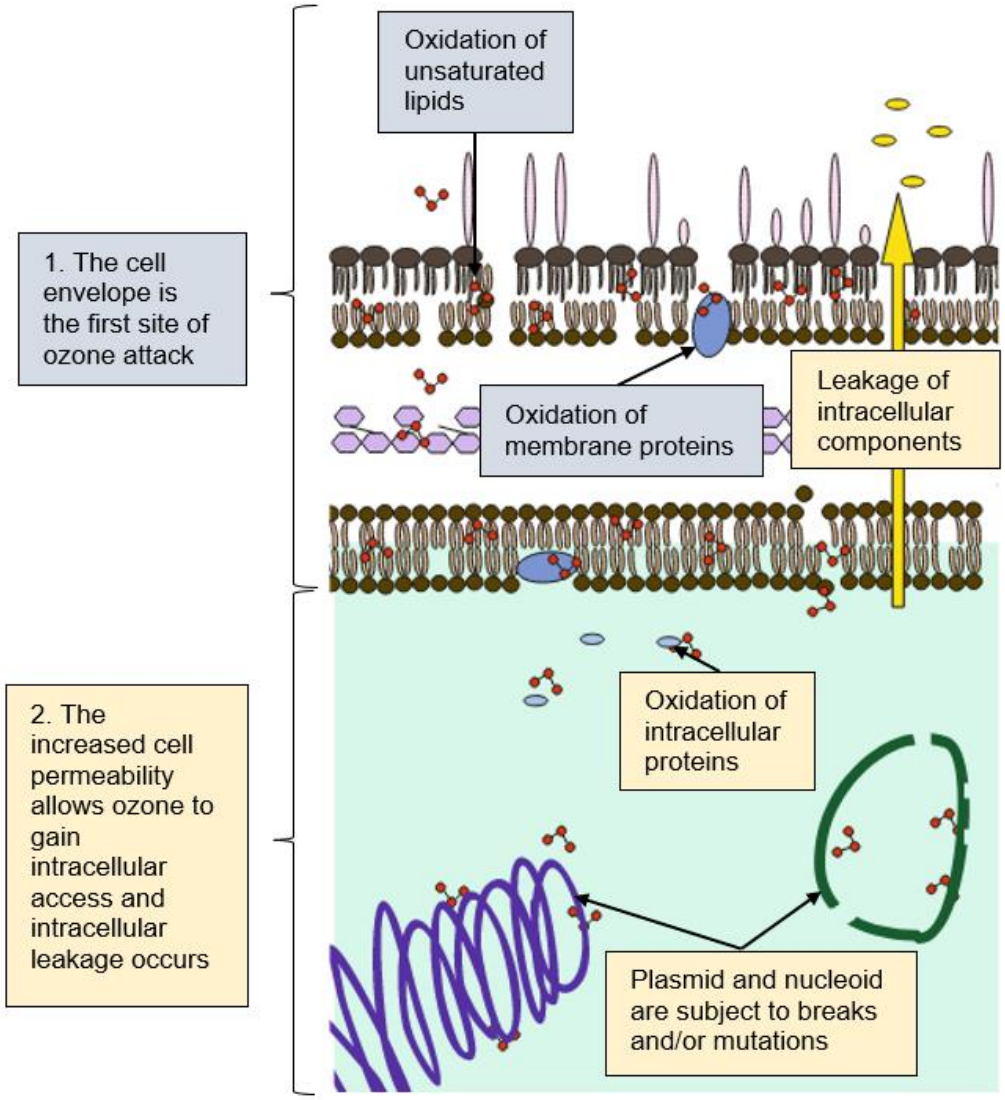


Figure 1.4: The bacterial cell envelope is initially targeted by ozone, leading to subsequent intracellular damage and leakage. A Gram-negative bacterium is represented because model pathogens selected for the project are Gram-negative. The cell envelope is the first site of ozone attack where unsaturated lipids and membrane proteins are oxidised (blue text boxes). The resultant increase in cell permeability allows ozone to gain intracellular access so that intracellular proteins and DNA are oxidised, and intracellular leakage also occurs (yellow text boxes).

1.6 Commercial systems for ozone generation

Commercial systems which generated gaseous ozone and aqueous ozone respectively were used for work in this project.

To compare the concentrations of ROS generated by commercial systems to those generated by eukaryotic hosts, it is to be mentioned that within the leaves of different plant species, physiological levels of hydrogen peroxide have been reported to range from

0.5 - 75 µmol/gram fresh weight (Rahman *et al.*, 2023), and in tobacco, *P. syringae* induced a ROS burst which increased hydrogen peroxide by 5 µmol/gram fresh weight above its physiological level (Mur *et al*., 2005). Since ROS in eukaryotic hosts are measured in µmol/gram fresh weight, it was difficult to compare this to the concentrations of commercially generated gaseous ozone, which is measured in ppm. Nevertheless, ~1 ppm commercially generated aqueous ozone was used for work in this project and this could be converted to 0.0208 µmol/gram water (Sunberg, 1986). While this can be tentatively compared to the physiological levels of ROS in eukaryotic hosts, it is essential to acknowledge the compositional differences between plant tissues and water. Plant tissues comprise a diverse array of biological constituents, capable of interacting with and sequestering ROS (Raja *et al.*, 2017), whereas water lacks such constituents. This disparity will affect the quantity of ROS available for reactions with micro-organisms.

Gaseous ozone production

Anacail Ltd developed the in-pack ozone system (model: F250) (figure 1.5: A) for the food industry, where the system head generates gaseous ozone by cold plasma technology for a varying number of seconds (figure 1.5: B).

(A) The in-pack ozone system



(B) The system head

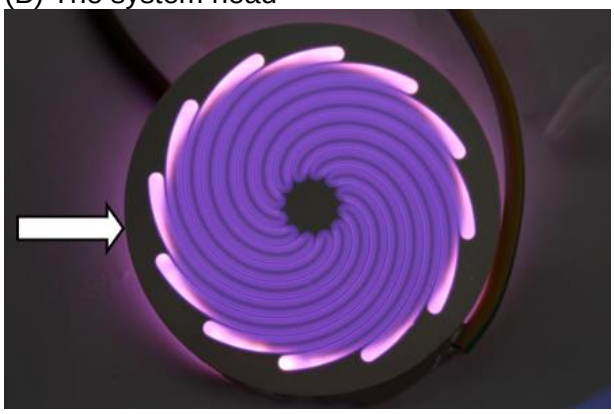


Figure 1.5 sourced from Anacail Ltd: (A) The in-pack ozone system (model: F250) and (B) a close-up of the system head generating cold plasma. The white arrows indicate the system head. The red arrow indicates where system information is presented.

Cold plasma technology is utilised to split oxygen molecules from air into singlet oxygen atoms by electron impact dissociation (figure 1.6: A) (Gibalov and Pietsch, 2006; Potts and Diver, 2012; Whitehead, 2016). These are highly reactive and unstable so can recombine with available oxygen molecules to form ozone molecules, which are also highly reactive and unstable (figure 1.6: B) (Gibalov and Pietsch, 2006). Other ROS may also form during this process, dependent on air humidity. This is because electron impact dissociation of water can form hydroxyl radicals, which could subsequently react with ozone to form perhydroxyl radicals (Whitehead, 2016). Hydroxyl radicals and perhydroxyl radicals are further sources of oxidative stress (table 1.1) (Epelle *et al.*, 2023). Since air is the input, electron impact dissociation of nitrogen can also occur, which can subsequently form nitrogen species, however this will be minimal since the electron mean energy in the system is optimum for the electron impact dissociation of oxygen (Penetrante, Bardsley and Hsiao, 1997).

(A) $O_2 + e^- \longrightarrow O + O + e^-$

(B) $O + O_2 \longrightarrow O_3$

Figure 1.6 adapted from Gibalov and Pietsch, 2006: (A) Electron impact dissociation of oxygen molecules for (B) ozone generation.

The decay of electronically excited states is a source of ultraviolet (UV) photons (Whitehead, 2016), which makes the surface of the system head purple (figure 1.5: B). The UV emission is not expected to have a significant role in the antimicrobial activity of cold plasma systems and reactive species are the biggest contributor to the antimicrobial activity (Laroussi and Leipold, 2004).

The system head generates ROS, primarily the form of ozone, inside a sealed food pack, when the system head is in contact with the seal of the pack (figure 1.7) (Potts and Diver, 2012). Inside the pack, ozone decays back to molecular oxygen (figure 1.7) (Potts and Diver, 2012), therefore safety issues associated with exposure to ozone gas, including respiratory tract and eye damage, are overcome (Health and Safety Executive, 2014). The generated ozone could take up to several hours to decay, therefore the contents of a sealed pack would remain exposed to ozone during this time (Potts and Diver, 2012).

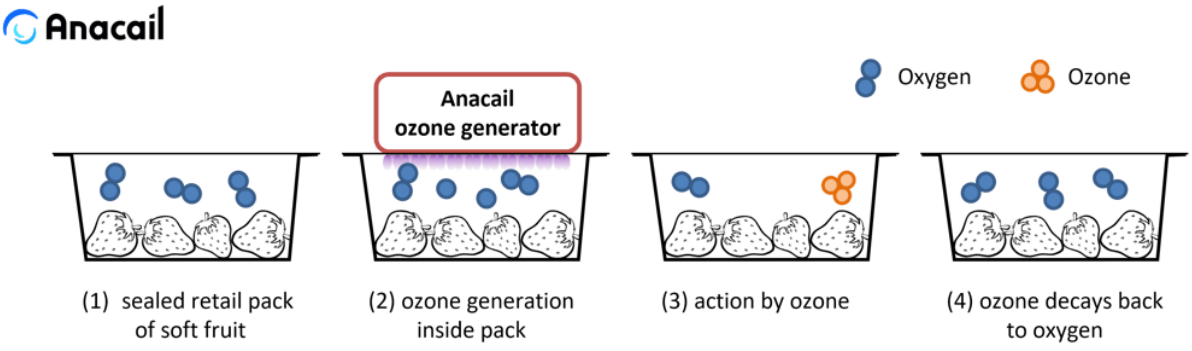


Figure 1.7 sourced from Anacail Ltd: The in-pack ozone system generates ozone inside a food pack, which subsequently decays inside the food pack.

For this project, 1 and 3 second ozone generation times were used because they were ‘low’ and ‘high’ doses that were recommended to treat produce in the food industry (Anacail Ltd, personal communication). Ozone doses to treat produce are limited because too much ozone could negatively impact organoleptic properties (Sarron *et al*., 2021).

For the execution of this project, two distinct in-pack ozone systems, each assigned a unique serial number, were employed. Initially, the ozone system bearing serial number 6 was used, which generally generated ~80 - 300 peak ppm ozone for a 1 second ozone generation time, and ~350 - 700 peak ppm ozone for a 3 second ozone generation time. Unfortunately, operational issues occasionally led to lower-than-expected peak ozone concentrations following ozone generation, which prompted the substitution of the system with an alternative. The replacement in-pack ozone system, identified by serial number 4, was subsequently used for further experiments. In this case, the system was exclusively used for 3 second ozone generations, which consistently generated peak ozone concentrations ranging from 663 - 827 ppm.

During the project, Anacail Ltd dissolved, therefore work with the in-pack ozone system was halted. To account for this, some work for this project was completed using a different ozone generating system, which generated aqueous ozone.

Aqueous ozone production

Aqueous ozone was continuously generated from water using electricity, by electrochemical cells in a commercial system. Within an electrochemical cell, ozone is generated at the electrolytic anode by two different reactions (figure 1.8) (Okada and Naya, 2012).

(1) $3H_2O \longrightarrow O_3 + 6H^+ + 6e^-$

(2a) $2H_2O \longrightarrow O_2 + 4H^+ + 4e^-$

(2b) $O_2 + H_2O \longrightarrow O_3 + 2H^+ + 2e^-$

Figure 1.8 adapted from Okada and Naya, 2012: Ozone is generated from water by two different reactions (1 and 2) within an electrochemical cell.

The concentration of ozone that can be achieved in water is limited by its solubility in water (Epelle *et al.*, 2023). Due to its low solubility, some of it is released as a gas, therefore appropriate controls require to be in place to minimise exposure to gaseous ozone, which, as previously described, is a safety risk (Epelle *et al.*, 2023).

The commercial system used a positive feedback loop to maintain a specific concentration of ozone in water. 0.7 - 1 ppm aqueous ozone was used for work in this project because in water that is clean, potable and free from debris, ozone is an effective sanitiser within the concentration range of 0.5 - 2 ppm (Suslow, 2004). Different half-lives have been reported for aqueous ozone because it is dependent on conditions such as temperature, pH and the presence of organic contaminants, however it typically ranges from 10 - 80 minutes (Epelle *et al.*, 2023).

The decomposition of aqueous ozone is a complex process, but it can result in the formation of other ROS including hydroxyl radicals, hydroperoxyl radicals and superoxide radicals, which are further sources of oxidative stress (table 1.1) (Gardoni *et al*., 2012; Epelle *et al.*, 2023). The extent of their production is dependent on water properties (Epelle *et al.*, 2023).

1.7 Ozone has benefits over current food industry treatments

Ozone has benefits over the treatments which are currently being used to control for pathogens in the food industry. These are mainly chlorine-based treatments (Rico *et al.*, 2007; Berger *et al.*, 2009; Deng *et al.*, 2020) but other treatments such as peracetic acid also exist (Chinchkar *et al.*, 2022).

Chlorine-based treatments

Chlorine-based treatments, particularly sodium hypochlorite, are frequently used in the food industry because they are low cost, easy to source and are effective against a range of bacteria (Rico *et al.*, 2007; Berger *et al.*, 2009; Ramos *et al.*, 2013; Deng *et al.*, 2020).

Sodium hypochlorite forms hypochlorous acid in water (figure 1.9: A), which subsequently exists in equilibrium with gaseous chlorine (Cl_2) and the hypochlorite ion (^{-}OCl) (figure 1.9: B), and the distribution of these chemical species within this equilibrium is highly dependent on pH (Fukuzaki, 2006; da Cruz Nizer *et al*., 2020). All of the chemical species

within this equilibrium are termed ‘free chlorine’ because they are available to oxidise micro-organisms (table 1.1). For this project, sodium hypochlorite with 100 ppm free chlorine was selected to represent a concentration relevant to the food industry (The Food and Agricultural Organisation of the United Nations and The World Health Organisation, 2008), and its pH ranged from 9.7 - 10.7, where the hypochlorite ion would have been the dominant species (Fukuzaki, 2006). Lower concentrations of sodium hypochlorite were also used for work in this project, which would have had a pH closer to neutral, so would have had a greater percentage of hypochlorous acid (Fukuzaki, 2006).

(A) $NaOCl + H_2O \rightarrow HOCl + NaOH$

(B) $Cl_2 \leftrightarrow HOCl \leftrightarrow {}^{-}OCl$

Figure 1.9: (A) taken from da Cruz Nizer *et al*., 2020. Sodium hypochlorite (NaOCl) reacts with water to form hypochlorous acid (HOCl). (B) Hypochlorous acid exists in equilibrium with gaseous chlorine (Cl_2) and the hypochlorite ion (^{-}OCl).

Within ‘free chlorine’, both hypochlorous acid and the hypochlorite ion are the strongest oxidants (table 1.1). Although the hypochlorite ion has a greater oxidising potential than hypochlorous acid (table 1.1), hypochlorous acid has the greatest antimicrobial activity due to its ability to diffuse through the bacterial cell membrane and cause intracellular damage (Fukuzaki, 2006).

Although hypochlorous acid is a weak acid, its oxidising action primarily contributes to its bactericidal activity (Fukuzaki, 2006). It reacts with nucleophilic structures which can exhaust antioxidants and inactivate enzymes involved in ROS destruction, subsequently causing the intracellular accumulation of superoxide and hydrogen peroxide produced during aerobic metabolism (Fukuzaki, 2006). Free iron is released by the cell in response to hypochlorous acid, which could react with hydrogen peroxide to generate extremely reactive hydroxyl radicals via the Fenton reaction (Fukuzaki, 2006). The direct reaction of hypochlorous acid with iron could be a further source of hydroxyl radicals (Fukuzaki, 2006).

The hypochlorite ion is negatively charged so does not readily cross bacterial cell membranes, therefore it oxidises extracellular components (Fukuzaki, 2006). It causes disintegration of the microbial cell wall and membrane, and can inactivate functional proteins located in the cell membrane via the oxidation of sulfhydryl groups and the chloramination of amino groups (Fukuzaki, 2006).

The use of chlorine-based treatments results in the formation of toxic disinfection by-products (DBPs) when free chlorine reacts with residues, such as organic matter, that are present in water. This includes trihalomethanes which have been linked to an increased risk of bladder cancer, colorectal cancer and adverse reproductive effects in humans (Committee on Toxicity of Chemicals in Food Consumer Products and the Environment, 2006; de Castro Medeiros *et al.*, 2019), and chlorates which can cause reduced iodine adsorption in humans, particularly in children (Food Standards Scotland, 2023). Due to this, a maximum reside limit (MRL) for chlorate is imposed on food products in the EU (EU regulation 2020/749) which the UK abides by (Health and Safety Executive, 2023), however there is no MRL for trihalomethanes since there is insufficient evidence for health risks associated with the levels of trihalomethanes which people are realistically exposed to (de Castro Medeiros *et al.*, 2019).

Peracetic acid

Peracetic acid ($C_2H_4O_3$) is also an intervention treatment in the food industry (Ramos *et al.*, 2013; Chinchkar *et al.*, 2022). It is a strong oxidant (table 1.1) composed of acetic acid ($C_2H_4O_2$) and hydrogen peroxide, which it exists in equilibrium with (figure 1.10) (Dul'neva and Moskvin, 2005; Ramos *et al.*, 2013).

$$C_2H_4O_2 + H_2O_2 \leftrightarrow C_2H_4O_3 + H_2O$$

Figure 1.10 adapted from Dul'neva and Moskvin, 2005: Peracetic acid ($C_2H_4O_3$) exists in equilibrium with acetic acid ($C_2H_4O_2$) and hydrogen peroxide (H_2O_2).

The mechanism of bactericidal action of peracetic acid is less well understood than hydrogen peroxide, ozone and sodium hypochlorite, however it can oxidise sulfhydryl groups and cause damage to the cell membrane, DNA, lipids, proteins, and enzymatic and transport systems (Vandekinderen *et al.*, 2009; Ao *et al.*, 2021). Peracetic acid can also spontaneously decompose in water into hydroxyl radicals which, as previously mentioned, is a potent oxidant (Coyle *et al*., 2014).

It has been reported that commercially available peracetic acid often contains considerable quantities of hydrogen peroxide, which would contribute to antimicrobial activity (Vandekinderen *et al.*, 2009). However, the disinfection efficiency of hydrogen peroxide is low compared to peracetic acid, so it has previously been concluded that the bactericidal action of peracetic acid is mainly due to peracetic acid (Koivunen and Heinonen-Tanski, 2005).

Peracetic acid has a benefit over chlorine-based treatments because it does not result in the formation of toxic DBPs (Ramos *et al.*, 2013). Peracetic acid primarily degrades to acetic acid, oxygen, and water, each of which is not a toxicological concern (Environmental Protection Agency, 2000).

Ozone

Ozone is an emerging intervention treatment (Deng *et al.*, 2020), which may be a better alternative to chlorine-based treatments and peracetic acid. This is because ozone does not form toxic DBPs since the only product of its decomposition is oxygen (Karaca and Velioglu, 2007), it is generated on-site, therefore there is no requirement for the transportation and storage of chemicals (Goodburn and Wallace, 2013), and the long-term operating costs of ozone treatments may be lower than the operating costs of chlorine-based treatments and peracetic acid *(*Aslam *et al*., 2020). Ozone can also remove residual pesticides from post-harvest produce (Chen *et al*., 2013; de Souza *et al.*,

2018) and can delay their ripening by oxidising ethylene (which is a hormone that accelerates ripening) (Martínez-Romero *et al.*, 2007; Tzortzakis and Chrysargyris, 2017).

1.8 Research aims and rationale

Different types of intervention treatments exist to control for pathogens on post-harvest produce, including sodium hypochlorite and peracetic acid (U.S. Food and Drug Administration, 1999), however ozone has benefits over these. The primary aim of this project was to determine if ozone could be used as an alternative treatment to effectively control pathogens on post-harvest produce. One specific aim of this project was therefore to compare the effectiveness of ozone, sodium hypochlorite and peracetic acid against pathogens on post-harvest produce.

The effect of factors which were hypothesised to affect the survival of pathogens to ozone treatment were also investigated in this project. For example, for pathogens to become established on eukaryotic hosts, they must tolerate a burst of ROS produced during host defences, which is mainly hydrogen peroxide (Lamb and Dixon, 1997; O'Brien *et al.*, 2012), and there is evidence that micro-organisms associated with these hosts have evolved a strong oxidative stress response to cope with this (Aussel *et al.*, 2011; Dublan *et al.*, 2014; Vassallo *et al.*, 2023). It was hypothesised that bacteria which had a particularly high tolerance to hydrogen peroxide could better survive ozone treatment, since both hydrogen peroxide and ozone are ROS which cause oxidative stress (Bayir, 2005), so they could be tolerated by the same mechanisms. For example, ROS in the form of hydroxyl radicals can form during ozone treatments (Epelle *et al.*, 2023), and from Fenton reactions, in which hydrogen peroxide participates in (Sen and Imlay, 2021). An aim of this project was to compare the physiological response of model pathogens to ozone and hydrogen peroxide, to gain a deeper understanding of whether they were both tolerated by the same mechanisms. The physiological response of model pathogens to sodium hypochlorite and peracetic acid was also compared against hydrogen peroxide as

another aim for this project. This was because, although the active components of sodium hypochlorite and peracetic acid are not ROS, they are strong oxidants, which in addition to hydrogen peroxide, are also associated with the formation of hydroxyl radicals (Fukuzaki, 2006; Coyle *et al*., 2014). They could therefore also be tolerated by similar molecular mechanisms to hydrogen peroxide in bacteria. Hence, bacteria with a particularly high tolerance to hydrogen peroxide could also better survive peracetic acid and sodium hypochlorite, so it was beneficial to gain a deeper understanding of whether they were tolerated by the same mechanisms.

Another factor that was hypothesised to affect the survival of pathogens to ozone treatment was the change induced in the whole microbiota of post-harvest produce by ozone treatment. It was hypothesised that the elimination of ozone-susceptible micro-organisms would reduce competition for the surviving population, which could then thrive after the decay of ozone. The altered microbiota could subsequently affect the ability of pathogens to survive and proliferate, so since the aim of ozone was to reduce pathogens, the effect of ozone on the native microbiota required consideration. Hence, an aim of this project was to assess the effect of ozone treatment on the native microbiota of post-harvest produce.

Anacail Ltd, which developed the in-pack ozone system, were the original industrial partner of this project, however since the organisation dissolved, this project would not benefit them. However, data generated using the in-pack ozone system may be applicable to similar technologies developed in the future. This project would benefit the company which supplied the commercial aqueous ozone system because data would be provided to them to demonstrate the suitability of their system as an intervention treatment for the food industry. The company could use the data to consider if any modifications of the intervention treatment would be required to provide the best service for the food industry. Results and potential modifications could also be applicable to the current sanitation services that the commercial aqueous ozone system is being used for.

Data generated from the project will also be relevant to the food industry because it will identify how effective ozone is against food-borne and plant pathogens. The project will also benefit the scientific community because further knowledge will be gained regarding oxidative stress tolerance mechanisms employed by bacteria to survive intervention treatments.

To summarise, post-harvest produce is subject to contamination by pathogens, and this is controlled in the food industry by intervention treatments including sodium hypochlorite and peracetic acid (U.S. Food and Drug Administration, 1999). However, these treatments necessitate the transportation and storage of chemicals, and sodium hypochlorite results in the formation of toxic DBPs (Committee on Toxicity of Chemicals in Food Consumer Products and the Environment, 2006; Food Standards Scotland, 2023). Ozone may be a better alternative because it is generated onsite so eliminates the requirement for transportation and storage, and it does not form toxic residues (Karaca and Velioglu, 2007; Goodburn and Wallace, 2013). The overall aim of this project was to investigate whether ozone could serve as a viable alternative treatment to effectively control pathogens on post-harvest produce. This will be investigated by assessing the impact of ozone on the native microbiota of post-harvest produce, considering that induced changes could influence the ability of pathogens to survive and proliferate (chapter 2). Furthermore, to investigate if tolerance to hydrogen peroxide, which is released during eukaryotic host defences against pathogens (O'Brien *et al.*, 2012), could prime pathogens to be more tolerant to ozone (and other oxidative treatments), the physiological response of pathogens to hydrogen peroxide and other treatments will be compared (chapter 3). Finally, the effectiveness of ozone, sodium hypochlorite and peracetic acid against pathogens on post-harvest produce will also be compared to determine if ozone is as efficient as current treatments (chapter 4).

Chapter 2: The impact of gaseous ozone treatment on the microbiota of post-harvest produce

2.1 Introduction

It was hypothesised that ozone treatment would alter the entire microbiota of post-harvest produce, which could affect the ability of pathogens to survive and proliferate during post-treatment storage before consumption. The ability of ozone treatment to reduce pathogens, and its effect on the native microbiota of post-harvest produce was investigated in this chapter. Gaseous ozone delivered by the in-pack ozone system (Anacail Ltd) (chapter 1, section 1.6) was used to study the effect of ozone for all work completed in this chapter.

2.1.1 The impact of high gaseous ozone concentrations on whole microbial communities is unknown

The impact of such high ozone concentrations that are delivered by the in-pack ozone system on whole microbial communities is unknown. The impact of ozone on microbial communities has mainly been studied by investigating the impact of elevated environmental levels of ozone on soil, rhizosphere or plant phyllosphere communities (J. Zhang *et al.*, 2019; Díaz-López *et al.*, 2022; Li *et al.*, 2022; Bhandari *et al.*, 2023; Yu *et al.*, 2023; Zhang *et al.*, 2023). In most studies, elevated environmental levels of ozone reduced the microbial community diversity and changed the microbial community composition, however mixed results have been reported (Agathokleous *et al.*, 2020).

Only a few studies have investigated the effect of ozone applied as an intervention treatment on whole microbial communities of food products, and of the studies found, very low concentrations of ozone were used in comparison to the concentrations that are generated by the in-pack ozone system (Qian *et al.*, 2022; Zhang *et al.*, 2022). In these studies, it was also reported that ozone caused differences in the microbial community

composition, however the effect of ozone on community diversity was not conclusive (Qian *et al.*, 2022; Zhang *et al.*, 2022).

2.1.2 The tomato calyx and pedicel as a model system

The tomato calyx and pedicel were selected as the model system to investigate the impact of ozone treatment on the microbiota of post-harvest produce (figure 2.1). This was because tomato was the model fruit for the project (chapter 1, section 1.1) and more micro-organisms reside on the calyx and pedicel than on the fruit surface (Smid *et al.*, 1996; Barak *et al.*, 2011). The calyx is a structure at the base of the fruit that are a remnant of the sepals (Lyle, 2006) and the pedicel is the stem structure that connects the base of the tomato fruit to the plant body (Ito and Nakano, 2015) (figure 2.1). Upon fruit maturation, an abscission zone, often referred to as the natural breakpoint, forms in the pedicel so that the fruit can become detached from the plant body (Ito and Nakano, 2015) (figure 2.1).

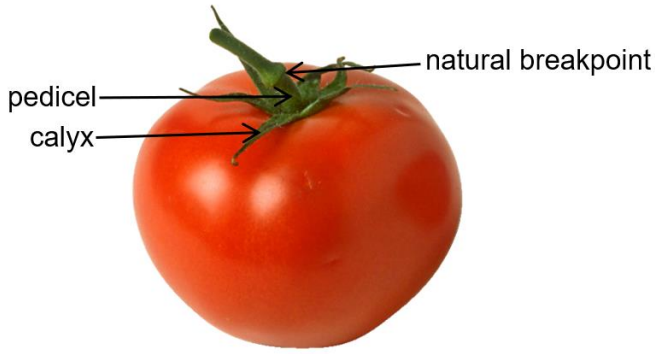


Figure 2.1: Tomato calyx, pedicel, and natural breakpoint.

Although the tomato calyx and pedicel are not for direct consumer consumption, implications could still arise if pathogens were selected for on these, due to an altered microbial community. For example, they could contribute to post-harvest fruit decay (Khaleghi *et al.*, 2013) and could be transferred to food preparation areas via cross-contamination (Barak *et al*., 2011) which could cause food-borne illness in consumers (U.S. Food and Drug Administration, 2012).

2.1.3 The microbiota of the tomato calyx and pedicel is unknown

Tomato fruit microbial communities have previously been studied (Ottesen *et al.*, 2013; Dong *et al.*, 2019; López *et al.*, 2020; Soto-Giron *et al.*, 2021), but tomato calyx and pedicel microbial communities remain uncharacterised, to current knowledge. Aims of this chapter were therefore to characterise the tomato calyx and pedicel microbiota, to investigate how this changed over time post-harvest, and to investigate the impact of ozone treatment on this.

2.1.4 Microbiota changes may occur during post-harvest storage of tomatoes

The tomato calyx and pedicel microbiota may change during post-harvest storage. This is because calyx senescence causes desiccation and browning, which starts from the calyx tips and moves towards the base as time progresses (Fathi-Najafabadi *et al.*, 2021). Browning arises due to the oxidation of phenolic compounds and is related to the degradation of chloroplast and chlorophylls (Selvarajan *et al*., 2018; Fathi-Najafabadi *et al.*, 2021). These changes in the calyx may influence the microbial community present. Also, ethylene is a hormone which accelerates fruit ripening and it continues to be produced post-harvest (figure 2.2), therefore it enhances senescence and fruit decay (de Poel *et al.*, 2012). This is because changes associated with ripening will still occur post-harvest, which include the tomato fruit becoming softer, sweeter and less acidic, and changes in volatile emission will occur (Quinet *et al.*, 2019). This can make conditions more or less favourable for specific micro-organisms, for example conditions may become more favourable for pathogens since tomato disease incidence and severity have been reported to increase with tomato storage duration (Sinha *et al.*, 2019). Since the calyx and pedicel are attached to the fruit, the microbiota of the calyx and pedicel may change due to changes in the fruit microbiota.

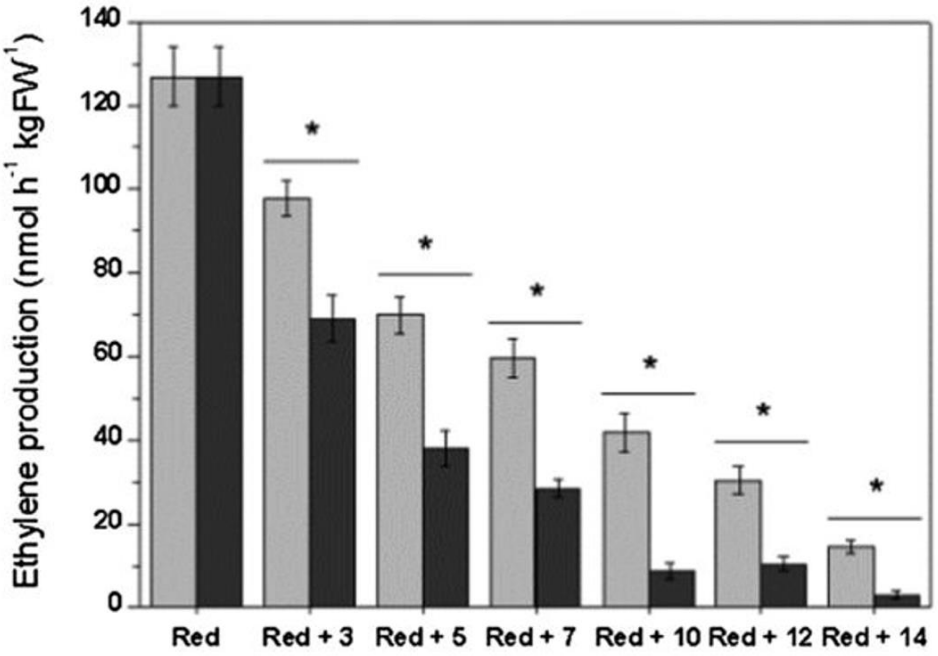


Figure 2.2 taken from De Poel *et al*., 2012: Ethylene production of harvested red tomatoes (dark gray) and red tomatoes kept on the plant (light gray). *In vivo* ethylene production was measured (mmol h^{-1} kg fresh $weight^{-1}$) from tomato fruits at different days after tomatoes were red ripe (displayed on x-axis). Mean and standard deviation are shown (n = 10). * = $p < 0.05$.

2.1.5 Ozone may induce changes in the microbiota

Ozone treatment may cause changes in the tomato calyx and pedicel microbiota because it would eliminate ozone susceptible micro-organisms, which would reduce competition for survivors, allowing them to thrive after the decay of ozone. Ozone may also induce stress responses in micro-organisms that it does not kill, which could alter their gene expression (Patil *et al.*, 2011). This could result in traits that affect the survival of the affected micro-organism and neighbouring micro-organisms, such as an increase in biofilm formation or the production of secondary metabolites (Kaplan, 2011; Li *et al.*, 2020).

Ozone also directly oxidises ethylene so can delay ripening (Martínez-Romero *et al.*, 2007; Tzortzakis and Chrysargyris, 2017), which could prevent changes in the microbiota that are associated with ripening. However, the in-pack ozone system only generates one dose of ozone within seconds, which then decays within a few hours (Potts and Diver, 2012), therefore the effect of ethylene depletion would only be short-term because ethylene is continuously produced during post-harvest storage (figure 2.2) (de Poel *et al.*,

2012). Nevertheless, ozone treatment is applied soon after harvest so it would deplete ethylene when it is at its highest levels post-harvest (figure 2.2).

Since ozone is a broad-spectrum antimicrobial agent, it will also attack the tomato host, inducing a stress response, which will subsequently activate signalling cascades (Vainonen and Kangasjarvi, 2015). It has previously been concluded that ozone can cause changes in a tomato fruit's interactions with pathogens (Tzortzakis *et al*., 2008), therefore it could cause changes in the tomato fruit's interactions with members of the microbial community. The physical damage that ozone may cause to the tomato calyx and pedicel may also affect the ability of microbiota members to survive on it (Sarron *et al*., 2021).

2.1.6 Sequence analysis of the 16S rRNA gene for bacterial community analysis

For work in this chapter, bacterial communities were assessed by sequence analysis of the bacterial 16S rRNA gene, which acts as a fingerprint for bacterial species identification (Ottesen *et al.*, 2013; Dong *et al.*, 2019). Since amplification of the 16S rRNA gene is DNA amplification, DNA from viable cells, dead cells and cell-free DNA would be amplified and included in results, therefore results would not distinguish between viable and non-viable members of a microbial community (Emerson *et al.*, 2017). However, after ozone treatment, the altered viability status of microbiota members would impact their growth, which would impact the dynamics of the microbial community over time. Therefore, for work in this chapter, the dynamics of the microbial community between selected different time-points, namely 0, 3 and 10 days post-treatment/post-harvest were compared to identify members of the microbiota that appeared to be active and viable. Only an untreated sample was analysed on day 0 because the differences in microbial viability, which would have been imposed in the ozone-treated sample, were not expected to be immediately detected. The comparison of 16S rRNA DNA at selected

timepoints after ozone application has previously been done to investigate ozone effects (Qian *et al.*, 2022).

2.1.7 Chapter aims

This chapter aimed to investigate if gaseous ozone, generated by the in-pack ozone system, could reduce pathogens. This chapter also aimed to characterise the microbial community of the tomato calyx and pedicel, and to investigate how this changed over time, after tomato harvest. The impact of ozone treatment on this bacterial community was also investigated.

2.2 Materials and methods

2.2.1 Bacterial strains and primers

Bacterial strains used for this study are listed in table 2.1.

Table 2.1: Bacterial strains used for this study

Strain	Description	Antibiotics	Reference
Pseudomonas syringae pv. tomato (Pst) DC3000	A rifampicin-resistant derivative of Pst DC52 (also referred to as NCPPB 1106), which was isolated from tomatoes on the island of Guernsey, UK (Buell *et al.*, 2003; Almeida *et al.*, 2009)	Rifampicin, nitrofurantoin	(Cuppels, 1986)
Pst T1	An isolate from tomatoes in Canada	Nitrofurantoin	(Almeida *et al.*, 2009)
Escherichia coli (*E. coli*) JHI-5025	An isolate from soil in Scotland	NA	(Holden, 2021)

Primers used for this study are listed in table 2.2.

Table 2.2: Primers used for this study

Primer	Sequence (5' – 3')	Use	Reference
515F (Parada)	TCGTCGGCAGCGTCAGAT GTGTATAAGAGACAGGTG YCAGCMGCCGCGGTAA	Forward primer for amplification of variable region 4 of the 16S rRNA gene	(Parada *et al*., 2016)
806R (Apprill)	GTCTCGTGGGCTCGGAGA TGTGTATAAGAGACAGGG ACTACNVGGGTWTCTAAT	Reverse primer for amplification of variable region 4 of the 16S rRNA gene	(Apprill *et al.*, 2015)

2.2.2 Media and growth conditions

Media

The following media were used in this study:

- Lysogeny broth (LB): 10 g/L tryptone, 5 g/L yeast extract, 10 g/L NaCl. For solid LB, agar was added at 1.5% (w/v).
- Plate count agar (PCA) (Merck, UK). For *Pseudomonas* selection, PCA was supplemented with 10 mg/L cetrimide, 10 mg/L fucidin and 50 mg/L cephaloridine (CFC) (Merck, UK)
- Potato dextrose agar (PDA): potato dextrose broth (Fisher Scientific, USA) supplemented with 1.2% (w/v) agar.
- Rose-Bengal chloramphenicol agar (RBCA) (Merck, UK)
- MacConkey agar (Merck, UK)

Growth conditions

All bacterial strains were stored in 25% glycerol at -80^{o}C. They were cultured onto LB agar and incubated at 28^{o}C for 1 - 2 days until single colonies appeared. Single colonies were used to inoculate 10 ml LB, which was incubated at 28^{o}C, 220 revolutions per minute (rpm) overnight (20 to 24 hours).

2.2.3 Tomato cultivation

Tomato cv. Brioso RZ F1 (72 - 130) (Rijk Zwaan) seeds (British Tomato Growers Association, UK) were planted on 4th March 2020 in a mixture of Levington Advance M2 compost (BHGS Ltd) and Sinclair Pro coarse vermiculite medium grade 2.0 - 5.0 mm (BHGS Ltd). They were germinated in a propagator within a glasshouse (22 - 24°C, 16 hour photoperiod) at the Department of Biology, University of Oxford. After germination, plants remained in the glasshouse and were re-potted, irrigated and treated with Levington Tomorite liquid plant feed (B&Q, UK) when necessary.

2.2.4 Tomato collection and packing

Sterile gloves and scissors were used to cut tomatoes from vines, so that each tomato had approximately 1 cm of vine above the natural breakpoint (figure 2.1). This was completed to mimic conditions of tomatoes being kept on the vine, since Tomato cv. Brioso RZ F1 (72 - 130) (Rijk Zwaan) is sold on the vine (Rijk Zwaan, 2021) and there were not enough tomatoes per vine to use complete vines in experiments. Only tomatoes which were red-ripe, firm, and looked healthy were collected (because all tomatoes grown in Britain are harvested when they are red ripe (British Tomato Growers' Association, 2023)). Tomatoes from the same plant were collected into a punnet (DUNI, UK), which was wrapped in cling-film for transportation to the laboratory. Five tomatoes from the same plant were then weighed and collectively transferred into a new punnet (DUNI, UK) before being ozone-treated or not.

2.2.5 Gaseous ozone treatments

Gaseous ozone was generated by the in-pack ozone system (Anacail, UK, model: F250, serial no: 6)), for either 1 or 3 seconds at a command voltage of 3.2 V. The ozone which was generated would have taken up to a few hours to completely decay (Potts and Diver, 2012) so micro-organisms would have remained exposed to ozone during this time.

For ozone treatments, samples had to be inside punnets (DUNI, UK), which were sealed with 5-lane custom microperforated film (Coveris, UK) at 100ºC. Before ozone treatments were performed on samples, 5 empty sealed punnets were used to record peak ozone concentrations produced by the relevant ozone generation times (appendix 1.1). This was because ozone concentrations could not be recorded in sample punnets without destruction of ozone. Peak ozone concentrations typically ranged from 80 - 300 ppm for a 1 second ozone generation and 350 - 700 ppm for a 3 second ozone generation (appendix 1.1). Occasionally, the peak ozone concentration recorded was very low due to issues with the in-pack ozone system (appendix 1.1). To account for this, samples in punnets which produced very different results to other samples within the same treatment group were removed as outliers.

2.2.6 Bactericidal action of gaseous ozone on pathogens *in vitro*

Overnight bacterial cultures of Pst DC3000, Pst T1 and *E. coli* JHI-5025 (table 2.1) were diluted into 10 ml fresh LB by a factor of 1:100 respectively, and incubated at 28ºC, 220 rpm until bacteria reached early exponential growth (OD_{600nm} = 0.35 - 0.6). Bacteria were adjusted to OD_{600nm} 0.35 in LB for exposure to ozone treatments. For non-treated samples, cultures at OD_{600nm} 0.35 were serially diluted by a factor of 10 in 10 mM $MgCl_2$ to provide cultures at a suitable dilution for counting bacterial colonies. Bacteria were spread onto LB agar plates (50 µl culture onto 10 ml agar in 50 x 20.3 mm plates) in triplicate for each treatment condition: 0, 1 and 3 second ozone generation times. Bacteria-inoculated agar plates were left to dry for 5 minutes in a laminar flow cabinet before being packed, unlidded, into punnets (DUNI, UK).

For *E. coli*, each plate replicate was packed individually into a punnet. For *P. syringae*, 3 plates were packed into the same punnet, but plate replicates from the same biological replicate were divided between punnets. For example, one punnet contained biological replicate 1: plate replicate 1, biological replicate 2: plate replicate 1 and biological

replicate 3: plate replicate 1. Punnets were either ozone-treated with a 1 or 3 second ozone generation time, or were not treated, before being incubated at 28ºC. *E. coli* was incubated for 18 hours and *P. syringae* was incubated for 48 hours before colonies were counted. Samples with a count of 0 were recorded as the limit of detection.

2.2.7 Impact of gaseous ozone on the tomato calyx and pedicel culturable microbiota

Tomatoes were collected and packed on 7th October 2020 so that 4 packs (which each contained 5 tomatoes from the same plant) were prepared for each of the 6 treatment conditions: either an ozone treatment or not and subsequent storage for 3 hours, 3 days or 10 days at 18ºC. The 4 packs within each treatment group contained tomatoes from 4 different plants, however the 4 different plants that were used for each treatment group were not always the same.

After the required storage time, the calyx and pedicel from the five tomatoes in each punnet were collected by breaking them from the vine at the natural breakpoint and removing them from the fruit (figure 2.1). They were pooled, weighed, and placed in a 101 x 152 stomacher bag with 5 ml PBS and stomached for 2 x 30 seconds on normal speed in a Stomacher® 80 Biomaster (Seward). The contents were serially diluted in PBS by a factor of 10 and 100 µl of each dilution was spread onto each of the agars listed in table 2.3, in duplicate. Agar plates were incubated at the conditions stated in table 2.3 before colonies were counted. The average count between duplicate plates was used. Samples with a count of 0 were recorded as their limit of detection, which was different for each sample due to different sample weights.

Table 2.3: Agars for the detection of culturable micro-organisms from the tomato calyx and pedicel

Agar	Selection	Incubation temperature (ºC)	Incubation time (hours)
Plate count agar (PCA)	Non-selective	35	24
PCA with cetrimide, fucidin and cephaloridine (CFC) supplementation	Pseudomonads	28	48
Potato dextrose agar (PDA)	Yeasts and moulds	25	48
Rose-Bengal chloramphenicol agar (RBCA)	Yeasts and moulds	25	48
MacConkey agar	Non-fastidious Gram-negative bacteria	35	24

2.2.8 Impact of gaseous ozone on the tomato calyx and pedicel bacterial community

To analyse bacterial communities of the tomato calyx and pedicel, variable region 4 of the 16S rRNA gene was amplified and assessed.

Sample preparation

Tomatoes were collected and packed between 19th June and 5th October 2020. Throughout this time period, a total of 25 tomatoes were collected from each plant, in the form of 5 punnets, which each contained 5 tomatoes collected at one time. Each punnet was subjected to either one of five conditions, so that a punnet from every plant was exposed to every condition: either an ozone treatment or not on the day of harvest, and subsequent storage for 3 or 10 days at 18^{o}C, or an untreated control that was not stored post-harvest (figure 2.3). Tomatoes were collected from 10 different plants, so that 10 punnets were exposed to each of the 5 treatment conditions.

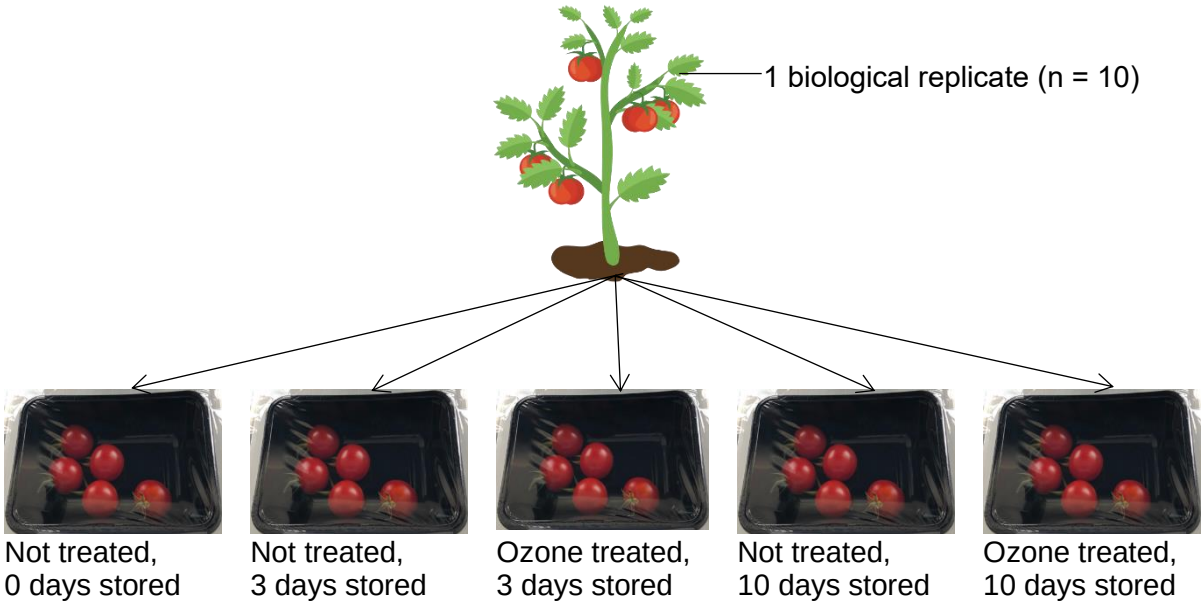


Figure 2.3: Experimental set-up for the effect of gaseous ozone treatment on the bacterial community of the tomato calyx and pedicel. 25 tomatoes were collected from each plant, in the form of 5 punnets, which each contained 5 tomatoes collected at one time. Each punnet was subjected to either one of the five conditions displayed, so that a punnet was exposed to every condition. Ozone treated punnets were subjected to an ozone treatment (3 second ozone generation, ~350 - 700 peak ppm). Post-harvest storage occurred at 18^{o}C. Tomatoes were collected from 10 different plants, so that 10 punnets were exposed to each of the 5 treatment conditions.

After the required storage time, the calyx and pedicel from tomatoes in each punnet were collected by breaking them from the vine at the natural breakpoint and removing them from the fruit (figure 2.1). They were stored at -80^{o}C before further sample processing.

Sample homogenisation

Tomato calyx and pedicel samples which originated from the same punnet were manually ground to a fine powder in liquid nitrogen with a sterile mortar and pestle. Homogenised samples were stored at -80^{o}C before DNA extractions.

DNA extractions

DNA was extracted from ~110 mg of each homogenised sample using the Zymo quick-DNA fecal/soil microbe miniprep kit (Zymo Research, USA) according to the manufacturer's instructions (version 2.4.5, revised 04/2021) with deviations: bead beating conditions were 2 x 2.5 minutes at maximum speed with a TissueLyser (Qiagen, UK)

(protocol step 2), bashing bead lysis tubes were centrifuged at 14,000 x g for 1 minute (protocol step 3), as much supernatant as possible was transferred to the Zymo-Spin™ III-F Filter tube (protocol step 4), Zymo-Spin™ IICR Column was centrifuged at 11,000 x g for 1 minute (protocol steps 8 and 9), 50 µl DNA elution buffer was used for elution's at 10,000 x g for 1 minute (protocol step 10). A DNA extraction negative control was collected by extracting DNA from buffers only.

DNA concentrations were measured on a Qubit 4 Fluorometer (ThermoFisher Scientific, UK) with an Invitrogen Qubit dsDNA HS and BR assay kit (ThermoFisher Scientific, UK), according to the manufacturer's instructions (revision A.0, 02/2015). DNA concentrations were adjusted to 4 ng/µl in sterile water, however since the DNA concentration of the DNA extraction negative control was below the detection limit (<0.2 ng/µl), the DNA concentration was not adjusted for this sample. DNA was stored at -20^{o}C.

PCR amplification and high-throughput sequencing

For 16S rRNA library preparation, the Illumina '16S Metagenomic Sequencing Library Preparation (15044223B)' protocol (revised 11/2013) was generally followed.

Variable region 4 of the 16S rRNA gene was PCR-amplified from 12 ng of each DNA extraction with Invitrogen Platinum SuperFI DNA Polymerase (ThermoFisher Scientific, UK), according to the manufacturer's instructions (revision B, 2017) using primers 515F (Parada) and 806R (Apprill) (table 2.2). Mitochondria rRNA blocker (mPNA) (PNA BIO INC, USA) and chloroplast rRNA blocker (pPNA) (PNA BIO INC, USA) were dissolved by a 55^{o}C incubation at 1400 rpm for 10 minutes, and then added to PCR reactions at a final concentration of 5 µM to prevent amplification of plant DNA. A preliminary test showed that the addition of these blockers visibly reduced 16S rRNA amplification (appendix 2). A PCR negative control was collected by PCR-amplifying sterile water only.

PCR products were cleaned up according to the Illumina protocol, however the beads used were Macherey-Nagel NucleoMag NGS Clean-up and Size Select (FisherScientific, USA). All PCR products were checked on a 1% agarose gel.

Indexes (DNA sequences that are used to identify sample origins) were added according to the Illumina protocol with KAPA HiFi HotStart ReadyMix (Roche Sequencing Store, USA), however the indexes used were from Nextera XT Index Kit v2 Set C (96 indexes, 384 samples) (Illumina, UK). PCR products were cleaned up and checked as previously described.

The DNA concentration of each sample was measured as previously described and adjusted to 4 nM in 10 mM Tris pH 8.5. The DNA concentration of the DNA extraction and PCR negative controls were below the detection limit (<0.2 ng/µl) (ThermoFisher Scientific, UK), therefore the DNA concentrations were not adjusted for these samples. 5 µl of each sample was pooled and subjected to high-throughput sequencing with an Illumina Miseq sequencing platform at the James Hutton Institute, UK.

Sequence processing for bacterial community analysis

All code that was used for sequence processing and bacterial community analysis is available at: https://github.com/AshleighMacdonald/tomato_calyx_and_pedicel_bacterial_community_analysis.

Reads (sequenced 16S rRNA amplicons) were received in a demultiplexed format, which meant that index DNA sequences had been removed and the sample origin of each read was known. Primer DNA sequences were removed from all reads with Cutadapt version 4.3 (Martin, 2011) in Linux.

In R, DADA2 version 1.20.0 (Callahan *et al.*, 2016) was used to filter, denoise and merge reads. Briefly, read quality profiles were inspected, and to account for poorer quality

scores of nucleotides at later positions in reads, reads were trimmed from ~290 bp to 160 bp for forward reads and to 150 bp for reverse reads. After trimming, reads were filtered so that reads which exceeded 3 expected errors (expected errors were calculated from quality scores) were removed. From the remaining reads, an error model was learned, which involved estimating the error rate for each possible nucleotide misplacement. The error model was applied to filtered reads in a process called denoising, which detected if differences in nucleotides between reads were true variation or were likely to be errors. Each read that was different due to true variation was called an amplicon sequence variant (ASV). Paired ASVs were merged using default parameters, which required a 12 bp minimum overlap region, and each nucleotide in the overlap region had to be identical base pairs. Chimeras were detected and removed from the list of ASVs.

DADA2 was then used to assign taxonomy to the ASVs using the naïve Bayesian classifier method which was trained on the Silva nr99 dataset version 138.1 (Quast *et al.*, 2013). Data which presents the ASVs detected in each sample, and sample metadata has been deposited in the Oxford University Research Archive (ORA) (DOI: 10.5287/ora-qmvk1g24g). ASVs that were assigned as “Eukaryota” kingdom, “mitochondria” family or “chloroplast” order were removed from the dataset. In R, phyloseq version 1.44.0 (McMurdie and Holmes, 2013) was used to combine all sample information (abundance of each ASV in each sample, sample metadata) and all ASV information (ASV sequences, ASV taxonomic information, ASV phylogenetic tree produced using phangorn version 2.11.1) into one object for bacterial community analysis.

2.2.9 Presentation and statistical analysis of data

Data was processed using R version 4.3.1 (R Core Team, 2023) and charts were produced using the ggplot2 package version 3.4.2 (Wickham, 2016).

Where ANOVAs were performed, diagnostic plots were used to check that linear models produced met linear model requirements: linearity of data, homogeneity of residuals

variance and normality of residuals (Kassambara, 2017). Where diagnostic plots looked insufficient, Levene's test was used to test for homogeneity of residuals and Shapiro-Wilk's test was used to test for normality of residuals.

For 16S rRNA sequence analysis, non-parametric tests were performed because ASV counts are not normally distributed (Wagner *et al*., 2011) and the assumption of true independence is not met in high-throughput sequencing experiments (Gloor *et al.*, 2017).

Statistical results with p-values < 0.05 were deemed significant, unless otherwise stated.

Bactericidal action of gaseous ozone on pathogens *in vitro*

Linear models were built for each dataset, where results from all plate replicates were included as independent data points. Log_{10}(colony forming units (CFU)/ml) was the response variable and treatment, experimental replicate, and punnets (where relevant) were fixed effects. ANOVAs were performed and where a significant result was generated, a post-hoc Tukeys honest significance difference (HSD) test was performed when necessary.

Effect of gaseous ozone on the tomato calyx and pedicel culturable microbiota

Linear models were built for each agar dataset, so that log_{10}(CFU/g) was the response variable and the interaction between treatment and storage time was a fixed effect. ANOVAs were performed on each model.

Effect of gaseous ozone on the tomato calyx and pedicel 16S rRNA bacterial community

Differences in the ASV library size (number of reads) between sample groups, before and after the removal of plant ASVs (Eukaryota, mitochondria, chloroplast), were tested for by a Kruskal-Wallis test followed by a post-hoc Dunn's test when required.

Charts to display the taxonomic profiles of sample groups were generated with non-normalised data, using the microbiome package version 1.22.0 (Lahti and Sudarshan, 2019).

Phyloseq version 1.44.0 (McMurdie and Holmes, 2013) was used to generate rarefaction curves, and to subsequently rarefy each sample to 7400 reads for alpha diversity analysis. It was then used to calculate the observed and Shannon's diversity metrics, which were used as measures of alpha diversity. Differences in the alpha diversity between sample groups were tested for by a Kruskal-Wallis test followed by a post-hoc Dunn's test.

Data was centred log ratio (CLR)-transformed for beta diversity analysis using the microbiome package version 1.22.0 (Lahti and Sudarshan, 2019). Since beta diversity analyses differences in community structure between samples, sample groups were separated so that only the data to answer each question, regarding the effect of time or treatment, was provided. A model which combined the effect of both time and treatment was not used to test time and treatment effects because the treatment effect may only have become apparent in the 16S rRNA sequence analysis at later time points of measurement (where treatment would have had time to impact the growth dynamics of the microbial community to a point that changes could be identified by 16S rRNA sequence analysis). The 16S rRNA sequence analysis would therefore not always consistently measure the true treatment effect at different time points. This meant that it would not be fair to include treatment effects collected at different times in the same model for the assessment of the treatment effect. Sample groups were as follows (days refer to days post-treatment/post-harvest):

- **For microbiota changes over time on untreated samples:** untreated day 0, untreated day 3, untreated day 10

- **For microbiota changes over time on treated samples:** untreated day 0, treated day 3, treated day 10
- **For the treatment effect on day 3 post-treatment:** untreated day 3, treated day 3
- **For the treatment effect on day 10 post-treatment:** untreated day 10, treated day 10

For beta diversity analysis, the R command ‘prcomp’ was used to complete a principal components analysis (PCA) with Aitchison distance, for each data subset (listed above). Scores were extracted for plotting using vegan version 2.6-4 (Oksanen *et al.*, 2015). Permutational analysis of variances (PERMANOVAs) (999 permutations) (Anderson, 2017) were completed using the vegan package version 2.6-4 (Oksanen *et al.*, 2015), to test if predictors of interest could significantly explain differences in beta diversity/community structure using the Aitchison distance matrix. The effect of time was tested for in datasets which were created to analyse microbiota changes over time, and the effect of treatment was tested for in datasets which were created to analyse treatment effects at a specific time. When significant differences were identified, the pairwiseAdonis package version 0.4.1 (Martinez Arbizu, 2020) was used to complete post-hoc pairwise PERMANOVA tests (999 permutations).

For differential abundance testing, DESeq2 version 1.40.1 (Love *et al*., 2014) was used to complete pairwise comparisons between all samples in each data subset (listed above). For pairwise comparisons that were completed to detect treatment effects, comparisons were completed on treated vs untreated sample groups, so that the changes in ASV abundance were calculated relative to the treated sample group. For pairwise comparisons that were completed to detect time effects, comparisons were completed on a sample group with a later time point vs a sample group with an earlier time point, so that the changes in ASV abundance were calculated relative to the sample group with the later

time point. Data which had not been normalised was fed into DESeq2 version 1.40.1 (Love *et al*., 2014) because it internally transformed data to account for library size and ASV composition bias (Love *et al*., 2014). This involved calculating size factors for each sample to normalise all ASV counts to within the sample (Love *et al*., 2014). Differential abundance testing was completed using a Wald test with Benjamini-Hochberg multiple testing correction (Love *et al*., 2014). Adjusted p-values <0.05 were considered significant when treatment effects were assessed at different time points, because only one pairwise comparison was completed in each analysis (treated vs untreated). When the effect of time, either on untreated or treated samples was assessed, 3 pairwise comparisons were completed within each analysis (day 3 vs day 0, day 10 vs day 0, day 10 vs day 3) so to account for this, adjusted p-values <0.0167 (equivalent to a Bonferroni correction of 0.05/3) were considered significant.

2.3 Results

2.3.1 Gaseous ozone reduced pathogens *in vitro*

To test if gaseous ozone could reduce pathogens at industry-recommended doses, Pst DC3000, Pst T1 or *E. coli* JHI-5025 (table 2.1) (OD_{600nm} = 0.35) were dried on LB agar and exposed to ozone, which was generated for either 1 (~80 - 300 peak ppm) or 3 (~350 - 700 peak ppm) seconds in a sealed punnet, before bacterial colonies were counted. Bacteria were presented on a surface because the aim of the in-pack ozone system was to control pathogens which would reside on produce.

After ozone exposure, *E. coli* and Pst colonies presented different morphologies in comparison to the controls because they were generally clustered together, irregularly shaped and some had a lighter centre (appendix 3).

Ozone which had been generated for 3 seconds significantly reduced *E. coli* by 6.1 $\log_{10}$ orders of magnitude, to beyond or close to the limit of detection [ANOVA, F(1, 14) =

4799.615, p <2e-16] (figure 2.4). Ozone which had been generated for 1 second produced mixed results because some samples had countable colonies, but other samples had too many to count. There was variability in ozone generation within punnets and at times, lower doses may have been generated than normal (appendix 1.1). Ozone was not measured in punnets containing samples because measurements resulted in ozone destruction, and since only one sample was present per punnet, it was a challenge to identify outlier punnets which had contained lower ozone than normal. Since outliers were not obvious, the effect of ozone which had been generated for 1 second on the number of *E. coli* was inconclusive, so results are not presented.

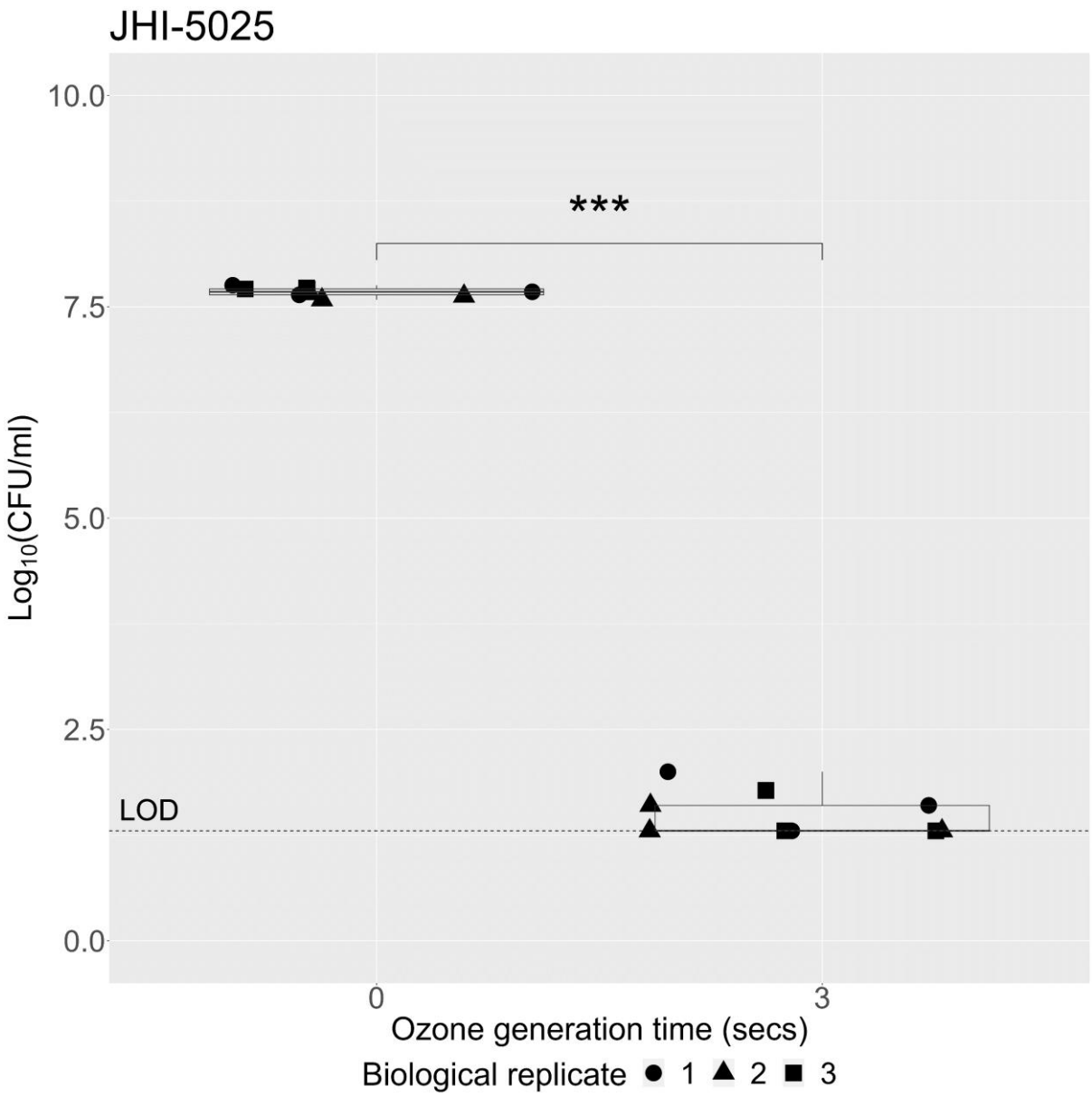


Figure 2.4: Gaseous ozone reduced *E. coli*. *E. coli* JHI-5025 (OD_{600nm} 0.35) was spread onto LB agar, subjected to an ozone treatment (3 second ozone generation, ~350 - 700 peak ppm) and incubated at 28°C for 18 hours before colony forming units (CFU)/ml were calculated. Samples with a count of 0 were recorded as the limit of detection (LOD). Boxplots display the median, interquartile range, minimum and maximum values (n = 9). Asterisks indicate significant differences (*** = $p < 0.001$) from ANOVA.

Since one sample per punnet made it difficult to identify outlier punnets, the set-up was modified so that 3 samples were present per punnet to test the bactericidal action of gaseous ozone against Pst. This was because results from all 3 samples would better indicate if the punnet was an outlier or not.

Ozone treatment (groups = 0, 1, 3 second ozone generation times) significantly affected Pst DC3000 [ANOVA, $F(2, 14) = 757.318$, $p = 5.4e\text{-}15$] and Pst T1 [ANOVA, $F(2, 14) = 318.585$, $p = 2.12e\text{-}12$] (figure 2.5). Both 1 and 3 second ozone generation times significantly reduced Pst DC3000 and Pst T1 compared to the untreated controls ($p < 0.001$), as determined by a post-hoc Tukeys HSD test (figure 2.5). 1 second of ozone generation reduced Pst DC3000 by 4.8 $\log_{10}$ orders of magnitude and Pst T1 by 3.3 $\log_{10}$ orders of magnitude. 3 seconds of ozone generation reduced Pst DC3000 by 6.2 $\log_{10}$ orders of magnitude and Pst T1 by 4.1 $\log_{10}$ orders of magnitude, so that they were both beyond, or close to the limit of detection (figure 2.5).

Within both the Pst DC3000 and Pst T1 datasets, a punnet in which ozone was generated for 1 second was removed as an outlier. This was because bacterial growth within these punnets was much greater than bacterial growth from other punnets in which ozone was generated for 1 second, within the same dataset. These punnets may have contained lower ozone doses than normal due to variability in ozone generation within punnets (appendix 1.1).

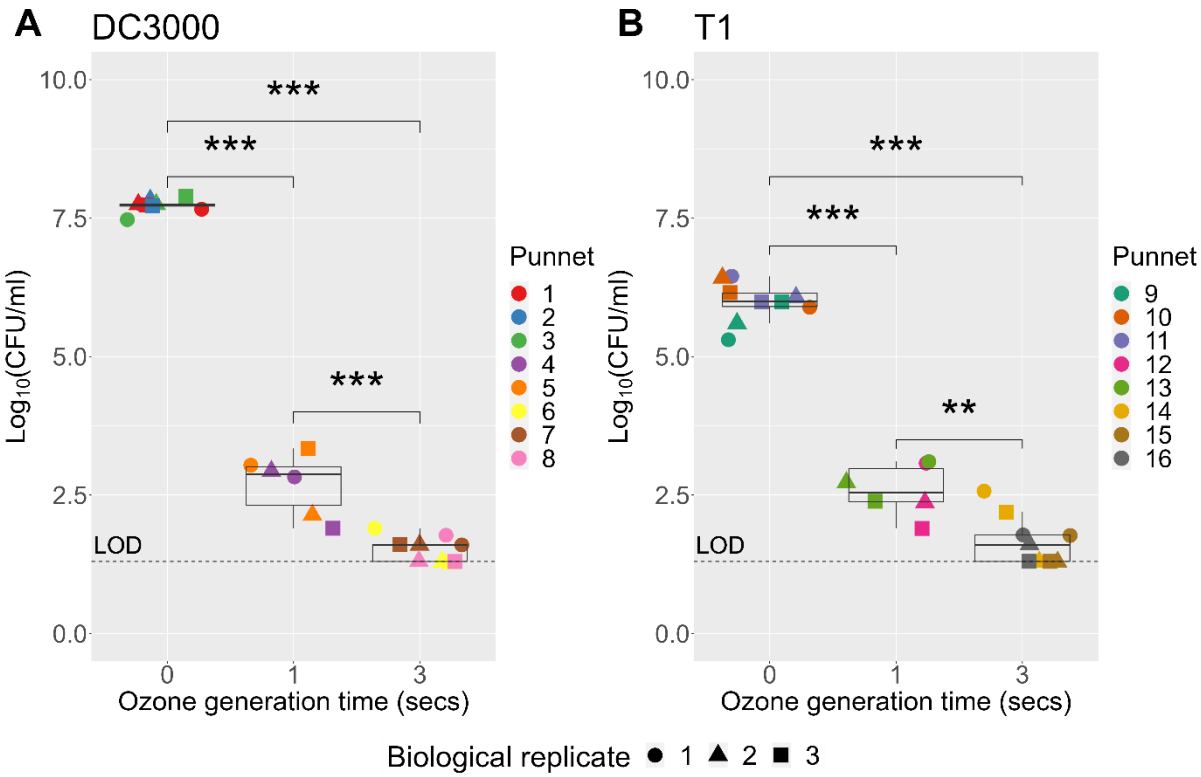


Figure 2.5: Gaseous ozone reduced *P. syringae*. (A) *P. syringae* pv. tomato DC3000 and **(B)** *P. syringae* pv. tomato T1 (OD_{600nm} 0.35) were spread onto LB agar and subjected to an ozone treatment with either a 1 (~80 - 300 peak ppm) or 3 (~350 - 700 peak ppm) second ozone generation time. *P. syringae* was incubated at 28°C for 48 hours before colony forming units (CFU)/ml were calculated. Samples with a count of 0 were recorded as the limit of detection (LOD). Boxplots display the median, interquartile range, minimum and maximum values (n = 6 - 9). Asterisks indicate significant differences (** = $p < 0.01$, *** = $p < 0.001$) from ANOVA and Tukeys HSD tests.

Since cell density (OD_{600nm}) could affect the sensitivity of micro-organisms to ozone (Khadre *et al.*, 2001), Pst DC3000, Pst T1 and *E. coli* JHI-5025 were each adjusted to the same density before ozone exposure so that comparisons could be made between their sensitivities to ozone. However, this did not represent the same number of cells because Pst DC3000 and *E. coli* JHI-5025 had approximately 7.5 log_{10}(CFU/ml) in the untreated control (see figures 2.4 and 2.5), whereas Pst T1 had approximately 6 log_{10}(CFU/ml) in the untreated control (see figure 2.5). Nevertheless, all bacteria were highly sensitive to a 3 second ozone treatment since they were all reduced to beyond or close to the limit of detection.

To summarise, all model pathogens tested (Pst DC3000, Pst T1 and *E. coli* JHI-5025) were very sensitive to ozone treatment with a 3 second ozone generation time. Pst DC3000 and Pst T1 were also significantly reduced after ozone treatment with a 1 second ozone generation time. Since gaseous ozone reduced pathogens *in vitro*, the impact of ozone on whole microbial communities on plant tissue was next characterised.

2.3.2 Yeasts and moulds on the tomato calyx and pedicel increased over time, and they were reduced by gaseous ozone

The effect of ozone treatment on the native microbiota of post-harvest produce was determined, and the tomato calyx and pedicel were used as a model system for this. This was because tomato was the model fruit for this project (chapter 1, section 1.1) and more micro-organisms reside on the calyx and pedicel than on the fruit surface (Smid *et al.*, 1996; Barak *et al.*, 2011).

Changes in the culturable microbiota of the untreated tomato calyx and pedicel (figure 2.1) during post-harvest storage, and the effect of ozone treatment on this was investigated. This was completed by analysing microbial communities from calyxes and pedicels of tomatoes which had been harvested when red-ripe and stored for 3 hours (0 days), 3 days and 10 days after an ozone treatment (3 second ozone generation, ~350 - 700 peak ppm), or no treatment, on their day of harvest. Assessments were completed up to 10 days post-treatment/post-harvest since ripe tomatoes can be typically stored for up to 10 days before consumption (Parnell *et al*., 2004; Do Nascimento Nunes, 2008). Microbial communities were analysed by completing colony counts on a range of different agars which selected for different groups of micro-organisms (table 2.3). This included PCA, which was a non-selective agar, and RBCA and PDA, which each selected for yeasts and moulds. MacConkey agar, which selected for non-fastidious Gram-negative bacteria, and PCA-CFC, which selected for Pseudomonads, were also included for microbial community analysis because they selected for groups of micro-organisms which

would have included model pathogens for the project, namely *E. coli*, *S. enterica* and Pst. Linear models were generated for each agar dataset, and significance testing was completed to identify if time alone, treatment alone, and both time and treatment had significant effects on the number of colonies recovered.

Yeasts and moulds significantly increased over time, as determined by colony counting on RBCA [ANOVA, $F(2, 16) = 24.735$, $p = 1.27e\text{-}05$] and PDA [ANOVA, $F(2, 18) = 31.569$, $p = 2.79e\text{-}06$] (figure 2.6: A, B), whereas the number of micro-organisms detected on PCA, non-fastidious Gram-negative bacteria detected on MacConkey agar, and Pseudomonads detected on PCA-CFC, did not significantly change over time (figure 2.6: C, D, E). It is to be mentioned that for significance testing, the linear model that was generated for the PDA dataset violated the normality of residuals assumption, which was confirmed by a Shapiro-Wilk's test ($p = 0.008599$). Nevertheless, since the main issue with this violation would be an inflated type 1 error (which would cause rejection of a null hypothesis of no differences when it should not have been rejected), the standard ANOVA was completed, but with a more conservative alpha significance threshold for result interpretation ($p < 0.01$).

Ozone treatment significantly reduced yeasts and moulds that were detected on both RBCA [ANOVA, $F(1, 16) = 32.725$, $p = 3.16e\text{-}05$] and PDA [ANOVA, $F(1, 16) = 23.269$, $p = 0.000187$] (figure 2.6: A, B), whereas ozone treatment did not significantly affect the number of micro-organisms detected on PCA, non-fastidious Gram-negative bacteria detected on MacConkey agar, or Pseudomonads detected on PCA-CFC (figure 2.6: C, D, E). One treated punnet which was stored for 3 hours (0 days) and one treated punnet which was stored for 3 days were removed from the results as outliers. This was because yeast and mould growth, which was detected on RBCA and PDA, was much greater on samples in these punnets, in comparison to other samples which had been treated and stored for the same length of time. These punnets may have contained lower ozone doses than normal due to variability in ozone generation within punnets (appendix 1.1).

Yeasts and moulds that were detected on RBCA and PDA remained reduced in comparison to non-treated samples over the 10 day period that was tested (figure 2.6: A, B).

Limits of detection for the detection of micro-organisms on each agar varied according to the weights of tomato calyxes and pedicels, therefore data points which were at the limit of detection have been coloured red in figure 2.6. Yeasts and moulds were always detected at levels well above the limit of detection in untreated samples, however this was not the case for the agars which specifically selected for bacterial species, namely MacConkey agar and PCA supplemented with CFC (figure 2.6). 5/12 of the untreated samples (regardless of post-harvest storage time) did not have any detectable colonies on MacConkey agar and PCA supplemented with CFC, and were subsequently recorded as the limit of detection. It was therefore difficult to determine the impact of ozone treatment on culturable bacteria in this experiment.

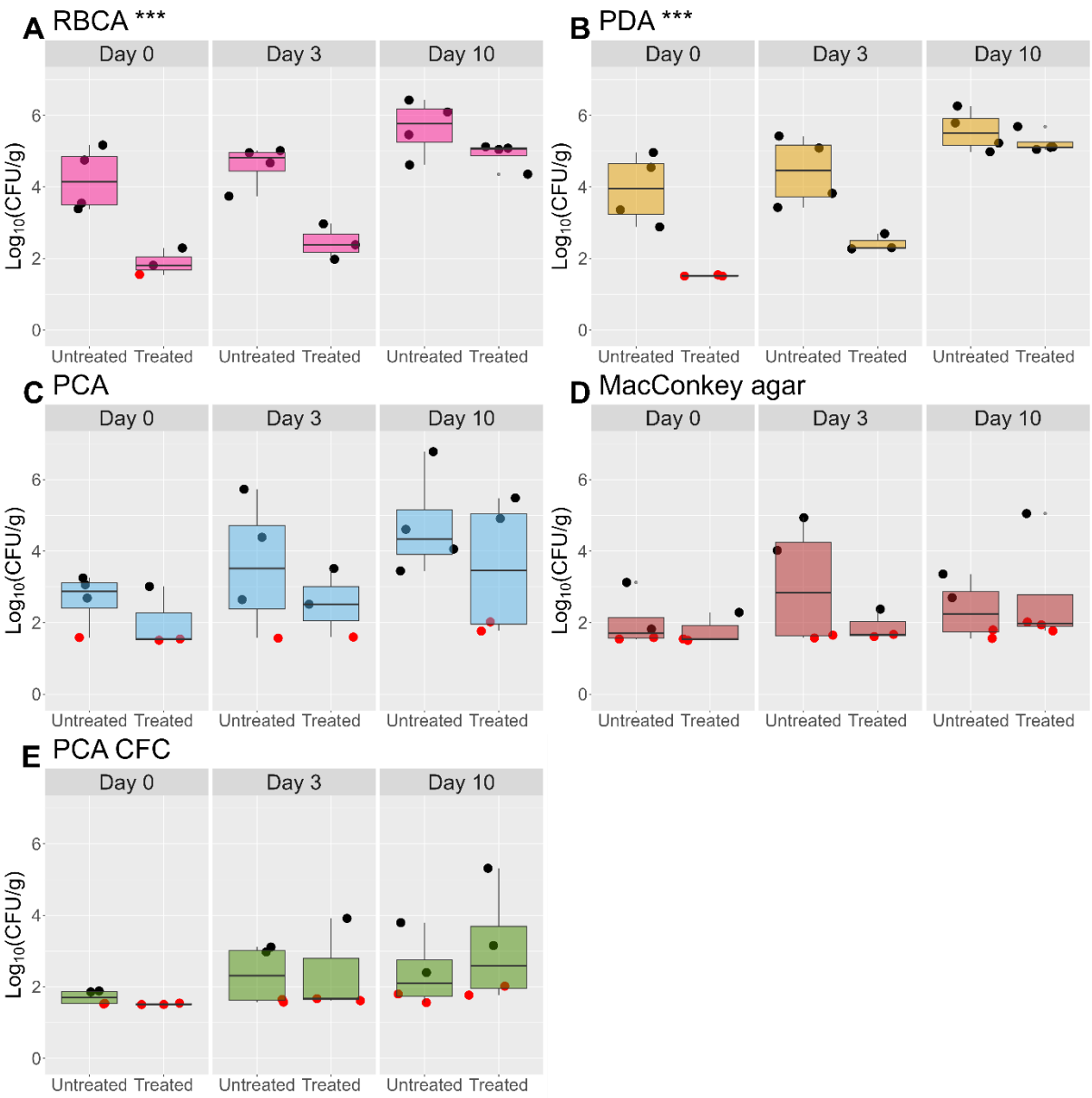


Figure 2.6: Yeasts and moulds on the tomato calyx and pedicel significantly increased post-harvest, and they were significantly reduced by gaseous ozone. Sealed punnets which contained 5 tomatoes were subjected to either one of six conditions; either an ozone treatment (3 second ozone generation, ~350 - 700 peak ppm) or not and stored at 18^{o}C for 3 hours (0 days), 3 days or 10 days. The calyxes and pedicels in each punnet were then pooled and colony forming units (CFU)/g were calculated for micro-organisms detected on different agars: Rose-Bengal chloramphenicol agar (RBCA) and potato dextrose agar (PDA) for yeast and mould recovery, plate count agar (PCA) for non-selective recovery, MacConkey agar for recovery of non-fastidious Gram-negative bacteria, and PCA with cetrimide, fucidin and cephaloridine supplementation (PCA CFC) for Pseudomonad recovery. Counts of 0 were recorded as the limit of detection and these data points have been coloured in red. Boxplots display the median, interquartile range, minimum and maximum values (n = 3 - 4). Asterisks next to dataset titles indicate datasets where time and ozone treatment respectively caused a significant difference in Log_{10}(CFU/g) (*** = $p < 0.001$) from ANOVA.

In summary, culturable yeasts and moulds significantly increased during post-harvest storage on the tomato calyx and pedicel, and they were significantly reduced by ozone treatment. The effect of post-harvest storage time and ozone treatment on bacteria which

resided on the tomato calyx and pedicel were however ambiguous and could not be determined by culturable plating alone. Since it was previously identified that ozone could affect bacteria (section 2.3.1), and since the effect of ozone treatment against bacteria on the tomato calyx and pedicel still required to be resolved, a culture-independent technique, namely sequence analysis of the 16S rRNA gene, was next used to assess the impact of post-harvest storage time and ozone treatment on the tomato calyx and pedicel bacterial community. This was because it was a more sensitive method which did not rely on specific bacterial recovery conditions for bacterial detection. It would also identify specific bacterial taxonomic groups that were impacted by ozone treatment (Johnson *et al*., 2019).

2.3.3 Gaseous ozone reduced the bacterial DNA library size from the tomato calyx and pedicel

The bacterial community of the tomato calyx and pedicel was characterised, and changes in the bacterial community during post-harvest storage, after ozone treatment had been applied or not, were investigated. Bacterial communities were analysed by sequence analysis of the 16S rRNA gene, therefore bacteria would be included in the analysis, regardless of their viability status (Emerson *et al.*, 2017). However, after ozone treatment, the altered viability status of microbiota members would impact their growth, which would impact the dynamics of the microbiota over time. Therefore, the dynamics of the bacterial community between different time points were compared to identify changes. Hence, bacterial communities from calyxes and pedicels of tomatoes which had been subjected to one of five conditions were assessed; either an ozone treatment (3 second ozone generation, ~350 - 700 peak ppm) or not on their day of harvest, and subsequent storage at 18^{o}C for 3 or 10 days (there was also an untreated day 0 control) (figure 2.3). Only an untreated sample was analysed on day 0 because the differences in microbial viability, which would have been imposed in the ozone-treated sample, were not expected to be immediately detected.

Bacterial 16S rRNA amplicons were sequenced and the percentage of original reads which passed the filtering, denoising, merging and chimera removal processes were on average 86% per sample (range = 79% - 89%). Each read that was different due to true variation was called an ASV.

After plant ASVs (assigned as Eukaryota, chloroplast or mitochondria) were removed, only 12.5% of reads remained on average per sample, however this ranged from 4.4% - 86.5%. The total number of reads, including both plant and bacterial ASVs, in each sample is displayed in figure 2.7. Sample B9-UT10 had a much higher percentage of bacterial ASVs in comparison to other samples (figure 2.7).

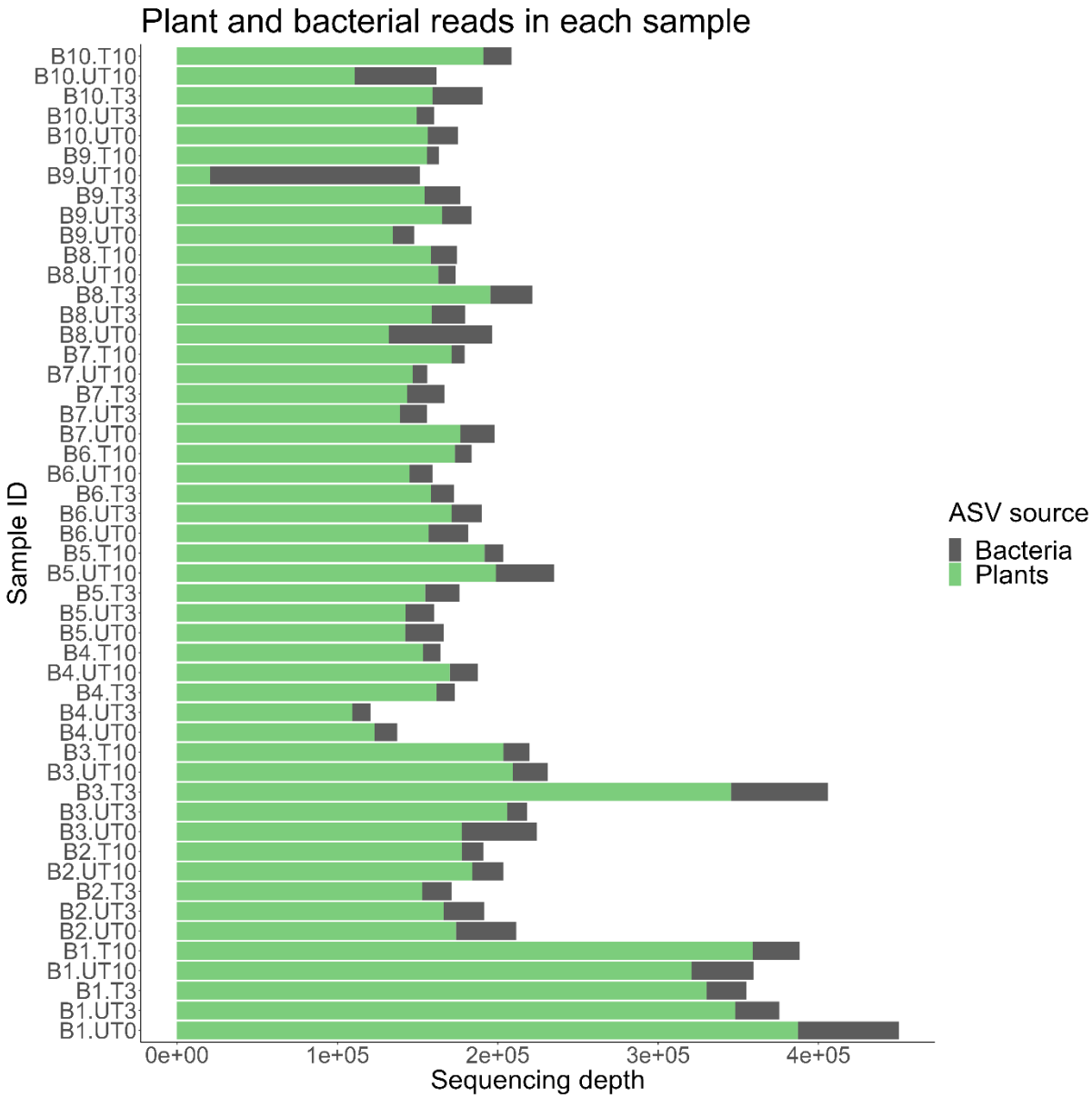


Figure 2.7: 16S rRNA reads from tomato calyxes and pedicels were mainly plant DNA. Tomatoes were subjected to either one of five conditions; either an ozone treatment (3 second ozone generation, ~350 - 700 peak ppm) or not and stored at 18ºC for 3 or 10 days (there was also an untreated day 0 control). DNA was extracted from tomato calyxes and pedicels, and 16S rRNA gene amplicons were sequenced. Chart shows sample ID where B number is biological replicate, T or UT is treated or untreated and 0, 3 or 10 refers to post-harvest/post-treatment storage days. Sequencing depth shows the number of reads detected in samples. Amplicon sequence variants (ASVs) were classified as plants if they were assigned as Eukaryota, chloroplast or mitochondria.

After plant ASVs were removed from all samples, a large proportion of reads that remained were ASV 2, and this ASV was also detected in the negative controls (figure 2.8). During the 16S rRNA experiment, one negative control was collected during genomic extractions, and another was collected during PCR. The negative controls did

not produce visible bands on an agarose gel however they contained reads. In total, 18 ASVs were detected in the negative controls, and 5 of these were also detected in samples. These were each assigned to the genus level: ASV 2 (*Pseudomonas*), ASV 9 (*Escherichia - Shigella*), ASV 29 (*Ralstonia*), ASV 80 (*Curvibacter*) and ASV 277 (*Pseudomonas*). ASV 2 made up 93% of the total reads of each of the negative controls, although the DNA extraction negative control had much more reads (1,051,118 reads) than the PCR negative control (59 reads). The number of reads from the DNA extraction negative control was also much larger than the original number of reads from samples (shown as sequencing depth in figure 2.7). This was because DNA concentrations of samples were diluted for high-throughput sequencing, but DNA concentrations of the negative controls could not be diluted because they had undetectable DNA concentrations.

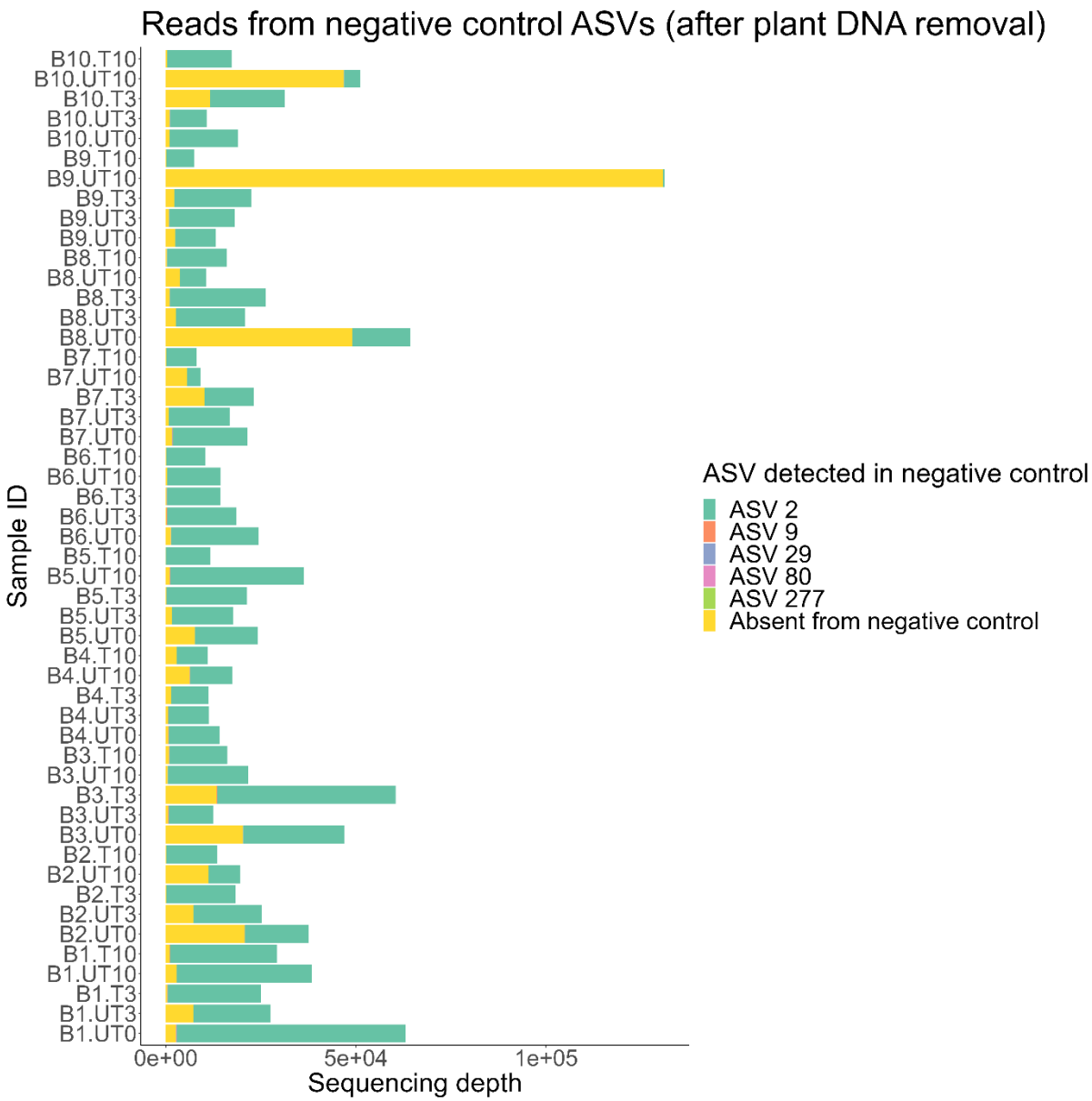


Figure 2.8: ASV 2, which was detected in the negative controls, had a strong presence in samples (after the removal of plant DNA). Tomatoes were subjected to either one of five conditions; either an ozone treatment (3 second ozone generation, ~350 - 700 peak ppm) or not and stored at 18ºC for 3 or 10 days (there was also an untreated day 0 control). DNA was extracted from tomato calyxes and pedicels, and 16S rRNA gene amplicons were sequenced. Charts show sample ID where B number is biological replicate, T or UT is treated or untreated and 0, 3 or 10 refers to post-harvest/post-treatment storage days. Sequencing depth shows the number of reads detected in samples. 5 ASVs which were detected in the negative controls were also detected in samples: ASV 2 (*Pseudomonas*), ASV 9 (*Escherichia shigella*), ASV 29 (*Ralstonia*), ASV 80 (*Curvibacter*) and ASV 277 (*Pseudomonas*).

All ASVs that were detected in the negative controls were kept in samples for bacterial community analysis. This was because the removal of ASVs detected in negative controls could potentially result in the elimination of ASVs from samples that were genuinely present (Karstens *et al.*, 2019), and the ASVs that were present in the negative control

included those which were expected to be detected in samples. ASV 2, which was predominant in both the negative controls and samples (figure 2.8), belonged to the *Pseudomonas* genus and Proteobacteria phylum, and since a very high abundance of *Pseudomonas* or Proteobacteria has previously been reported in tomato bacterial communities (Ottesen *et al.*, 2013; Dong *et al.*, 2019; López *et al.*, 2020; Soto-Giron *et al.*, 2021), it was likely that it was truly present in samples.

There were no significant differences between the library size (number of reads) of each sample group before plant DNA was removed (figure 2.9: A). The library sizes of each sample group after the removal of plant DNA were however significantly different (Kruskal-Wallis, $p = 0.01509$) (figure 2.9: B). Bacterial reads recovered from tomato calyxes and pedicels which had been ozone-treated and stored for 10 days were significantly lower than bacterial reads recovered from tomato calyxes and pedicels which had not been treated or stored (Dunn test, $p = 0.01752727$) (figure 2.9: B).

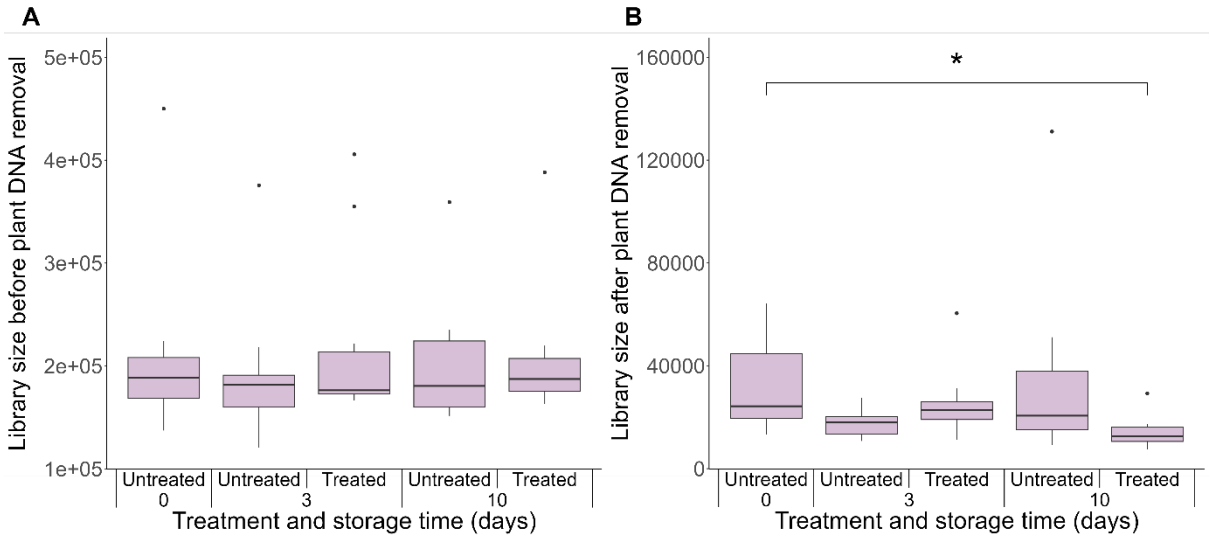


Figure 2.9: After plant DNA removal, the library size of ozone-treated samples which had been stored for 10 days was significantly lower than that of samples which had not been treated or stored. Tomatoes were subjected to either one of five conditions; either an ozone treatment (3 second ozone generation, ~350 - 700 peak ppm) or not and stored at 18^{o}C for 3 or 10 days (there was also an untreated day 0 control). DNA was extracted from tomato calyxes and pedicels, and 16S rRNA gene amplicons were sequenced. The 16S rRNA DNA library size within each sample group (**A**) before the removal of plant DNA and (**B**) after the removal of plant DNA are displayed. Boxplots display the median, interquartile range, minimum and maximum values of bacterial DNA library sizes per sample group (n = 10). Asterisks indicate significant differences (* = $p < 0.05$) from Kruskal-Wallis and Dunn tests.

To conclude, the number of bacterial 16S rRNA reads was significantly lower in ozone-treated samples which had been stored for 10 days, in comparison to samples which had not been treated or stored. Next, the bacterial taxonomic profiles between sample groups were compared.

2.3.4 The tomato calyx and pedicel bacterial community changed over time, and with ozone treatment

Changes in the bacterial community of the tomato calyx and pedicel that occurred during post-harvest storage, after the application of ozone treatment or not, were visualised by taxonomic profiling. The relative abundances of all phyla detected, which were 23 in total, were visualised in figure 2.10. The relative abundances of only the top 20 families and genera that were detected across all samples were visualised in figures 2.11 and 2.12

respectively, because a total of 211 families/445 genera were detected and so could not all be presented.

Proteobacteria/*Pseudomonadaceae/Pseudomonas* dominated all sample groups, regardless of post-harvest storage time and if ozone treatment had been applied (figures 2.10, 2.11 and 2.12). Proteobacteria/*Pseudomonadaceae*/*Pseudomonas* had a hierarchical relationship. 87.3% of the total Proteobacteria detected in the dataset (which included all samples) were *Pseudomonadaceae* and all *Pseudomonadaceae* that were detected were *Pseudomonas*. In the dataset, 41 different ASVs were *Pseudomonas*, however 'ASV 2' contributed to 88.3% of the *Pseudomonas* detected, and it was previously reported that this ASV was also detected in the negative controls.

The dominance of Proteobacteria/*Pseudomonadaceae/Pseudomonas* made it difficult to visualise the differences in the relative abundances of other, rarer taxa between sample groups (figures 2.10, 2.11 and 2.12), therefore the findings were also presented to show differences in specific taxonomic groups (appendix 4). There were generally high rates of standard error, which was likely because the relative abundances of all phyla/families/genera, apart from Proteobacteria/*Pseudomonadaceae*/*Pseudomonas*, were very low so were prone to greater variation (appendix 4).

The bacterial community of the tomato calyx and pedicel was characterised using the taxonomic profiles of the untreated samples, pre-storage. The relative abundances of all phyla/families/genera which had a mean relative abundance >1%, in regard to all of the phyla/families/genera detected in the untreated day 0 dataset, were reported (the mean and standard error are shown). The relative abundances of all phyla which had a mean >1% were: Proteobacteria (83.4% +/- 5.8%), Actinobacteriota (7.1% +/- 3.3%), Firmicutes (3.2% +/- 1.7%), Bacteroidota (1.9% +/- 1.1%) and Planctomycetota (1.7% +/- 1.2%). The relative abundances of all families which had a mean >1% were: *Pseudomonadaceae* (75.3% +/- 8.0%), *Nocardiopsaceae* (3.1% +/- 2.7%), *Planococcaceae* (1.7% +/- 1.5%)

and *Rhizobiaceae* (1.3% +/- 0.7%). The relative abundances of all genera which had a mean >1% were: *Pseudomonas* (75.3% +/- 8.0%), unknown (3.3% +/- 1.6%), *Nocardiopsis* (3.1% +/- 2.7%) and *Planomicrobium* (1.2% +/- 1.2%).

Although Proteobacteria/*Pseudomonadaceae*/*Pseudomonas* were always dominant, there were changes in the bacterial community of the tomato calyx and pedicel over time, and ozone treatment affected these changes. Changes in the phyla/family/genera profiles were seen between the untreated samples which were stored for 0, 3 and 10 days respectively. Notably, the relative abundance of Proteobacteria/*Pseudomonadaceae*/*Pseudomonas* increased from day 0 to day 3 but decreased from day 3 to day 10 (figures 2.10, 2.11 and 2.12 and/or appendix 4). (When the ASVs that were detected in the negative control were removed from the dataset, Proteobacteria/*Pseudomonadaceae*/*Pseudomonas* still increased from day 0 to day 3, but then further increased from day 3 to day 10 (data not shown)). When ozone-treatment was applied at day 0, the profiles underwent different changes over time, for example, the relative abundance of Proteobacteria/*Pseudomonadaceae*/*Pseudomonas* increased from day 0 to day 3 and then further increased from day 3 to day 10 (figures 2.10, 2.11 and 2.12 and/or appendix 4). (When the ASVs that were detected in the negative control were removed from the dataset, Proteobacteria still increased from day 0 to day 3, but then slightly decreased from day 3 to day 10, and *Pseudomonadaceae*/*Pseudomonas* increased from day 0 to day 3, and then increased further from day 3 to day 10 (data not shown)).

Since *P. syringae*, *E. coli* and *S. enterica* were model pathogens for the project, it was beneficial to see how the taxonomic groups which these micro-organisms belonged to survived in the bacterial community after ozone treatment. *P. syringae* belonged to the *Pseudomonas* genus and the behaviour of this in the bacterial community was just described. *E. coli* belonged to the *Escherichia* genus and *S. enterica* belonged to the *Salmonella* genus, neither of which were present in the dataset. *E. coli* and *S. enterica*

both belonged to the *Enterobacteriaceae* family, which was present, but at a very low abundance with high standard error (appendix 4.2). This therefore made it difficult to determine its changes in the bacterial community.

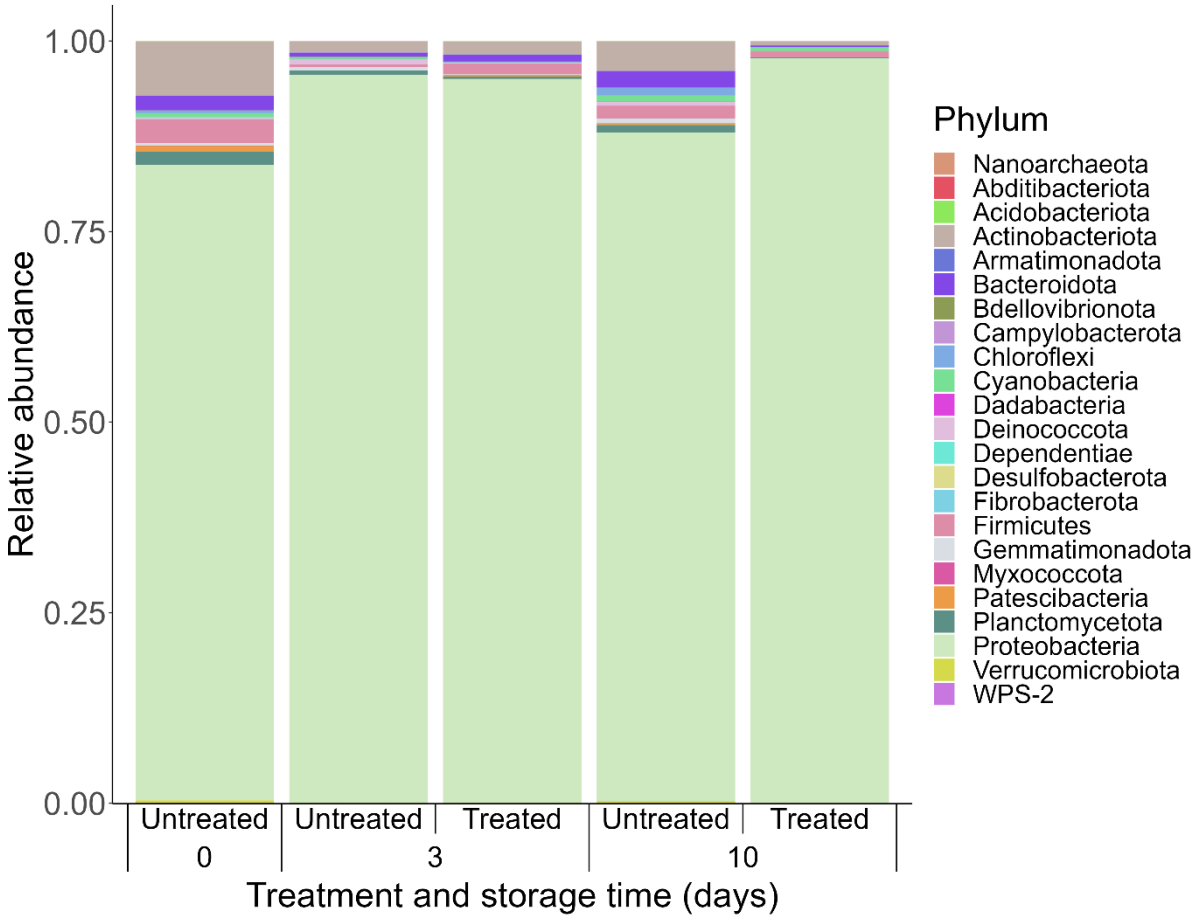


Figure 2.10: The relative abundance of bacterial phyla in the tomato calyx and pedicel changed over time and with ozone treatment. Tomatoes were subjected to either one of five conditions; either an ozone treatment (3 second ozone generation, ~350 - 700 peak ppm) or not and stored at 18^{o}C for 3 or 10 days (there was also an untreated day 0 control). DNA was extracted from tomato calyxes and pedicels, and 16S rRNA gene amplicons were sequenced. The mean relative abundance of all phyla detected in each sample group is displayed (n = 10).

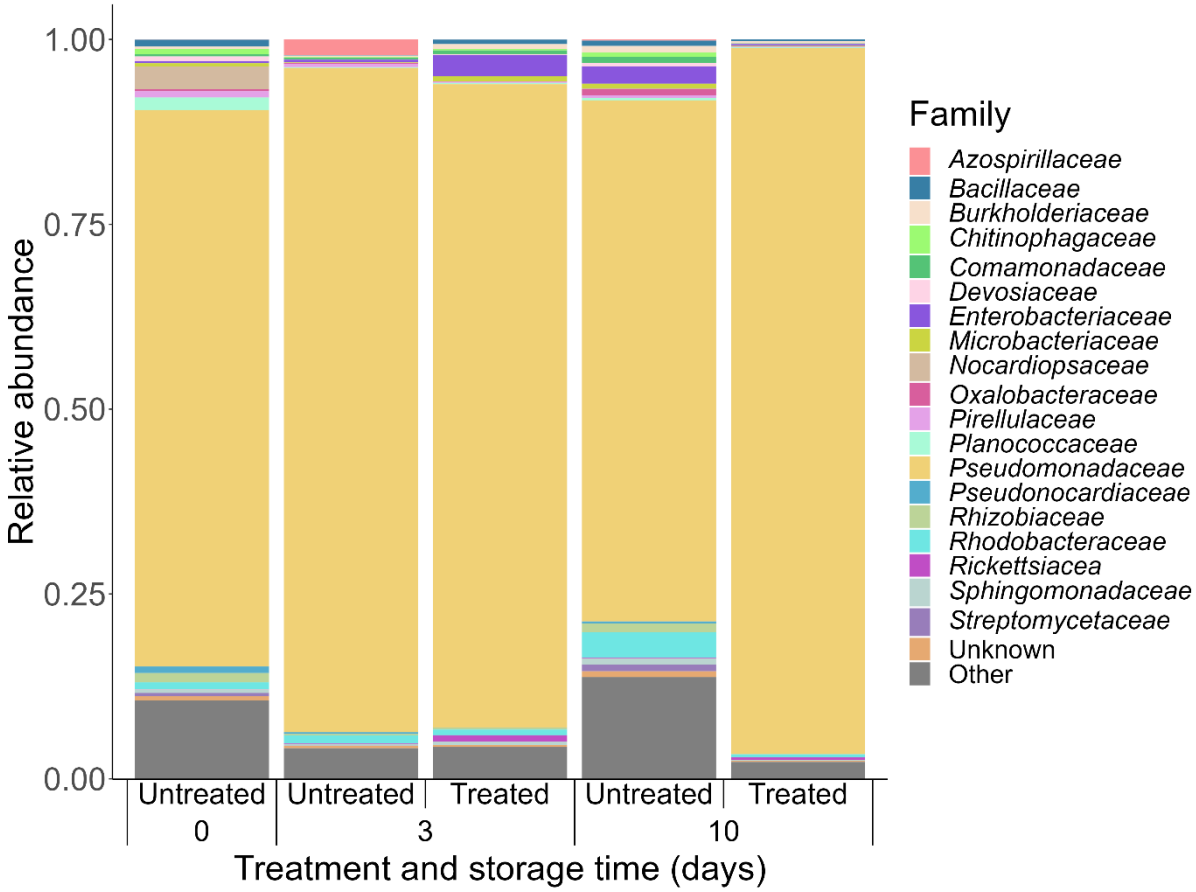


Figure 2.11: The relative abundance of bacterial families in the tomato calyx and pedicel changed over time and with ozone treatment. Tomatoes were subjected to either one of five conditions; either an ozone treatment (3 second ozone generation, ~350 - 700 peak ppm) or not and stored at 18^{o}C for 3 or 10 days (there was also an untreated day 0 control). DNA was extracted from tomato calyxes and pedicels, and 16S rRNA gene amplicons were sequenced. The mean relative abundance of the top 20 families (which were detected across all samples) in each sample group is displayed (n = 10).

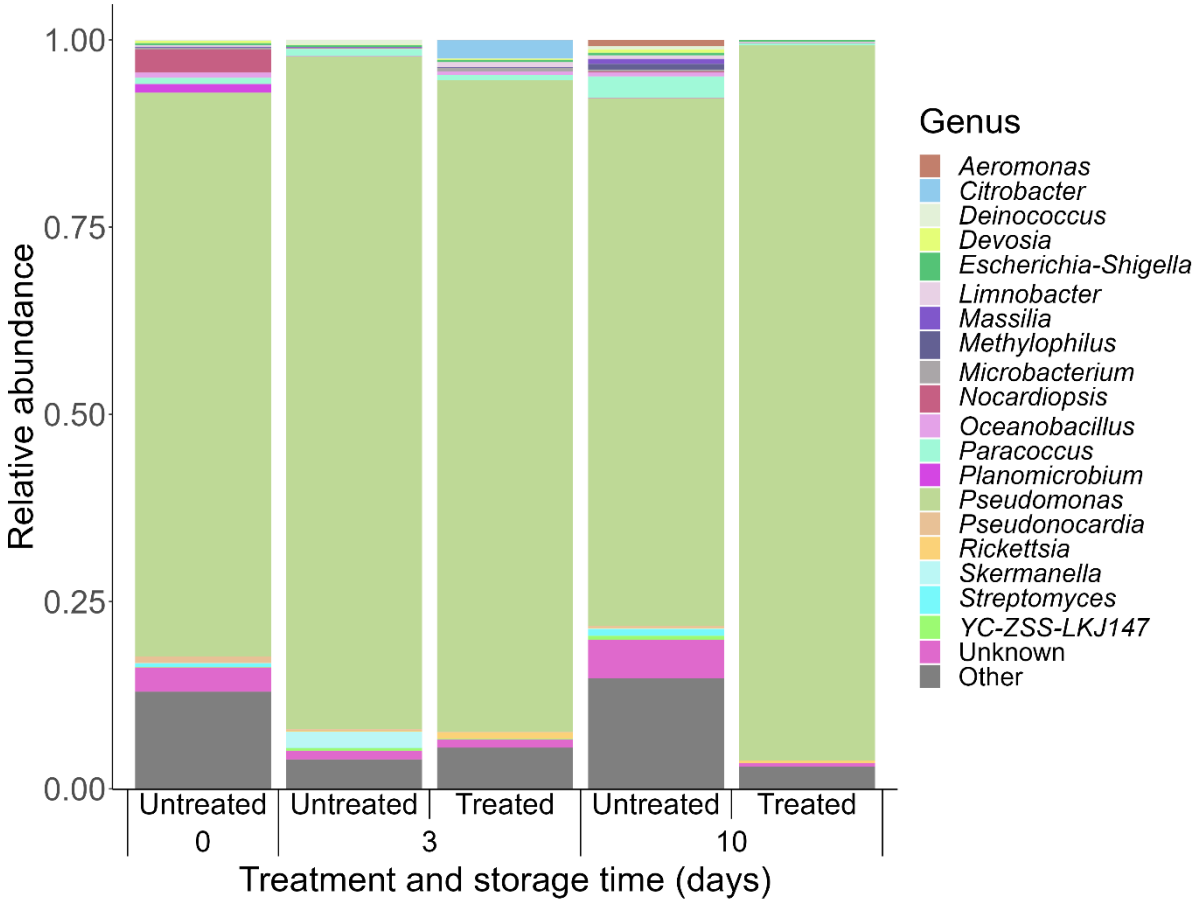


Figure 2.12: The relative abundance of bacterial genera in the tomato calyx and pedicel changed over time and with ozone treatment. Tomatoes were subjected to either one of five conditions; either an ozone treatment (3 second ozone generation, ~350 - 700 peak ppm) or not and stored at 18ºC for 3 or 10 days (there was also an untreated day 0 control). DNA was extracted from tomato calyxes and pedicels, and 16S rRNA gene amplicons were sequenced. The mean relative abundance of the top 20 genera (which were detected across all samples) in each sample group is displayed (n = 10).

Taxonomic profiles showed that although Proteobacteria/*Pseudomonadaceae*/*Pseudomonas* always dominated the bacterial community of the tomato calyx and pedicel, there were changes in the bacterial community over time, and ozone treatment affected these changes. Next, the diversity of the community within each sample group was measured and compared.

2.3.5 Gaseous ozone reduced the bacterial community diversity of the tomato calyx and pedicel

The impact of post-harvest storage and ozone treatment on the alpha diversity ('within sample' diversity) of the tomato calyx and pedicel bacterial community was assessed. The observed number of ASVs within samples was used as an alpha diversity metric because it measures community richness. Shannon's index was also used as an alpha diversity metric because it measures community richness and evenness (Shannon, 1948), and it has previously been used to assess tomato-associated microbiota (Dong *et al.*, 2019; Cheng *et al.*, 2020).

7400 reads were randomly selected from each sample for alpha diversity analysis. This was necessary for a fair assessment of alpha diversity because richness will vary dependent upon sampling depth, since there is a greater opportunity to find more species in samples which have been sequenced deep (Willis, 2019). 7400 was the selected quantity because the lowest sequencing depth of a sample was 7408, and rarefaction curves identified that most of the alpha diversity within samples had been captured by 7400 reads, since the curves of most samples had plateaued by 7400 reads (figure 2.13).

The rarefaction curves presented for each sample in figure 2.13 do not show the complete rarefaction curves because the x-axis limit was constrained to 25,000 reads. This was because the sequencing depth of each sample was highly variable, so when the full sequencing depth of all samples were shown on the x-axis, it was difficult to see the curves of samples which had a much smaller sequencing depth (appendix 5 shows rarefaction curves with an unconstrained x-axis). Constraining the x-axis to 25,000 reads in order to present the rarefaction curves was not problematic for samples which had a sequencing depth >25,000 reads, because the alpha diversity metrics for most of these samples had plateaued by 25,000 reads (appendix 5).

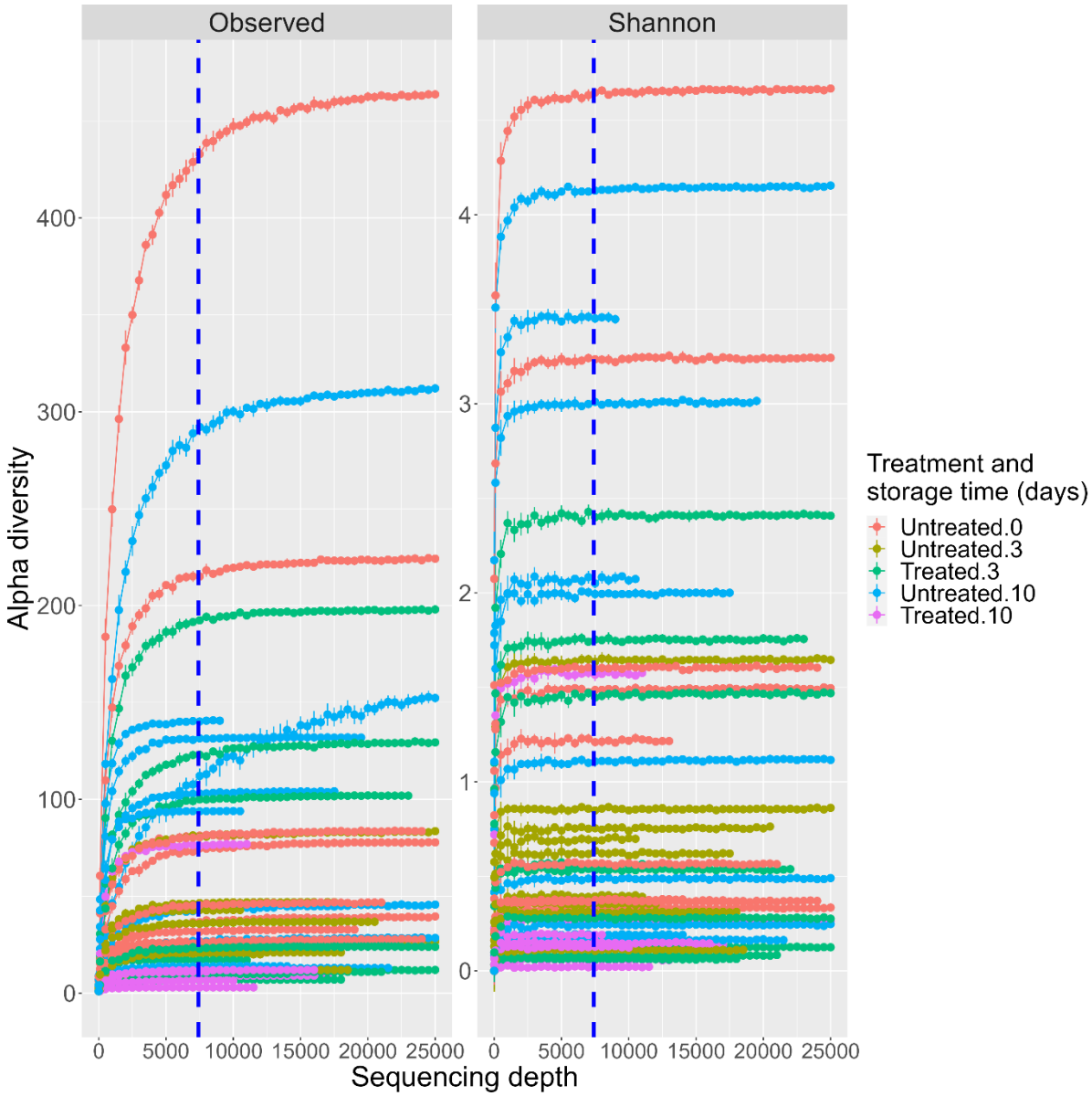


Figure 2.13: Most bacterial diversity was captured within 7400 reads. Tomatoes were subjected to either one of five conditions; either an ozone treatment (3 second ozone generation, ~350 - 700 peak ppm) or not and stored at 18ºC for 3 or 10 days (there was also an untreated day 0 control). DNA was extracted from tomato calyxes and pedicels, and 16S rRNA gene amplicons were sequenced. The charts show the observed and Shannon's diversity for all samples, when an increasing number of sequences from each sample were randomly selected and measured. The mean observed or Shannon's diversity metric from 10 groups of randomly selected reads were calculated at the following sequencing depths for each sample: 1, 10, 100, and then at 500 intervals from 500 reads. A blue dashed line was added at a sequencing depth of 7400 because all samples were rarefied at 7400 reads. The x axis limit was constrained to 25,000 reads so completed rarefaction curves are not shown for all samples.

Bacterial community diversity was significantly different between sample groups, as measured by the observed number of ASVs (Kruskal-Wallis, p = 0.000548) and the Shannon's index (Kruskal-Wallis, p = 0.007053) (figure 2.14). Post-hoc Dunn tests

identified that the significant differences were between the untreated day 0 sample and the treated day 10 sample (observed $p < 0.01$, Shannon's index $p < 0.05$), and between the untreated day 10 sample and the treated day 10 sample (observed $p < 0.01$, Shannon's index $p < 0.05$) (figure 2.14).

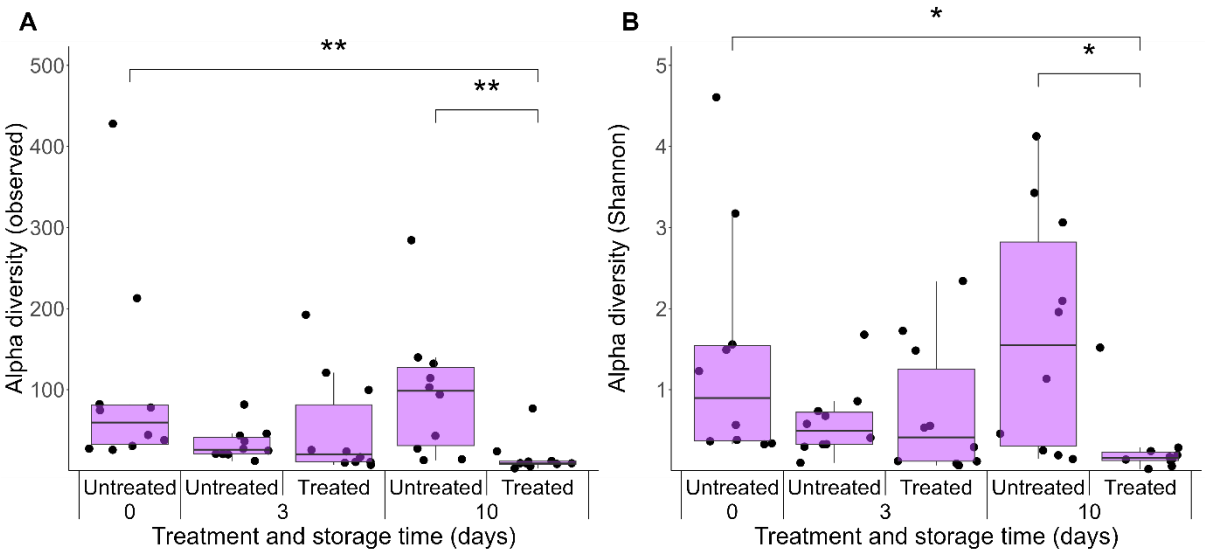


Figure 2.14: Ozone significantly reduced the bacterial community diversity of the tomato calyx and pedicel. Tomatoes were subjected to either one of five conditions; either an ozone treatment (3 second ozone generation, ~350 - 700 peak ppm) or not and stored at 18^{o}C for 3 or 10 days (there was also an untreated day 0 control). DNA was extracted from tomato calyxes and pedicels, and 16S rRNA gene amplicons were sequenced. (**A**) Observed and (**B**) Shannon alpha diversity metrics, calculated from samples rarefied at 7400 reads, are displayed. Boxplots display the median, interquartile range, minimum and maximum values (n = 10). Asterisks indicate significant differences (* = $p < 0.05$, ** = $p < 0.01$) from Kruskal-Wallis and Dunn tests.

To conclude, no significant changes in bacterial community diversity were detected in untreated samples over time, however when ozone treatment was applied at day 0, there was a significant reduction in the bacterial community diversity over time, between day 0 and day 10. The significant reduction in bacterial community diversity that was caused by ozone-treatment, was also evident when the ozone-treated and non-treated samples which had each been stored for 10 days were compared. Next, the bacterial community composition between relevant sample groups was compared.

2.3.6 Gaseous ozone changed the bacterial community composition of the tomato calyx and pedicel

The impact of post-harvest storage and ozone treatment on the bacterial community composition of the tomato calyx and pedicel was assessed by beta diversity ('between sample' diversity) analysis. This involved the measurement of Aitchison distance (Quinn *et al.*, 2018) between sample community compositions, which was visualised by a PCA. Since beta diversity analyses differences in community structure between samples, sample groups were separated into different subsets, so that only the sample groups required to assess a particular effect were provided in a data subset. Sample groups were as follows (days refer to days post-treatment/post-harvest):

- **For microbiota changes over time on untreated samples:** untreated day 0, untreated day 3, untreated day 10
- **For microbiota changes over time on treated samples:** untreated day 0, treated day 3, treated day 10
- **For the treatment effect on day 3 post-treatment:** untreated day 3, treated day 3
- **For the treatment effect on day 10 post-treatment:** untreated day 10, treated day 10

As noted previously, samples were rarefied so that differences in sequencing depth did not introduce bias in the number of different ASVs detected within a sample, which was a key measurement for alpha diversity analysis (Willis, 2019). Rarefaction is however not an ideal normalisation method because data is lost in the filtering process, sub-sampling introduces artificial uncertainty and the number of reads selected for rarefaction is arbitrary (Lin and Peddada, 2020). Since beta diversity assesses differences between samples based on their compositional data, read count normalisation was not required

(Gloor *et al.*, 2017). Instead, data underwent a CLR transformation, which normalised the abundance of ASVs, relative to other ASVs in the dataset (Gloor *et al.*, 2017). CLR transformed values are scale-invariant, so values would be expected to be the same, regardless of the number of reads within a sample (Gloor *et al.*, 2017).

All samples had similar community compositions, regardless of the time that untreated or treated samples were stored for (figure 2.15: A, B) and regardless of whether treatment had been applied before samples were assessed 3 or 10 days later (figure 2.15: C, D). There were however variable divergences of the sample groups within each data subset, which are indicated by the size of ellipses (95% confidence level) (figure 2.15). The divergence of a sample group was an indicator of the variability in community composition within a sample group. Figure 2.15: A shows that the variability between bacterial communities within a selected group of samples reduced from day 0 to day 3 but was largest at day 10 post-harvest, when no treatment had been applied. Figure 2.15: B shows that the variability between bacterial communities within a selected group of samples reduced over time after ozone-treatment had been applied, so that it was lowest at 10 days post-treatment/post-harvest. Figure 2.15: C shows that at day 3 post-treatment/post-harvest, the ozone-treated samples had a larger variability in bacterial community composition than the untreated samples, however this result was mainly caused by the communities of few treated samples and not the majority. Figure 2.15: D shows that this was the opposite at day 10 post-treatment/post-harvest, for which results appeared to be more robust.

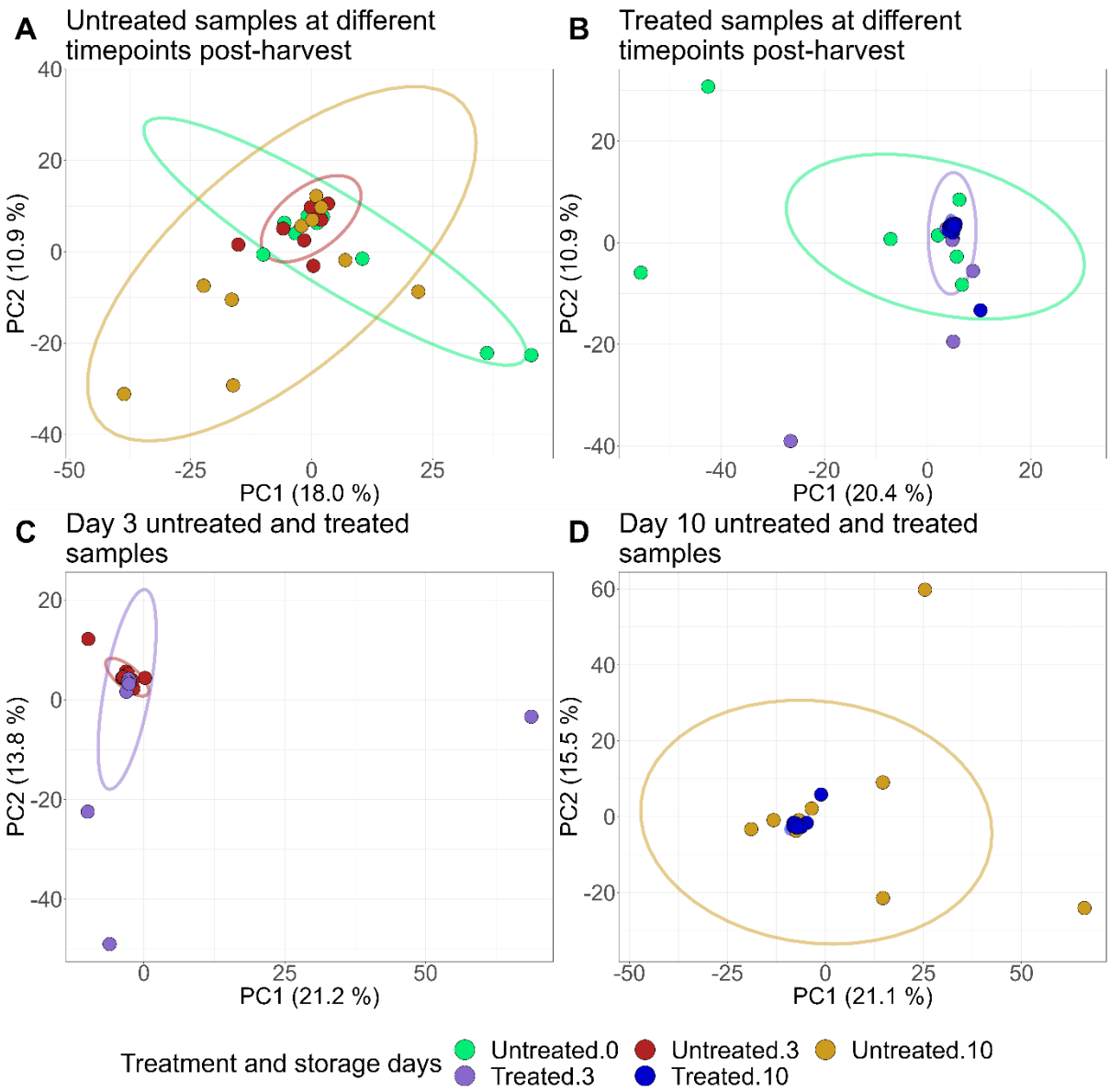


Figure 2.15: All sample groups within each data subset had a similar community composition but sample groups demonstrated different variances of this. Tomatoes were subjected to either one of five conditions; either an ozone treatment (3 second ozone generation, ~350 - 700 peak ppm) or not and stored at 18ºC for 3 or 10 days (there was also an untreated day 0 control). DNA was extracted from tomato calyxes and pedicels, and 16S rRNA gene amplicons were sequenced. Sample scores for the two principal components which explained the most variation within each dataset (identified by a principal component analysis) are displayed on charts. The percentage of variation explained by the principal components are shown on axes. Ellipses were drawn around sample groups at a 95% confidence level.

Storage time did not cause a significant difference in community structure between the untreated samples tested at 0, 3 and 10 days post-harvest. It did however cause significant differences in community structure between the untreated samples at day 0, and treated samples tested at 3 and 10 days post-treatment/post-harvest [PERMANOVA,

F(2, 27) = 1.2024, p = 0.038]. A pairwise PERMANOVA post-hoc test revealed that the significant difference was between the untreated day 0 and treated day 10 samples (p = 0.001). Comparison of untreated and treated samples on days 3 and 10 post-treatment/post-harvest respectively, identified that treatment significantly affected community composition at both day 3 [PERMANOVA, F(1, 18) = 1.158, p = 0.034] and day 10 [PERMANOVA, F(1, 18) = 1.3902, p = 0.024].

To conclude, when ozone treatment was not applied, there were no significant differences in community composition over time. However, when ozone treatment was applied on the day of harvest, there was a significant difference in community composition over time, specifically at 10 days post-treatment/post-harvest. Bacterial community compositions of treated samples were significantly different from untreated samples at both 3 and 10 days post-treatment/post-harvest. Next, differential abundance analysis was completed to identify significant differences in the abundance of each ASV caused by either the effect of time or treatment.

2.3.7 Gaseous ozone caused changes in the abundance of specific ASVs

ASVs which had a significantly different abundance in one sample group, in comparison to another sample group were identified to highlight changes caused by either time or treatment. This was completed by a differential abundance analysis using DESeq2. Since only pairwise comparisons could be completed, the effect of time was investigated by completing multiple pairwise comparisons between different time-points, relative to the later time point (day 10 vs day 0, day 3 vs day 0, day 10 vs day 3). Pairwise comparisons for the effect of treatment were completed, relative to the treated sample.

For differential abundance analysis, data was transformed to account for library size and ASV composition bias (Love *et al*., 2014). This involved calculating size factors for each sample, to normalise all ASV counts to within the sample (Love *et al*., 2014). It was important to account for library size because a sample with a bigger library size would

have higher ASV counts, therefore ASVs would be more likely to be identified as differently expressed, in comparison to a sample with a smaller library size, and therefore smaller ASV counts. It was also important to account for ASV composition bias which could occur because the number of reads obtained to represent bacterial communities is limited by a fixed number of slots to be filled for sequencing (Gloor *et al.*, 2017). ASV composition bias would occur when, for example, a high abundance of one ASV within a sample would reduce the number of 'slots' in the library that were free to collect other ASVs from the sample. This could therefore misrepresent the abundance of the 'other' ASVs in the sample, which could make them appear to be artificially lower in comparison to a sample with the same library size, but with a more balanced abundance of ASVs and hence more 'slots' for the collection of the 'other' ASVs (Robinson and Oshlack, 2010).

Results to present the significant changes that were detected between time points, in both untreated and treated samples, have been summarised in figure 2.16. Figure 2.16 presents simplified data so only indicates where significant increases or decreases were detected and does not provide qualitative information about the significant change in abundance (this information is provided in appendix 6).

5 different patterns of significant change were displayed by different groups of ASVs in the untreated microbiota over time (figure 2.16: A). This included an 'early increase' and an 'early decrease', which was a significant increase or decrease in ASVs between the day 0 and day 3 samples. The significant increase or decrease in these groups were also detected between the day 0 and day 10 samples, which validated that they had increased or decreased over time and remained increased or decreased at day 10 (figure 2.16: A). Other patterns included a 'late increase' and a 'late decrease', which was a significant increase or decrease in ASVs between the day 3 and day 10 samples. The significant increase or decrease in these groups were also detected between the day 0 and day 10 samples, which validated that they had increased or decreased over time (figure 2.16: A). The other pattern of significant change was an 'early decrease, late increase' which was a

significant decrease in ASVs between the day 0 and day 3 samples, followed by a significant increase of the same ASVs between the day 3 and day 10 samples (figure 2.16: A).

3 different patterns of significant change were displayed by different groups of ASVs in the ozone-treated microbiota over time, and all patterns were reductions (figure 2.16: B). The patterns included an ‘early decrease’ or ‘late decrease’, which were significant decreases between the day 0 and day 3, or day 3 and day 10 samples, respectively. Significant decreases were also detected between the day 0 and day 10 samples for each of the ASVs which displayed these patterns, which validated that reductions had occurred over time (figure 2.16: B).

A. Patterns of significant changes in genera abundance on untreated samples over time

B. Patterns of significant changes in genera abundance on treated samples over time (day 0 was an untreated control)

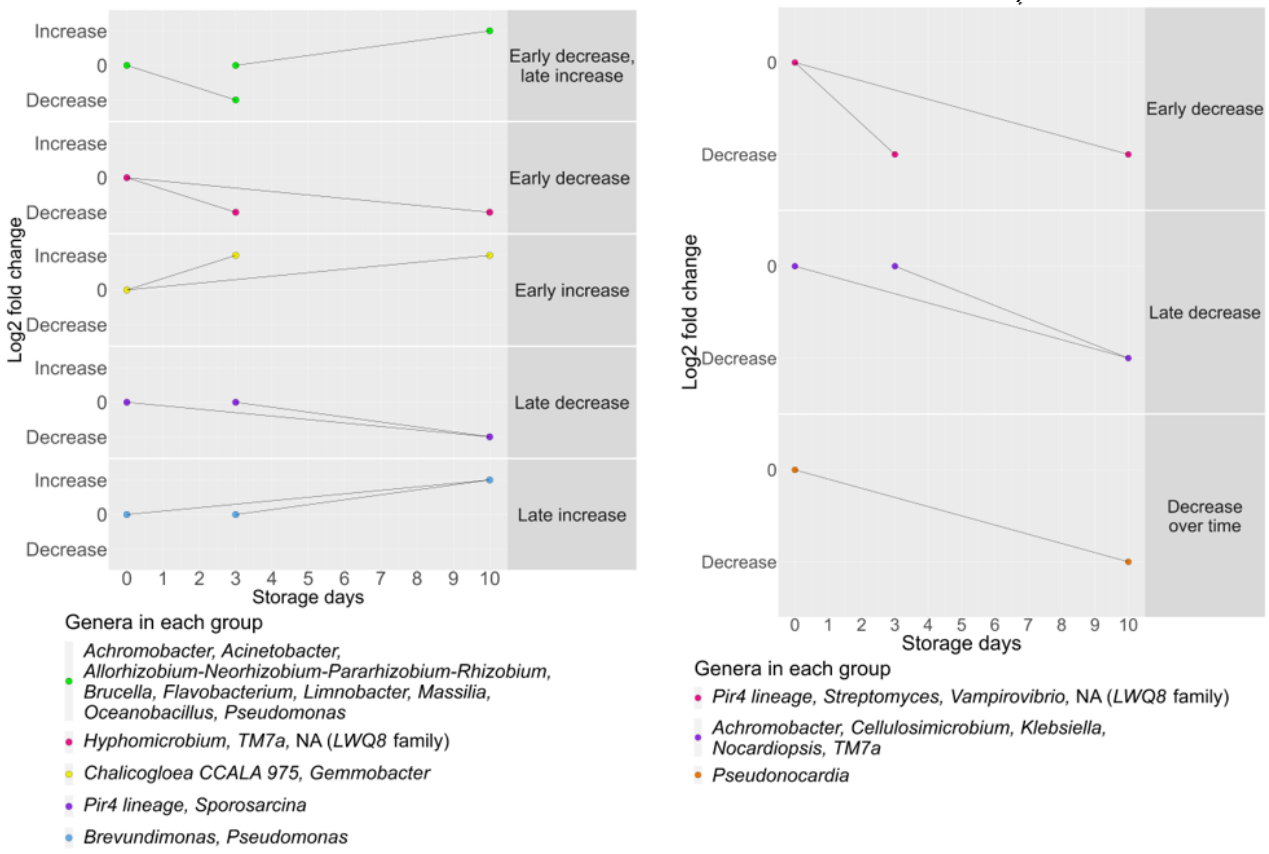


Figure 2.16: Gaseous ozone caused differences in the ASVs which changed in abundance post-harvest. Tomatoes were subjected to either one of five conditions; either an ozone treatment (3 second ozone generation, ~350 - 700 peak ppm) or not and stored at 18°C for 3 or 10 days (there was also an untreated day 0 control). DNA was extracted from tomato calyxes and pedicels, and 16S rRNA gene amplicons were sequenced. Significant differences in the number of every type of ASV, either between **(A)** all untreated samples at each time point, or **(B)** all ozone-treated samples at each time point (with inclusion of the untreated day 0 control), were tested for with DeSeq2. ASVs which significantly increased or decreased over time were presented as their genus, and they were grouped with other genera that presented the same significant pattern of change over time. The pattern of change that occurred within each group was presented by an individual subplot, where the time points at which significant increases or decreases were detected, were indicated by lines and their directions. A pattern description was provided next to each subplot.

When the treated and untreated samples were compared at day 3 post-treatment/post-harvest, only one ASV significantly changed in abundance, and this was a significant increase of an ASV in treated samples which was predicted to belong to the *Limnobacter* genus (figure 2.17: A). The abundance of this ASV was however significantly lower in the treated sample, in comparison to the untreated sample, at 10 days post-treatment/post-

harvest (figure 2.17: B). At 10 days post-treatment/post-harvest, other ASVs also showed a significant reduction in the treated sample, in comparison to the untreated sample. No ASVs showed a significantly higher abundance (figure 2.17: B).

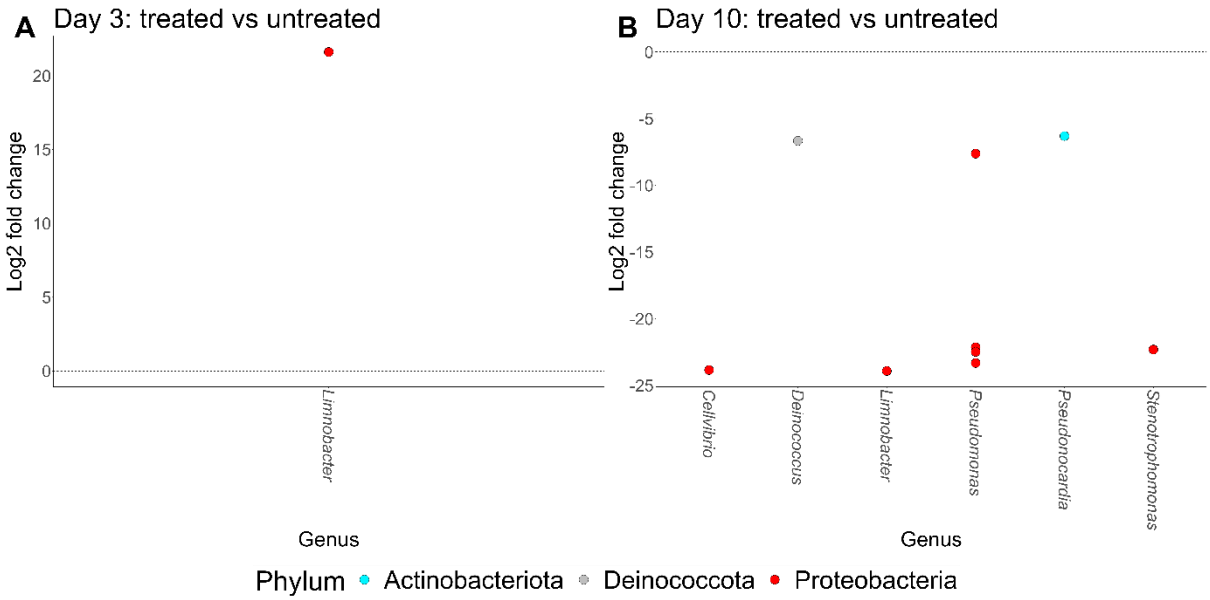


Figure 2:17: Gaseous ozone caused the abundance of ASVs to significantly change. Tomatoes were subjected to either one of five conditions; either an ozone treatment (3 second ozone generation, ~350 - 700 peak ppm) or not and stored at 18ºC for 3 or 10 days (there was also an untreated day 0 control). DNA was extracted from tomato calyxes and pedicels, and 16S rRNA gene amplicons were sequenced. Significant differences in the number of every type of ASV, between treated and untreated samples, either at **(A)** 3 days, or **(B)** 10 days post-treatment/post-harvest, were tested for with DeSeq2. ASVs which significantly increased or decreased over time were presented on the x-axis of charts as their genus and have been coloured according to their phylum. The log2 fold change is presented on the y-axis which shows the quantitative change in abundance of each organism, relative to the treated sample.

To conclude, dynamic changes in the bacterial population of the tomato calyx and pedicel occurred over time, during post-harvest storage. However, when ozone treatment was applied, these dynamic changes were interrupted, because only significant reductions of microbiota members occurred over time.

2.4 Discussion

The ability of gaseous ozone, generated by the in-pack ozone system, to reduce pathogens was tested in this chapter. Then, the effects of gaseous ozone on the

microbiota of the tomato calyx and pedicel (which was the selected model system) was investigated by culture and culture-independent means.

2.4.1 Gaseous ozone reduced pathogens *in vitro*

Gaseous ozone treatment with 1 (~80 - 300 peak ppm) and 3 (~350 - 700 peak ppm) second ozone generation times caused a high level of bacterial inactivation. Gaseous ozone has previously been reported to reduce bacterial pathogens including *Salmonella*, *E. coli* and *Pseudomonas*. However, this involved much lower ozone concentrations and much longer treatment times than those generated by the in-pack ozone system (Torlak *et al*., 2013; Alwi and Ali, 2014; Wani *et al*., 2016; Oliver *et al.*, 2019). Since the in-pack ozone system was a unique system, its ability to reduce pathogens was tested, and since it caused a high level of *E. coli* and *P. syringae* inactivation, it could be a promising intervention treatment for the food industry.

For the experiment, *E. coli* and *P. syringae* were dried on agar immediately before ozone exposure, so would have been in a surface-attached state but would not have had time to establish a biofilm. This is an important consideration because the in-pack ozone system is designed to control pathogens on produce, where pathogens may exist in a biofilm, and biofilms can increase bacterial tolerance to ozone (Ölmez and Temur, 2010). The sensitivity of pathogens in a biofilm to ozone, generated by the in-pack ozone system, could be investigated in future work. Also, for the experiment *E. coli* and *P. syringae* were presented on a smooth agar surface for ozone exposure, however the efficiency of ozone against bacteria may depend on the structure of the surface to which bacteria are attached, or whether bacteria are present endophytically within plant tissues. This is because bacteria may attach to or colonise sites which are inaccessible to ozone (Ölmez and Temur, 2010). The ability of gaseous ozone to reduce pathogens, when they are presented on the surface of different produce, may therefore vary and this was investigated during work for chapter 4.

2.4.2 Gaseous ozone reduced yeasts and moulds on the tomato calyx and pedicel

Yeasts and moulds significantly increased over time on the tomato calyx and pedicel. This could have been because yeasts and moulds were unaffected by desiccation (Barnard *et al*., 2013), which would occur to the calyx and pedicel tissue over time (Fathi-Najafabadi *et al.*, 2021). Ozone significantly reduced these yeasts and moulds, and the anti-fungal activity of gaseous ozone has previously been reported (Hudson and Sharma, 2009). This could benefit the food industry because some species of fungi cause food spoilage, and some fungi produce mycotoxins, which can be harmful to human health (Pitt and Hocking, 2022; Rodrigues and Furlong, 2022).

Specific changes in the fungal community that were caused by ozone could be investigated in future work. This would be beneficial because it was hypothesised that ozone would alter the entire microbial community, which could influence pathogen survival, and changes in both the bacterial and fungal community could influence bacterial and fungal pathogen survival, since bacteria interact with fungi (Peleg *et al*., 2010). Changes in both the native bacterial and fungal communities should therefore be considered. Fungal communities could be assessed by sequence analysis of 18S rRNA (Ottesen *et al.*, 2013) or the internal transcribed spacer 1 (ITS1) region (Liu *et al.*, 2020).

2.4.3 The tomato calyx and pedicel had a low bacterial abundance

It seems likely that the tomato calyx and pedicel had a low bacterial abundance. This was because amplification of the bacterial 16S rRNA gene from tomato calyxes and pedicels resulted in a high percentage of the host DNA being amplified, even though rRNA blockers were used. On average, 87.5% of 16S rRNA amplicons were identified as plant DNA (Eukaryota, chloroplast or mitochondria) per sample. Sample B9-UT10 had a much lower percentage of plant DNA in comparison to other samples, however the reason for this could not be identified. The relative abundance of bacteria and host 16S rRNA counts provides information about the bacterial density on the host (Humphrey and Whiteman,

2020), therefore it was likely that there was a low bacterial abundance on the tomato calyx and pedicel. High percentages of plant 16S rRNA amplification have also previously been reported in studies which investigated bacterial communities of tomato samples. For example, López *et al.*, 2020 and Dong *et al.*, 2019 respectively reported that 73 - 80% and 0 - 68% of 16S rRNA reads from tomato samples were plant DNA. This supports that there is likely a low bacterial abundance on tomatoes.

A low bacterial abundance on the tomato calyx and pedicel was further supported by the fact that 16S rRNA sequencing identified that *Pseudomonas* was the most abundant bacterial genus in all tomato calyx and pedicel samples, however when tomato calyx and pedicel samples were plated on PCA-CFC agar, which specifically selected for Pseudomonads, the Pseudomonads counts from many samples were below the limit of detection.

2.4.4 Gaseous ozone reduced the bacterial abundance on the tomato calyx and pedicel

It seems likely that ozone treatment with a 3 (~350 - 700 peak ppm) second ozone generation time further reduced the bacterial abundance on the tomato calyx and pedicel. Changes in the microbiota that were caused by ozone treatment, or no treatment, were identified by comparing 16S rRNA sequence results between 0, 3 and 10 days, since the results would have included DNA from viable and non-viable bacteria (Emerson *et al.*, 2017). Before host DNA removal, there were no significant differences between the 16S rRNA amplicon library size of each sample group. However, after host DNA removal, the bacterial 16S rRNA amplicon library sizes from tomato calyxes and pedicels which had been ozone-treated and stored for 10 days were significantly lower than bacteria recovered from tomato calyxes and pedicels which had not been treated or stored. It was therefore likely that the ozone-treated samples which had been stored for 10 days had less bacteria than the samples which had not been treated or stored. After host DNA

removal, there were no significant differences between the bacterial library sizes of untreated samples which had been stored for 0, 3 and 10 days. This indicated that the bacterial abundance on the host likely did not change over time when no ozone treatment was applied.

Samples which had been ozone-treated and stored for 10 days would have had a starting population equivalent to the samples which had not been ozone-treated or stored. Since bacterial populations were assessed by DNA amplification of viable cells, non-viable cells and extracellular DNA (Emerson *et al.*, 2017), bacterial DNA must have degraded within the environment to result in lower bacterial counts. Ozone exposure can cause DNA to leak from bacterial cells into the extracellular environment and it can also directly damage DNA (Komanapalli and Lau, 1996; Ersoy *et al*., 2019). Extracellular DNA can be degraded by nuclease-producing micro-organisms and the ability of extracellular DNA to persist in the environment is highly dependent on environmental conditions (Nielsen *et al.*, 2007; Kunadiya *et al.*, 2021). Ozone treatment and/or the environmental conditions were therefore likely sufficient to degrade DNA from inactivated bacterial cells, which would have contributed to the identification of the differences between bacterial communities.

2.4.5 Proteobacteria/*Pseudomonadaceae*/*Pseudomonas* dominated the tomato calyx and pedicel bacterial community

The bacterial community of the tomato calyx and pedicel was characterised by assessing the relative abundance of phyla, families and genera that were present on untreated samples which had not been stored. It showed that the dominating bacteria were Proteobacteria/*Pseudomonadaceae*/*Pseudomonas*. The *Pseudomonas* genus is comprised of 538 species (Parte *et al.*, 2020), some of which are plant pathogens or spoilage organisms (Höfte and De Vos, 2006). It has previously been reported that Proteobacteria made up nearly 100% of the endophytic bacterial community of tomato stems and leaves (Dong *et al.*, 2019). The dominant nature of *Pseudomonas* on tomato

fruit and flowers (Ottesen *et al.*, 2013; Soto-Giron *et al.*, 2021) has also been reported and the flower sepal ultimately forms the calyx (Lyle, 2006). There are contradictions regarding the other highly abundant genera which have been detected on tomato fruit. For example, Soto-Giron *et al.*, 2021 reported that *Rahnella* and *Pantoea* were also highly abundant genera whereas Ottesen *et al.*, 2013 reported that *Xanthomonas* and *Sphingomonas* were. Neither of these organisms were detected to be highly abundant on the tomato calyx and pedicel in this study. Many differences could contribute to variation in the bacterial communities of tomatoes, for example cultivation approach (Cheng *et al.*, 2020; Rodríguez *et al.*, 2021). Nevertheless, López *et al.*, 2020 concluded that bacteria in tomato plants mainly belonged to the Actinobacteria, Bacteroidota, Firmicutes and Proteobacteria phyla, and these were the four most abundant phyla in the bacterial community of the tomato calyx and pedicel, which had not been treated or stored.

2.4.6 The tomato calyx and pedicel bacterial community changed over time; however, ozone treatment impacted these changes

After tomatoes were stored for 10 days post-harvest (after no treatment had been applied), some changes in the bacterial community occurred over time, which was evident from taxonomic profiles. Although Proteobacteria/*Pseudomonadaceae*/*Pseudomonas* remained dominant, the profiles were different for the untreated samples which had been stored for 0, 3 and 10 days. Notably, the relative abundance of *Pseudomonas* increased from day 0 to day 3 but decreased from day 3 to day 10. When ozone-treatment with a 3 second ozone generation time (~350 - 700 peak ppm) was applied, the profiles underwent different changes over time. For example, although Proteobacteria/*Pseudomonadaceae*/*Pseudomonas* remained dominant, the relative abundance of *Pseudomonas* was evidently greater in the treated sample which had been stored for 10 days, in comparison to the untreated sample.

Although changes in the bacterial community of the tomato calyx and pedicel had occurred after 10 days of post-harvest storage, no significant changes in community diversity or composition occurred. It has previously been shown that the community diversity of the tomato fruit bacterial community increased from day 0 to day 8 but decreased from day 8 to day 12 during post-harvest storage at 10^{o}C for 8 days, then 20^{o}C for 4 days (Shi *et al.*, 2022). The same study also showed that each of these sample groups displayed different community structures (Shi *et al.*, 2022). The study however assessed bacteria on the tomato fruit, and used different storage conditions, which can significantly affect bacterial communities (Wang *et al.*, 2023), therefore it is not completely comparable to work completed in this study.

When ozone treatment had been applied, the tomato calyx and pedicel bacterial community diversity significantly reduced after 10 days of storage. The significant reduction in bacterial community diversity that was caused by ozone-treatment, was also evident when the ozone-treated and non-treated samples which had each been stored for 10 days were compared. Since there was reduced community diversity, significantly fewer species were present, which could have been due to the indicated loss of bacterial abundance in ozone-treated samples. Since it was hypothesised that ozone would kill a wide range of bacteria, due to its broad-spectrum antimicrobial activity (Kim and Yousef, 2003), the reduction in community diversity that was caused by ozone treatment was unsurprising.

Ozone treatment also caused significant changes in the bacterial community composition of the tomato calyx and pedicel. These significant changes were however driven by the differences in community composition variability within a sample group rather than differences in the community because PCA plots identified that sample groups were always overlaid but had different divergences. The community structure became less variable within the sample group as time post-treatment/post-harvest increased and

ozone-treated samples were less variable than non-treated samples after 10 days of storage.

The impact of gaseous ozone on microbial communities has mainly been studied by investigating the impact of ozone concentrations which are much lower than the ozone concentrations generated by the in-pack ozone system, therefore it was difficult to compare results generated from other studies to this study. Nevertheless, Qian *et al.*, 2022 showed that the community diversity of the bacterial community on salmon reduced after it had been stored in the refrigerator for 10 days, regardless of if ozone treatment (1 or 3 mg/m^3 for <10 minutes) had been applied or not. The authors also showed that the community composition of sample groups that had been exposed to different concentrations of ozone for different times, were different to the untreated control when comparisons were made at 0 and 10 days post-treatment. This was not due to differences in variation within sample groups. The authors completed DNA-based 16S rRNA sequencing for bacterial community analysis, and since their results showed that the effect of ozone treatment on the bacterial community could be immediately detected on the day of treatment, an ozone-treated sample which had not been stored could have been included as a sample group in this study. Zhang *et al.*, 2022 treated winter jujube fruit with gaseous ozone (2.5, 5 or 10 μL L^{-1}, 1 hour per day for >15 days) and concluded that ozone caused changes in community diversity but the changes did not present a conclusive pattern. Zhang *et al.*, 2022 also showed that ozone caused differences in the bacterial community structure of sample groups, which was not due to differences in variation within sample groups.

Dynamic changes in the bacterial community of the tomato calyx and pedicel occurred during post-harvest storage, as identified by a differential abundance analysis. The genera of the ASVs which underwent significant changes in abundance over time have been detailed in appendix 7.1. ASVs which decreased over time included those with long reported doubling times (for example *Hyphomicrobium* and *Sporosarcina*), whereas ASVs

which increased over time included those with much shorter reported doubling times (for example *Brevundimonas* and *Pseudomonas*) (appendix 7.1). Therefore, the doubling time could have impacted the ability of bacteria to adapt to post-harvest changes in the tomato calyx and pedicel through competitive growth.

When ozone treatment had been applied, there were differences in the bacteria which significantly changed in abundance over time and only significant bacterial reductions occurred. This was unexpected because it was hypothesised that ozone would eliminate ozone-susceptible micro-organisms which would reduce competition for other micro-organisms to thrive, however results showed that no micro-organisms thrived within the timescale tested. The genera of the ASVs which were significantly reduced over time after ozone treatment have been detailed in appendix 7.2, and the genera of ASVs which were significantly increased or decreased on the tomato calyx and pedicel after ozone treatment in comparison to non-treated samples at 3 and 10 days post-harvest have been detailed in appendix 7.3. No common features were identified within the genera which ASVs affected by ozone treatment belonged to. For example, no observable pattern was found regarding ozone susceptibility based on the Gram stain classification of genera, however it has previously been reported that Gram-positive cells are generally more susceptible to ozone than Gram-negative cells (Alwi and Ali, 2014; Ersoy *et al*., 2019). However, factors that are not attributed to the taxonomy of bacteria could have also contributed to a bacterium's tolerance to ozone when it was a member of the tomato calyx and pedicel microbial community. For example, if micro-organisms were attached to sites on the tomato calyx or pedicel which were inaccessible to ozone, or were presented in a biofilm, this could have increased their tolerance to ozone (Ölmez and Temur, 2010; Wani *et al*., 2016; Panebianco *et al.*, 2021). Also, older bacterial cells and cells which were pre-exposed to cold stress have been shown to be more tolerant to ozone (Wani *et al.*, 2015, 2016). This could have masked the contributions of taxonomic-related factors to bacterial tolerance.

The differential abundance analysis identified that some Pseudomonads significantly changed in abundance. For example, three types of Pseudomonads significantly increased from day 3 to day 10 post-harvest when no treatment had been applied. Also, four types of Pseudomonads were significantly reduced on the treated sample at 10 days post-treatment/post-storage, in comparison to the untreated sample. Nevertheless, there were 41 different Pseudomonads in the 16S rRNA dataset, therefore the abundance of other Pseudomonads would have been involved in driving the overall relative abundance of *Pseudomonas*.

2.4.7 Ozone-induced changes in the native microbiota might impact pathogen survival and proliferation

Ozone treatment significantly changed the native bacterial community of the tomato calyx and pedicel, which could affect the ability of pathogens to survive and proliferate until the point of consumption. During this time, pathogens could damage post-harvest produce (in particular, opportunistic pathogens could take advantage of ozone-induced damage to the host) or they could become a health risk to the consumer. It was identified that ozone treatment reduced the bacterial community diversity of the tomato calyx and pedicel, whereas the bacterial community diversity did not reduce when no treatment had been applied. A reduced microbial community diversity has been reported to be more invasible by pathogens (Matos *et al*, 2005; van Elsas *et al.*, 2012), therefore ozone treatment could make the tomato calyx and pedicel more susceptible to pathogen attack after the treatment had been applied. However, since the in-pack ozone system treats produce in its packaging, in which it is intended to remain until the point of consumption, produce would not likely be exposed to pathogens post-treatment, therefore an increased risk of pathogen colonisation post-treatment would not be of concern. Nevertheless, this could be a concern for produce treated with ozone, which would then be exposed to potential pathogen sources after treatment but before consumption, such as personnel, insects or transportation equipment (Balali *et al.*, 2020). It is to be mentioned that an increased risk

of pathogen colonisation post-treatment, due to a reduced bacterial community diversity, could also be applied to peracetic acid and sodium hypochlorite treated produce, since they have both reduced the bacterial community diversity of lettuce wash water (Gu *et al.*, 2020). Since the in-pack ozone system would reduce the risk of produce being exposed to pathogens post-treatment (which could be a time period where there is an increased vulnerability to pathogen colonisation), this highlights a benefit of the system, in comparison to the treatments which are currently being used.

Since reduced microbial community diversities have been reported to be more invasible by pathogens (Matos *et al*, 2005; van Elsas *et al.*, 2012), the reduced bacterial community diversity could also favour the proliferation of pathogens that were already present in the community which could have survived ozone treatment.

The genera of ASVs which significantly changed over time on the tomato calyx and pedicel, both with and without ozone treatment, often had species with pathogenic properties, for example *Flavobacterium* and *Pseudomonas* could be plant pathogens (appendix 7), however since pathogenic properties are species specific, the effect of ozone against pathogens could not be interpreted. Future work could involve spiking the native microbiota with food-borne and post-harvest pathogens and monitoring their survival in the altered microbiota after ozone treatment.

2.4.8 Conclusion

Gaseous ozone generated by the in-pack ozone system reduced *E. coli* and *P. syringae in vitro*, therefore it could be a promising intervention treatment to control for pathogens in the food industry. Ozone treatment however significantly affected the native microbiota of the tomato calyx and pedicel, which could impact pathogen survival. For example, it caused reductions in the general microbial abundance and although Proteobacteria/*Pseudomonadaceae*/*Pseudomonas* always dominated the bacterial community, ozone treatment caused taxonomic profiles to undergo different changes over

time. Ozone treatment also caused bacterial community diversity to reduce over time, and the bacterial community structure to change over time, and these changes did not occur when no treatment had been applied. Ozone treatment also resulted in differences in the ASVs which significantly changed in abundance over time.

Since ozone treatment changed the native microbiota of the tomato calyx and pedicel, future work could investigate the ability of pathogens to survive in this.

Chapter 3: Contribution of the oxidative stress tolerance pathway to ozone, peracetic acid and sodium hypochlorite tolerance in enterics and *P. syringae*

3.1 Introduction

Bacteria associated with eukaryotic hosts have evolved a strong oxidative stress response to the oxidative burst, which is primarily composed of hydrogen peroxide (Lamb and Dixon, 1997; O'Brien *et al.*, 2012). Since hydrogen peroxide, ozone, peracetic acid and the active components of sodium hypochlorite are all strong oxidants (chapter 1, table 1.1), they could be tolerated by the same molecular mechanisms in bacteria. Hence, bacteria with a particularly high tolerance to hydrogen peroxide could better survive ozone, peracetic acid, or sodium hypochlorite that could be applied in the food industry to control for pathogens.

The overall aim of this chapter was to gain a deeper understanding of whether hydrogen peroxide, ozone, peracetic acid, and sodium hypochlorite were tolerated by the same mechanisms in bacteria. The response of enterics and Pst to each treatment was therefore characterised and compared, to identify if they responded to each treatment in a similar way, and to identify if hydrogen peroxide tolerance was correlated with tolerance to other treatments.

3.1.1 roGFP is a biosensor for the intracellular redox state

In this chapter, roGFP was used to monitor the intracellular redox state of bacteria in response to treatments. roGFP is a reduction-oxidation sensitive GFP (Hanson *et al.*, 2004). It contains surface-exposed cysteines in the β-barrel of GFP so that the configuration of a disulfide switch between the cysteines affects the fluorescence excitation spectrum (Hanson *et al.*, 2004). Oxidation of the cysteine residues causes a disulfide bond to form between them, which causes an increase in the fluorescence

intensity when the roGFP is excited at ~405 nm (figure 3.1) (Hanson *et al.*, 2004). Reduction of the cysteine residues, and the subsequent disulfide bond reduction, causes an increase in fluorescence intensity when the roGFP is excited at ~488 nm (figure 3.1) (Hanson *et al.*, 2004). Thus, the ratio of fluorescence intensity upon excitation at ~405 nm and ~488 nm respectively indicates the redox status of roGFP and therefore its environment. Since roGFP is a ratiometric indicator, it reduces or eliminates measurement errors due to differences in roGFP concentration or photobleaching (Hanson *et al.*, 2004).

Different versions of roGFP exist, which each differ by either the location of their introduced cysteines and/or by their GFP background so that they each have differences in spectral properties, mid-point potentials and pH sensitivity (Hanson *et al.*, 2004). roGFP1 and roGFP2 are the most commonly used in the literature (Vevea *et al.*, 2013) and roGFP2 is preferred for measurements under mild to strong oxidative stress conditions (Schwarzländer *et al.*, 2008). Therefore, roGFP2 was used for work in this chapter and its excitation spectra has been presented in figure 3.1.

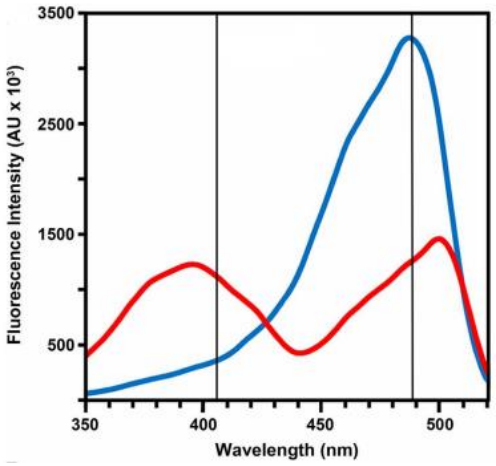


Figure 3.1 taken from Aller *et al*., 2013: The excitation spectra of roGFP2 is dependent on its redox status. The excitation spectra of fully oxidised (red) and fully reduced (blue) roGFP2 is displayed. Fluorescence intensity was measured at 540 nm emission. The ratio of fluorescence intensity upon excitation at 405 nm and 488 nm (black lines) is often used to determine the redox status of roGFP2.

The disulfide switch of roGFP2 is primarily specific for glutathione via glutaredoxins (figure 3.2) (Meyer *et al.*, 2007; Schwarzländer *et al.*, 2008). Glutathione is a thiol-containing antioxidant which acts as a major redox buffer in Gram-negative bacteria (Carmel-Harel and Storz, 2000). This is because in its reduced form (GSH), it donates electrons to neutralise ROS, and hence becomes oxidised in this process (GSSG) (Carmel-Harel and Storz, 2000). The ratio of GSH and GSSG can therefore indicate the redox status of a cell, since more GSSG will form under conditions of oxidative stress, and GSSG will become reduced back to GSH when the oxidative stress dissipates (Beer *et al.*, 2004). Both GSSG and GSH primarily react with roGFP2 cysteines to subsequently oxidise or reduce them, using glutaredoxins as electron shuttles in the process (figure 3.2) (Meyer *et al.*, 2007; Schwarzländer *et al.*, 2008).

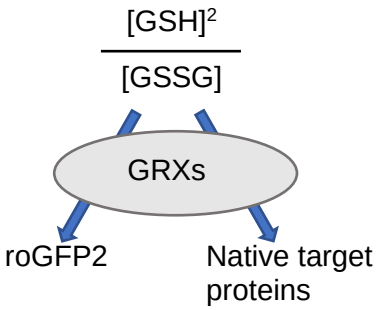


Figure 3.2 modified from Meyer et al., 2007: roGFP2 is primarily specific for glutathione via glutaredoxins. roGFP2 acts as an artificial target for the reversible transfer of electrons between the glutathione pool and target proteins by glutaredoxins (GRXs). The redox potential of the glutathione pool is dependent on the $[GSH]^2/[GSSH]$ ratio (GSH = reduced glutathione, GSSG = oxidised glutathione).

Although roGFP2 is primarily specific for glutathione via glutaredoxins, purified roGFP2 can also slowly react with GSH alone (to become reduced) and hydrogen peroxide alone (to become oxidised) (Meyer *et al.*, 2007). This indicates that although roGFP2 is primarily specific for glutathione via glutaredoxins, the specificity is not absolute.

3.1.2 Transcriptional fusion fluorescent reporters are biosensors for the transcriptional response of genes

Transcriptional fusion fluorescent reporters were used to monitor the transcriptional response of selected, individual genes in enterics to treatments. They were generated by positioning a promoter region for a selected gene of interest behind a promoter-less fluorescent protein, namely GFP (figure 3.3), in a plasmid. This was so that GFP expression would be regulated by the selected promoter. Hence, within a bacterium, GFP expression would represent the transcriptional activity of the gene of interest. Plasmid-borne transcriptional fusion reporters can only be used to monitor promoter induction because a reduction in fluorescence might be due to plasmid loss, caused by the accumulation of GFP to toxic levels (Hautefort *et al*., 2003).

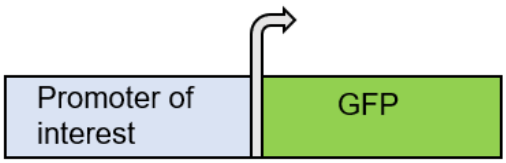


Figure 3.3: A promoter for a gene of interest is used to regulate the expression of a fluorescent protein in a transcriptional fusion fluorescent reporter.

GFP does not require any substrates or co-factors for its production (Chalfie *et al.*, 1994), however oxygen is required for its maturation (the process of GFP chromophore formation) (Heim *et al*., 1994; Iizuka *et al*., 2011). The maturation rate will affect the time at which the fluorescent protein can be detected after upregulation and within *E. coli*, the maturation rates of fluorescent proteins typically range from several minutes to several hours (Balleza *et al.*, 2018). Several factors including the bacterial strain, growth rate and temperature will impact the maturation time (Macdonald *et al*., 2012; Hebisch *et al.*, 2013).

Genes selected to produce the reporters were *oxyR*, *katG*, *soxS*, *soxR*, *ramA* and *lexA*, and their role in the oxidative stress response of enterics will now be described in detail.

3.1.3 The role of *oxyR*, *katG*, *soxS*, *soxR*, *ramA* and *lexA* in enterics

oxyR

The *oxyR* regulon is a primary regulon for the response of *E. coli* and *S. enterica* to oxidative stress (Imlay, 2009). Under oxidative stress conditions (primarily hydrogen peroxide), a cysteine residue (C199) within OxyR becomes oxidised to form a sulfenic acid (-SOH) (figure 3.4: A) (Sen and Imlay, 2021). This residue then moves from the hydrophobic pocket, in which it was originally located, to come into close proximity with a different cysteine residue (C208) located within OxyR (Sen and Imlay, 2021). A reversible disulfide bond/disulfide bridge is then formed between these residues (figure 3.4: B) (Sen and Imlay, 2021). This occurs within four monomers of OxyR, which transforms it into its activated state (figure 3.5) (Sen and Imlay, 2021). OxyR can only bind to most members of the regulon in its activated state, where it recruits RNA polymerase to initiate the transcription of genes required for the activation of resistance mechanisms (chapter 1, figure 1.3) (Sen and Imlay, 2021).

(A) $Cys\text{-}SH + H_2O_2 \longrightarrow Cys\text{-}SOH + H_2O$

(B) $Cys\text{-}SOH + Cys\text{-}SH \longrightarrow Cys\text{-}SS\text{-}Cys + H_2O$

Figure 3.4 taken from Imlay, 2009: (A) a sulfenic acid forms from a cysteine residue under conditions of oxidative stress and (B) a disulfide bond forms between the sulfenic acid and a cysteine residue.

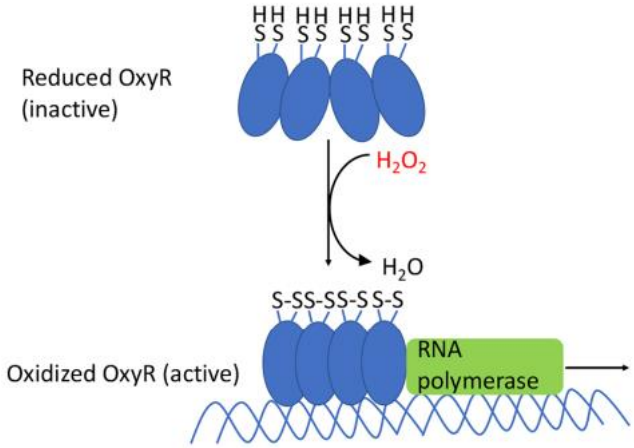


Figure 3.5 taken from Sen and Imlay, 2021: OxyR activation.

katG

katG is one of the most strongly induced genes by OxyR (Zheng *et al.*, 2001) and KatG (also known as catalase HPI) is involved in ROS detoxification, since it is a cytoplasmic enzyme with catalase and peroxidase activity (Hillar *et al*., 1999) (chapter 1, figure 1.3).

In addition to KatG, *E. coli* also has another cytoplasmic catalase, namely KatE (also known as catalase HPII), which only has catalase activity (Hillar *et al*., 1999). In addition to KatE and KatG, which use haem as a co-factor, *Salmonella* has another non-haem catalase which uses manganese as a co-factor, namely KatN (Robbe-Saule *et al.*, 2001; Diaz-Ochoa *et al.*, 2016). In *E. coli* and *Salmonella*, KatG is the only catalase which is upregulated in response to hydrogen peroxide. KatE and KatN are only produced during the stationary phase of growth, under control of the *rpoS* regulon (Iwase *et al.*, 2013; Hahn *et al*., 2021).

soxRS

In addition to the *oxyR* regulon, the *soxRS* regulon is another key regulon involved in the oxidative stress response of *E. coli* and *S. enterica* (Imlay, 2009). The *soxRS* regulon has been shown to be induced by redox-cycling drugs which induce oxidative stress (Gu and

Imlay, 2011). SoxR binds near the *soxS* promoter site and acts as a sensor of the cellular redox state (Imlay, 2009). SoxR is composed of two subunits, which each have a [2Fe-2S]$^{+}$ cluster in unstressed cells (Imlay, 2009). Under oxidative stress conditions, the clusters become oxidised to [2Fe-2S]$^{2+}$, which causes contortion of the SoxR region that is bound near the *soxS* promoter site (Imlay, 2009). This improves the RNA polymerase binding site for the transcription of *soxS*. SoxS is subsequently upregulated which initiates the transcription of genes required for the activation of resistance mechanisms (chapter 1, figure 1.3) (Imlay, 2009; Seo *et al.*, 2015).

ramA

In addition to the *soxRS* and *oxyR* regulons, other regulons are also involved in the oxidative stress response of enterics. For example, RamA is a transcriptional activator in an oxidative stress regulon, and it has a role in protection against intracellular ROS generated by redox-cycling drugs and extracellular hydrogen peroxide in *S. enterica* (van der Straaten *et al.*, 2004). However, its protective role only becomes apparent in the absence of the *soxRS* regulon (van der Straaten *et al.*, 2004). Interestingly, *E. coli* lacks *ramA*, however, the expression of *ramA* on a plasmid in *E. coli* significantly increased its resistance to the redox-cycling drug menadione, which generates intracellular ROS (van der Straaten *et al.*, 2004).

ramA is locally regulated by *ramR* which encodes a repressor of *ramA* transcription, and it is thought that the repressor mechanism is via the binding of RamR to the *ramA* promoter site (Ricci *et al*., 2012). It is therefore presumed that the prevention of RamR binding to the *ramA* promoter site induces the *ramA* overexpression which allows elevated oxidative stress tolerance (Bailey *et al.*, 2010).

Bailey *et al.*, 2010 and Zheng *et al.*, 2011 each reported that the genes which were upregulated by *ramA* included those involved in drug efflux in *S. enterica* (such as *acrAB* and *tolC* (chapter 1, figure 1.3)).

lexA

Since ROS damages DNA, this can trigger the SOS response in *E. coli* and *S. enterica*, which induces the production of proteins to repair DNA and maintain DNA integrity (Maslowska *et al*., 2019; Mérida-Floriano *et al.*, 2021).

The response is positively regulated by RecA when it binds to single-stranded DNA, downstream of a DNA lesion (Simmons *et al.*, 2008). RecA then cleaves and inactivates LexA, which is a negative regulator of the SOS response, so that genes required for the SOS response which are normally repressed by LexA can be relieved (Simmons *et al.*, 2008). Genes regulated by LexA include *uvrAB* which is involved in nucleotide excision repair, *sulA* which is an inhibitor of cell division, and *grxA*, which is also regulated by OxyR and is involved in the maintenance of the cellular redox balance (chapter 1, figure 1.3) (Simmons *et al.*, 2008; Sen and Imlay, 2021). LexA represses its own promoter, therefore when the SOS response is induced, LexA will be upregulated (Simmons *et al.*, 2008).

3.1.4 The role of *oxyR* and catalases in Pst DC3000 treatment tolerance

The *oxyR* regulon is highly conserved in Pst, and it has a critical role in the detoxification of exogenous and endogenous hydrogen peroxide (Ishiga and Ichinose, 2015). The *oxyR* regulon in Pst is however not as well characterised as the *oxyR* regulon in enterics, so much less information is available regarding the genes that it controls. Nevertheless, Ishiga and Ichinose, 2015 showed that OxyR could regulate the expression of catalases in Pst DC3000, namely KatB and KatG (table 3.1), in response to ROS.

Catalases are important enzymes for the detoxification of hydrogen peroxide (Guo *et al.*, 2012). Pst DC3000 has three catalases, namely KatB, KatE and KatG, and a summary of these catalases is provided in table 3.1 (Guo *et al.*, 2012). Notably, no major role has

been identified for KatE, however it may become important under specific environmental conditions (Guo *et al.*, 2012).

Table 3.1: Summary of catalases in Pst DC3000

Catalase	Proposed functional activity	Proposed substrate	Proposed cellular location	Role in H_2O_2 detoxification
KatB	Monofunctional catalase	Exclusively H_2O_2	Periplasm and cytoplasm	• **Major role in the detoxification of exogenous H_2O_2** • Minor house-keeping role for H_2O_2 detoxification in culture • Minor role in the detoxification of intracellular H_2O_2 generated by menadione
KatE	Monofunctional catalase	Exclusively H_2O_2	Cytoplasm	• Minor house-keeping role for H_2O_2 detoxification in culture • Very minor role in the detoxification of exogenous H_2O_2, linked with the role of KatB
KatG	Bifunctional catalase (has catalase and peroxidase activity)	H_2O_2 and other organic peroxides	Cytoplasm	• **Major house-keeping role for H_2O_2 detoxification in culture** • **Major role in the detoxification of intracellular H_2O_2 generated by menadione** • Moderate role in the detoxification of exogenous H_2O_2

All information was sourced from Guo *et al*., 2012. The proposed functional activity, substrate and cellular location of each catalase was inferred from studies of related catalases.

3.1.5 Chapter aims

This chapter aimed to gain a deeper understanding of whether hydrogen peroxide, ozone, peracetic acid, and sodium hypochlorite were tolerated by the same mechanisms in bacteria. The effect of each treatment on the growth, culturability and redox state of each

model bacterium, the transcriptional response of selected genes in enterics, and the redox state of Pst DC3000 deletion mutants were therefore investigated and compared.

3.2 Methods

3.2.1 Antimicrobial chemicals

Antimicrobial chemicals that were sourced for this study are listed in table 3.2. Ozone was also an antimicrobial chemical that was used for this study; however, it did not require to be sourced because it was generated on-site at working concentrations.

Table 3.2: Antimicrobial chemicals sourced for this study

Chemical	Source	Stored stock concentration	Working stock concentration
Hydrogen peroxide (H_2O_2)	Merck, UK	30% hydrogen peroxide, 9.8 M	variable
Peracetic acid ($C_2H_4O_3$)	ThermoFisher Scientific, UK	ca. 35% peracetic acid	≤ 0.008% (80 ppm)
Sodium hypochlorite (NaClO)	ThermoFisher Scientific, UK	15.3% sodium hypochlorite	≤ 0.01% (100 ppm) free chlorine
Dithiothreitol (DTT)	ThermoFisher Scientific, UK	NA	5 mM

To generate working stocks of peracetic acid and sodium hypochlorite, 80 ppm peracetic acid or sodium hypochlorite with 100 ppm free chlorine were made first so that their concentrations could be confirmed with MQuant™ peracetic test strips (Merck, UK) and MQuant™ free chlorine test strips (Merck, UK) respectively. Then, dilutions were completed to generate working concentrations.

It is to be noted that to produce 80 ppm peracetic acid from the ca. 35% stock solution, the calculated volume of stock required to be added to distilled water (229 µl/L) produced a concentration which was detected as too high on the MQuant™ peracetic test strip. The volume of stock added was therefore modified to 152 µl/L because this produced a concentration which was detected as 80 ppm on the MQuant™ peracetic test strip. To produce 100 ppm free chlorine from the 15.3% sodium hypochlorite stock, the calculated

volume of stock required to be added to distilled water (778 µl/L) produced a concentration which was confirmed as 100 ppm on the MQuant™ free chlorine test strip.

3.2.2 Bacterial strains, plasmids and primers

Bacterial strains used for this study are listed in table 3.3.

Table 3.3: Bacterial strains used for this study

Strain	Description	Antibiotics	Reference
Wildtype strains			
Pseudomonas syringae pv. tomato (Pst) DC3000	A rifampicin-resistant derivative of *P. syringae* pv. tomato DC52 (also referred to as NCPPB 1106), which was isolated from tomatoes on the island of Guernsey, United Kingdom (Buell *et al.*, 2003; Almeida *et al.*, 2009)	Rifampicin, nitrofurantoin	(Cuppels, 1986)
Pst T1	An isolate from tomato in Canada	Nitrofurantoin	(Almeida *et al.*, 2009)
Escherichia coli (*E. coli*) JHI-5025	An isolate from soil in Scotland	NA	(Holden, 2021)
Salmonella enterica (*S. enterica*) sv. Typhimurium (Stm) SL1344	A histidine auxotroph (due to *hisG46* mutation) of strain *Salmonella enterica* sv. Typhimurium 4/74 (Jones, 1988), which was isolated from a calf with salmonellosis (Rankin and Taylor, 1966)	NA	(Hoiseth and Stocker, 1981)
S. enterica serovar Senftenberg (Ssf) 20070885	An isolate from contaminated ready to eat basil	NA	(Elviss *et al.*, 2009)
Strains for initial transformations of assembled plasmids			
E. coli DH5-α (Subcloning Efficiency™ DH5α Competent Cells)	Genotype: F^- Φ80*lac*ZΔM15 Δ(*lac*ZYA-*arg*F) U169 *rec*A1 *end*A1 *hsd*R17(r_k^-, m_k^+) *pho*A *sup*E44 *thi*-1 *gyr*A96 *rel*A1 λ^-.	NA	ThermoFisher Scientific, UK
E. coli AAEC185A	Genotype: $F^-\lambda^-$supE44 hsdR17 μrA endA1 thi-1Δ(fimBEACDFGH) ΔrecA	NA	(Blomfield *et al.*, 1991)
Strains carrying plasmids for conjugations			
E. coli SM10/λ pir (pUX-BF13)	*E. coli* SM10/λ pir with pUX-BF13	Carbenicillin	(Miller and Mekalanos, 1988)
E. coli DH5α (pRK2013)	*E. coli* DH5α with pRK2013	Kanamycin	(Figurski and Helinski, 1979)
E. coli DH5α (pK18mobsacB_oxyR_deletion)	*E. coli* DH5α with pK18mobsacB_oxyR_deletion	Kanamycin	This study
E. coli DH5α (pUC18T-mini_Tn7T-Gm-oxyR)	*E. coli* DH5α with pUC18T-mini_Tn7T-Gm-oxyR	Gentamicin	This study
Pst DC3000 deletion mutants and complement strains			

Pst DC3000 Δ*oxyR*	Pst DC3000 with deletion of *oxyR*	Rifampicin, nitrofurantoin	This study
Pst DC3000 Δ*oxyR* + Tn7_*oxyR*	Pst DC3000 Δ*oxyR* with a genomic integration of *oxyR* and its native promoter in the Tn7 attachment site.	Rifampicin, nitrofurantoin, gentamicin	This study
Pst DC3000 Δ*katBEG* (also known as UNL254)	Pst DC3000 with deletion of *katB*, *katE* and *katG*	Rifampicin, nitrofurantoin	(Guo *et al.*, 2012)
Pst DC3000 Δ*katBEG* + Tn7_*katG*	Pst DC3000 Δ*katBEG* with a genomic integration of *katG* and its native promoter in the Tn7 attachment site.	Rifampicin, nitrofurantoin, gentamicin	(Guo *et al.*, 2012)
roGFP reporter strains			
Pst DC3000 (pDSK-roGFP)	Pst DC3000 expressing roGFP via pDSK-roGFP	Rifampicin, nitrofurantoin, kanamycin	This study
Pst DC3000 Δ*oxyR* (pDSK-roGFP)	Pst DC3000 Δ*oxyR* expressing roGFP via pDSK-roGFP	Rifampicin, nitrofurantoin, kanamycin	This study
Pst DC3000 Δ*oxyR* + Tn7_*oxyR* (pDSK-roGFP)	Pst DC3000 Δ*oxyR* + Tn7_*oxyR* expressing roGFP via pDSK-roGFP	Rifampicin, nitrofurantoin, kanamycin, gentamicin	This study
Pst DC3000 Δ*katBEG* (pDSK-roGFP)	Pst DC3000 Δ*katBEG* expressing roGFP via pDSK-roGFP	Rifampicin, nitrofurantoin, kanamycin	This study
Pst DC3000 Δ*katBEG* + Tn7_*katG* (pDSK-roGFP)	Pst DC3000 Δ*katBEG* + Tn7_*katG* expressing roGFP via pDSK-roGFP	Rifampicin, nitrofurantoin, kanamycin, gentamicin	This study
Pst T1 (pDSK-roGFP)	Pst T1 expressing roGFP via pDSK-roGFP	Kanamycin	This study
E. coli JHI-5025 (pDSK-roGFP)	*E. coli* JHI-5025 expressing roGFP via pDSK-roGFP	Kanamycin	This study
Strains to act as controls in roGFP experiments			
Pst DC3000 (pDSK519)	Pst DC3000 with pDSK519	Rifampicin, nitrofurantoin, kanamycin	This study
Pst DC3000 Δ*oxyR* (pDSK519)	Pst DC3000 Δ*oxyR* with pDSK519	Rifampicin, nitrofurantoin, kanamycin	This study
Pst DC3000 Δ*oxyR* + Tn7_*oxyR* (pDSK519)	Pst DC3000 Δ*oxyR* + Tn7_*oxyR* with pDSK519	Rifampicin, nitrofurantoin, kanamycin, gentamicin	This study
Pst DC3000 Δ*katBEG* (pDSK519)	Pst DC3000 Δ*katBEG* with pDSK519	Rifampicin, nitrofurantoin, kanamycin	This study
Pst DC3000 ΔkatBEG +	Pst DC3000 Δ*katBEG* + Tn7_*katG* with pDSK519	Rifampicin, nitrofurantoin,	This study

Tn7_*katG* (pDSK519)		kanamycin, gentamicin	
Pst T1 (pDSK519)	Pst T1 roGFP with pDSK519	Kanamycin	This study
E. coli JHI-5025 (pDSK519)	*E. coli* JHI-5025 roGFP with pDSK519	Kanamycin	This study
Transcriptional fusion fluorescent reporter strains[a]			
E. coli JHI-5025 (p_{gyrA}-GFP+, pOPS0378)	*E. coli* JHI-5025 with a *gyrA* transcriptional fusion fluorescent reporter via p_{gyrA}-GFP+ and constitutive mCherry expression via pOPS0378	Chloramphenicol, kanamycin, neomycin	This study
E. coli JHI-5025 (p_{oxyR}-GFP+, pOPS0378)	*E. coli* JHI-5025 with an *oxyR* transcriptional fusion fluorescent reporter via p_{oxyR}-GFP+ and constitutive mCherry expression via pOPS0378	Chloramphenicol, kanamycin, neomycin	This study
E. coli JHI-5025 (p_{katG}-GFP+, pOPS0378)	*E. coli* JHI-5025 with a *katG* transcriptional fusion fluorescent reporter via p_{katG}-GFP+ and constitutive mCherry expression via pOPS0378	Chloramphenicol, kanamycin, neomycin	This study
E. coli JHI-5025 (p_{soxR}-GFP+, pOPS0378)	*E. coli* JHI-5025 with a *soxR* transcriptional fusion fluorescent reporter via p_{soxR}-GFP+ and constitutive mCherry expression via pOPS0378	Chloramphenicol, kanamycin, neomycin	This study
E. coli JHI-5025 (p_{soxS}-GFP+, pOPS0378)	*E. coli* JHI-5025 with a *soxS* transcriptional fusion fluorescent reporter via p_{soxS}-GFP+ and constitutive mCherry expression via pOPS0378	Chloramphenicol, kanamycin, neomycin	This study
E. coli JHI-5025 (p_{lexA}-GFP+, pOPS0378)	*E. coli* JHI-5025 with a *lexA* transcriptional fusion fluorescent reporter via p_{lexA}-GFP+ and constitutive mCherry expression via pOPS0378	Chloramphenicol, kanamycin, neomycin	This study
E. coli JHI-5025 (p_{ramA}-GFP+, pOPS0378)	*E. coli* JHI-5025 with a *ramA* transcriptional fusion fluorescent reporter via p_{ramA}-GFP+ and constitutive mCherry expression via pOPS0378	Chloramphenicol, kanamycin, neomycin	This study
E. coli JHI-5025 (pKC026, pOPS0378)	*E. coli* JHI-5025 with a transcriptional fusion fluorescent reporter negative control via pKC026 and	Chloramphenicol, kanamycin, neomycin	This study

	constitutive mCherry expression via pOPS0378		
Strains for flow cytometry compensations			
E. coli JHI-5025 (pKC026)	*E. coli* JHI-5025 with a transcriptional fusion fluorescent reporter negative control via pKC026	Chloramphenicol	This study
E. coli JHI-5025 (p_{gyrA}-GFP+)	*E. coli* JHI-5025 with a *gyrA* transcriptional fusion fluorescent reporter via p_{gyrA}-GFP+	Chloramphenicol	Gifted from Holden lab
E. coli JHI-5025 (pOPS0378)	*E. coli* JHI-5025 with constitutive mCherry expression via pOPS0378	Kanamycin, neomycin	This study
Strains for plasmid extractions[b]			
E. coli S17-1 (pK18mobsacB)	*E. coli* S17-1 with pK18mobsacB	Kanamycin	(Schäfer *et al.*, 1994) (strain with plasmid was received from Alan Collmer lab)
E. coli (pUC18T-mini_Tn7T-Gm-dsRedExpress)	*E. coli* with pUC18T-mini_Tn7T-Gm-dsRedExpress	Gentamicin, carbenicillin	(Choi and Schweizer, 2006)
E. coli AAEC185A (pKC026)	*E. coli* AAEC185A with pKC026	Chloramphenicol	(Holden *et al.*, 2007)
E. coli ST18 (pOPS0378)	*E. coli* ST18 with pOPS0378	Kanamycin	(Mendoza-Suárez *et al.*, 2020)
E. coli S17 λpir (pDSK-roGFP)	*E. coli* S17 λpir with pDSK-roGFP	Kanamycin	(Solmi *et al.*, 2023)
E. coli (pDSK519)	*E. coli* with pDSK519	Kanamycin	(Keen *et al.*, 1988)

[a]transcriptional fusion reporter strains before transformation with pOPS0378 have not been included in this table, apart from those that were used for flow cytometry compensations.

[b]strains for plasmid extractions of plasmids that were constructed in this study have not been included in this table.

Plasmids used for this study are listed in table 3.4.

Table 3.4: Plasmids used in this study

Plasmid	Description	Antibiotic resistance	Reference
For production of transcriptional fusion fluorescent reporters			
pKC026 (also referred to as pKC26)	Promoter-less GFP+ plasmid	Chloramphenicol	(Holden *et al.*, 2007)
p_{gyrA}-GFP+	pKC026 with *gyrA* upstream region (from *E. coli*) fused to GFP+	Chloramphenicol	(Holden *et al.*, 2006)
p_{oxyR}-GFP+	pKC026 with *oxyR* upstream region (from Stm SL1344) fused to GFP+	Chloramphenicol	This study
p_{katG}-GFP+	pKC026 with *katG* upstream region (from Stm SL1344) fused to GFP+	Chloramphenicol	This study
p_{soxR}-GFP+	pKC026 with *soxR* upstream region (from Stm SL1344) fused to GFP+	Chloramphenicol	This study
p_{soxS}-GFP+	pKC026 with *soxS* upstream region (from Stm SL1344) fused to GFP+	Chloramphenicol	This study
p_{lexA}-GFP+	pKC026 with *lexA* upstream region (from Stm SL1344) fused to GFP+	Chloramphenicol	This study
p_{ramA}-GFP+	pKC026 with *ramA* upstream region (from Stm SL1344) fused to GFP+	Chloramphenicol	This study
pOPS0378	Constitutive mCherry expression under regulation of the *nptII* promoter	Kanamycin, neomycin	(Mendoza-Suárez *et al.*, 2020)
For production of Pst DC3000 Δ*oxyR* and complement strain			
pK18mobsacB	Backbone used for plasmid construction for the production of deletion mutants	Kanamycin	(Schäfer *et al.*, 1994)
pK18mobsacB_ oxyR_deletion	pk18mobsacB backbone fused with flanking regions from *oxyR* in Pst DC3000 for the production of Pst DC3000 Δ*oxyR*	Kanamycin	This study
pUC18T-mini_Tn7T-Gm-dsRedExpress	pUC18T backbone used for plasmid construction for the production of deletion mutant complement strains	Gentamicin, carbenicillin	(Choi and Schweizer, 2006)
pUC18T-mini_Tn7T-Gm-oxyR	pUC18T backbone fused with *oxyR* from Pst DC3000 for the production of Pst DC3000 Δ*oxyR* complement	Gentamicin, carbenicillin	This study
pRK2013	Suicide plasmid required for the production of a secretion system for the mobilisation of non-self-transmissible plasmids.	Kanamycin	(Figurski and Helinski, 1979)

pUX-BF13	Suicide plasmid for the delivery of the Tn7 transposase complex: *TnsABCDE.*	Carbenicillin	(Miller and Mekalanos, 1988)
For production of roGFP transformants and control strains			
pDSK-roGFP	Broad host range plasmid: roGFP2 in pDSK519 backbone	Kanamycin	(Solmi *et al.*, 2023)
pDSK519	Broad host range plasmid.	Kanamycin	(Keen *et al.*, 1988)

Primers used for this study are listed in table 3.5.

Table 3.5: Primers used in this study

Primer	Sequence (5' – 3')	Use
For production of transcriptional fusion fluorescent reporters[a]		
oxyR_For_2	GCTCTAGAGCCATCAACGATGCGAAGGC	Forward primer for amplification of Stm SL1344 *oxyR* upstream region
oxyR_Rev_2	GCTCTAGATCCGTCGCCACGATAGTTCAT	Reverse primer for amplification of Stm SL1344 *oxyR* upstream region
katG_F	GCTCTAGACCTCCAGCTCCCTGCCGGGAGC	Forward primer for amplification of Stm SL1344 *katG* upstream region
katG_R	GCTCTAGACCCTTTTAAAGTGTTACCGTTACG	Reverse primer for amplification of Stm SL1344 *katG* upstream region
soxR_For_1	GCTCTAGAGCAAATACCACTTGGAGTAGC	Forward primer for amplification of Stm SL1344 *soxR* upstream region
soxR_Rev_2	GCTCTAGACTCAAGTTAACTTGAGGAATTATAC	Reverse primer for amplification of Stm SL1344 *soxR* upstream region
soxS_For_1	GCTCTAGAGCTTAACGTATGTCCTTCCG	Forward primer for amplification of Stm SL1344 *soxS* upstream region
soxS_Rev_2	GCTCTAGATCTTAAACAGTATTCGATTCG	Reverse primer for amplification of Stm SL1344 *soxS* upstream region
lexA_F	GCTCTAGAGCATCGGTTCTGAATACCATGAGC	Forward primer for amplification of Stm SL1344 *lexA* upstream region
lexA_Stm_R	GCTCTAGACCCTGGGTGTATATACAATCATGC	Reverse primer for amplification of Stm SL1344 *lexA* upstream region
ramA_For_1	GCTCTAGAGCCGCTTCCAGTAATGC	Forward primer for amplification of Stm SL1344 *ramA* upstream region
ramA_Rev_1	GCTCTAGACCTCTATCAAACTCGTCAGC	Reverse primer for amplification of Stm SL1344 *ramA* upstream region
pKC026_For	GAACGGGTGCGCATAGAAA	Forward primer for checking inserts in pKC026 by colony PCR and sequencing
GFP+Fusion	CCGTATGTAGCATCACCT	Reverse primer for checking inserts in pKC026 by colony PCR and sequencing
For production of Pst DC3000 Δ*oxyR*[b]		
oxyR_L_F	TACCGCCTTTGAGTGAGCTGATACCGCTATAGCGGTAGTCTGTTGTTGGT	Forward primer for amplification of Pst DC3000 *oxyR* upstream region
oxyR_L_R	TCTACTGCCTAGCTCGCGACTGTAAGAGTCATAACGTGCGTCCATG	Reverse primer for amplification of Pst DC3000 *oxyR* upstream region
oxyR_R_F	CATGGACGCACGTTATGACTCTTACAGTCGCGAGCTAGGCAGTAGA	Forward primer for amplification of Pst DC3000 *oxyR* downstream region
oxyR_R_R	TTCCCTTGTCCAGATAGCCCAGTAGCGAACCGACATCACCCTGAATCAAG	Reverse primer for amplification of Pst DC3000 *oxyR* downstream region
pK18mobsacB_GA_F	GCTACTGGGCTATCTGGACAAGGGAA	Forward primer for amplification of pK18mobsacB plasmid backbone
pK18mobsacB_GA_R	CGGTATCAGCTCACTCAAAGGCGGTA	Reverse primer for amplification of pK18mobsacB plasmid backbone

pK18mobsacB_seq_F	TTGCTCACATGTTCTTTCCTGCG	Forward primer for checking inserts in pK18mobsacB by colony PCR and sequencing
pK18mobsacB_seq_R	TTCGCTTGCTGTCCATAAAACCG	Reverse primer for checking inserts in pK18mobsacB by colony PCR and sequencing
DC3000_oxyR_seq_F	ATGGACGTCATGAACACGCTTCGC	Forward primer for checking for Pst DC3000 Δ*oxyR* by colony PCR
DC3000_oxyR_seq_R	GCGCTGAAAGTTGATGTAATGCTGC	Reverse primer for checking for Pst DC3000 Δ*oxyR* by colony PCR
For production of Pst DC3000 Δ*oxyR* complement strain[b]		
oxyR_KO_comp_F_real	TTTTGAAGCTAATTCGATCATGCATGACGCTGGATAAACGCTGAATTGC	Forward primer for amplification of Pst DC3000 *oxyR* and its upstream region
oxyR_KO_comp_R_real	ACTAGATTTCACTTATCTGGTTGGCCTCTACTGCCTAGCTCGCGAC	Reverse primer for amplification of Pst DC3000 *oxyR* and its upstream region
BB_F	GGCCAACCAGATAAGTGAAATCTAGT	Forward primer for amplification of pUC18T miniTn7T-Gm plasmid backbone
BB_R	TCATGCATGATCGAATTAGCTTCAAAA	Reverse primer for amplification of pUC18T miniTn7T-Gm plasmid backbone
Tn7_lux_seq_F	TGCTGTTGACAAAGGGAATCAG	Forward primer for checking inserts in pUC18T miniTn7T-Gm by colony PCR and sequencing
Tn7_seq_R	GCAGCGCCCAAACATAACAG	Reverse primer for checking inserts in pUC18T miniTn7T-Gm by colony PCR and sequencing
glms_F	AATCCGACCTGACCCTGCT	Forward primer for confirmation that Tn7 transposon had inserted into expected genomic site of *P. syringae*
Right_end_Tn7_transposon	CACGCCCCTCTTTAATACGACGG	Reverse primer for confirmation that Tn7 transposon had inserted into expected genomic site of *P. syringae*
For confirmation of pDSK519 presence		
New_Pdsk_F	TGACCATGATTACGCCAAGC	Forward primer for checking presence of pDSK519
New_Pdsk_R	CCGTCAAGTCAGCGTAATGC	Reverse primer for checking presence of pDSK519

[a] 5' nucleotide tails that were added for XbaI digestion have been underlined.

[b] 5' nucleotide tails that were added for Gibson assembly have been underlined.

3.2.3 Media and growth conditions

Media

The following media were used in this study:

- Lysogeny broth (LB) medium: 10 g/L tryptone, 5 g/L yeast extract, 10 g/L NaCl
- Kings B (KB) medium: 20 g/L proteose peptone no. 3, 1.5 g/L K_2HPO_4, 12.5 mM $MgSO_4.7H_2O$, 1% (v/v) glycerol
- M9 medium: 6 g/L $Na_2HPO_4.7H_2O$, 3 g/L KH_2PO_4, 0.5 g/L NaCl, 1 g/L NH_4Cl, 0.1 mM $CaCl_2$, 2 mM $MgSO_4.7H_2O$, 0.4% (v/v) glucose
- Super optimal broth with catabolite repression (SOC) medium: 20 g/L tryptone, 5 g/L yeast extract, 0.5 g/L NaCl, 2.5 mM KCl, 0.4 mM $MgCl_2$, 0.8 mM glucose, pH adjusted to 7

For solid media, agar was added at 1.5% (w/v). Antibiotics were generally used at the following concentrations, unless otherwise stated: 50 µg/ml carbenicillin, 25 µg/ml chloramphenicol, 10 µg/ml gentamicin, 50 µg/ml kanamycin, 25 µg/ml nitrofurantoin.

Growth conditions

All bacterial strains were stored in 25% glycerol at -80^{o}C. They were cultured onto LB agar and incubated at 28^{o}C (37^{o}C for *S. enterica* only) for 1 - 2 days until single colonies appeared. Single colonies were used to inoculate 10 ml LB (or an otherwise stated medium), which was incubated at 28^{o}C (37^{o}C for *S. enterica* only), 220 rpm overnight (20 to 24 hours). If required, antibiotics were added to liquid or solid media at the working stock concentrations mentioned above. Bacteria hosting plasmids were always grown in the presence of the relevant antibiotic. Bacteria which had a genomic integration at the Tn7 attachment (attTn7) site were only grown in the presence of the relevant antibiotics

for the chromosomal insertion on LB agar but not liquid medium because the chromosomal insertion is stable in the absence of antibiotics (Choi *et al.*, 2005).

3.2.4 Production of transcriptional fusion fluorescent reporters

Restriction enzyme digestion and ligation were used to insert gene promoter regions (amplified from *S. enterica* sv. Typhimurium (Stm) SL1344) into the XbaI site of the promoter-less GFP+ pKC026 plasmid, respectively, to produce GFP+ transcriptional fusion reporters (table 3.4). Assembled plasmids were placed into *E. coli* JHI-5025, which were then subsequently transformed with a constitutive mCherry plasmid so that they could be identified during flow cytometry for the measurement of GFP+ reporter activity.

Plasmid construction for transcriptional fusion fluorescent reporters

A plasmid preparation of pKC026 (table 3.4) was obtained from *E. coli* AAEC185A (pKC026) (table 3.3).

Plasmid preparation: Macherey-Nagel Nucleospin Plasmid Quickpure Kit (FisherScientific, UK) was used according to the manufacturer's instructions (revision 07, 07/2010). A modification to the manufacturer's protocol was that 10 ml overnight culture was centrifuged at 3214 x g for 8 minutes before supernatant removal and pellet resuspension. Plasmids to be used for electrotransformation were eluted in sterile water.

Promoter regions of genes involved in the oxidative stress response (*oxyR*, *katG*, *soxR*, *soxS*, *lexA*, *ramA*) were PCR-amplified from Stm SL1344 (table 3.3) genomic DNA (which had been prepared using the Blood & cell culture DNA kit (Qiagen, UK)) using Phusion high-fidelity DNA polymerase (New England Biolabs, UK) or Q5 high-fidelity DNA polymerase (New England Biolabs, UK). Primers for this (table 3.5) were designed using the published sequence for Stm SL1344 (ASM21085v2) so that genomic upstream regions up to 550 bp long were amplified. PCR products were cleaned up using the Wizard® SV gel and PCR clean up system (Promega, UK) and were subjected to XbaI

(Promega, UK) digestion at 37ºC for 2 hours, along with the pKC026 plasmid respectively, so that compatible sticky ends were generated for the ligation of PCR products into pKC026, respectively. To prevent the digested pKC026 from religating with itself, thermosensitive alkaline phosphatase (TSAP) (Promega, UK) was applied according to the manufacturer's instructions (revised 03/2018) for dephosphorylation of 5' ends. Digested products were cleaned up with the Wizard® SV gel and PCR clean up system (Promega, UK) and T4 DNA ligase was used for ligations according to the manufacturer's instructions (revised 04/2018) to generate transcriptional fusion plasmids: p_{oxyR}-GFP+, p_{katG}-GFP+, p_{soxR}-GFP+, p_{soxS}-GFP+, p_{lexA}-GFP+, p_{ramA}-GFP+ (table 3.4).

Assembled plasmids were heat-shock transformed (New England Biolabs, 2019) into *E. coli* AAEC185A competent cells or Invitrogen subcloning efficiency DH5α competent cells (ThermoFisher Scientific, UK) (table 3.3), which were recovered in SOC at 37ºC, static for 1 hour before being spread onto LB agar with chloramphenicol and incubated overnight at 37ºC. The presence of assembled plasmids in resultant colonies was checked by colony PCR with GoTaq G2 DNA polymerase (Promega, UK) using the primer pair pKC026_For, GFP+Fusion (table 3.5). A colony of a successful transformant was grown overnight in LB at 37ºC, 220 rpm with chloramphenicol and used for a plasmid preparation, as previously described. Promoter sequences within plasmids were confirmed by Sanger sequencing (Source Bioscience, UK) with the primer pair pKC026_For, GFP+Fusion (table 3.5).

<u>*E. coli* JHI-5025 transformation with transcriptional fusion reporters</u>

p_{oxyR}-GFP+, p_{katG}-GFP+, p_{soxR}-GFP+, p_{soxS}-GFP+, p_{lexA}-GFP+, p_{ramA}-GFP+ and pKC026 plasmids (table 3.4) were respectively delivered into electrocompetent *E. coli* JHI-5025 (table 3.3) by electrotransformation (p_{gyrA}-GFP+ in *E. coli* JHI-5025 was gifted from the Holden lab).

Electrocompetent cell preparation: Electrocompetent cells were made by diluting an overnight culture into fresh LB by a factor of 1:100, and incubating it at 28ºC, 220 rpm

until it had an OD_{600nm} of 0.3 - 0.5. Cultures were then chilled on ice for 10 - 15 minutes, centrifuged at 4ºC, 3214 x g (maximum speed of Centrifuge 5810R (Eppendorf, Germany)) for 8 minutes, washed in ice cold 10% glycerol twice and resuspended in ice cold 10% glycerol equivalent to 0.01 x the original volume.

Electrotransformation: 200 ng plasmid was added to 80 µl electrocompetent cells and incubated on ice for 10 minutes. The mixture was then transferred to a pre-chilled Fisherbrand Electroporation Cuvette Plus with a 2 mm width gap (FisherScientific, USA) and electrotransformation was completed using a Biorad gene pulser, Biorad pulse controller and Biorad capacitance extender at 2500 volts, 200-ohm resistance, 25-µF capacitance. *E. coli* was recovered in 0.5 ml SOC and incubated at 37ºC, 220 rpm for 1 hour. Cultures were then spread onto LB agar with the relevant antibiotic(s) for plasmid selection and *E. coli* was incubated at 37ºC overnight.

The presence of plasmids in resultant colonies was checked by colony PCR with GoTaq G2 DNA polymerase (Promega, UK) using the primer pair pKC026_For, GFP+Fusion (table 3.5).

Addition of a constitutive mCherry plasmid into *E. coli* JHI-5025 transcriptional fusion reporters

A plasmid preparation of pOPS0378 (table 3.4) was obtained from *E. coli* ST18 (pOPS0378) as previously described (table 3.3).

pOPS0378 was delivered into the following GFP+ reporter strains (which had previously been made electrocompetent) by electrotransformation, as previously described: *E. coli* JHI-5025 (pKC026), *E. coli* JHI-5025 (p_{gyrA}-GFP+), *E. coli* JHI-5025 (p_{oxyR}-GFP+), *E. coli* JHI-5025 (p_{katG}-GFP+), *E. coli* JHI-5025 (p_{soxR}-GFP+), *E. coli* JHI-5025 (p_{soxS}-GFP+), *E. coli* JHI-5025 (p_{lexA}-GFP+), *E. coli* JHI-5025 (p_{ramA}-GFP+). pOPS0378 was also delivered into electrocompetent wild-type *E. coli* JHI-5025 by electrotransformation, which was required for flow cytometry compensations. Colonies of successful transformants were

grown overnight in LB at 37ºC, 220 rpm with the relevant antibiotics. The presence of pOPS0378 and GFP+ reporter plasmids in the cultures were confirmed by fluorescence measurements with an Infinite M200 plate reader (Tecan, Switzerland). mCherry in pOPS0378 was detected by excitation at 565 - 575 nm and emission at 620 - 640 nm and GFP+ in GFP+ reporter plasmids was detected by excitation at 465 - 475 nm and emission at 500 - 520 nm.

3.2.5 Production of Pst DC3000 Δ*oxyR* and its complemented strain

Two-step allelic exchange was used to produce Pst DC3000 Δ*oxyR* (Kvitko and Collmer, 2011; Hmelo *et al.*, 2015). A complemented strain was also generated by the insertion of *oxyR* into the attTn7 site of the deletion mutant by four parental mating conjugation.

Plasmid construction for Pst DC3000 Δ*oxyR*

~1 kb regions which flanked each side of *oxyR* were PCR-amplified from Pst DC3000 genomic DNA with Q5 high-fidelity DNA polymerase (New England Biolabs, UK) using primer pairs oxyR_L_F, oxyR_L_R for the upstream region and oxyR_R_F, oxyR_R_R for the downstream region (table 3.5). Primers were designed using the published sequence for Pst DC3000 (NC_004578.1), so that the upstream and downstream regions contained the start and stop codons of *oxyR*, respectively, plus a few adjacent in-frame codons of *oxyR*. This was so that the end result of the deletion would be a drastically truncated OxyR protein. Gibson assembly (Gibson *et al.*, 2009) was used to assemble the two flanking regions into a pK18mobsacB plasmid backbone, which was PCR-amplified from the pK18mobsacB plasmid (Schäfer *et al.*, 1994) with Q5 high-fidelity DNA polymerase (New England Biolabs, UK) using the primer pair pK18mobsacB_GA_F, pK18mobsacB_GA_R (table 3.5). The assembled plasmid, pK18mobsacB_oxyR_deletion (table 3.4), was heat-shock transformed (New England Biolabs, 2019) into Invitrogen subcloning efficiency DH5α competent cells (ThermoFisher Scientific, UK), which were recovered in LB broth at 37ºC, 220 rpm for 1 hour before being spread onto LB agar with

kanamycin and incubated at 37ºC overnight. The presence of pK18mobsacB_oxyR_deletion in resultant colonies was checked by colony PCR with GoTaq G2 DNA polymerase (Promega, UK) using the primer pair pK18mobsacB_seq_F, pK18mobsacB_seq_R (table 3.5). A colony of a successful transformant was grown overnight in LB at 37ºC, 220 rpm with kanamycin and used for a plasmid preparation (section 3.2.4). The sequence of the combined flanking regions within pK18mobsacB_oxyR_deletion was validated by Sanger sequencing (Source Bioscience, UK) with the primer pair pK18mobsacB_seq_F, pK18mobsacB_seq_R (table 3.5).

Production of Pst DC3000 Δ*oxyR*

pK18mobsacB_oxyR_deletion (table 3.4) was transformed into Pst DC3000 by triparental mating conjugation. This was completed to allow for a single crossover event between either the upstream or downstream region of *oxyR* in the plasmid and the homologous region in the Pst DC3000 genome, which would result in the integration of the entire assembled plasmid into the genome of Pst DC3000.

Triparental mating: Overnight cultures of the donor, recipient (strain to be transformed) and helper *E. coli* DH5α (pRK2013) (table 3.3)) were centrifuged at 4000 x g for 5 minutes, washed with LB (prewarmed to 50°C) once and resuspended in LB equivalent to 0.5 x the original volume. 700 µl recipient, 300 µl host and 100 µl of helper were centrifuged together at 4000 x g for 5 minutes and the pellet was resuspended in 50 µl LB (prewarmed to 50°C). This was spotted onto LB agar, left to dry, and incubated at 28°C overnight (20 to 24 hours). The spot was scraped from the plate using a sterile loop, resuspended in 400 µl LB, spread onto LB agar with nitrofurantoin for selection against *E. coli* and the appropriate antibiotic for selection of the plasmid integration, and then incubated at 28°C for 2 days.

A resultant colony from triparental mating was grown in LB at 28ºC, 220 rpm overnight. This was completed to allow for a double crossover event, which would occur between

either the two upstream or two downstream regions of *oxyR* that now existed in the genome. This would remove the assembled plasmid from the genome and result in either a gene deletion or wild-type revertant. To select for a double crossover event, the culture was spread onto KB agar containing 10% (w/v) sucrose and 0.1 mg/ml catalase, and then incubated at 28°C for 2 days. Sucrose allowed for counterselection of the *sacB* marker on the integrated assembled plasmid, and catalase was previously used to select for an *oxyR* deletion mutant (Ishiga and Ichinose, 2015). The presence of the deletion in resultant colonies was checked by colony PCR with GoTaq G2 DNA polymerase (Promega, UK) using the primer pair DC3000_oxyR_seq_F, DC3000_oxyR_seq_R (table 3.5).

Plasmid construction for Pst DC3000 Δ*oxyR* complement

oxyR was PCR-amplified from Pst DC3000 genomic DNA with Q5 high-fidelity DNA polymerase (New England Biolabs, UK) using primers oxyR_KO_comp_F_real and oxyR_KO_comp_R_real (table 3.5). Primers were designed using the published sequence for Pst DC3000 (NC_004578.1) so that the *oxyR* amplicon included the native promoter and ribosome binding site. Gibson assembly (Gibson *et al.*, 2009) was used to assemble the *oxyR* amplicon into a pUC18T miniTn7T-Gm plasmid backbone which was amplified from plasmid pUC18T miniTn7T-Gm-PA1/04/03 DsRedexpress TOT1 (unpublished) (table 3.4) with Q5 high-fidelity DNA polymerase (New England Biolabs, UK) using primers BB_F and BB_R (table 3.5). The assembled plasmid, pUC18T-mini_Tn7T-Gm-oxyR (table 3.4), was heat-shock transformed (New England Biolabs, 2019) into Invitrogen subcloning efficiency DH5α competent cells (ThermoFisher Scientific, UK), which were recovered in LB at 37ºC, 220 rpm for 1 hour before being spread onto LB agar with gentamicin and incubated overnight at 37ºC. The presence of pUC18T-mini_Tn7T-Gm-oxyR in resultant colonies was checked by colony PCR with GoTaq G2 DNA polymerase (Promega, UK) using primers Tn7_lux_seq_F and Tn7_seq_R (table 3.5). A colony of a successful transformant was grown overnight in LB

at 37°C, 220 rpm with gentamicin and used for a plasmid preparation (section 3.2.4). The sequence of the *oxyR* amplicon within pUC18T-mini_Tn7T-Gm-oxyR was validated by Sanger sequencing (Source Bioscience, UK) with primers Tn7_lux_seq_F and Tn7_seq_R (table 3.5).

Production of Pst DC3000 Δ*oxyR* complement

Four parental mating conjugation was used to deliver the *oxyR* amplicon into the attTn7 site of Pst DC3000 Δ*oxyR*. *E. coli* DH5α (pK18mobsacB_oxyR_deletion) (table 3.3) was the donor.

Four parental mating: Overnight cultures of the donor, recipient (strain to be transformed) and helpers (*E. coli* SM10/λ pir (pUX-BF13) and *E. coli* DH5α (pRK2013) (table 3.3)) were centrifuged at 4000 x g for 5 minutes, washed with LB (prewarmed to 50°C) once and resuspended in LB equivalent to 0.5 x the original volume. 700 µl recipient, 300 µl host and 100 µl of each helper were centrifuged together at 4000 x g for 5 minutes and the pellet was resuspended in 50 µl LB (prewarmed to 50°C). This was spotted onto LB agar, left to dry, and incubated at 28°C overnight (20 to 24 hours). The spot was scraped from the plate using a sterile loop, resuspended in 400 µl LB, spread onto LB agar with nitrofurantoin for selection against *E. coli* and the appropriate antibiotic for transposon selection, and then incubated at 28°C for 2 days.

To verify that *oxyR* had integrated into the expected genomic site, colony PCR with GoTaq G2 DNA polymerase (Promega, UK) was performed using the primer pair glms_F (anneals to *glms* which is upstream of the attTn7 site) and Right_end_Tn7_transposon (anneals to the right end of the Tn7 transposon) (table 3.5).

3.2.6 Introduction of pDSK-roGFP and pDSK519 by electrotransformation

To assess the intracellular redox state of bacteria exposed to different treatments, the pDSK-roGFP plasmid (table 3.4) was introduced into the following strains: Pst DC3000,

Pst T1, *E. coli* JHI-5025, Pst DC3000 Δ*oxyR*, Pst DC3000 Δ*oxyR* + Tn7_*oxyR*, Pst DC3000 Δ*katBEG* and Pst DC3000 Δ*katBEG* + Tn7_*katG* (table 3.3). These strains were also transformed with the pDSK519 plasmid (table 3.4), to provide a control for background signal in roGFP experiments.

Plasmid preparations of pDSK-roGFP and pDSK519 were obtained from *E. coli* S17 λpir (pDSK-roGFP) and *E. coli* (pDSK519) respectively (table 3.3) (section 3.2.4). Plasmids were introduced into electrocompetent cells by electrotransformation, and kanamycin was used for pDSK-roGFP and pDSK519 selection. Electrocompetent *E. coli* JHI-5025 was made, and subsequent electrotransformation was completed as previously described (section 3.2.4). Electrocompetent Pst was made from overnight bacterial cultures which were centrifuged at 4ºC, 3214 x g for 8 minutes, washed twice in ice cold 10% glycerol, 1 mM HEPES, and resuspended in ice cold 10% glycerol, 1 mM HEPES equivalent to 0.06 x the original volume. Pst electroporation was completed as previously described (section 3.2.4), however Pst was recovered in 0.5 ml SOC and incubated at 28ºC, 220 rpm for 2 hours. Transformed Pst was then plated on LB agar with kanamycin, and transformed Pst deletion mutants and complement strains were plated on KB agar with 0.1 mg/ml catalase and kanamycin. All Pst stains were then incubated at 28°C for 2 days.

The presence of pDSK-roGFP in transformed colonies was confirmed by fluorescence screening using a FastGene blue light LED illuminator (Geneflow Ltd, UK). The presence of pDSK519 in transformed colonies was confirmed by colony PCR with GoTaq G2 DNA polymerase (Promega, UK) using the primer pair New_Pdsk_F, New_Pdsk_R (table 3.5).

3.2.7 Treatment effects on bacterial growth and culturability

Bacteria preparation

Overnight LB bacterial cultures were diluted into 200 ml fresh LB by a factor of 1:100, which was incubated at 28ºC, 220 rpm until OD_{600nm} 0.35 - 0.6. Bacteria were centrifuged

at 2500 x g for 15 minutes, washed in M9 once, resuspended in M9 equivalent to 0.08 x the original volume and adjusted to OD_{600nm} 0.75 in 5 ml M9.

Treatment application

To account for ozone's reactivity with plastic (Altshuller *et al*., 1961), bacteria were exposed to each treatment in a final volume of 5 ml in a sterile, small glass bottle. This involved the addition of the following components in the listed order, so that all final concentrations would dilute to 1X (bottles were swirled after the addition of each component):

- 867 µl 5X concentrated M9
- 3466 µl 1.33X concentrated treatment (prepared in distilled water)
- 667 µl 7.5X concentrated bacteria (prepared in 1X M9)

The final concentration of bacteria was OD_{600nm} 0.1.

Growth curves

Ozone growth curves with a hydrogen peroxide positive control (no colony counts): bacteria were kept in the glass bottle for 30 minutes before 3 x 150 µl of each sample was dispensed into a 96-well plate.

Hydrogen peroxide, peracetic acid and sodium hypochlorite growth curves (with colony counts): after bacterial addition to each treatment, 3 x 150 µl of each sample was immediately dispensed into a 96-well plate.

96-well plates were incubated at 28^{o}C with shaking in an Infinite M200 plate reader (Tecan, Switzerland), which measured the OD_{600nm} every 30 minutes.

Where colony counts were required, the plate reader was stopped 1 hour after incubation. 5 µl from each well replicate for each sample was pooled and diluted in PBS by a factor of

1:100 so that treatments would be diluted. Serial dilutions by a factor of 10 were completed in PBS and 3 x 20 µl spots from each dilution were dispensed onto LB agar. Plates were left to dry in the laminar flow cabinet and were incubated at 28^{o}C for 22 hours before *E. coli* colonies were counted, and 40 hours before Pst colonies were counted. The mean count for 3 spot replicates was the experimental mean. Samples with a count of 0 were recorded as the limit of detection.

3.2.8 Measurement of the intracellular redox state

Measurement of the intracellular redox state in wildtype strains

A bacterial strain which exclusively carried pDSK-roGFP and the same bacterial strain which exclusively carried pDSK519 were used in experiments to measure the intracellular redox state of the bacterial strain. Bacteria was prepared as described in section 3.2.7, however the final M9 resuspension was equivalent to 0.03 x the original volume and cultures were adjusted to OD_{600nm} 7.5 in 5 ml M9.

Treatments were applied to bacteria as described in section 3.2.7, and the final concentration of bacteria was OD_{600nm} 1.

Separate assays to test various concentrations of a single treatment (aqueous ozone, hydrogen peroxide, peracetic acid or sodium hypochlorite) were conducted. There was an exception for aqueous ozone, where only the highest achievable concentration was tested, and a 2.5 mM hydrogen peroxide positive control was included.

In every assay, bacteria were also exposed to distilled water and final concentrations of 100 mM hydrogen peroxide and 5 mM dithiothreitol (DTT) (table 3.2), in the same way as the other treatments. The hydrogen peroxide and DTT were required to provide controls for the maximum oxidised, and maximum reduced intracellular redox state respectively, which were required for data normalisation.

Since the intracellular redox state of bacteria could change rapidly after being exposed to a treatment, all of the bottles required in each assay were set up with M9 and treatments before the addition of any bacteria. Then, bacteria which exclusively expressed pDSK-roGFP and bacteria which exclusively expressed pDSK519 were added to a treatment at a single concentration in different bottles. The bottles were swirled, and 200 µl of each bacterium was dispensed into adjacent wells in a row of a black 96-well plate (figure 3.6). This was then repeated for other treatments/concentrations, one treatment/concentration at a time, with 45 second gaps between them. Bacteria were always added to 5 mM DTT, 100 mM hydrogen peroxide and water first, because these were expected to provide stable intracellular redox states. Then bacteria were added to the treatment to be tested, starting from the highest concentration (for ozone, the 2.5 mM hydrogen peroxide positive control was measured before ozone). After all samples had been dispensed into the 96-well plate (figure 3.6), the plate was placed into a pre-warmed Infinite M200 plate reader (Tecan, Switzerland) at 28^{o}C, which was started at exactly one minute after the addition of bacteria to the final treatment/concentration. Bacteria were incubated at 28^{o}C and fluorescence was measured at 405 nm (400 - 410 nm bandwidth) and 480 nm (475 - 485 nm bandwidth) excitation, 510 nm (500 - 520 nm bandwidth) emission, at a gain of 120. For fluorescence measurements, the plate reader measured wells row by row continuously, and after each round of measurements had been completed for all samples, the plate was shaken for 2 seconds. Measurements were taken for 1 hour.

	Column 1: (pDSK-roGFP)	Column 2: (pDSK519)
A	5 mM DTT	5 mM DTT
B	100 mM H_2O_2	100 mM H_2O_2
C	Water	Water
D	Treatment concentration 1	Treatment concentration 1
E	Treatment concentration 2	Treatment concentration 2
F	Treatment concentration 3	Treatment concentration 3
G	Treatment concentration 4	Treatment concentration 4

Figure 3.6: 96-well plate set-up for roGFP and control sample measurements in wildtype strains (only the relevant wells are displayed). The brackets indicate the plasmid which the bacterial strain contained in the entire column. Treatments in wells are indicated. Treatment concentration 1 is the highest concentration, which reduced until treatment concentration 4. Some treatments may not have had 4 concentrations. For ozone, the 2.5 mM hydrogen peroxide positive control was measured in the place of treatment concentration 1 and ozone was measured in the place of treatment concentration 2. The arrow indicates the direction in which wells were measured.

Measurement of the intracellular redox state in Pst DC3000 deletion mutants and complement strains

pDSK-roGFP-expressing variants and pDSK519-expressing variants of either Pst DC3000 Δ*oxyR* and Pst DC3000 Δ*oxyR* + Tn7_*oxyR* or Pst DC3000 Δ*katBEG* and Pst DC3000 Δ*katBEG* + Tn7_*katG* were used in a roGFP assay at one time with the wildtype Pst DC3000 (table 3.3).

Overnight KB bacterial cultures were diluted into 20 ml fresh KB by a factor of 1:50, which was incubated at 28^{o}C, 220 rpm until OD_{600nm} 0.35 - 0.6. Bacteria were centrifuged at 2500 x g for 15 minutes, washed in M9 once, resuspended in M9 equivalent to 0.05 x the original volume and adjusted to OD_{600nm} 2 in 1.5 ml M9.

100 µl of cultures were dispensed into the relevant wells of a black 96-well plate (figure 3.7), which was placed into a pre-warmed Infinite M200 plate reader (Tecan, Switzerland) at 28^{o}C. Fluorescence measurements were taken as previously described for the wild-type strains, for 15 minutes. Then a multichannel pipette was used to dispense 100 µl of each treatment, which was 2X concentrated and made in M9, into the relevant row of the 96-well plate (figure 3.7). M9, and final concentrations of 100 mM hydrogen peroxide and 5 mM DTT were included as treatments in every assay to provide controls for reasons

previously described. After treatment additions, wells were mixed with a multichannel pipette. The plate was put back into the plate reader and fluorescence measurements were taken for 1 hour, as previously described.

	Column 1: strain 1 (pDSK-roGFP)	**Column 2: strain 1 (pDSK519)**	**Column 3: strain 2 (pDSK-roGFP)**	**Column 4: strain 2 (pDSK519)**	**Column 5: strain 3 (pDSK-roGFP)**	**Column 6: strain 3 (pDSK519)**
A	5 mM DTT	5 mM DTT	5 mM DTT	5 mM DTT	5 mM DTT	5 mM DTT
B	100 mM H_2O_2	100 mM H_2O_2	100 mM H_2O_2	100 mM H_2O_2	100 mM H_2O_2	100 mM H_2O_2
C	M9	M9	M9	M9	M9	M9
D	Treatment concentration 1	Treatment concentration 1	Treatment concentration 1	Treatment concentration 1	Treatment concentration 1	Treatment concentration 1
E	Treatment concentration 2	Treatment concentration 2	Treatment concentration 2	Treatment concentration 2	Treatment concentration 2	Treatment concentration 2
F	Treatment concentration 3	Treatment concentration 3	Treatment concentration 3	Treatment concentration 3	Treatment concentration 3	Treatment concentration 3

Figure 3.7: 96-well plate set-up for roGFP and control sample measurements in Pst DC3000 deletion mutants and complement strains (only the relevant wells are displayed). Bacterial strains were the same in every column, and the brackets indicate the plasmid which the bacterial strain contained. Treatments in wells are indicated. Treatment concentration 1 is the lowest concentration, which increased until treatment concentration 3. The arrow indicates the direction in which wells were measured.

3.2.9 Measurement of GFP+ transcriptional fusion reporter activity

Transcriptional fusion fluorescent reporter strains, which carried both a GFP+ reporter plasmid and pOPS0378 for constitutive mCherry expression (table 3.3), were prepared as described in section 3.2.7, however the final M9 resuspension was equivalent to 0.03 x the original volume and cultures were adjusted to OD_{600nm} 7.5 in 5 ml M9.

Treatments were applied to bacteria as described in section 3.2.7 and the final concentration of bacteria was OD_{600nm} 1.

After each treatment application, 150 µl of each sample was dispensed into individual wells of a black 96-well plate which was incubated at 28^{o}C with shaking for a total of 24 hours in an Infinite M200 plate reader (Tecan, Switzerland). During the incubation,

bacterial growth and GFP+ reporter activity was monitored by measuring OD_{600nm}, and fluorescence (465 - 475 nm excitation, 500 - 520 nm emission) respectively. Measurements were taken every 15 minutes for the first 5 hours, and then every 30 minutes. At 1, 5, and 18 hours, the plate reader was stopped and 10 µl of each sample was diluted into Gibco flow cytometry grade PBS (ThermoFisher Scientific, UK) for flow cytometry analysis. At 1 and 5 hours, dilutions were made by a factor of 1:100 and at 18 hours, dilutions were made by a factor of 1:1000. (Only GFP+ data from flow cytometry analysis was used to present reporter activity since it provided data at the single cell level).

For flow cytometry measurements, diluted samples were transferred to a round-bottomed 96-well plate which was sealed with X-pierce film (Merck, UK). Samples were measured row by row from the 96-well plate using the ‘autosampler’ function with a CellStream flow cytometer (Merck, Germany). Samples were positioned in the 96-well plate so that 100 µl of 0.9% NaCl, 0.02% Silwet was positioned in every alternate column, to allow for flow cytometer ‘washing’ between sample measurements (figure 3.8). Samples were also positioned to minimise the time between measurements for each reporter exposed to each treatment (figure 3.8).

	1	2	3	4	5	6	7	8
A	No promoter, H_2O	Wash	No promoter, H_2O_2	Wash	No promoter, $C_2H_4O_3$	Wash	No promoter, NaClO	Wash
B	*gyrA*, H_2O	Wash	*gyrA*, H_2O_2	Wash	*gyrA*, $C_2H_4O_3$	Wash	*gyrA*, NaClO	Wash
C	*soxR*, H_2O	Wash	*soxR*, H_2O_2	Wash	*soxR*, $C_2H_4O_3$	Wash	*soxR*, NaClO	Wash
D	*soxS*, H_2O	Wash	*soxS*, H_2O_2	Wash	*soxS*, $C_2H_4O_3$	Wash	*soxS*, NaClO	Wash
E	*oxyR*, H_2O	Wash	*oxyR*, H_2O_2	Wash	*oxyR*, $C_2H_4O_3$	Wash	*oxyR*, NaClO	Wash
F	*katG*, H_2O	Wash	*katG*, H_2O_2	Wash	*katG*, $C_2H_4O_3$	Wash	*katG*, NaClO	Wash
G	*lexA*, H_2O	Wash	*lexA*, H_2O_2	Wash	*lexA*, $C_2H_4O_3$	Wash	*lexA*, NaClO	Wash
H	*ramA*, H_2O	Wash	*ramA*, H_2O_2	Wash	*ramA*, $C_2H_4O_3$	Wash	*ramA*, NaClO	Wash

Figure 3.8: 96-well plate set-up for flow cytometry analysis (only the relevant wells are displayed). The gene name indicates the reporter gene in the GFP+ transcriptional fusion reporter in *E. coli* JHI-5025. The treatment that reporter strains were exposed to is also indicated. Wash is 0.9% NaCl, 0.02% Silwet. The arrow indicates the direction that wells were sampled by the flow cytometer.

Sample settings were a ‘slow’ rate with the following lasers all switched on at 100%: forward scatter (FSC), side scatter (SSC), 488 nm (for GFP+ excitation) and 561 nm (for mCherry excitation). Events collected per sample ranged from 10,000 - 20,000. For washes, 25 µl of 0.9% NaCl, 0.02% Silwet was fed into the flow cytometer from the 96 well plate at a ‘fast’ rate.

3.2.10 Detection of viable but non-culturable (VBNC) *S. enterica*

Overnight bacterial cultures of Stm SL1344 and *S. enterica* serovar Senftenberg (Ssf) 20070885 (table 3.3) were diluted into 10 ml fresh LB by a factor of 1:100, which was incubated at 37ºC, 220 rpm until OD_{600nm} 0.8 - 1.0. Then, cultures were diluted to OD_{600nm} 0.02 in 1 ml PBS, and 200 µl (in a 1.5 ml Eppendorf tube) was incubated at 70ºC for 3.25 minutes in a pre-heated heat block. Then, cultures were incubated on ice for 10 minutes before being serially diluted by a factor of 10 in PBS. 100 µl of each serial dilution was plated onto both LB agar and LB agar with 0.1% sodium pyruvate, which were incubated at 37ºC for 24 hours before colonies were counted.

3.2.11 Presentation and statistical analysis of data

Data was processed using R version 4.3.1 (R Core Team, 2023) and charts were produced using the ggplot2 package version 3.4.2 (Wickham, 2016). Statistical results with p-values < 0.05 were deemed significant.

Treatment effects on bacterial growth and culturability

To assess the effect of treatments on bacteria, the time before exponential growth was used as a metric, which was referred to as the 'apparent' lag phase. This was defined as the time at which a 50% increase from the initial OD_{600nm} had occurred. The average 'apparent' lag phase length of well replicates was used to present the result of the experimental replicate. Kruskal-Wallis tests were used to determine if concentrations of each treatment had a significant effect on the length of the 'apparent' lag phase in growth curves, and on colony forming units respectively.

Measurement of the intracellular redox state

The data which was collected from roGFP experiments was analysed as described by van der Heijden and Finlay, 2015. Briefly, background fluorescence signal was corrected for at each treatment condition by subtracting the fluorescence values measured from the pDSK519-expressing strain, from the fluorescence values measured from the pDSK-roGFP-expressing strain, at each time point. Then, the corrected fluorescence values which were measured at 405 nm excitation were divided by the corrected fluorescence values which were measured at 480 nm excitation at the same time point, to provide a '405/480 nm ratio'. Then in every individual assay, the data was normalised using 405/480 nm ratio measurements from the same bacterial strain in a maximum oxidised and maximum reduced state. A normalised 405/480 ratio of 1 was made to be equal to the maximum oxidised signal, and 0.1 was made to be equal to the maximum reduced signal.

Because of the experimental design of the roGFP assays for the deletion and complement strains, fluorescence measurements were able to be acquired from bacteria prior to the introduction of any treatments. The 405/480 nm ratio (which had been corrected for background fluorescence signal) was stable in wells prior to the addition of treatments, however its value occasionally, slightly varied between different wells which contained the same bacterium. To account for this, data from the last time-point before the addition of treatments, was used to calculate the difference between the 405/480 nm ratio in all wells, and the 405/480 nm ratio in the well which contained the same bacterium and would be exposed to M9 only. The difference that was calculated for each well was applied to every 405/480 nm ratio that was calculated post-treatment from the same well. The subsequent 405/480 nm ratios were then normalised using the maximum oxidised and maximum reduced signals.

All roGFP charts present the average and standard error from independent experiments.

Measurement of GFP+ transcriptional fusion reporter activity

CellStream Analysis software version 1.4.76 was used for flow cytometry data analysis. Fluorescence compensation settings were determined using the following strains: *E. coli* JHI-5025 (pKC026) as a non-reporter strain, *E. coli* JHI-5025 (p_{gyrA}-GFP+) as a single-coloured GFP+ strain, and *E. coli* JHI-5025 (pOPS0378) as a single-coloured mCherry strain (table 3.3).

Events were gated for bacterial cells to exclude background noise (figure 3.9: A), bacterial cells were gated for single cells (figure 3.9: B), single bacterial cells were gated for mCherry expression (dependent on fluorescence emission at 611 - 631 nm) (figure 3.9: C), and the GFP+ expression (fluorescence emission at 528 - 546 nm) of mCherry cells was visualised (figure 3.9: D). The co-ordinates of these gates remained the same for the analysis of all reporters. The GFP+ expression of mCherry cells had long tails at the end of the normal distribution, which encompassed a very small percentage of the population

(figure 3.9: D), therefore further gating was completed to minimise the presence of these outliers (figure 3.9: D). The co-ordinates of this additional gate remained the same for the analysis of each individual GFP+ reporter strain. A histogram of the GFP+ expression in this final gated region was used to present GFP+ activity (figure 3.9: E). For result presentation, these histograms were overlaid with histograms from the same reporter, which were sampled at the same time point, but were exposed to different treatments.

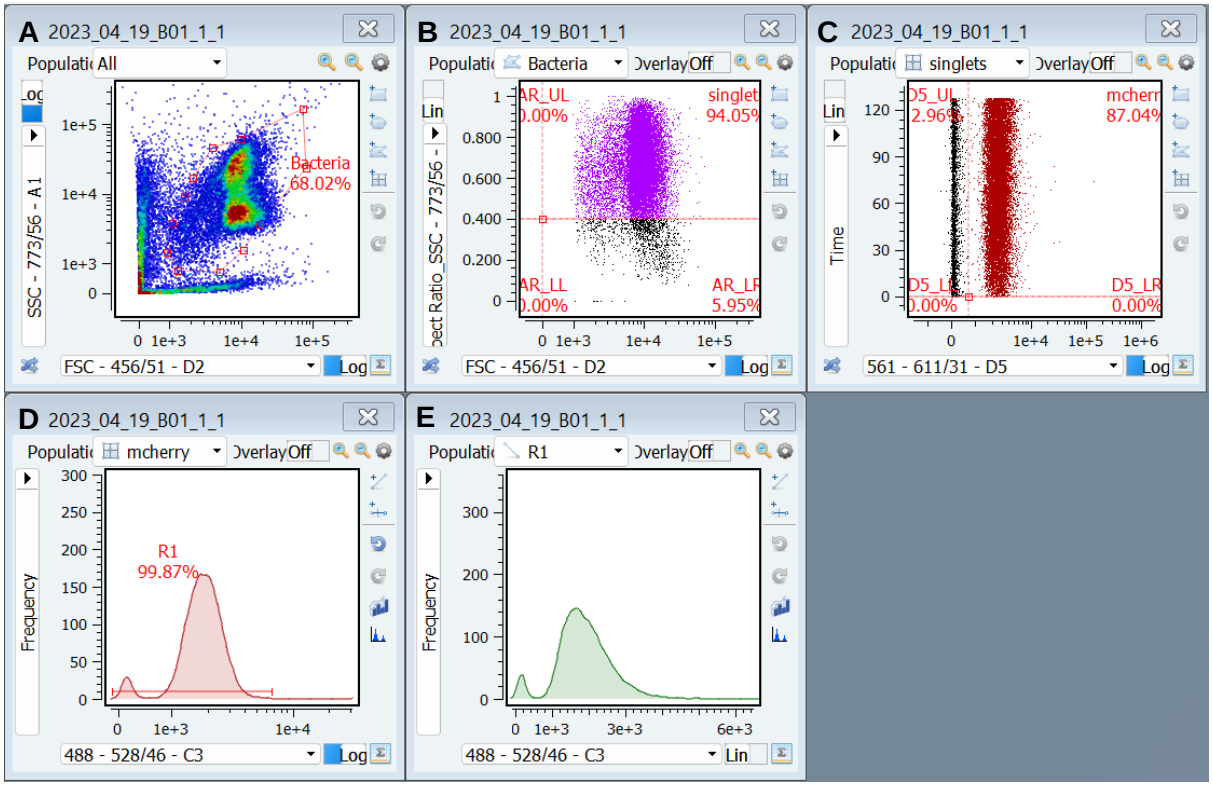


Figure 3.9: Example of flow cytometry data analysis. The charts display data from events collected from *E. coli* JHI-5025 (p_{gyrA}-GFP+, pOPS0378) exposed to distilled water, after 1 hour of incubation at 28ºC, with shaking in an Infinite M200 plate reader. The analysis was completed in CellStream Analysis software version 1.4.76. (**A**) Events were gated for bacterial cells, (**B**) bacterial cells were gated for single cells (**C**), single bacterial cells were gated for mCherry expression, (**D**) mCherry, single bacterial cells were gated to remove outliers with high GFP+ expression. (**E**) A histogram of the GFP+ expression in this final gated region was used to present GFP+ activity.

Only the results from one experiment were presented, but similar results were obtained from two further experimental replicates.

3.3 Results

3.3.1 Aqueous ozone did not extend the 'apparent' lag growth phase

The effect of 1 ppm aqueous ozone (the maximum concentration that could be achieved with the experimental set-up) on the growth of Pst DC3000, Pst T1 and *E. coli* JHI-5025 (table 3.3) was tested. 2 mM hydrogen peroxide was included as a positive control to validate that if ozone did not induce stress, this would not have been due to issues with the experimental set-up.

Bacteria in the early exponential growth phase were exposed to ozone because they would be more susceptible to oxidative stress, in comparison to those in the stationary growth phase. This is because during stationary phase, the *rpoS* regulon is induced which activates genes whose products protect bacteria from oxidative stress (Imlay, 2008, 2015). Bacteria were exposed to treatments in M9 in a glass bottle (final OD_{600nm} 0.1), since ozone can react with plastic (Altshuller *et al*., 1961). Bacteria interacted with treatments in the glass bottle for 30 minutes before being dispensed into a 96-well plate (incubated at 28^{o}C with shaking) for growth (OD_{600nm}) measurements over time. To present the effect of ozone on bacterial growth, the time before exponential growth was used as a metric. The lag phase is typically used to describe this time, however since it refers to the time that is required for bacteria to adapt to a new environment before exponential growth (Rolfe *et al.*, 2012), it was not used. This was because treatments could have caused reductions in bacterial viability which could have prolonged the time before exponential growth was observed by cell density. (Cell density measures the presence of cells regardless of their viability status, and a reduction in viability could increase the time it would take for cells to recover to a population level at which the increase in growth could then become observable by the OD_{600nm} value). Therefore, the time before exponential growth was termed the 'apparent' lag phase. This was used to present the effect of ozone on bacterial growth because antimicrobial treatments which

are strong oxidants, including hydrogen peroxide, sodium hypochlorite and peracetic acid, have been reported to extend it (Watson and Schubert, 1969; Zhang *et al.*, 2019).

Ozone did not significantly affect the 'apparent' lag phase length of any bacterium, whereas the hydrogen peroxide positive control did (Dunn test, $p < 0.05$) (figure 3.10). The full growth curves can be viewed in appendix 8. Interestingly, they show that Pst T1 grew to a higher density when it was grown in aqueous ozone, compared to distilled water.

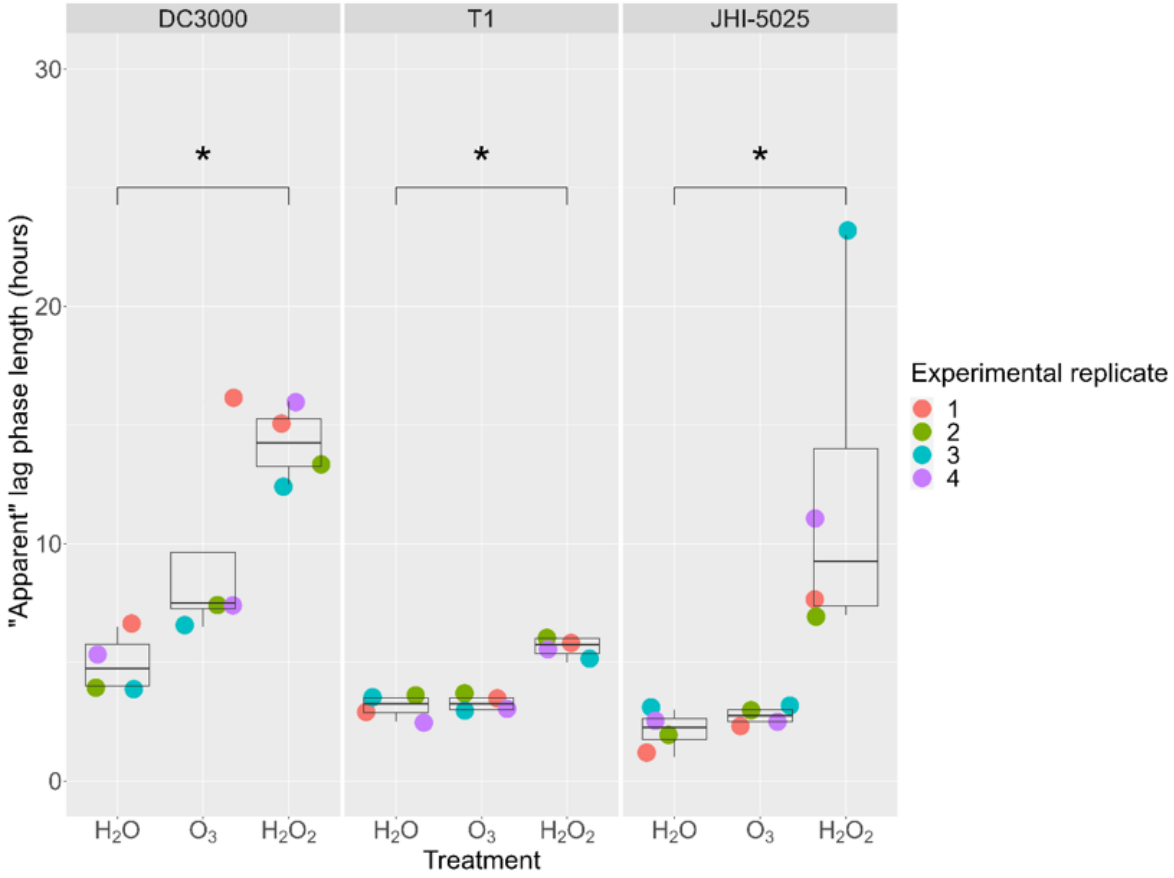


Figure 3.10: Aqueous ozone did not extend the 'apparent' lag growth phase of bacteria, whereas hydrogen peroxide did. Bacteria (*P. syringae* pv. tomato DC3000, *P. syringae* pv. tomato T1, *E. coli* JHI-5025) which had grown to early exponential phase were added into M9 with distilled water, 1 ppm ozone (O_3) or 2 mM hydrogen peroxide (H_2O_2) in a glass bottle (final OD_{600nm} = 0.1). After 30 minutes, bacterial growth (OD_{600nm}) was monitored in a 96-well plate at 28ºC with shaking. The length of the 'apparent' lag phase in growth curves was defined as the time at which a 50% increase from the initial OD_{600nm} had occurred. Boxplots display the median, interquartile range, minimum and maximum values (n = 4). Asterisks indicate significant differences (* = $p <$ 0.05) from Kruskal-Wallis and Dunn tests.

The effect of the other treatments (hydrogen peroxide, peracetic acid and sodium hypochlorite) on bacterial growth and culturability was next investigated.

3.3.2 Hydrogen peroxide, peracetic acid and sodium hypochlorite extended the 'apparent' lag growth phase and reduced culturability

The effect of increasing concentrations of hydrogen peroxide, peracetic acid and sodium hypochlorite on the growth and culturability of Pst DC3000, Pst T1 and *E. coli* JHI-5025 (table 3.3) was tested in the same assay, to determine if bacteria responded similarly to each of these treatments, and to identify if hydrogen peroxide tolerance was correlated with tolerance to other treatments.

Bacteria in the early exponential growth phase were exposed to treatments because as previously described, they would be more susceptible to oxidative stress than those in the stationary growth phase would be (Imlay, 2008, 2015). Bacteria were exposed to treatments in M9 in a glass bottle (final OD_{600nm} 0.1), before being immediately dispensed into a 96-well plate (incubated at 28^{o}C with shaking) for growth (OD_{600nm}) measurements over time. After 1 hour, small aliquots of each sample were extracted and diluted in PBS by a factor of 1:100, to dilute treatments and subsequently halt their effects on bacteria. Then, the number of CFUs in these samples were calculated after incubation on LB agar at 28^{o}C. To present the effect of treatments on bacterial growth, the length of the 'apparent' lag phase was used as a metric because this has been a previously reported effect caused by hydrogen peroxide, sodium hypochlorite and peracetic acid (Watson and Schubert, 1969; Zhang *et al.*, 2019).

Hydrogen peroxide, peracetic acid and sodium hypochlorite all caused significant increases in the length of the 'apparent' lag growth phase (Kruskal-Wallis test, $p < 0.05$), which was generally associated with a reduction in culturability (figures 3.11, 3.12 and 3.13). Each individual experimental replicate for results presented in figures 3.11, 3.12 and 3.13 was completed at the same time, so that the tolerance of bacteria to each

treatment could be more fairly compared. The full growth curves can be viewed in appendix 9. They show that occasionally, the cell density at stationary phase was greater in treated cultures, in comparison to the control.

Since an extended ‘apparent’ lag phase was generally associated with a reduction in culturability, which could have been due to loss of viability, the length of the extended ‘apparent’ lag phase could have been dependent on the time required for each bacterium to resuscitate from a reduced state of viability and the doubling rate of each bacterium. This is because these factors could prolong the time for cells to recover to a population level at which growth would become observable by the OD_{600nm} value. Since resuscitation and doubling times may be factors which affect the post-treatment ‘apparent’ lag phase time, it would not be fair to use this measurement to compare the response of different bacteria to the same treatment, without accounting for these differences. Therefore, the effect of treatments on culturability was used to compare the sensitivity of bacteria to each treatment.

E. coli was the most tolerant bacterium to hydrogen peroxide because after 2 mM hydrogen peroxide exposure, its culturability was not as affected as that of Pst DC3000 or Pst T1 (figure 3.11). *E. coli* was however the most sensitive bacterium to sodium hypochlorite because 1 ppm sodium hypochlorite always reduced the culturability of *E. coli* to below the limit of detection, whereas this was not always the case for Pst T1 or Pst DC3000 (figure 3.13). There were no obvious differences between the sensitivity of each bacterium to peracetic acid (figure 3.12).

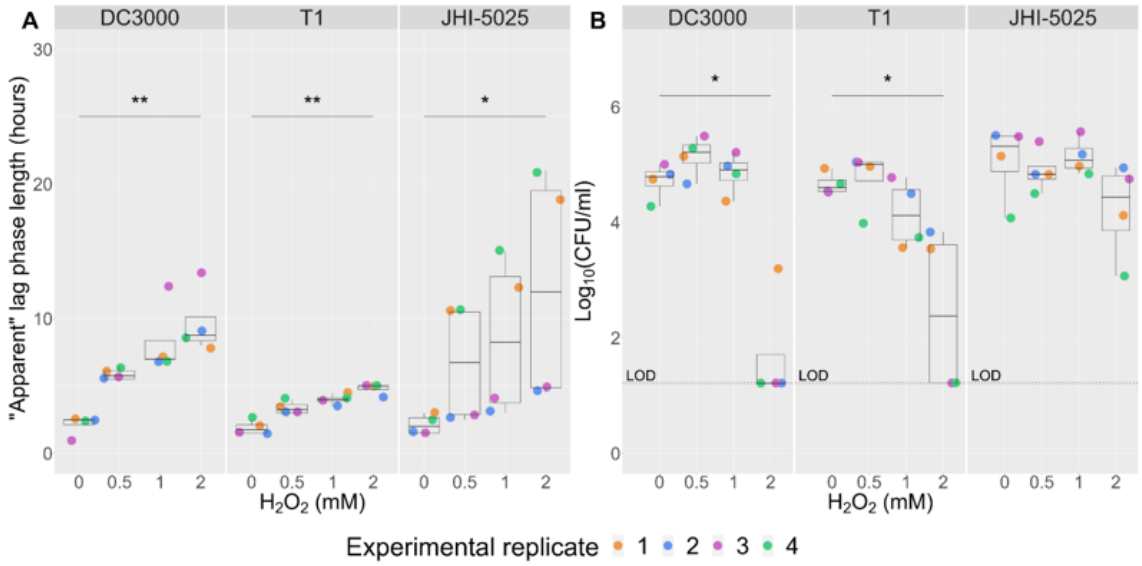


Figure 3.11: Increasing concentrations of hydrogen peroxide caused (A) an extended 'apparent' lag growth phase and (B) a reduction in culturability. Bacteria (*P. syringae* pv. tomato DC3000, *P. syringae* pv. tomato T1, *E. coli* JHI-5025) which had grown to early exponential phase were added into M9 with hydrogen peroxide (H_2O_2) in a glass bottle (final OD_{600nm} = 0.1). Bacterial growth (OD_{600nm}) was immediately monitored in a 96-well plate at 28ºC with shaking. The length of the 'apparent' lag phase was defined as the time at which a 50% increase from the initial OD_{600nm} had occurred. After 1 hour of incubation, cultures were diluted in PBS by a factor of 1:100, which was serially diluted, plated onto LB agar, and incubated at 28ºC. After 22 hours for *E.* coli, and 40 hours for *P. syringae*, colony forming units (CFUs)/ml were calculated. Samples with a count of 0 were recorded as the limit of detection (LOD). Boxplots display the median, interquartile range, minimum and maximum values (n = 3 - 4). Asterisks indicate significant differences (** = $p < 0.01$, * = $p < 0.05$) from Kruskal-Wallis tests.

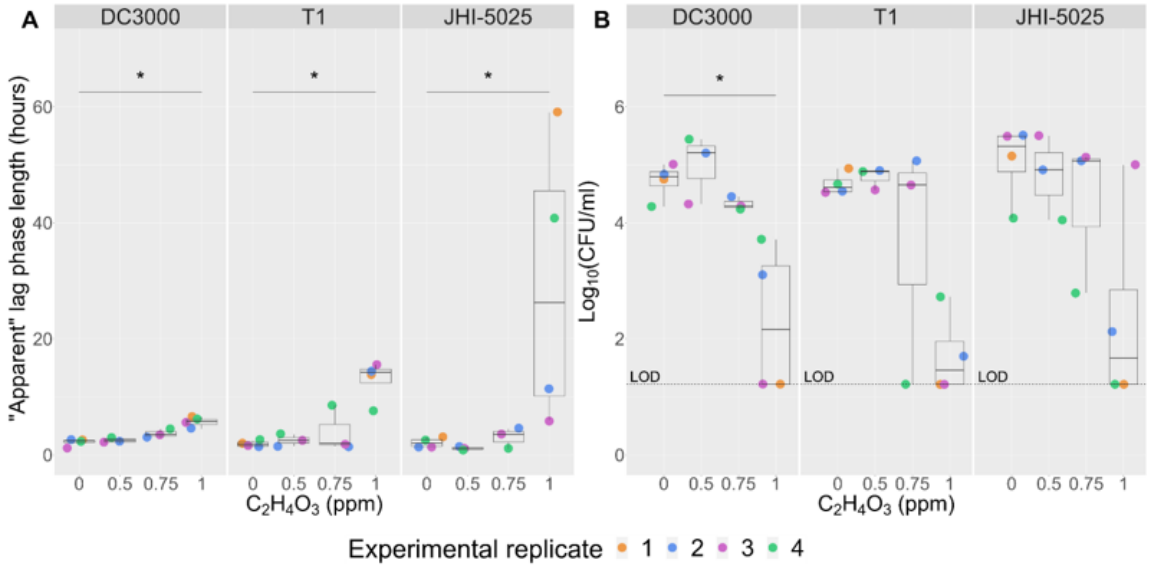


Figure 3.12: Increasing concentrations of peracetic acid caused (A) an extended 'apparent' lag growth phase and (B) a reduction in culturability. Bacteria (*P. syringae* pv. tomato DC3000, *P. syringae* pv. tomato T1, *E. coli* JHI-5025) which had grown to early exponential phase were added into M9 with peracetic acid ($C_2H_4O_3$) in a glass bottle (final OD_{600nm} = 0.1). Bacterial growth (OD_{600nm}) was immediately monitored in a 96-well plate at 28°C with shaking. The length of the 'apparent' lag phase was defined as the time at which a 50% increase from the initial OD_{600nm} had occurred. After 1 hour of incubation, cultures were diluted in PBS by a factor of 1:100, which was serially diluted, plated onto LB agar, and incubated at 28°C. After 22 hours for *E.* coli, and 40 hours for *P. syringae*, colony forming units (CFUs)/ml were calculated. Samples with a count of 0 were recorded as the limit of detection (LOD). Boxplots display the median, interquartile range, minimum and maximum values (n = 3 - 4). Asterisks indicate significant differences (* = $p < 0.05$) from Kruskal-Wallis tests.

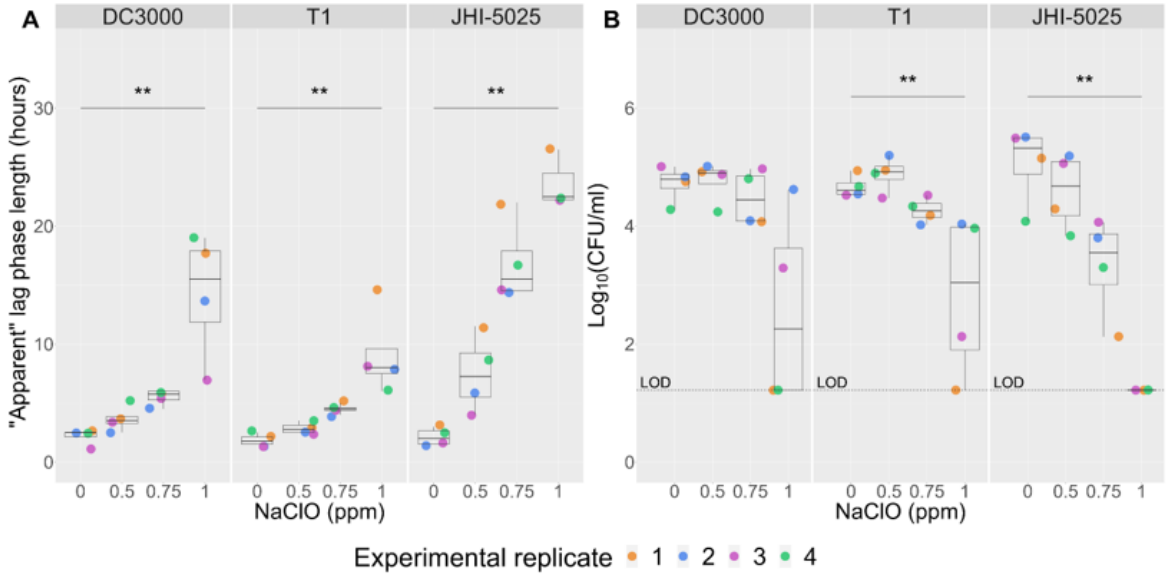


Figure 3.13: Increasing concentrations of sodium hypochlorite caused (A) an extended 'apparent' lag growth phase and (B) a reduction in culturability. Bacteria (*P. syringae* pv. tomato DC3000, *P. syringae* pv. tomato T1, *E. coli* JHI-5025) which had grown to early exponential phase were added into M9 with sodium hypochlorite (NaClO) in a glass bottle (final OD_{600nm} = 0.1). Bacterial growth (OD_{600nm}) was immediately monitored in a 96-well plate at 28°C with shaking. The length of the 'apparent' lag phase was defined as the time at which a 50% increase from the initial OD_{600nm} had occurred. After 1 hour of incubation, cultures were diluted in PBS by a factor of 1:100, which was serially diluted, plated onto LB agar, and incubated at 28°C. After 22 hours for *E.* coli, and 40 hours for *P. syringae*, colony forming units (CFUs)/ml were calculated. Samples with a count of 0 were recorded as the limit of detection (LOD). Boxplots display the median, interquartile range, minimum and maximum values (n = 3 - 4). Asterisks indicate significant differences (** = p < 0.01) from Kruskal-Wallis tests.

To summarise, hydrogen peroxide, peracetic acid and sodium hypochlorite all caused significant increases in the length of the 'apparent' lag growth phase, which was generally associated with a reduction in culturability. *E. coli* was more tolerant than Pst to hydrogen peroxide, but was more sensitive than Pst to sodium hypochlorite, therefore a tolerance to hydrogen peroxide was not always associated with a tolerance to other oxidants. Next, the effect of treatments on the intracellular redox state of bacteria was compared.

3.3.3 All treatments except aqueous ozone increased the intracellular redox state of bacteria

The effect of hydrogen peroxide, ozone, peracetic acid and sodium hypochlorite on the intracellular redox state of Pst DC3000, Pst T1 and *E. coli* JHI-5025 (table 3.3) was investigated and compared, to determine if bacteria responded similarly to each of these

treatments. The experiment was also completed to further identify if there were any correlations in treatment tolerance. For this experiment, bacteria were tagged to express roGFP, a tool for measuring the intracellular redox state (Hanson *et al.*, 2004). roGFP is primarily oxidised or reduced by glutathiones (via glutaredoxins) in bacteria, and the redox state of roGFP affects its fluorescence excitation spectra (Meyer *et al.*, 2007; Schwarzländer *et al.*, 2008). Therefore, the ratio of fluorescence intensity at excitation wavelengths of 405 and 480 nm was used to measure the intracellular redox state of bacteria. A higher ratio indicated a more oxidised state (Hanson *et al.*, 2004).

Bacteria in the early exponential growth phase were exposed to treatments because as previously described, they would be more susceptible to oxidative stress than those in the stationary growth phase would be (Imlay, 2008, 2015). Bacteria were exposed to treatments in M9 in a glass bottle (final OD_{600nm} 1), before being dispensed into a 96-well plate (incubated at 28^{o}C with intermittent shaking) for roGFP fluorescence measurements.

Hydrogen peroxide, peracetic acid and sodium hypochlorite all quickly increased the intracellular redox state of bacteria within minutes (figures 3.14, 3.15, 3.16). 1 ppm aqueous ozone (which was the highest concentration that could be achieved with the experimental set-up) did not affect the intracellular redox state of bacteria, whereas the hydrogen peroxide positive control did (figure 3.17). The ‘starting points’ of signals displayed on the charts in figures 3.14, 3.15, 3.16 and 3.17 represent the time between the addition of bacteria to the treatment and the first measurement.

Increasing concentrations of hydrogen peroxide, peracetic acid and sodium hypochlorite increased the maximum oxidised signal that bacteria reached until very high maximum oxidised signals, near the value of 1, were obtained (which represented the maximum oxidised signal) (figures 3.14, 3.15, 3.16). Occasionally, the peaks of the oxidation states could not be seen, because the start of the redox state measurement occurred during

redox state recovery, therefore oxidation peaks below values near 1 were not seen for Pst DC3000 or *E. coli* in response to peracetic acid (figure 3.15).

Increasing concentrations of hydrogen peroxide, peracetic acid and sodium hypochlorite also increased the length of time that it took for bacteria to recover to a more stable redox state (figures 3.14, 3.15, 3.16). Interestingly, the addition of M9 and water only, increased the intracellular redox state of Pst DC3000 and Pst T1, which they then slowly recovered from. This did not occur in *E. coli* (figures 3.14, 3.15, 3.16, 3.17).

Since the water alone caused an increased intracellular redox state in Pst, it was difficult to make comparisons regarding whether *E. coli* or Pst were more tolerant to each treatment. There were no obvious differences in the tolerance between Pst DC3000 and Pst T1 to hydrogen peroxide or sodium hypochlorite, however Pst T1 was more sensitive to peracetic acid than Pst DC3000 (figures 3.14, 3.15, 3.16).

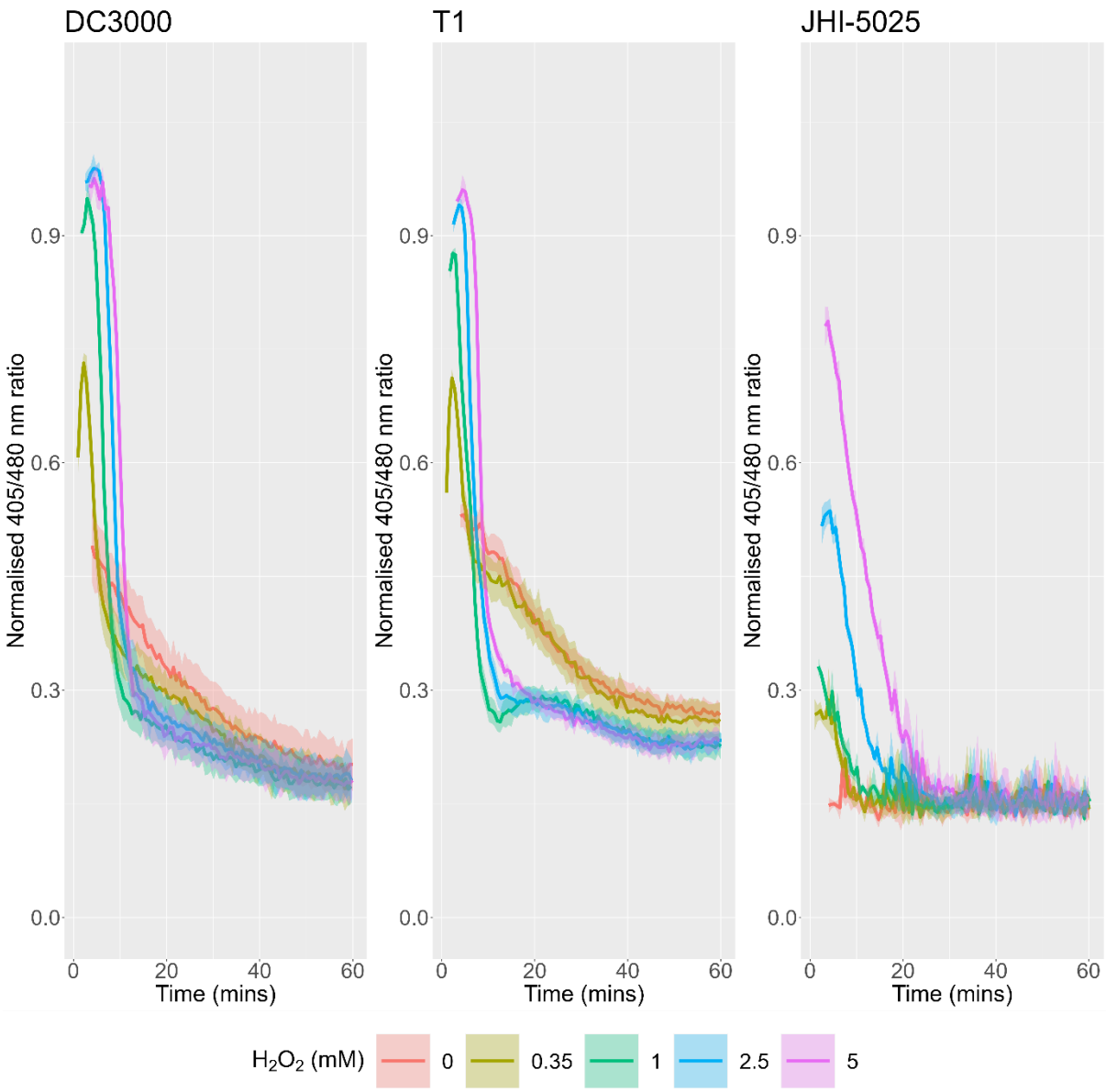


Figure 3.14: Hydrogen peroxide increased the intracellular redox state of all bacteria. Bacteria (*P. syringae* pv. tomato DC3000, *P. syringae* pv. tomato T1, *E. coli* JHI-5025) which had been tagged with pDSK-roGFP were grown to early exponential phase and added into M9 with hydrogen peroxide (H_2O_2) in a glass bottle (final OD_{600nm} = 1). Bacteria were added to each treatment concentration at 45 second intervals, and the 'starting points' of signals displayed on the charts represent the time between the addition of bacteria to the treatment and the first measurement. Data points represent the intracellular redox state of bacteria, which is a ratio of the fluorescence intensity measured at 405 nm (400 - 410 nm bandwidth) and 480 nm (475 - 485 nm bandwidth) excitation, 500 - 520 nm emission, at 28°C with intermittent shaking. The data was normalised using measurements from bacteria in a maximum oxidised and maximum reduced state, so that a normalised 405/480 ratio of 1 was equal to the maximum oxidised signal and 0.1 was equal to the maximum reduced signal. Mean and standard error are shown (n = 3).

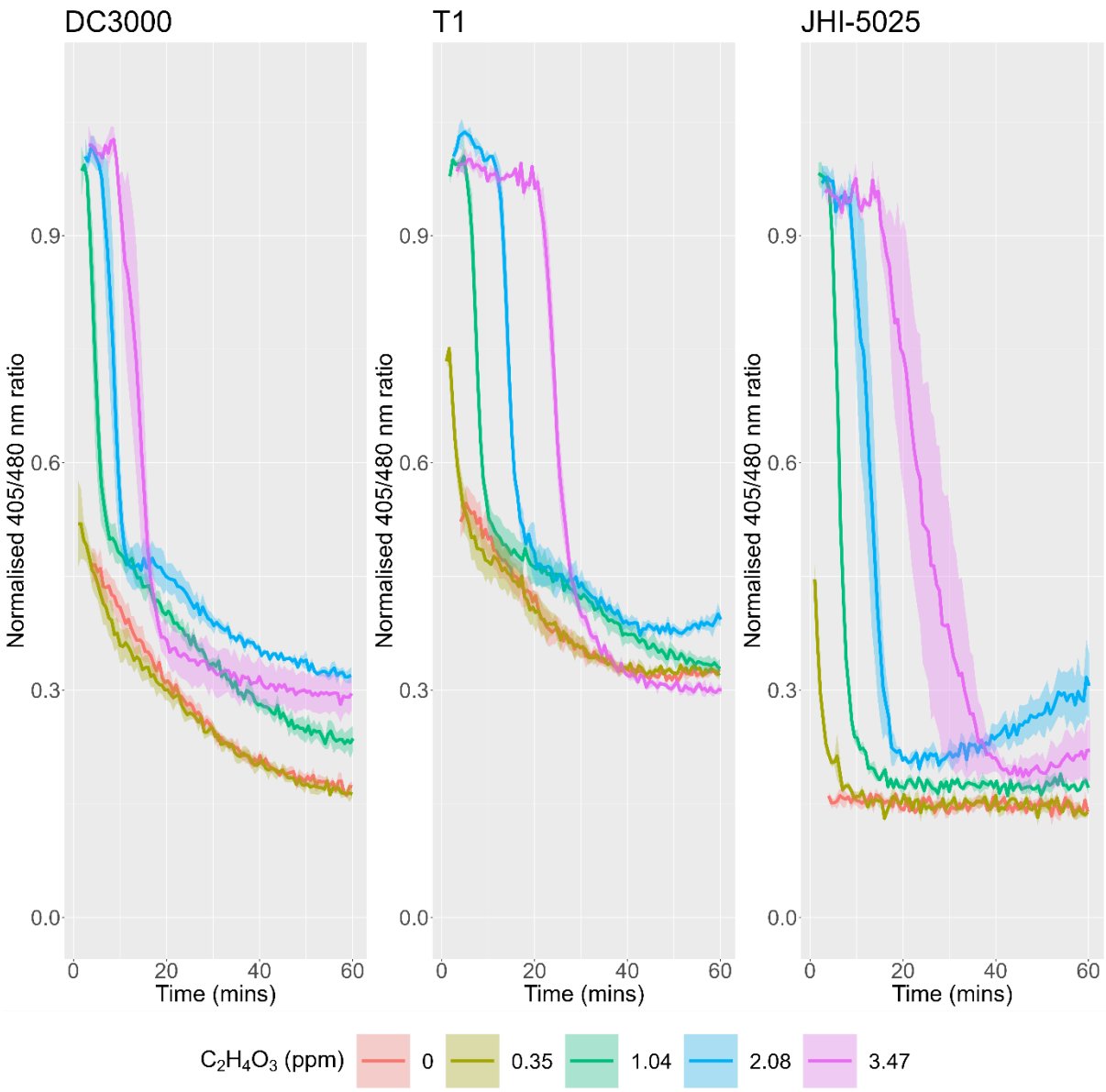


Figure 3.15: Peracetic acid increased the intracellular redox state of all bacteria. Bacteria (*P. syringae* pv. tomato DC3000, *P. syringae* pv. tomato T1, *E. coli* JHI-5025) which had been tagged with pDSK-roGFP were grown to early exponential phase and added into M9 with peracetic acid ($C_2H_4O_3$) in a glass bottle (final OD_{600nm} = 1). Bacteria were added to each treatment concentration at 45 second intervals, and the 'starting points' of signals displayed on the charts represent the time between the addition of bacteria to the treatment and the first measurement. Data points represent the intracellular redox state of bacteria, which is a ratio of the fluorescence intensity measured at 405 nm (400 - 410 nm bandwidth) and 480 nm (475 - 485 nm bandwidth) excitation, 500 - 520 nm emission, at 28°C with intermittent shaking. The data was normalised using measurements from bacteria in a maximum oxidised and maximum reduced state, so that a normalised 405/480 ratio of 1 was equal to the maximum oxidised signal and 0.1 was equal to the maximum reduced signal. Mean and standard error are shown (n = 3).

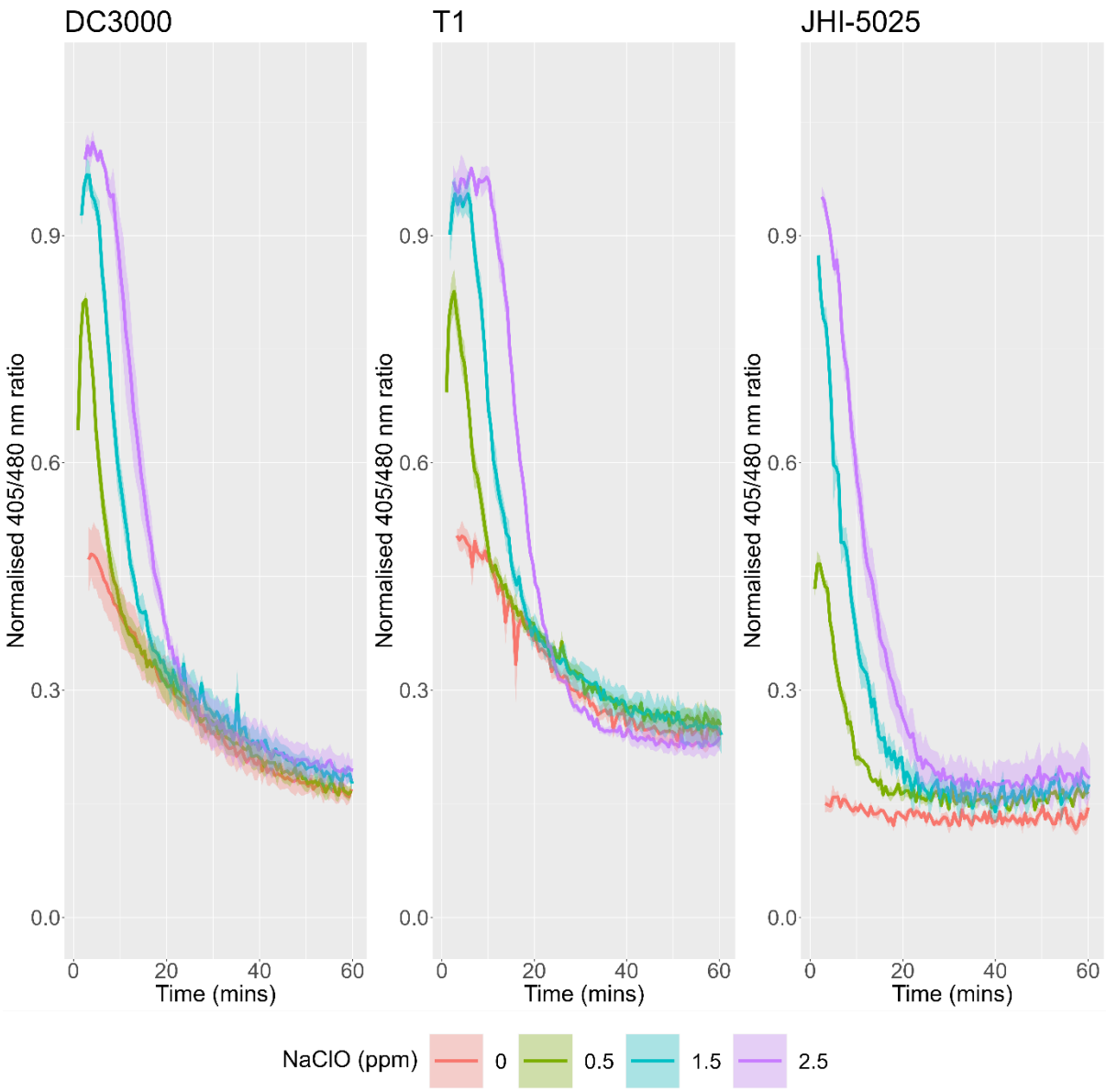


Figure 3.16: Sodium hypochlorite increased the intracellular redox state of all bacteria. Bacteria (*P. syringae* pv. tomato DC3000, *P. syringae* pv. tomato T1, *E. coli* JHI-5025) which had been tagged with pDSK-roGFP were grown to early exponential phase and added into M9 with sodium hypochlorite (NaClO) in a glass bottle (final OD_{600nm} = 1). Bacteria were added to each treatment concentration at 45 second intervals, and the 'starting points' of signals displayed on the charts represent the time between the addition of bacteria to the treatment and the first measurement. Data points represent the intracellular redox state of bacteria, which is a ratio of the fluorescence intensity measured at 405 nm (400 - 410 nm bandwidth) and 480 nm (475 - 485 nm bandwidth) excitation, 500 - 520 nm emission, at 28°C with intermittent shaking. The data was normalised using measurements from bacteria in a maximum oxidised and maximum reduced state, so that a normalised 405/480 ratio of 1 was equal to the maximum oxidised signal and 0.1 was equal to the maximum reduced signal. Mean and standard error are shown (n = 3).

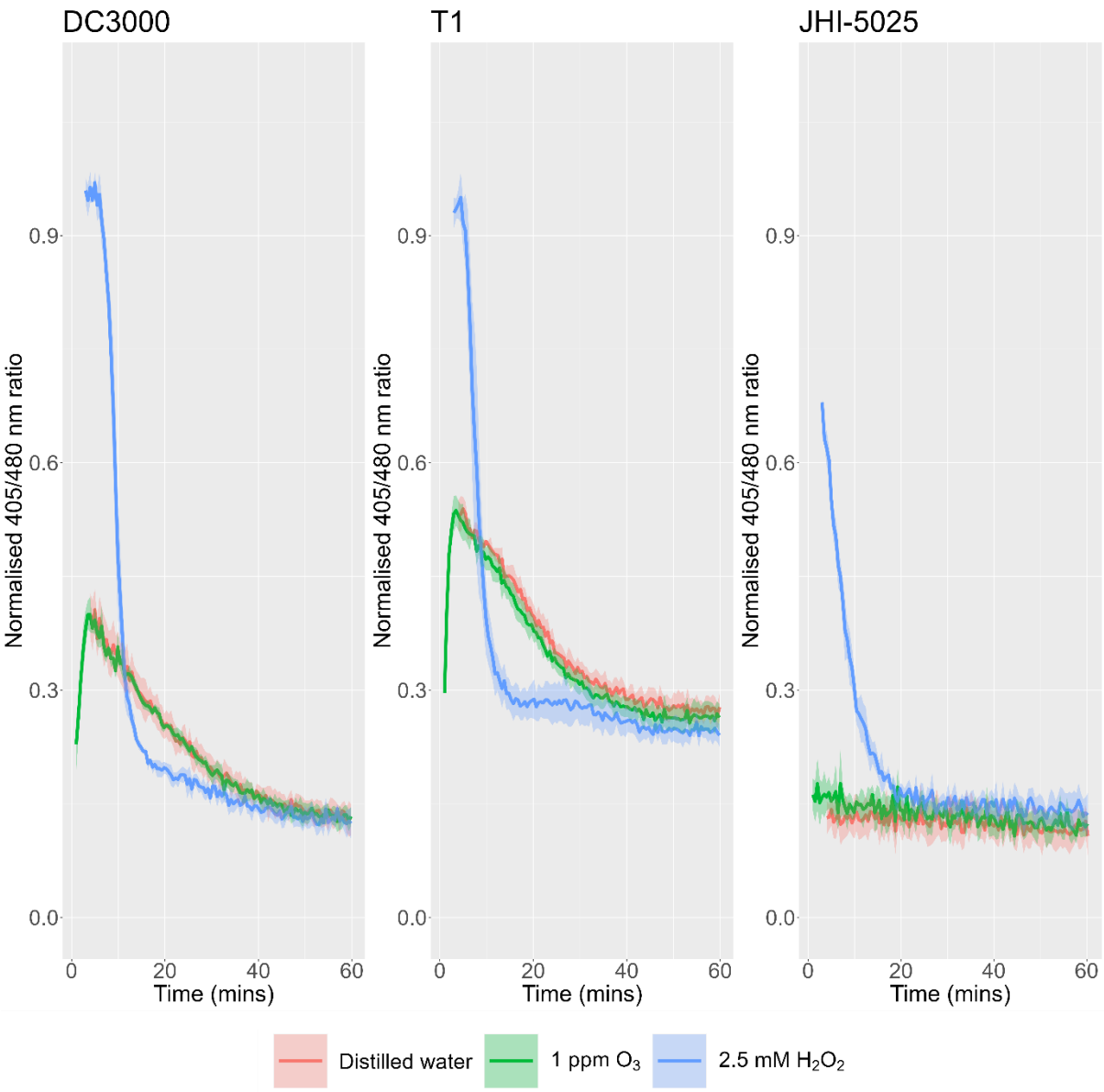


Figure 3.17: Aqueous ozone did not increase the intracellular redox state of any bacterium. Bacteria (*P. syringae* pv. tomato DC3000, *P. syringae* pv. tomato T1, *E. coli* JHI-5025) which had been tagged with pDSK-roGFP were grown to early exponential phase and added into M9 with distilled water, 1 ppm ozone (O_3) or 2.5 mM hydrogen peroxide (H_2O_2) in a glass bottle (final OD_{600nm} = 1). Bacteria were added to treatments at 45 second intervals, and the 'starting points' of signals displayed on the charts represent the time between the addition of bacteria to the treatment and the first measurement. Data points represent the intracellular redox state of bacteria, which is a ratio of the fluorescence intensity measured at 405 nm (400 - 410 nm bandwidth) and 480 nm (475 - 485 nm bandwidth) excitation, 500 - 520 nm emission, at 28°C with intermittent shaking. The data was normalised using measurements from bacteria in a maximum oxidised and maximum reduced state, so that a normalised 405/480 ratio of 1 was equal to the maximum oxidised signal and 0.1 was equal to the maximum reduced signal. Mean and standard error are shown (n = 3).

To conclude, hydrogen peroxide, peracetic acid and sodium hypochlorite all quickly increased the intracellular redox state of bacteria, whereas ozone did not. The response that was caused by increasing concentrations of each treatment was characterised by an

increase in the maximum oxidised signal that bacteria reached, until very high maximum oxidised signals were obtained, and a prolonged time for bacteria to recover to a more stable redox state. Aqueous ozone was no longer used for work in this chapter since bacteria were not being stressed by it.

Since hydrogen peroxide, sodium hypochlorite and peracetic acid all caused bacteria to have an extended 'apparent' lag growth phase, a reduced culturability and an increased intracellular redox state, the transcriptional response of individual genes in enterics to each treatment was next characterised and compared. This was to identify further similarities in the response of enterics to each of these treatments.

3.3.4 Oxidative stress tolerance genes were upregulated in response to hydrogen peroxide, peracetic acid and sodium hypochlorite

The transcriptional response of oxidative stress tolerance genes (*oxyR, katG, soxR, soxS, ramA*, *lexA*) in enterics was compared after exposure to hydrogen peroxide, sodium hypochlorite and peracetic acid. For this experiment, gene promoter regions were amplified from Stm SL1344 and were used to produce transcriptional fusion GFP+ reporters. GFP+ is a GFP variant which allows for increased sensitivity of GFP detection and has previously been used to accurately quantify gene expression (Scholz *et al.*, 2000). The reporters were transformed into *E. coli* JHI-5025 for testing because unlike Stm SL1344, *E. coli* JHI-5025 is a non-pathogenic enteric. Nevertheless, the oxidative stress response of *E. coli* and *S. enterica* are very similar (Imlay, 2009).

Since Stm promoter regions were placed into *E. coli* for testing, a BLAST nucleotide alignment was completed (with default settings) to identify how similar their gene promoter regions were. The Stm-amplified promoter regions were up to 550 bp long, and they always contained the full intergenic region between the previous gene (5' - 3' direction) and the gene of interest, just up to or intersecting the expected ribosome binding site for the gene of interest, however some amplified regions also included the tail

end of the previous genes coding sequence. Since the promoter was expected to be within the intergenic region, only the intergenic regions were aligned. *E. coli* K-12 MG1655 (accession NC_000913.3) was used for the alignment against Stm SL1344 because it displayed a high similarity to the *E. coli* JHI-5025 contig genome (Holden, 2021). A *ramA* intergenic region was not aligned because *E. coli* does not have this gene (van der Straaten *et al.*, 2004).

Table 3.6: Comparison of *E. coli* K-12 MG1655 and Stm SL1344 selected intergenic regions

Gene	Intergenic region aligned	*E. coli* K-12 intergenic region size (bp)	Stm SL1344 intergenic region size (bp)	Identified regions of similarity (bp) (*E. coli* K-12 vs Stm SL1344)
oxyR	Between *oxyS* and *oxyR*	95	94	80/87 (92%)
katG	Between *metF* and *katG*	328	164	108/139 (78%)
soxR	Between *soxS* and *soxR*	85	86	67/81 (83%)
soxS	Between *soxR* and *soxS* (same region as for *soxR* but reverse-complemented)	85	86	67/81 (83%)
lexA	Between *dgkA* and *lexA*	109	108	93/106 (88%)

As there were regions of sequence similarity between the intergenic regions which were expected to contain the promoters for all of the genes of interest (table 3.6), we predicted that the Stm transcriptional fusion reporters would be similarly regulated in *E. coli* to their regulation in Stm. However, interestingly, the intergenic region which was expected to contain the *katG* promoter was double the size in *E. coli* than Stm, nevertheless a large section of sequence similarity to Stm was still identified within this region, which could be the promoter (table 3.6).

Transcriptional fusion fluorescent reporters with no promoter behind GFP+, and an *E. coli*-amplified *gyrA* promoter behind GFP+, were used as negative and positive controls respectively. *E. coli* JHI-5025 (p_{gyrA}-GFP+) has previously been used as a constitutive

GFP reporter (Wright *et al.*, 2017), however since *gyrA* is involved in DNA supercoiling, changes in its expression could occur in response to treatments (Weinstein-Fischer *et al*., 2000). This is because DNA supercoiling is a tool for introducing rapid changes in protein expression, which is often required for bacteria to survive stress (Weinstein-Fischer *et al*., 2000). All *E. coli* JHI-5025 transcriptional fusion fluorescent reporters also contained a plasmid with constitutive mCherry expression so that they could be identified during flow cytometry.

Transcriptional fusion fluorescent reporter strains (table 3.3) in the early exponential growth phase were exposed to treatments because as previously described, they would be more susceptible to oxidative stress than those in the stationary growth phase would be (Imlay, 2008, 2015). Treatments included 5 mM hydrogen peroxide, 1.040 ppm peracetic acid and 2.5 ppm sodium hypochlorite because all three treatments largely increased the intracellular redox state of bacteria (figures 3.14, 3.15 and 3.16). The reporter strains were exposed to treatments in M9 in a glass bottle (final OD_{600nm} 1), before being dispensed into a 96-well plate (incubated at 28^{o}C with intermittent shaking) for growth (OD_{600nm}) measurements over time. At 1, 5, and 18 hours, aliquots of samples were diluted in PBS and the GFP+ expression of mCherry cells was measured by flow cytometry.

Each transcriptional fusion fluorescent reporter was active to some extent, without the addition of any treatment and *ramA* was notably the most active (figure 3.18: A). In the water control, there were changes in the GFP+ expression of reporters over time (figure 3.18: A). It could be proposed that the preparation of cells for treatment exposure (which included cell pelleting, washing, and resuspension) could have triggered the initial induction of some of the reporters. Alternatively, or in addition to this, the bacterial growth phase could have also contributed to the differences in GFP+ expression that occurred over time in the water control.

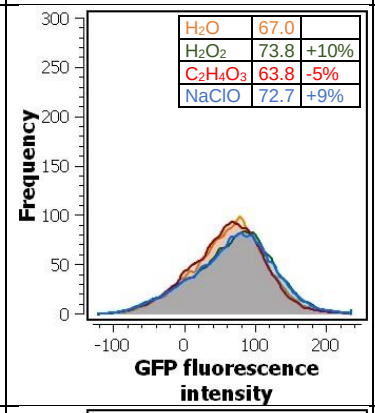
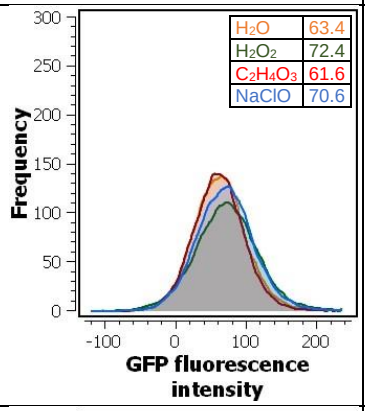
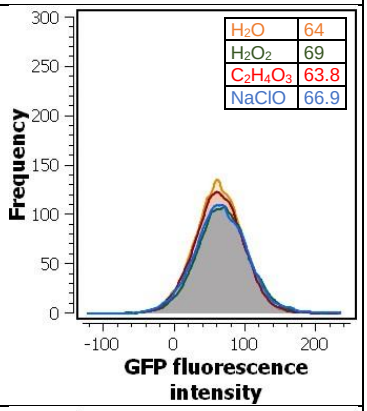
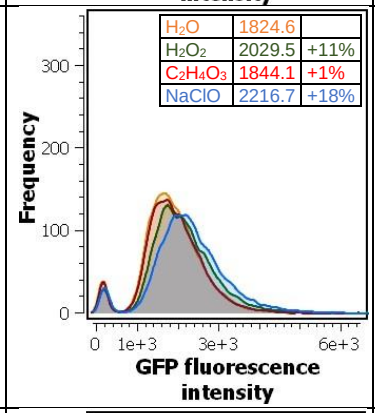
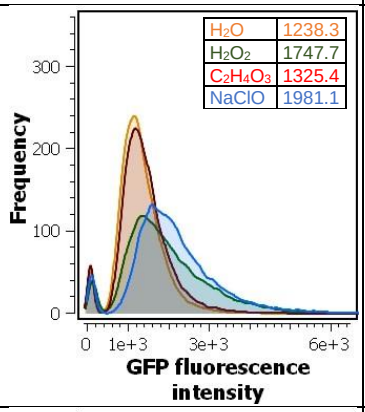
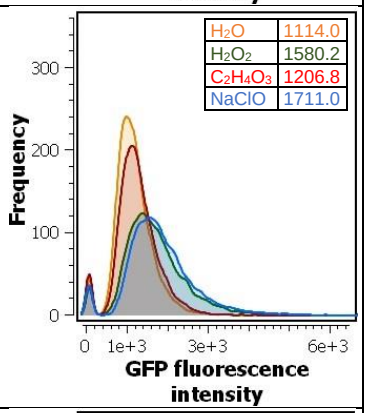
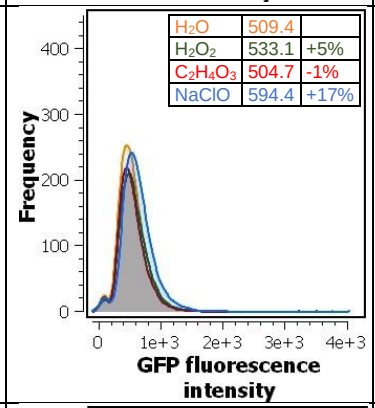
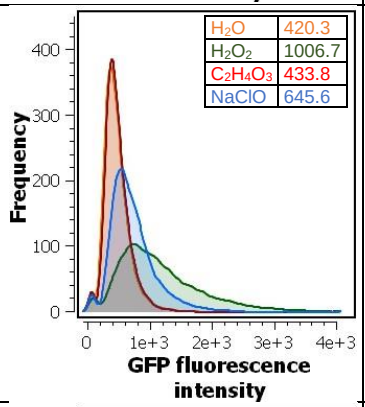
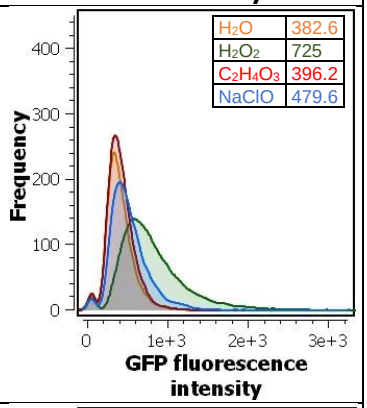
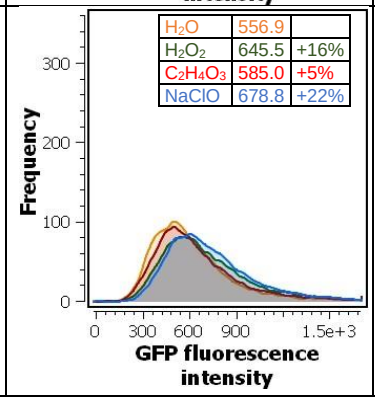
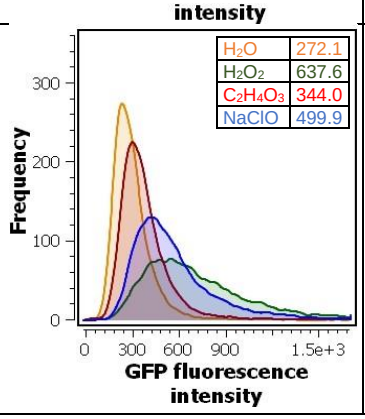
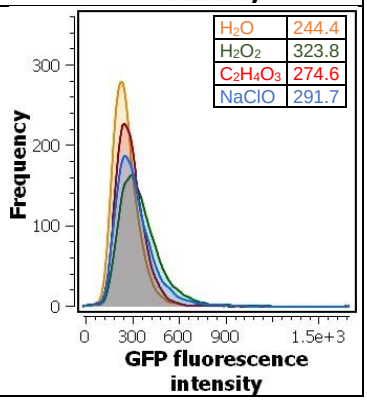
Since all reporters were still in the ‘apparent’ lag growth phase 1 hour after treatment (appendix 10 shows the first 8 hours of the growth curves presented in figure 3.18: B), the 1 hour time-point was used to compare the response of each reporter to different treatments. This was because the growth phase would not have contributed to differences in GFP+ expression and a GFP+ ‘dilution effect’ of the original population that were exposed to treatments (caused by the presence of progeny) would have been minimal. Although all treatments imposed stress, the level of stress imposed was not equivalent for all treatments, with hydrogen peroxide causing the most stress, followed by sodium hypochlorite and peracetic acid respectively (appendix 10 and figure 3.18: B). Therefore, conclusions were drawn based on the expression observed for each stress relative to water at the 1 hour time-point, rather than from direct comparisons between treatments.

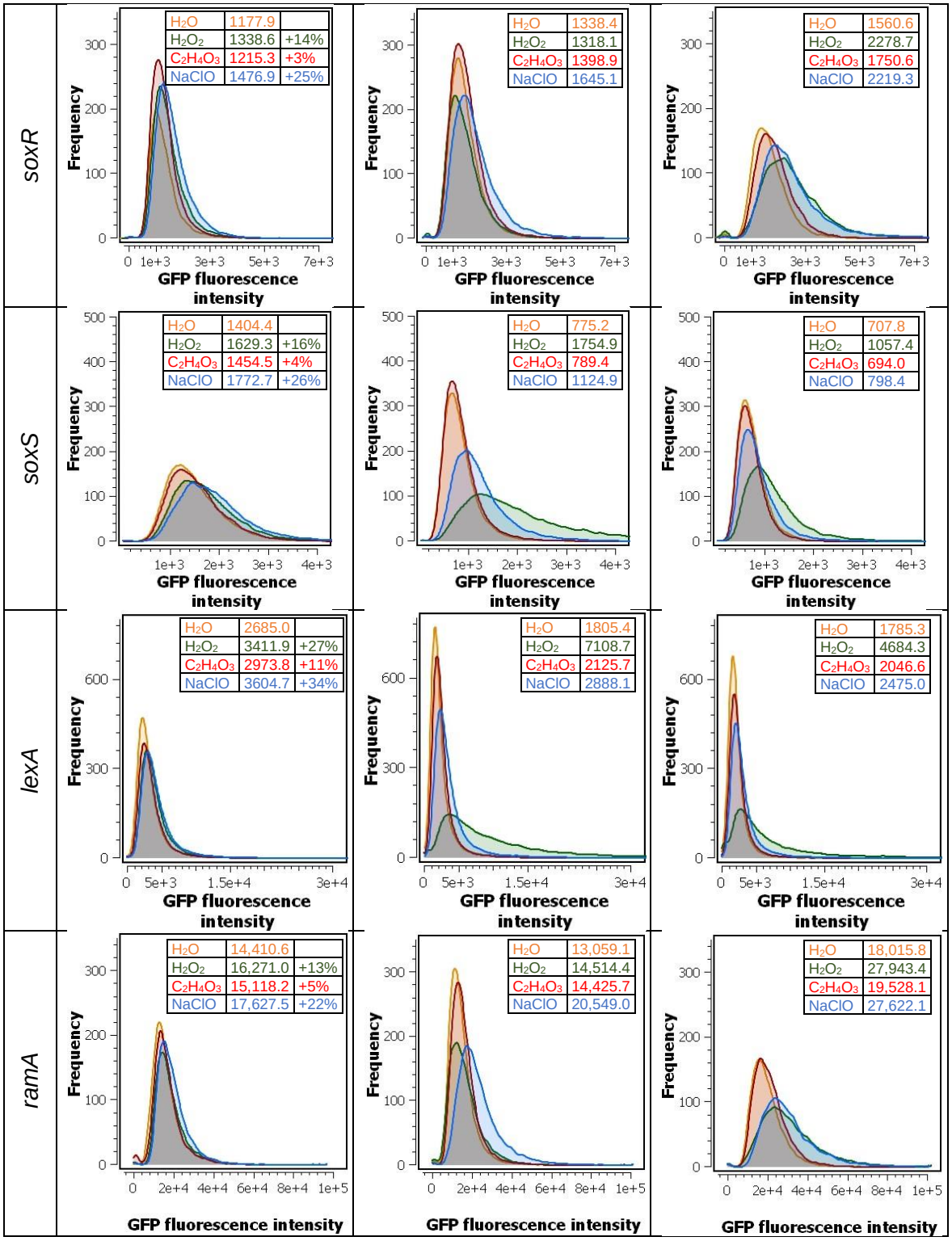
The GFP+ expression of each treatment-exposed reporter was compared over time (at 1, 5 and 18 hours post-treatment) to identify if there were increases in GFP+ expression due to delayed upregulation or GFP+ maturation. This was compared to the GFP+ expression of the same reporter over time in water, to identify if further inductions were likely growth phase dependent or not.

Compared to the water control, slight fluctuations in the median GFP+ expression were observed when the no promoter reporter was exposed to each treatment (figure 3.18: A). Therefore, after exposure to each treatment, only the reporters which had a larger percentage increase in median GFP+ expression from the water control than the no promoter reporter did (by at least 2%), were considered as increases, which indicated upregulation.

The median of *soxR*, *soxS*, *katG*, *ramA* and *lexA* controlled GFP+ expression increased within 1 hour after exposure to all treatments, in comparison to the water control (figure 3.18: A). The median of *soxR* and *ramA* controlled GFP+ expression peaked at 18 hours after exposure to all treatments and the water control (figure 3.18: A). After hydrogen

peroxide exposure only, the median of *soxS* and *lexA* controlled GFP+ expression continued to increase to 5 hours, whereas it decreased over time in all other samples (figure 3.18: A). The median of *oxyR* controlled GFP+ expression did not increase within 1 hour of hydrogen peroxide or peracetic acid exposure but did after sodium hypochlorite exposure (figure 3.18: A). The median of *oxyR* controlled GFP+ expression drastically increased from 1 to 5 hours after hydrogen peroxide, and slightly further increased from 1 to 5 hours after sodium hypochlorite (figure 3.18: A). The median of *gyrA* controlled GFP+ expression was not increased by hydrogen peroxide or peracetic acid but was increased by sodium hypochlorite within 1 hour of exposure (figure 3.18: A).

(A)	1 hour	5 hours	18 hours
No promoter			
gyrA			
oxyR			
katG			


soxR
soxS
lexA
ramA
Frequency
GFP fluorescence intensity
H2O 1177.9
H2O2 1338.6 +14%
C2H4O3 1215.3 +3%
NaClO 1476.9 +25%
H2O 1338.4
H2O2 1318.1
C2H4O3 1398.9
NaClO 1645.1
H2O 1560.6
H2O2 2278.7
C2H4O3 1750.6
NaClO 2219.3
H2O 1404.4
H2O2 1629.3 +16%
C2H4O3 1454.5 +4%
NaClO 1772.7 +26%
H2O 775.2
H2O2 1754.9
C2H4O3 789.4
NaClO 1124.9
H2O 707.8
H2O2 1057.4
C2H4O3 694.0
NaClO 798.4
H2O 2685.0
H2O2 3411.9 +27%
C2H4O3 2973.8 +11%
NaClO 3604.7 +34%
H2O 1805.4
H2O2 7108.7
C2H4O3 2125.7
NaClO 2888.1
H2O 1785.3
H2O2 4684.3
C2H4O3 2046.6
NaClO 2475.0
H2O 14,410.6
H2O2 16,271.0 +13%
C2H4O3 15,118.2 +5%
NaClO 17,627.5 +22%
H2O 13,059.1
H2O2 14,514.4
C2H4O3 14,425.7
NaClO 20,549.0
H2O 18,015.8
H2O2 27,943.4
C2H4O3 19,528.1
NaClO 27,622.1

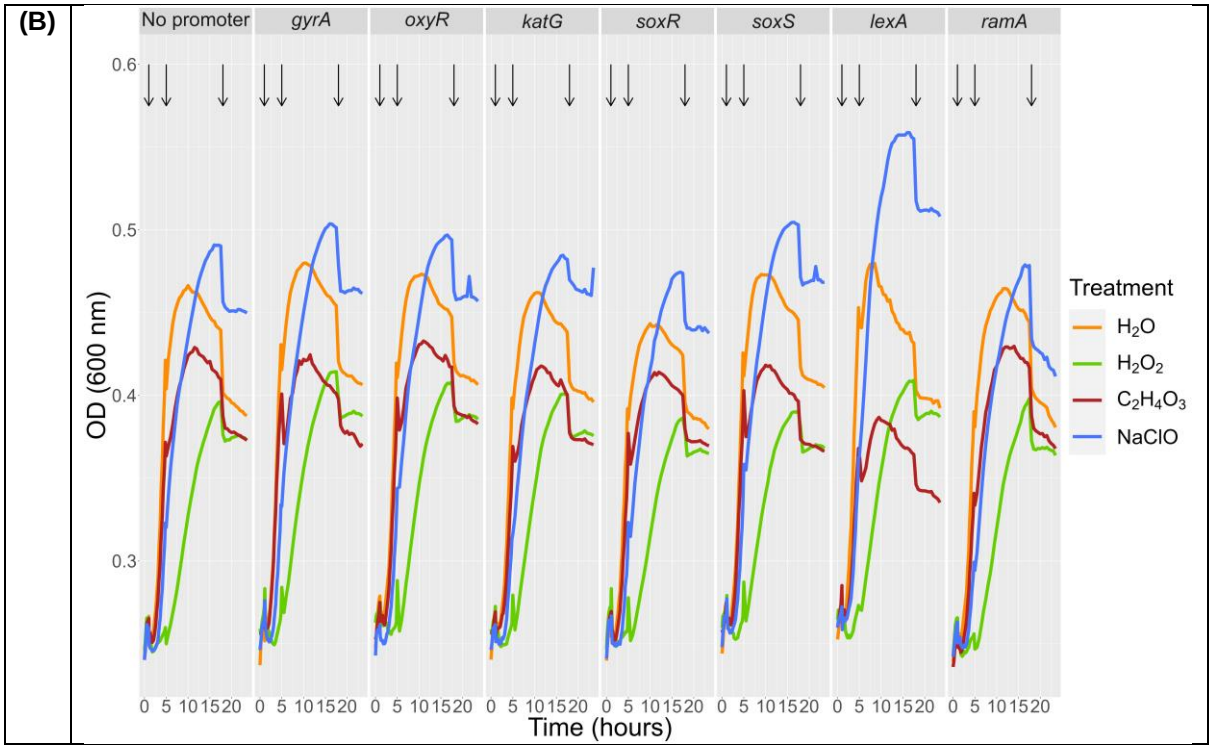


Figure 3.18: Oxidative stress tolerance genes were upregulated in response to hydrogen peroxide, peracetic acid and sodium hypochlorite. mCherry *E. coli* JHI-5025, which had been transformed with a GFP+ transcriptional fusion reporter for a selected gene (named in the figure), was grown to early exponential phase and added into M9 with either water, 5 mM hydrogen peroxide (H_2O_2), 1.040 ppm peracetic acid ($C_2H_4O_3$) or 2.5 ppm sodium hypochlorite (NaClO) in a glass bottle (final OD_{600nm} = 1). The reporter strains were then dispensed into a 96-well plate (incubated at 28ºC with intermittent shaking) for growth (OD_{600nm}) measurements over time. At 1, 5, and 18 hours, aliquots of samples were diluted in PBS and the GFP+ expression of mCherry cells was measured by flow cytometry. (**A**) Histograms of the GFP+ expression of mCherry cells are displayed, and the numbers in tables represent the median GFP+ expression of the reporter, after exposure to each treatment at that time-point. At the 1 hour time-point only, the percentage changes of the fluorescence, in comparison to the water control, have also been displayed in tables. (**B**) Growth curves of the reporters are displayed, and the arrows represent the time points (1, 5, 18 hours) at which aliquots were removed for flow cytometry analysis.

To summarise, oxidative stress tolerance genes were upregulated in response to hydrogen peroxide, peracetic acid and sodium hypochlorite. Next, the role of *oxyR* and catalases in the tolerance to Pst DC300 against treatments was investigated.

3.3.5 *oxyR* is required for hydrogen peroxide but not peracetic acid or sodium hypochlorite tolerance

To determine if *oxyR*, a key regulon involved in the response of Pst DC3000 to oxidative stress (Ishiga and Ichinose, 2015), was required for hydrogen peroxide, peracetic acid and sodium hypochlorite tolerance, the intracellular redox state of an *oxyR* deletion

mutant (Δ*oxyR*) was compared to the Pst DC3000 wildtype after exposure to treatments (table 3.3). Pst DC3000 Δ*oxyR* + Tn7_*oxyR* (table 3.3) was also used in experiments to validate that any observed variations in tolerance were a result of the *oxyR* deletion. All of the strains for the assay were tagged to express roGFP, since roGFP is a tool for measuring the intracellular redox state, as previously described (Hanson *et al.*, 2004).

Bacteria in the early exponential growth phase were exposed to treatments because as previously described, they would be more susceptible to oxidative stress than those in the stationary growth phase would be (Imlay, 2008, 2015). Bacteria were exposed to treatments in M9 in a 96-well plate (final OD_{600nm} 1), which was incubated at 28^{o}C with intermittent shaking for roGFP fluorescence measurements.

The oxidised intracellular redox state of Pst DC3000 Δ*oxyR* took longer to recover than Pst DC3000 from the same concentrations of hydrogen peroxide (figure 3.19). Since the complemented strain Pst DC3000 Δ*oxyR* + Tn7_*oxyR* behaved similarly to Pst DC3000 in its response to hydrogen peroxide (figure 3.19), this validated that the increased sensitivity of Pst DC3000 Δ*oxyR* was due to the *oxyR* deletion. Hence, it was concluded that *oxyR* was required for hydrogen peroxide tolerance.

Pst DC3000, Pst DC3000 Δ*oxyR* and Pst DC3000 Δ*oxyR* + Tn7_*oxyR* all behaved similarly in their response to peracetic acid and sodium hypochlorite (figure 3.20 and 3.21), therefore it was concluded that *oxyR* was not required for an increased tolerance to these treatments.

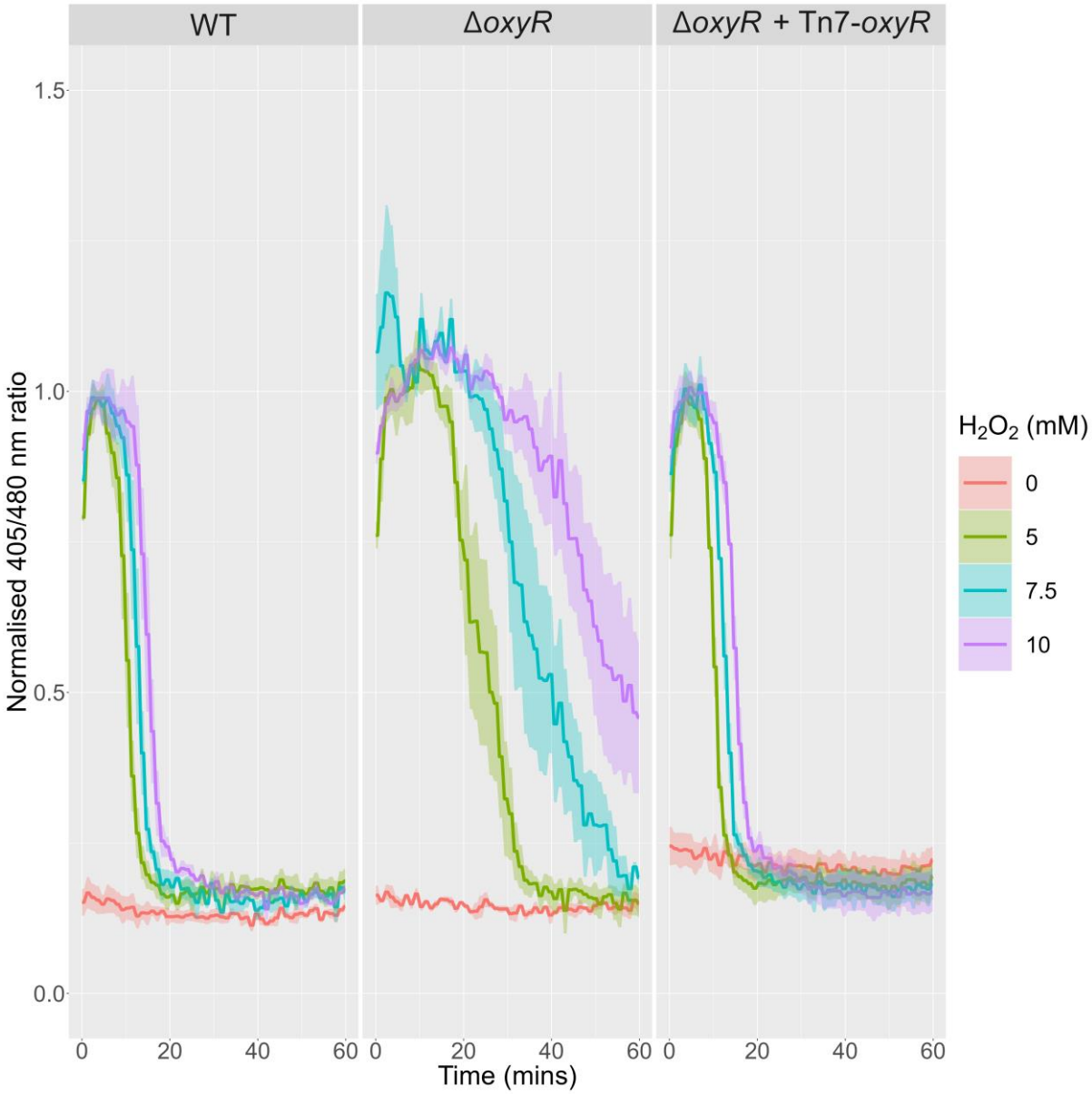


Figure 3.19: *oxyR* is required for hydrogen peroxide tolerance. Bacteria (*P. syringae* pv. tomato DC3000, *P. syringae* pv. tomato DC3000 Δ*oxyR*, *P. syringae* pv. tomato DC3000 Δ*oxyR* + Tn7_*oxyR*) which had been tagged with pDSK-roGFP were grown to early exponential phase and exposed to hydrogen peroxide (H_2O_2) in M9 (final OD_{600nm} = 1). Treatments were added to each bacterium at the same time. Data points represent the intracellular redox state of bacteria, which is a ratio of the fluorescence intensity measured at 405 nm (400 - 410 nm bandwidth) and 480 nm (475 - 485 nm bandwidth) excitation, 500 - 520 nm emission, at 28°C with intermittent shaking. The data was normalised using measurements from the same bacterial strain, in a maximum oxidised and maximum reduced state, so that a normalised 405/480 ratio of 1 was equal to the maximum oxidised signal and 0.1 was equal to the maximum reduced signal. Mean and standard error are shown (n = 3).

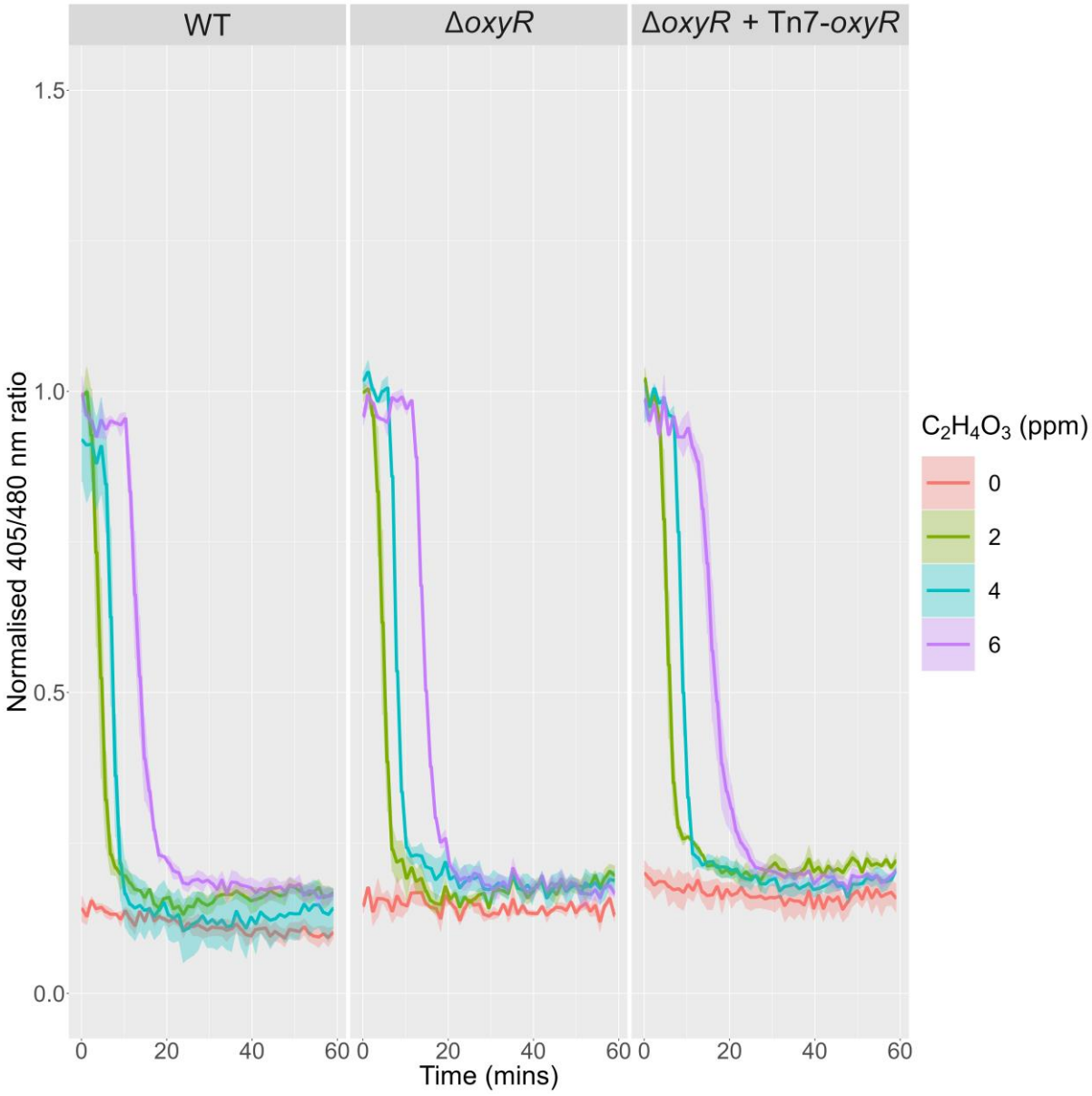


Figure 3.20: *oxyR* is not required for peracetic acid tolerance. Bacteria (*P. syringae* pv. tomato DC3000, *P. syringae* pv. tomato DC3000 Δ*oxyR*, *P. syringae* pv. tomato DC3000 Δ*oxyR* + Tn7_*oxyR*) which had been tagged with pDSK-roGFP were grown to early exponential phase and exposed to peracetic acid ($C_2H_4O_3$) in M9 (final OD_{600nm} = 1). Treatments were added to each bacterium at the same time. Data points represent the intracellular redox state of bacteria, which is a ratio of the fluorescence intensity measured at 405 nm (400 - 410 nm bandwidth) and 480 nm (475 - 485 nm bandwidth) excitation, 500 - 520 nm emission, at 28°C with intermittent shaking. The data was normalised using measurements from the same bacterial strain, in a maximum oxidised and maximum reduced state, so that a normalised 405/480 ratio of 1 was equal to the maximum oxidised signal and 0.1 was equal to the maximum reduced signal. Mean and standard error are shown (n = 3).

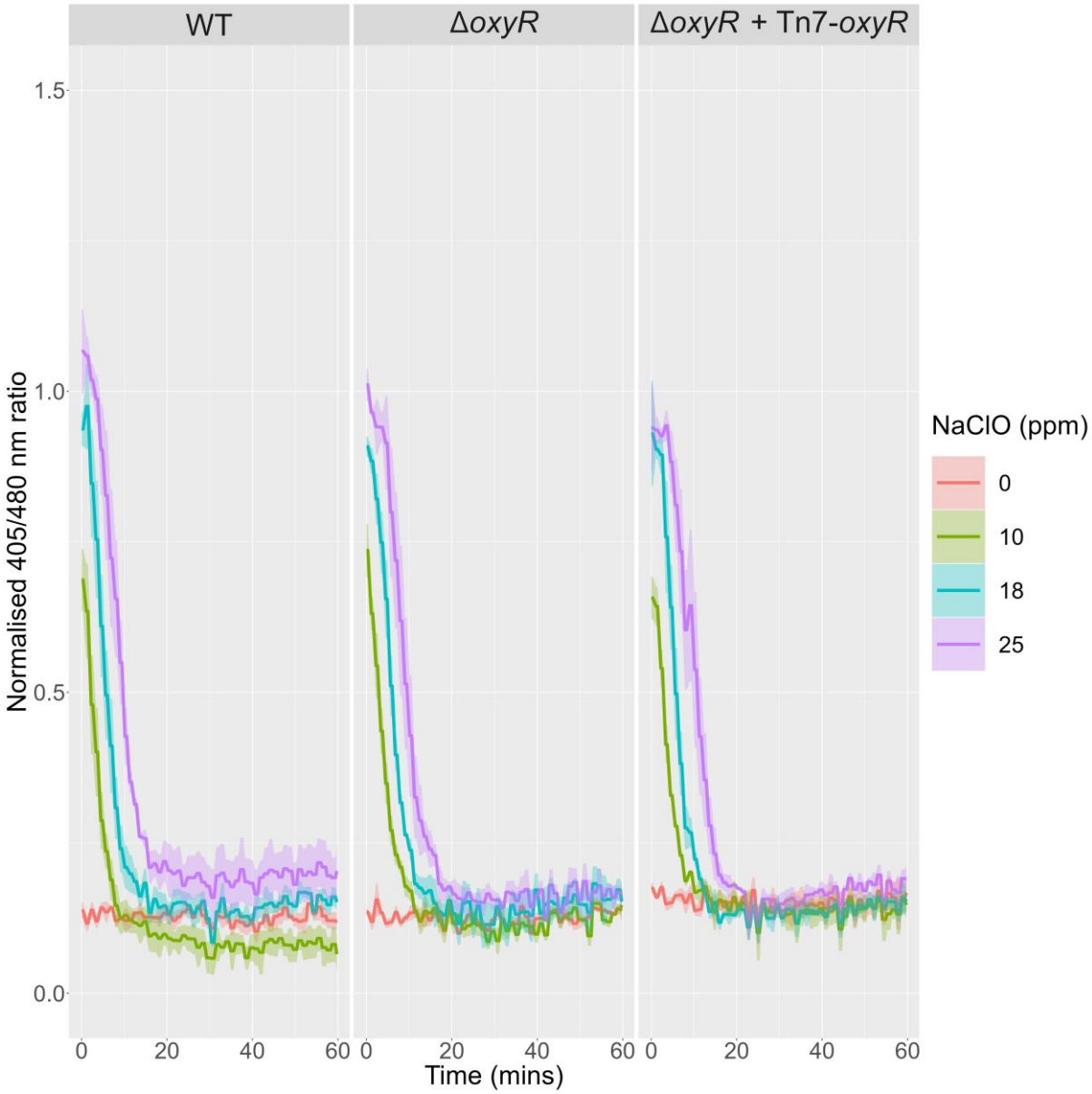


Figure 3.21: *oxyR* is not required for sodium hypochlorite tolerance. Bacteria (*P. syringae* pv. tomato DC3000, *P. syringae* pv. tomato DC3000 Δ*oxyR*, *P. syringae* pv. tomato DC3000 Δ*oxyR* + Tn7_*oxyR*) which had been tagged with pDSK-roGFP were grown to early exponential phase and exposed to sodium hypochlorite (NaClO) in M9 (final OD_{600nm} = 1). Treatments were added to each bacterium at the same time. Data points represent the intracellular redox state of bacteria, which is a ratio of the fluorescence intensity measured at 405 nm (400 - 410 nm bandwidth) and 480 nm (475 - 485 nm bandwidth) excitation, 500 - 520 nm emission, at 28°C with intermittent shaking. The data was normalised using measurements from the same bacterial strain, in a maximum oxidised and maximum reduced state, so that a normalised 405/480 ratio of 1 was equal to the maximum oxidised signal and 0.1 was equal to the maximum reduced signal. Mean and standard error are shown (n = 3).

oxyR was required in Pst DC3000 for tolerance to hydrogen peroxide, but not peracetic acid or sodium hypochlorite. Since catalases are involved in hydrogen peroxide

detoxification, their role in the tolerance of Pst DC3000 to hydrogen peroxide, peracetic acid and sodium hypochlorite was next determined.

3.3.6 Catalases are required for hydrogen peroxide and peracetic acid but not sodium hypochlorite tolerance

To determine if catalases, the primary enzymes involved in the detoxification of hydrogen peroxide in Pst DC3000 (Guo *et al.*, 2012), were required for hydrogen peroxide, peracetic acid and sodium hypochlorite tolerance, the intracellular redox state of Pst DC3000 with all of its catalases deleted (Δ*katBEG*) was compared to the wildtype after exposure to treatments. Pst DC3000 Δ*katBEG* + Tn7_*katG* (table 3.3), was also used in experiments to investigate if *katG*, which is the only proposed bifunctional catalase (table 3.1), could restore tolerance of Pst DC3000 Δ*katBEG* to any treatments in which it displayed an increased sensitivity to, in comparison to Pst DC3000. All of the strains for the assay were tagged to express roGFP since roGFP is a tool for measuring the intracellular redox state, as previously described (Hanson *et al.*, 2004).

Bacteria in the early exponential growth phase were exposed to treatments because as previously described, they would be more susceptible to oxidative stress than those in the stationary growth phase would be (Imlay, 2008, 2015). Bacteria were exposed to treatments in M9 in a 96-well plate (final OD_{600nm} 1), which was incubated at 28^{o}C with intermittent shaking for roGFP fluorescence measurements. It is to be mentioned that Pst DC3000 Δ*katBEG* (pDSK-roGFP) and Pst DC3000 Δ*katBEG* + Tn7_*katG* (pDSK-roGFP) clustered together in liquid culture, whereas Pst D3000 (pDSK-roGFP) did not, which may have affected OD_{600nm} measurements (appendix 11).

Pst DC3000 Δ*katBEG* was more sensitive to hydrogen peroxide than Pst DC3000, since its oxidised intracellular redox state took longer to recover at 0.5 mM hydrogen peroxide than Pst DC3000 did, and its redox state did not recover at 2.5 or 5 mM hydrogen peroxide, whereas the redox state of Pst DC3000 did (figure 3.22). Hence, it was

concluded that catalases were required for hydrogen peroxide tolerance. Pst DC3000 Δ*katBEG* + Tn7_*katG* was able to recover at 2.5 and 5 mM hydrogen peroxide, however the length of time that the recovery took was distinctly longer than the wildtype (figure 3.22). Therefore, it was concluded that the addition of *katG* to Pst DC3000 Δ*katBEG* was able to restore some, but not all hydrogen peroxide tolerance.

Pst DC3000 Δ*katBEG* was more sensitive to peracetic acid than Pst DC3000, since its oxidised intracellular redox state took longer to recover at 4 ppm peracetic acid than Pst DC3000 did, and the redox state that it recovered to after 8 ppm peracetic acid was much higher than what Pst DC3000 recovered to (figure 3.23). Hence, it was concluded that catalases were required for peracetic acid tolerance. The intracellular redox state of Pst DC3000 Δ*katBEG* + Tn7_*katG* recovered more similarly to Pst DC3000 at 4 ppm peracetic acid, and at 8 ppm peracetic acid it was able to recover to the same baseline redox state that Pst DC3000 was able to recover to, although the recovery was slower. Therefore, it was concluded that the addition of *katG* to Pst DC3000 Δ*katBEG* was able to restore some, but not all peracetic acid tolerance.

Pst DC3000, Pst DC3000 Δ*katBEG* and Pst DC3000 Δ*katBEG* + Tn7_*katG* all behaved similarly in their response to sodium hypochlorite (figure 3.24), therefore it was concluded that catalases were not required for an increased tolerance to sodium hypochlorite. Since the effect of peracetic acid on the deletion mutants only became apparent at higher concentrations, the results of the two independent replicates that were used to present the sodium hypochlorite results in figure 3.24 have been displayed in appendix 12 to demonstrate that there were still no differences between the wildtype and the deletion mutants when sodium hypochlorite caused very high levels of stress (because one replicate caused very high levels of stress in comparison to the other).

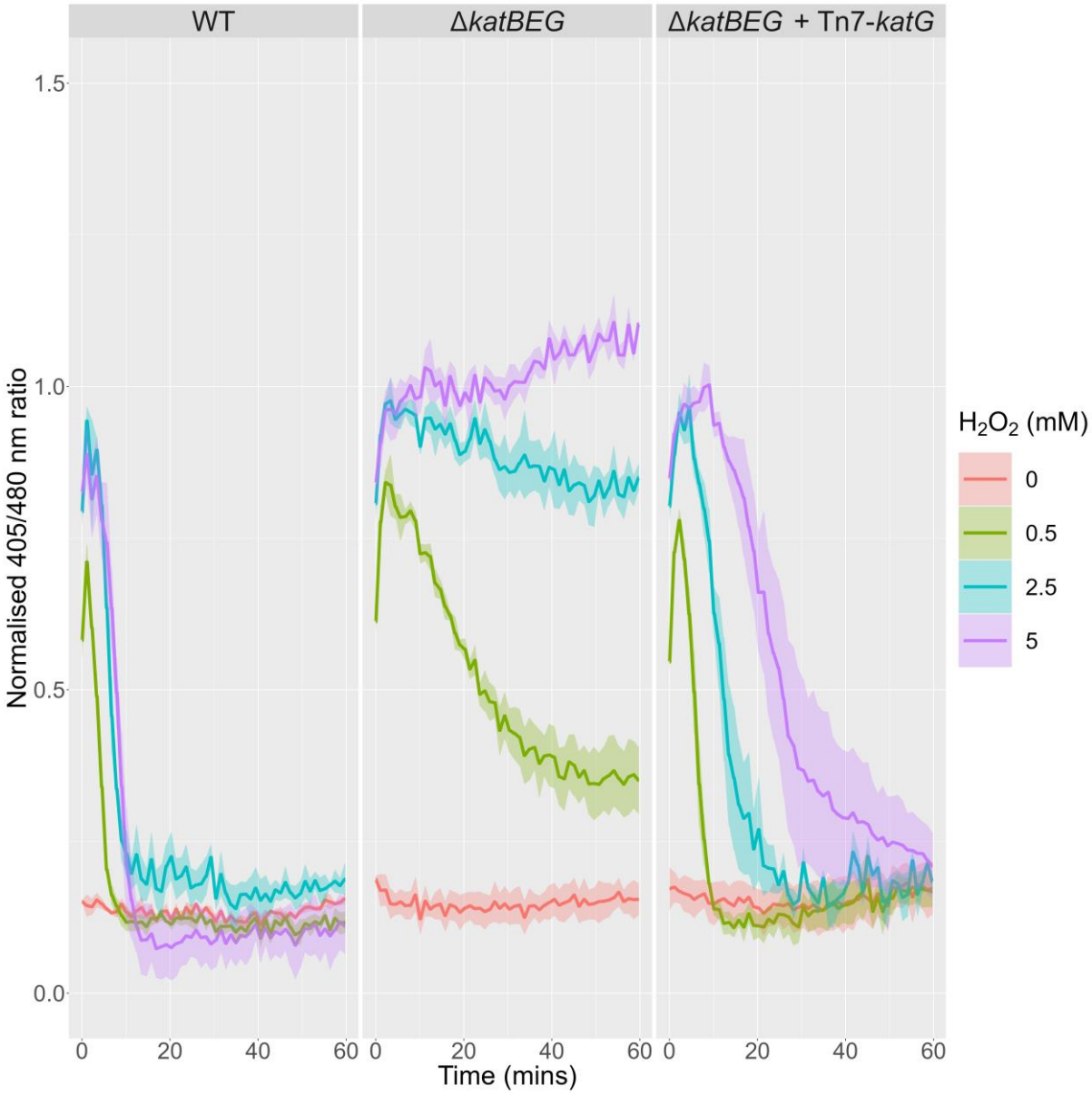


Figure 3.22: Catalases are required for hydrogen peroxide tolerance. Bacteria (*P. syringae* pv. tomato DC3000, *P. syringae* pv. tomato DC3000 Δ*katBEG*, *P. syringae* pv. tomato DC3000 Δ*katBEG* + Tn7_*katG*) which had been tagged with pDSK-roGFP were grown to early exponential phase and exposed to hydrogen peroxide (H_2O_2) in M9 (final OD_{600nm} = 1). Treatments were added to each bacterium at the same time. Data points represent the intracellular redox state of bacteria, which is a ratio of the fluorescence intensity measured at 405 nm (400 - 410 nm bandwidth) and 480 nm (475 - 485 nm bandwidth) excitation, 500 - 520 nm emission, at 28°C with intermittent shaking. The data was normalised using measurements from the same bacterial strain, in a maximum oxidised and maximum reduced state, so that a normalised 405/480 ratio of 1 was equal to the maximum oxidised signal and 0.1 was equal to the maximum reduced signal. Mean and standard error are shown (n = 3).

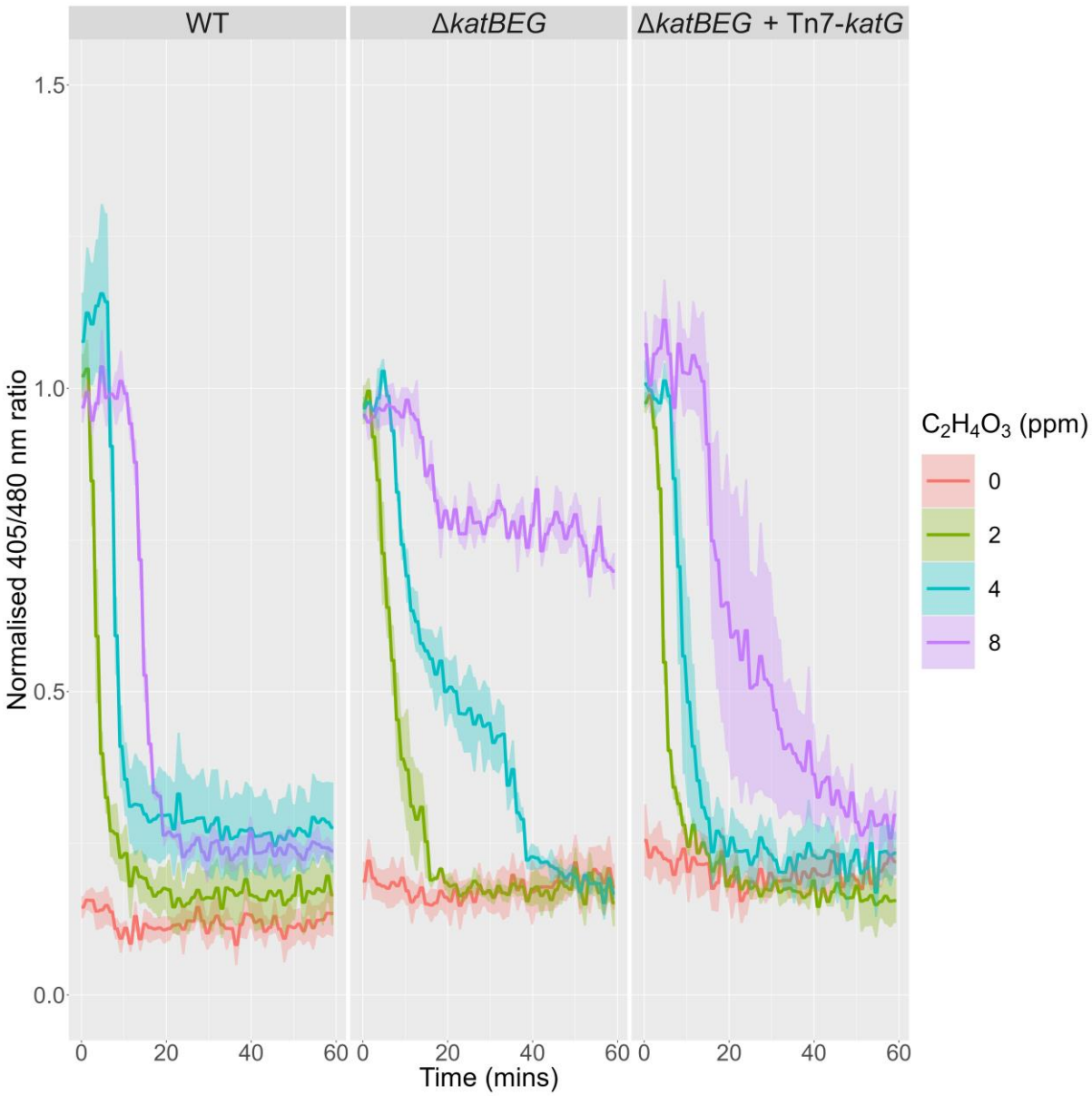


Figure 3.23: Catalases are required for peracetic acid tolerance. Bacteria (*P. syringae* pv. tomato DC3000, *P. syringae* pv. tomato DC3000 Δ*katBEG*, *P. syringae* pv. tomato DC3000 Δ*katBEG* + Tn7_*katG*) which had been tagged with pDSK-roGFP were grown to early exponential phase and exposed to peracetic acid ($C_2H_4O_3$) in M9 (final OD_{600nm} = 1). Treatments were added to each bacterium at the same time. Data points represent the intracellular redox state of bacteria, which is a ratio of the fluorescence intensity measured at 405 nm (400 - 410 nm bandwidth) and 480 nm (475 - 485 nm bandwidth) excitation, 500 - 520 nm emission, at 28°C with intermittent shaking. The data was normalised using measurements from the same bacterial strain, in a maximum oxidised and maximum reduced state, so that a normalised 405/480 ratio of 1 was equal to the maximum oxidised signal and 0.1 was equal to the maximum reduced signal. Mean and standard error are shown (n = 3).

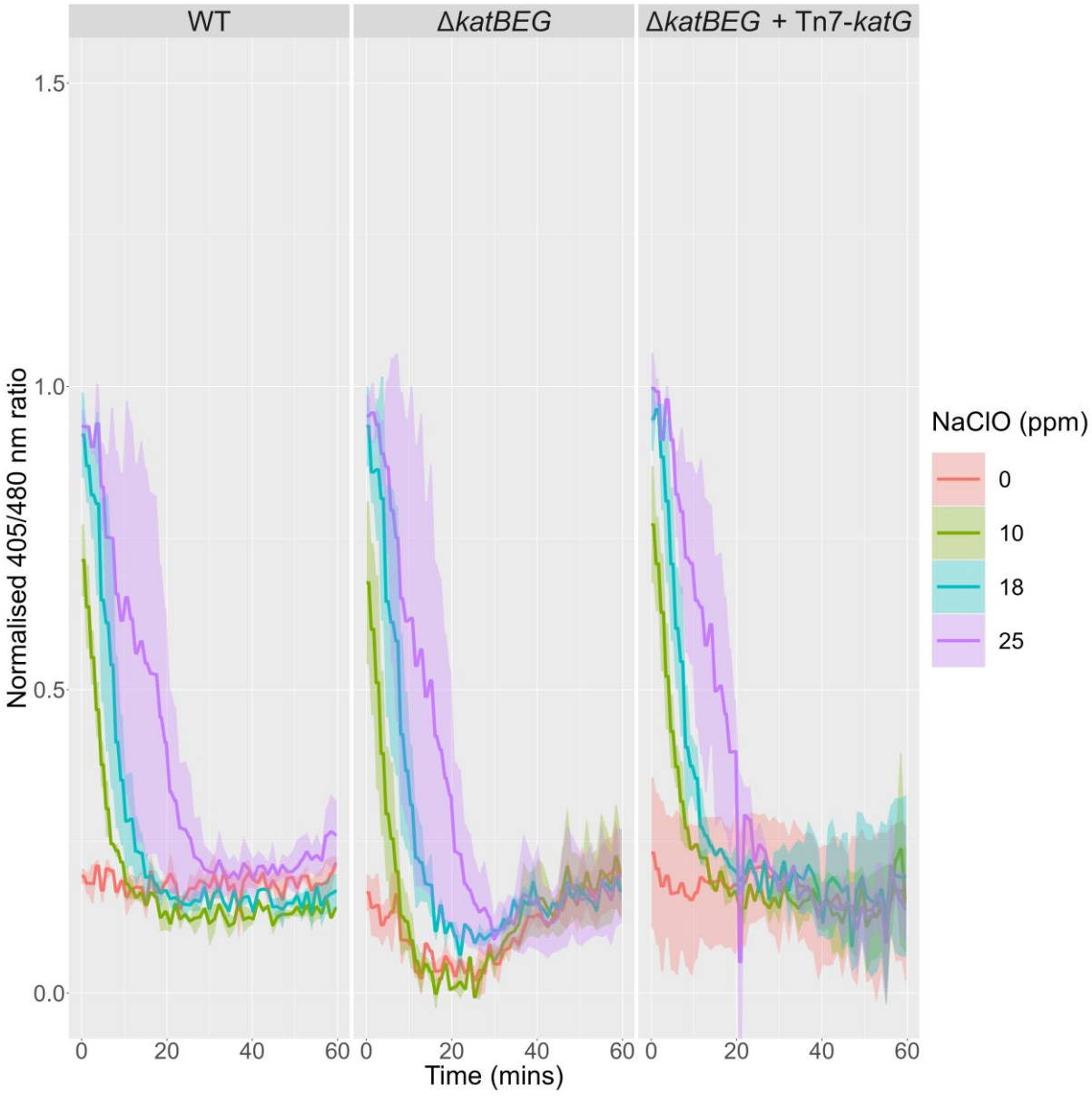


Figure 3.24: Catalases are not required for sodium hypochlorite tolerance. Bacteria (*P. syringae* pv. tomato DC3000, *P. syringae* pv. tomato DC3000 Δ*katBEG*, *P. syringae* pv. tomato DC3000 Δ*katBEG* + Tn7_*katG*) which had been tagged with pDSK-roGFP were grown to early exponential phase and exposed to sodium hypochlorite (NaClO) in M9 (final OD_{600nm} = 1). Treatments were added to each bacterium at the same time. Data points represent the intracellular redox state of bacteria, which is a ratio of the fluorescence intensity measured at 405 nm (400 - 410 nm bandwidth) and 480 nm (475 - 485 nm bandwidth) excitation, 500 - 520 nm emission, at 28°C with intermittent shaking. The data was normalised using measurements from the same bacterial strain, in a maximum oxidised and maximum reduced state, so that a normalised 405/480 ratio of 1 was equal to the maximum oxidised signal and 0.1 was equal to the maximum reduced signal. Mean and standard error are shown (n = 2).

To summarise, catalases (*katBEG*) were required in Pst DC3000 for tolerance to hydrogen peroxide and peracetic acid but not sodium hypochlorite. Since the addition of *katG* to Pst DC3000 Δ*katBEG* was able to restore some, but not all tolerance to hydrogen

peroxide and peracetic acid, this indicated that this catalase had an important role in the tolerance, but one or both of the other catalases, namely *katB* or *katE* must have also had a role.

3.4 Discussion

The effect of hydrogen peroxide, aqueous ozone, peracetic acid and sodium hypochlorite on the growth and intracellular redox state of bacteria was investigated. The data that was collected indicated that aqueous ozone did not stress bacteria, therefore the effect of only hydrogen peroxide, peracetic acid and sodium hypochlorite on the culturability, the transcriptional response of selected genes in enterics, and the redox state of Pst DC3000 *oxyR* and catalase deletion mutants were investigated and compared.

3.4.1 Aqueous ozone did not stress bacteria in this study

1 ppm aqueous ozone, which was the maximum concentration that could be achieved with the experimental set-up, did not extend the ‘apparent’ lag growth phase, or increase the intracellular redox state of Pst DC3000, Pst T1 or *E. coli* JHI-5025, whereas all of the other strong oxidant treatments (hydrogen peroxide, sodium hypochlorite, peracetic acid) did. It was expected that if ozone did stress bacteria, there would be an increase in the ‘apparent’ lag growth phase because it has previously been reported to cause an extended ‘apparent’ lag growth phase in bacteria (Selma *et al.*, 2007). Ozone has also been reported to reduce the culturability of bacteria (Westover *et al.*, 2022), which could cause an extended ‘apparent’ lag phase by increasing the time required for bacterial repair and adaption (Selma *et al.*, 2007). It was also expected that ozone would increase the intracellular redox state of bacteria if it induced stress, because gaseous ozone has previously been reported to cause roGFP2 oxidation via the glutathione pool in human airway epithelial cells (Gibbs-Flournoy *et al.*, 2013). An increase in bacterial intracellular ROS after ozone exposure has also been reported (Rangel *et al.*, 2021), so an increase in the oxidised redox state would be expected.

In the experiments, a high density (OD_{600nm} = 0.1 or 1) of bacteria was exposed to ozone in M9, therefore it was possible that the instantaneous ozone demand (IOD) (the consumption of ozone by reactive components at the initial stage of ozonation (Cruz-Alcalde *et al*., 2019)) would have depleted the ozone available to stress bacteria. For example, it has previously been reported that an ozone concentration below the IOD did not reduce bacteria, but when the ozone concentration was increased above the IOD, there was a reduction (Selma *et al.*, 2007). Since ozone increased the density which Pst T1 grew to, this could have indicated that Pst T1 was exposed to a non-lethal concentration of ozone, which could have primed it to become more tolerant to the ROS that it would have produced during bacterial growth, hence allowing it to grow to a higher density (Imlay, 2009; Rodríguez-Rojas *et al.*, 2020). Future work could aim to establish conditions to sufficiently stress bacteria in order to study the impact of ozone on bacterial responses. Since conditions were insufficient in this study, only the bacterial responses to hydrogen peroxide, peracetic acid and sodium hypochlorite were investigated and compared.

3.4.2 Hydrogen peroxide, peracetic acid and sodium hypochlorite extended the 'apparent' lag growth phase, reduced culturability and increased the intracellular redox state of bacteria

Hydrogen peroxide, peracetic acid and sodium hypochlorite all caused an extended 'apparent' lag growth phase, which was generally associated with a reduction in culturability in Pst DC3000, Pst T1 and *E. coli* JHI-5025. Although culturability was reduced this did not necessarily mean that there was a reduction in viability, since some cells may have entered into a viable but non-culturable (VBNC) state. This is an intermediate state of viability that some bacteria enter upon exposure to environmental stress, where they remain metabolically active but are incapable of cell division, therefore they would not be detected by culturable means (Zhao *et al.*, 2017). Future work could determine if hydrogen peroxide, peracetic acid and sodium hypochlorite could induce the

VBNC state in model pathogens. For this, preliminary work was completed to establish that the addition of sodium pyruvate (an antioxidant (Zhang *et al.*, 2021)) to LB agar could be used to resuscitate VBNC *S. enterica* (appendix 13) (resuscitation may not simply be achieved by the removal of the factor that induced the VBNC state, and resuscitation conditions are different for different bacteria (Zhao *et al.*, 2017)).

Based on the culturability data, it was concluded that *E. coli* was more tolerant to hydrogen peroxide but was more sensitive to sodium hypochlorite than Pst was. This indicated that although hydrogen peroxide and the active ingredients of sodium hypochlorite were strong oxidants, there were likely differences in the mechanisms by which bacteria could tolerate them. Occasionally, some of the treatments caused bacteria to grow to a higher density, which as previously explained, could have been due to bacteria being primed to be more tolerant against its self-produced ROS (Imlay, 2009; Rodríguez-Rojas *et al.*, 2020).

In addition to an increased ‘apparent’ lag growth phase and a reduced culturability, hydrogen peroxide, peracetic acid and sodium hypochlorite all quickly increased the intracellular redox state of Pst DC3000, Pst T1 and *E. coli* JHI-5025, which was measured using the redox state of the intracellular probe, roGFP. Increasing concentrations of each treatment increased the maximum oxidised signal that bacteria reached, until very high maximum oxidised signals were obtained, and increased the time for bacteria to recover to a more stable redox state. Since roGFP is primarily specific for gluthathione via glutaredoxin (Meyer *et al.*, 2007; Schwarzländer *et al.*, 2008), this indicated that all treatments rapidly increased the intracellular ratio of oxidised to reduced glutathione in bacteria, and then this ratio decreased for intracellular redox state recovery. Therefore, glutathione which is a major redox buffer (Carmel-Harel and Storz, 2000), must be involved in the bacterial response to each of these treatments.

3.4.3 Oxidative stress tolerance genes were upregulated in response to hydrogen peroxide, peracetic acid and sodium hypochlorite

The effect of 5 mM hydrogen peroxide, 1.040 ppm peracetic acid and 2.5 ppm sodium hypochlorite on the transcriptional response of selected genes (*oxyR*, *soxR*, *soxS*, *katG*, *ramA*, *lexA*, *gyrA*) in *E. coli* JHI-5025 were tested using transcriptional fusion fluorescent reporters. Each reporter was active to some extent, without the addition of any treatment, and there were differences in the expression of each gene. As previously mentioned in section 3.3.4, the preparation of cells for treatment exposure could have initially induced the transcription of some genes. Also, the presence of antibiotics in the medium, which were required for plasmid persistence, could have contributed to the continuous induction of genes relevant to the oxidative stress response. This is because genes under the control of the *ramA* and *soxRS* regulons include those which are involved in drug efflux, such as *acrAB* and *tolC* (Imlay, 2009; Bailey *et al.*, 2010, Zheng *et al.*, 2011). *ramA* was the most active gene in the absence of treatment and since its overexpression upregulates *arcAB* and *tolC* (Bailey *et al.*, 2010), the presence of antibiotics likely contributed to the high level of *ramA* transcription.

The response of transcriptional fusion fluorescent reporters in *E. coli* JHI-5025 to each treatment would likely be completed quickly because the intracellular redox state of *E. coli* JHI-5025 recovered within 30 minutes after exposure to each of the treatments. However, the expression of GFP+ produced by transcriptional fusion reporters was tested at 1, 5 and 18 hours post-treatment because time would be required for maturation of the GFP+ after its upregulation. Increases in GFP+ expression over time by a reporter could therefore be due to continued upregulation, or GFP+ that was produced may have continued to mature.

OxyR and SoxR are ‘first responders’ to oxidative stress (chapter 1, figure 1.3), because oxidative stress can directly alter their configuration, which results in the activation of their

regulons (Imlay, 2009). Their upregulation was therefore not required for the response to oxidative stress, so their upregulation during the response to treatments was not expected. When SoxR is in its oxidised state, it allows for the increased production of SoxS, which is required to switch on members of its regulon (chapter 1, figure 1.3) (Imlay, 2009). Therefore, the transcription of *soxS* was expected to increase under conditions of oxidative stress. When OxyR is in its oxidised state, *katG* is one of the genes which it most strongly upregulates (chapter 1, figure 1.3) (Zheng *et al.*, 2001). Therefore, under conditions of oxidative stress, *katG* was expected to be upregulated. RamA is a transcriptional activator and its overexpression has a role in oxidative stress, but its protective role only becomes apparent in the absence of the *soxRS* regulon (van der Straaten *et al.*, 2004), therefore, it was unknown if *ramA* would be upregulated by oxidative stress. *lexA* is upregulated in response to DNA damage, because under DNA damage conditions, LexA is cleaved so that it no longer represses its own promoter (Simmons *et al.*, 2008), therefore it was expected to be upregulated under conditions of DNA damage. *gyrA* is not known to be specifically involved in the oxidative stress response, however since it is required for DNA supercoiling its transcription could change under conditions of stress. This is because DNA supercoiling is a tool for introducing rapid changes in protein expression, which is often required for bacteria to survive stress (Weinstein-Fischer *et al*., 2000). Therefore, it was unknown if *gyrA* would be upregulated in response to treatments. The transcriptional response of each of these genes in Stm, in response to hydrogen peroxide was previously investigated, which mostly supported expectations (table 3.7) (Kröger *et al.*, 2013). *soxR* did however show a slight increase in upregulation after hydrogen peroxide exposure (table 3.7) (Kröger *et al.*, 2013).

Table 3.7: The fold change in relative expression levels of genes in Stm after hydrogen peroxide exposure

Promoter	Fold change in relative expression levels after H_2O_2 exposure (Kröger *et al*, 2013)
gyrA	0.22
oxyR	0.28
katG	35.66
soxR	1.34
soxS	16.98
ramA	1
lexA	2.69

All information was sourced from Kröger *et al.*, 2013. *S. enterica* sv. Typhimurium 4/74 was grown in PCN medium (Löber *et al.*, 2006) to OD_{600nm} 0.3 and then hydrogen peroxide (H_2O_2) was added to a final concentration of 1 mM for 12 minutes.

In this study, the median of *soxR*, *soxS*, *katG*, *ramA* and *lexA* controlled GFP+ expression increased within 1 hour after exposure to all treatments, in comparison to the water control. This indicated that their transcription was upregulated in response to each of these treatments. This was expected for all of the genes (there was previously no expectation for *ramA*), apart from *soxR* however a small increase in its upregulation was previously reported after hydrogen peroxide exposure (table 3.7) (Kröger *et al.*, 2013). The median of *soxR* and *ramA* controlled GFP+ expression peaked at 18 hours after exposure to all treatments and the water control. Since GFP maturation typically occurs within a few hours (Balleza *et al.*, 2018), there must have been a continued upregulation of *soxR* and *ramA* over time, both with and without treatment. *soxR* and *ramA* have not previously been reported to be upregulated during later growth phases in Stm (Kröger *et al.*, 2013) so another factor could have contributed to its continued upregulation, such as the presence of antibiotics in the medium. After hydrogen peroxide exposure only, the median of *soxS* and *lexA* controlled GFP+ expression continued to increase to 5 hours, whereas it decreased over time in all other samples. This could have been due to continued upregulation or GFP+ that was produced may have continued to mature after the 1 hour time-point and was not detected until the 5 hour time-point.

The median of *oxyR* controlled GFP+ expression did not increase within 1 hour of hydrogen peroxide or peracetic acid exposure but did after sodium hypochlorite exposure. The median of the *oxyR* controlled GFP+ expression drastically increased from 1 to 5 hours after hydrogen peroxide, and slightly further increased from 1 to 5 hours after sodium hypochlorite. Therefore, it may have had a delayed upregulation after hydrogen peroxide exposure or continued upregulation after sodium hypochlorite exposure. Alternatively, these results could have been due to a delay in GFP+ maturation as previously described. *oxyR* was not expected to be upregulated by treatments, however *oxyR* has previously been shown to be upregulated in response to petrol and diesel oil which increased intracellular ROS (Zhang *et al.*, 2018). The median of *gyrA* controlled GFP+ expression was not increased by hydrogen peroxide or peracetic acid but was increased by sodium hypochlorite within 1 hour of exposure.

Since hydrogen peroxide, peracetic acid and sodium hypochlorite caused an upregulation of *soxR*, *soxS*, *katG*, *ramA* and *lexA*, this highlighted that there must be similarities in the bacterial response to each of the treatments, since they would have all caused oxidative stress and DNA damage. Differences that were highlighted between the response of the transcriptional fusion reporters to each treatment could have been due to the differences in the level of stress that each treatment imposed.

Similarities in the transcriptional response of bacteria to hydrogen peroxide, peracetic acid and sodium hypochlorite have previously been reported. For example, Small *et al.*, 2007 identified that there were overlaps between the genes which were up and downregulated in the response of *Pseudomonas aeruginosa* to sub-lethal concentrations of hydrogen peroxide, peracetic acid and sodium hypochlorite, and all treatments caused transcriptional changes in many genes associated with membrane proteins, small molecule transport and putative enzymes. Small *et al.*, 2007 also showed that there were unique changes in the transcriptome associated with each treatment. Ceragioli *et al.*,

2010 showed that hydrogen peroxide, peracetic acid and sodium hypochlorite all induced genes involved in the general and oxidative stress response in *Bacillus cereus*.

3.4.4 *oxyR* and catalases were required for hydrogen peroxide but not always peracetic acid or sodium hypochlorite tolerance

oxyR was required for hydrogen peroxide tolerance in Pst DC3000, which was unsurprising because this has previously been reported (Ishiga and Ichinose, 2015). Although *oxyR* has also been reported to be required for tolerance to other oxidants, including tolerance to ozone in *E. coli* (Patil *et al.*, 2011), this study showed that it was not required for an increased tolerance to peracetic acid and sodium hypochlorite in Pst DC3000. Other regulons could therefore be responsible for driving the defence response to these treatments. For example, in *E. coli* other transcriptional activators and repressors, in addition to OxyR, are involved in the response to hypochlorous acid (an active component of sodium hypochlorite). These include HypT, RclR and NemR (da Cruz Nizer *et al*., 2020), which Pst DC3000 may have homologues to.

Catalases were collectively required for hydrogen peroxide tolerance in Pst DC3000, which again was unsurprising because this has previously been reported (Guo *et al.*, 2012). Catalases were also collectively required for peracetic acid tolerance but not sodium hypochlorite tolerance. This was interesting because it has previously been reported that the transcriptional response of *Bacillus cereus* to hydrogen peroxide and peracetic acid was very similar, whereas there were much greater differences exhibited in the response to sodium hypochlorite (Ceragioli *et al.*, 2010). Catalases have however previously been reported to be upregulated in the response to sodium hypochlorite (in addition to hydrogen peroxide and peracetic acid) in species including *Bacillus cereus* (Ceragioli *et al.*, 2010), enterics (this study) and *Pseudomonas aeruginosa* (Small *et al.*, 2007). Therefore, although catalases were not required for an increased tolerance to

sodium hypochlorite in Pst DC3000, they could have still been upregulated and involved in a redundant role.

Since OxyR upregulates all Pst DC3000 catalases to some extent (Ishiga and Ichinose, 2015) in the response to hydrogen peroxide, it was interesting that *oxyR* was not required for an increased tolerance to peracetic acid, but catalases were. Nevertheless, in the presence of hydrogen peroxide, *katE* and *katG* could also be upregulated in Pst DC3000 Δ*oxyR*, which suggests that these catalases are not solely under the control of OxyR (Ishiga and Ichinose, 2015).

The addition of *katG* back into the Pst DC3000 triple catalase deletion mutant (Pst DC3000 Δ*katBEG*) was able to restore some of its tolerance to hydrogen peroxide and peracetic acid, which indicated that *katG* was important for the tolerance to these treatments. The addition of *katG* back into Pst DC3000 Δ*katBEG* has previously been shown to restore some of its tolerance to hydrogen peroxide (Guo *et al.*, 2012).

Since OxyR was required for hydrogen peroxide tolerance but not peracetic acid or sodium hypochlorite tolerance, and catalases were required for hydrogen peroxide and peracetic acid tolerance but not sodium hypochlorite tolerance, this highlights that there are differences in the response of Pst DC3000 to each of these treatments.

3.4.5 Conclusion

Aqueous ozone did not cause bacterial stress in this study.

There were similarities and differences in the response of bacteria to hydrogen peroxide, peracetic acid and sodium hypochlorite. Similarities included an increased ‘apparent’ lag growth phase, reduced culturability, an increased intracellular redox state, and the induction of some genes involved in the oxidative stress response and DNA damage response in enterics. There were however differences since in Pst DC3000, *oxyR* and catalases were required for hydrogen peroxide tolerance, but not always peracetic acid or

sodium hypochlorite tolerance. Also, *E. coli* was more tolerant to hydrogen peroxide than Pst, but this did not mean it was any more tolerant to peracetic acid or sodium hypochlorite than Pst.

Overall, this study provided a deeper understanding of the bacterial response to each treatment. Although pathogens may have evolved a strong oxidative stress response to cope with the oxidative burst from eukaryotic hosts, which is mainly hydrogen peroxide (Lamb and Dixon, 1997; O'Brien *et al.*, 2012), this may not necessarily make them more tolerant to treatments used in the food industry which are strong oxidants, including peracetic acid and sodium hypochlorite.

Chapter 4: Bioluminescence imaging to demonstrate the effectiveness of different intervention treatments to control pathogens in the food industry

4.1 Introduction

The aim of this chapter was to investigate how effective gaseous ozone, aqueous ozone, sodium hypochlorite and peracetic acid were at reducing selected food-borne and plant pathogens on post-harvest produce.

The ability of ozone, sodium hypochlorite and peracetic acid to control pathogens relevant to the food industry has been well-studied, however the technique that is typically used to measure bacterial viability involves counting bacterial colonies formed on a selected medium after an incubation period (Selma *et al.*, 2006; Hassenberg *et al.*, 2008; Brilhante São José and Dantas Vanetti, 2012; Torlak *et al*., 2013; Wani *et al.*, 2015; Singh *et al*., 2018; Dharmarha *et al.*, 2019). This method is labour intensive, requires days before results are generated, and conditions may be insufficient for counting the true number of viable cells (Davey, 2011). A bioluminescence imaging technique was therefore developed to monitor the effect of ozone, sodium hypochlorite and peracetic acid on the viability of pathogens directly on the surface of post-harvest produce. This method involved the insertion of the *luxCDABE* operon into pathogens so that they could produce bioluminescence, which acts as an indicator of bacterial viability (Gregor *et al.*, 2018). Post-harvest produce, which had been inoculated with a *luxCDABE* tagged pathogen, was then subjected to bioluminescence imaging before and after the application of an intervention treatment, in order to demonstrate the effectiveness of the treatment. This method allowed results to be generated *in situ*, rapidly after treatment application.

4.1.1 *P. viridiflava* and *D. chrysanthemi* as additional model pathogens

As reported in chapter 1, section 1.1, Pst DC3000 and Pst T1 were selected as model plant pathogens, and *E. coli* JHI-5025 was selected as a proxy for an enteric pathogen, all of which are associated with the model fruit *Solanum lycopersicum* (tomato). Although Pst is a plant pathogen that is relevant to the food industry, it has only been reported to cause bacterial speck on tomatoes by infecting fruit at an early stage in fruit development (Getz *et al*., 1983), and no post-harvest outbreaks of bacterial speck have been reported. Plant pathogens and associated produce, which were more relevant models for post-harvest infection, were therefore also selected for work in this chapter. These included *Pseudomonas viridiflava* (*P. viridiflava*) and *Dickeya chrysanthemi* (*D. chrysanthemi*, formerly *Erwinia chrysanthemi* and *Pectobacterium chrysanthemi* (Hauben *et al.*, 1998; Samson *et al.*, 2005)), which have each caused post-harvest outbreaks of bacterial soft rot on the root of susceptible *Daucus carota* (carrot) plants (Farrar *et al*., 2000; Godfrey and Marshall, 2002). Therefore, carrots which had been colonised by each of these bacteria were used as model systems for work in this chapter. Bacterial soft rot is characterised by soft, slimy, brown flesh which often has a putrid odour due to secondary infections (Godfrey and Marshall, 2002). This presents a problem to the food industry because produce with bacterial soft rot have been abandoned by farmers or rejected by customers, which has subsequently resulted in large financial losses for farmers (Farrar *et al*., 2000; Godfrey and Marshall, 2002).

P. viridiflava and *D. chrysanthemi* are particularly relevant pathogens for this chapter because they each have a broad host range extending to more than 50 different plants, where a variety of disease symptoms on different parts of the host have been demonstrated (Centre for Agriculture and Bioscience International, 2022; Lipps and Samac, 2022). They could therefore present a risk to a range of post-harvest produce. For example, the host range of *P. viridiflava* and *D. chrysanthemi* includes other commercial crops such as cabbage, cauliflower, melon, onion, and tomato (Centre for

Agriculture and Bioscience International, 2022; Lipps and Samac, 2022). The capability of *P. viridiflava* and *D. chrysanthemi* to cause disease on a specific host is however strain dependent (Collmer *et al*., 1994; Lipps and Samac, 2022).

The different model systems which were selected to address the aims of this chapter are summarised in table 4.1.

Table 4.1: Selected model systems

Model pathogen	**Associated produce**	**Disease caused by model pathogen on associated produce**
Pseudomonas syringae pv. tomato DC3000	Solanum lycopersicum (tomato)	Bacterial speck
Pseudomonas syringae pv. tomato T1	Solanum lycopersicum (tomato)	Bacterial speck
Escherichia coli JHI-5025	Solanum lycopersicum (tomato)	N/A
Pseudomonas viridiflava PC006	Daucus carota (carrot)	Bacterial soft rot
Dickeya chrysanthemi EC16	Daucus carota (carrot)	Bacterial soft rot

4.1.2 Concentrations and applications of intervention treatments in the food industry

To control for the potential contamination of post-harvest produce by pathogens, fruits and vegetables are commonly subjected to an intervention treatment (Ramos *et al.*, 2013). Chlorine-based treatments, peracetic acid and ozone could each be used (Ramos *et al.*, 2013; Chinchkar *et al.*, 2022), and the benefits and constraints of these treatments have previously been discussed in chapter 1, section 1.7. For work in this chapter, it was important that the concentration and application of each treatment tested was representative of those used in the food industry.

Concentration limits for intervention treatments are in place in the U.S. (21 C.F.R. §173.315), however they are not in the UK. Instead, authorised treatments for post-harvest produce are restricted by MRLs. If a MRL does not exist for the treatment, or associated degradation products, and a MRL exemption is not in place, the default MRL

of 0.01 mg/kg will apply based on the assumption it should not be present on food (Health and Safety Executive, 2023). The U.S. also has MRLs in place (40 C.F.R. §180).

Chlorine-based treatments

Chlorine-based treatments are used for washing fruits and vegetables in the UK (Chilled Food Association, 2010), and are typically applied by a 1 - 2 minute submersion, where free chlorine concentrations in the wash are measured at the start and end of each wash (Food Standards Scotland, personal communication). 50 - 100 ppm free chlorine concentrations are generally used (The Food and Agricultural Organisation of the United Nations and The World Health Organisation, 2008). In the U.S., sodium hypochlorite is a chlorine-based treatment approved for washing fruits and vegetables with no concentration limit, but a subsequent rinse with potable water is required (21 C.F.R. §173.315).

Peracetic acid

In the U.S., <80 ppm peracetic acid can be used in wash water for fruit and vegetables that are not raw agricultural commodities, without the need for a subsequent rinse with potable water (21 C.F.R. §173.315). It is recommended that a test strip is used to measure the concentration of peracetic acid in the wash, and that produce are submerged in peracetic acid for at least 1 minute (Hadad, 2018).

Ozone

In water that is clean, potable and free from debris, ozone is an effective sanitiser within the concentration range of 0.5 - 2 ppm (Suslow, 2004) and is typically applied to produce using a continuous flow chamber (Sarron *et al*., 2021). Ozone is affirmed as generally recognised as safe (GRAS) by the United States Food and Drug Administration. In the U.S., it can be added directly to bottled water to serve as an antimicrobial agent (21

C.F.R. §184.1563) and can also be used as a food contact antimicrobial agent (21 C.F.R. §173.368).

In this chapter, the following treatment concentrations and applications were therefore used:

- Sodium hypochlorite with 100 ppm free chlorine (confirmed with a test strip), applied to produce by a 1 minute submersion. Produce was then submerged in water for a further minute.
- 80 ppm peracetic acid (confirmed with a test strip), applied to produce by a 1 minute submersion.
- 0.7 - 1.0 ppm aqueous ozone, applied to produce via a set-up designed to mimic a continuous flow set-up.
- Gaseous ozone with a 3 second ozone generation time (recommended by Anacail Ltd), applied to produce via the in-pack ozone system.

4.1.3 Bioluminescence imaging is a technique for bacterial viability determination

To test if an intervention treatment can be used to effectively control pathogens on post-harvest produce, it is important to measure the viability of pathogens after exposure to the treatment. The gold standard method for this involves processing post-harvest produce in buffer to release bacteria, and then counting bacterial colonies formed on a selected medium after an incubation period (Selma *et al.*, 2006; Hassenberg *et al.*, 2008; Brilhante São José and Dantas Vanetti, 2012; Torlak *et al*., 2013; Wani *et al.*, 2015; Singh *et al*., 2018; Dharmarha *et al.*, 2019). This method is labour intensive, often requires large volumes of media and reagents, and is time-consuming, both in regard to labour time and in regard to days being required before results are generated. Conditions for bacterial recovery may also be insufficient, and specific bacterial phyla and bacteria in intermediate states of viability may not be able to be detected. The true number of viable cells may also be underestimated due to a single colony being produced by more than one viable

cell, or due to the bacterial density being too low to form observable growth (Jasson *et al.*, 2010; Davey, 2011).

The expression of bioluminescence (light emitted from an organism due to an enzymatic reaction catalysed by luciferases) from bioluminescent bacterial cells can be used as an alternative method for bacterial viability determination (Morrissey *et al*., 2013). This is because the cell must continuously supply adenosine triphosphate (ATP) and NADPH for the regeneration of substrates to keep the bioluminescence reaction ongoing, therefore only metabolically active cells are bioluminescent (Gregor *et al.*, 2018). Bioluminescence imaging can image, and subsequently quantify, bioluminescence expressed from bacteria *in situ*, therefore it could be used to quantify bacterial viability directly on post-harvest produce, after exposure to an intervention treatment (Karsi *et al.*, 2008; Huang and Nitin, 2017). This technique provides rapid results (Morrissey *et al*., 2013) and since results are provided *in situ* without the requirement for sample destruction, multiple bacterial viability measurements could be taken from the same sample over a time course and the precise locations of pathogens could be identified (Morrissey *et al*., 2013). In addition to these benefits, *in situ* bioluminescence imaging does not require time for sample destruction and further processing or media preparation, therefore it is much less labour-intensive and time-consuming than bacterial colony counting (Morrissey *et al*., 2013). Some limitations are however associated with this technique, for example, expensive equipment is required (Nyhan *et al.*, 2020) and like bacterial colony counts, it cannot detect all cells in a reduced state of viability (Duncan *et al.*, 1994). Multiple bacterial cells are also typically required to detect bioluminescence (Karsi *et al.*, 2008; Soldan *et al.*, 2021), whereas single bacterial cells can be detected by colony counts (Davey, 2011). Oxygen is also required for the expression of bioluminescence (Gregor *et al.*, 2018), therefore bioluminescence can not be used as a viability marker in anaerobic conditions (Morrissey *et al*., 2013). Since the majority of bacteria which express natural bioluminescence are from marine environments, bacteria also need to be genetically modified to produce

bioluminescence, which can be completed by the introduction of a *luxCDABE* operon (Morrissey *et al*., 2013).

Since bioluminescence imaging provides rapid results *in situ*, it was used for work in this chapter to determine the effectiveness of intervention treatments against pathogens on post-harvest produce. This involved imaging post-harvest produce which had been inoculated with a *luxCDABE* tagged pathogen, before and after the application of an intervention treatment.

In situ imaging of bioluminescent pathogens on food, to assess the ability of treatments to reduce pathogens on food, has previously been used. For example, it has been used to assess if commercial surfactants, with or without the addition of soil, could reduce *E. coli* and *Listeria* on lettuce leaves (Huang and Nitin, 2017), if water reduced *Salmonella* on chicken skin (Karsi *et al.*, 2008), and if heat treatment reduced *Salmonella* on different meat surfaces (Lewis *et al.*, 2006). To current knowledge, the suitability of the technique for assessing the effect of peracetic acid, sodium hypochlorite, or ozone to reduce bacteria on foodstuffs, and the suitability of the technique to assess the effect of any treatment against pathogens colonised on carrots or tomatoes has never been tested. An aim of this study was therefore to validate bioluminescence imaging as a technique for this.

4.1.4 The *luxCDABE* operon makes bacteria bioluminescent

Model pathogens for this chapter were tagged with the *luxCDABE* operon so that they could express bioluminescence (Gregor *et al.*, 2018). In bioluminescent bacterial cells, *luxA* and *luxB* encode a luciferase (figure 4.1) which catalyse a luciferin, namely reduced flavin mononucleotide ($FMNH_2$), to emit light in the form of a blue photon (figure 4.2). *luxC*, *luxD* and *luxE* encode a fatty acid reductase complex (figure 4.1), so it can reduce the fatty acid (RCOOH) which is produced by this reaction, to the aldehyde substrate (RCHO) which is required to keep the reaction ongoing (figure 4.2). Flavin

mononucleotide (FMN) is also produced by the bioluminescence reaction, and all cell types encode a flavin mononucleotide reductase (FMN reductase) so are able to reduce FMN to $FMNH_2$, which is also required to keep the bioluminescence reaction ongoing (figure 4.2). A continuous supply of ATP and NADPH is required for the regeneration of the $FMNH_2$ and RCHO substrates to keep the bioluminescence reaction ongoing, therefore bioluminescence is expected to disappear on cell death, where the supply of ATP and NADPH would cease. The addition of the *luxCDABE* operon into bacterial cells would therefore allow the production of bioluminescence to be used as a measure of viability (Gregor *et al.*, 2018).

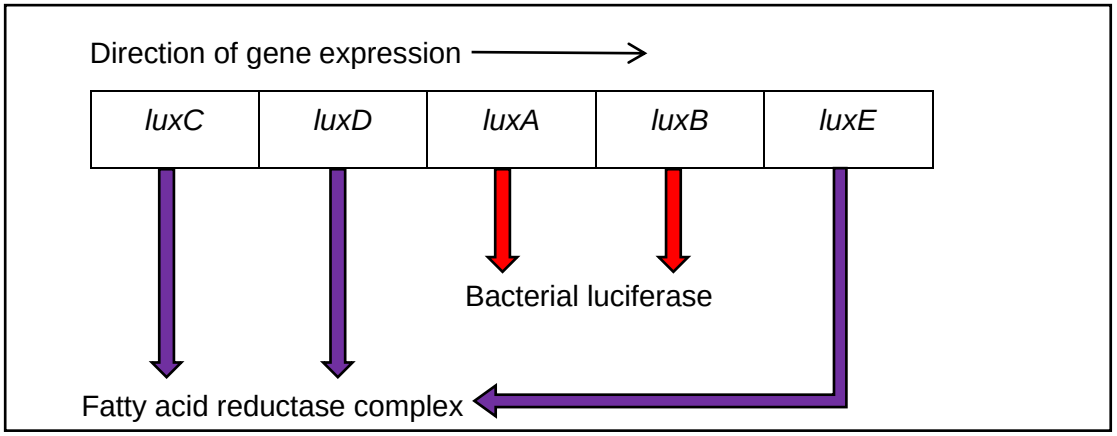


Figure 4.1: The *luxCDABE* operon

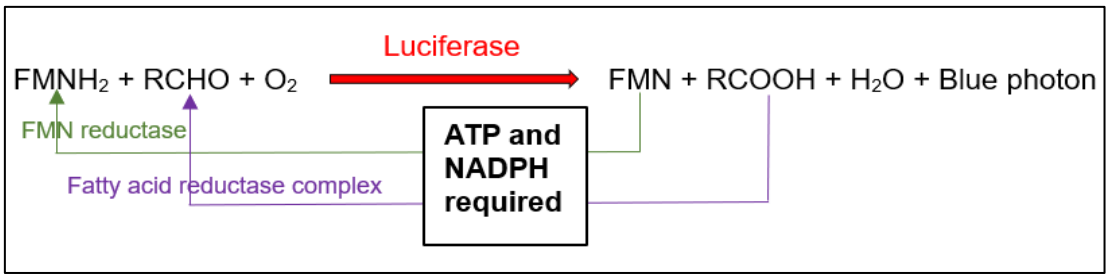


Figure 4.2: The bioluminescence reaction

4.1.5 Chapter aims

This chapter aimed to develop a bioluminescence imaging technique to monitor the effect of gaseous ozone, aqueous ozone, sodium hypochlorite and peracetic acid on the viability of pathogens directly on the surface of post-harvest produce (carrots and tomatoes).

4.2 Materials and methods

4.2.1 Antimicrobial chemicals

Antimicrobial chemicals that were sourced for this study are listed in table 4.2. Ozone was also an antimicrobial chemical that was used for this study; however, it did not require to be sourced because it was generated on-site at working concentrations.

Table 4.2: Antimicrobial chemicals sourced for this study

Chemical	Source	Concentration of stored stock	Concentration of working stock
Peracetic acid ($C_2H_4O_3$)	ThermoFisher Scientific, UK	ca. 35% peracetic acid	0.008% (80 ppm)
Sodium hypochlorite (NaClO)	ThermoFisher Scientific, UK	15.3% sodium hypochlorite	0.01% (100 ppm) free chlorine

80 ppm peracetic acid and sodium hypochlorite with 100 ppm free chlorine were made as described in chapter 3, section 3.2.1.

4.2.2 Bacterial strains, plasmids and primers

Bacterial strains used for this study are listed in table 4.3.

Table 4.3: Bacterial strains used for this study

Strain	Description	Antibiotics	Reference
Wildtype model pathogens			
Pseudomonas syringae pv. tomato (Pst) DC3000	A rifampicin-resistant derivative of Pst DC52 (also referred to as NCPPB 1106), which was isolated from tomatoes on the island of Guernsey, UK (Buell *et al.*, 2003; Almeida *et al.*, 2009)	Rifampicin, nitrofurantoin	(Cuppels, 1986)
Pst T1	An isolate from tomatoes in Canada	Nitrofurantoin	(Almeida *et al.*, 2009)
Pseudomonas viridiflava (*P. viridiflava*) PC006	An isolate from carrots exported from New Zealand which had bacterial soft rot during post-harvest refrigerated storage	Nitrofurantoin	(Godfrey and Marshall, 2002)
Escherichia coli (*E. coli*) JHI-5025	An isolate from soil in Scotland	NA	(Holden, 2021)
Dickeya chrysanthemi (*D. chrysanthemi*) EC16	An isolate from Chrysanthemum morifolium	NA	(Burkholder *et al.*, 1953)
Luminescent model pathogens			
Pst DC3000 p_{nptII}::lux	Pst DC3000 expressing *luxCDABE* under the *nptII* promoter via a genomic integration at the Tn7 attachment site	Gentamicin, rifampicin, nitrofurantoin	This study
Pst T1 p_{nptII}::lux	Pst T1 expressing *luxCDABE* under the *nptII* promoter via a genomic integration at the Tn7 attachment site	Gentamicin, nitrofurantoin	This study
P. viridiflava PC006 p_{nptII}::lux	*P. viridiflava* PC006 expressing *luxCDABE* under the *nptII* promoter via a genomic integration at the Tn7 attachment site	Gentamicin, nitrofurantoin	This study
E. coli JHI-5025 (pIJ11282)	*E. coli* JHI-5025 expressing *luxCDABE* under the *nptII* promoter via the pIJ11282 plasmid	Carbenicillin, tetracycline	This study
D. chrysanthemi EC16 (pIJ11282)	*D. chrysanthemi* EC16 expressing *luxCDABE* under the *nptII* promoter via the pIJ11282 plasmid	Carbenicillin, tetracycline	This study
Fluorescent model pathogens			
E. coli JHI-5025 (p_{gyrA}-GFP+)	*E. coli* JHI-5025 expressing constitutive fluorescence via p_{gyrA}-GFP+	Chloramphenicol	Gifted from Holden lab
Strains for plasmid extractions			
E. coli DH5α (pIJ11282)	*E. coli* DH5α with pIJ11282	Carbenicillin, tetracycline	(Frederix *et al.*, 2014)
Strains for mating conjugations			
E. coli DH5α (pRS-p_{nptII}::lux)	*E. coli* DH5α with pRS-p_{nptII}::lux	Gentamicin, carbenicillin	(Soldan *et al.*, 2021)
E. coli SM10/λ pir (pUX-BF13)	*E. coli* SM10/λ pir with pUX-BF13	Carbenicillin	(Miller and Mekalanos, 1988)

E. coli DH5α *(*pRK2013)	*E. coli* DH5α with pRK2013	Kanamycin	(Figurski and Helinski, 1979)

Plasmids used for this study are listed in table 4.4.

Table 4.4: Plasmids used for this study

Plasmid	**Description**	**Antibiotic resistance**	**Reference**
pIJ11282	Allows host strains to express *luxCDABE* under the *nptII* promoter	Carbenicillin, tetracycline	(Frederix *et al.*, 2014)
p_{gyrA}-GFP+	pKC026 with *gyrA* upstream region (from *E. coli*) fused to GFP+	Chloramphenicol	(Holden *et al.*, 2006)
pRS-p_{nptII}::lux	Suicide plasmid for the delivery of *luxCDABE* under the *nptII* promoter	Gentamicin (within Tn7 insertion region) and carbenicillin (within backbone)	(Soldan *et al.*, 2021)
pRK2013	Suicide plasmid required for the production of a secretion system for the mobilisation of non-self-transmissible plasmids	Kanamycin	(Figurski and Helinski, 1979)
pUX-BF13	Suicide plasmid for the delivery of the Tn7 transposase complex: *TnsABCDE*	Carbenicillin	(Miller and Mekalanos, 1988)

Primers used for this study are listed in table 4.5.

Table 4.5: Primers used for this study

Primer	Sequence (5' – 3')	Use
glms_F	AATCCGACCTGACCCTGCT	Forward primer for confirmation that Tn7 transposon has inserted into the expected genomic site of *P. syringae*
glms_F_viri	CGAATCCGACCTCACTCTGCT	Forward primer for confirmation that Tn7 transposon has inserted into the expected genomic site of *P. viridiflava*
Right_end_Tn7_transposon	CACGCCCCTCTTTAATACGACGG	Reverse primer for confirmation that Tn7 transposon has inserted into the expected genomic site of *P. syringae* and *P. viridiflava*

4.2.3 Media and growth conditions

Media

The following media were used in this study:

- Lysogeny broth (LB): 10 g/L tryptone, 5 g/L yeast extract, 10 g/L NaCl
- Super optimal broth with catabolite repression (SOC) medium: 20 g/L tryptone, 5 g/L yeast extract, 0.5 g/L NaCl, 2.5 mM KCl, 0.4 mM $MgCl_2$, 0.8 mM glucose, pH adjusted to 7

For solid media, agar was added at 1.5% (w/v). Antibiotics were used at the following concentrations: 50 µg/ml carbenicillin, 25 µg/ml chloramphenicol, 10 µg/ml gentamicin, 50 µg/ml kanamycin, 25 µg/ml nitrofurantoin.

Growth conditions

All bacterial strains were stored in 25% glycerol at -80^{o}C. They were cultured onto LB agar and incubated at 28^{o}C for 1 - 2 days until single colonies appeared. Single colonies were used to inoculate 10 ml LB, which was incubated at 28^{o}C, 220 rpm overnight (20 to 24 hours). If required, antibiotics were added to liquid or solid media at the working stock concentrations mentioned above. Bacteria hosting plasmids were always grown in the

presence of the relevant antibiotic. Bacteria which had a genomic integration at the attTn7 site were only grown in the presence of relevant antibiotics on LB agar but not liquid medium because the chromosomal insertion is stable in the absence of antibiotics (Choi *et al.*, 2005).

4.2.4 Produce

Tomatoes cv. Arlintia (300 g packs from either Thanet Earth, UK, or the Netherlands) and carrots (500 g packs from UK, either from grower B. Madarrasi or R. Abrey) were sourced from a local retailer (Marks & Spencer, UK). After purchase, tomatoes and carrots were stored at 4^{o}C and were transferred to room temperature the day before experimental work. 6 tomatoes totalling 0.24 kg +/- 10% or 6 carrots totalling 0.28 kg +/- 10% were used per treatment group in each experiment. All produce were used for experimental work before or on their best before date. Tomatoes were broken from the vine at the natural break point (chapter 2, figure 2.1). A thin slice was cut from the bottom of each tomato and the back of each carrot to provide produce with a straight edge to sit on. The weight of each tomato or carrot was then recorded before they were labelled with permanent marker, pre-rinsed with distilled water and left to dry on tissue in a laminar flow cabinet.

4.2.5 Chromosomal integration of the *luxCDABE* operon by four parental mating conjugation

Pst DC3000, Pst T1 and *P. viridiflava* PC006 were respectively tagged with a chromosomal integration of the *luxCDABE* operon in the attTn7 site by four parental mating conjugation as described in section 3.2.5, however *E. coli* DH5α (pRS-p_{nptII}::lux) was the donor (table 4.3).

Transformed colonies were screened for luminescence by viewing the plate with the NightOWL LB 983 NC100 *in vivo* imaging system (Berthold Technologies). To verify that

luxCDABE had integrated into the expected genomic site, colony PCR with GoTaq G2 DNA polymerase (Promega, UK) was performed using the primer pair glms_F (for *P. syringae*) or glms_F_viri (for *P. viridiflava*) and Right_end_Tn7_transposon (table 4.5).

4.2.6 Delivery of the *luxCDABE* operon by the introduction of pIJ11282

D. chrysanthemi EC16 and *E. coli* JHI-5025 (table 4.3) were tagged with the *luxCDABE* operon by the introduction of the pIJ11282 plasmid (table 4.4) into electrocompetent cells via electrotransformation. (They were not transformed by a chromosomal integration in the attTn7 site because a donor plasmid for this, with *luxCDABE* under the control of *nptII*, was not readily available for transformation into *Enterobacteriaceae*).

A plasmid preparation of pIJ11282 was obtained from *E. coli* DH5α (pIJ11282) (chapter 3, section 3.2.4). Electrocompetent cells for both *E. coli* JHI-5025 and *D. chrysanthemi* EC16 were made as previously described in chapter 3, section 3.2.4. Electrotransformation for *E. coli* JHI-5025 was completed as previously described in chapter 3, section 3.2.4. Electrotransformation for *D. chrysanthemi* EC16 was also completed in the same way however after electrotransformation, cells were recovered in 0.5 ml LB and incubated at 30^{o}C, 220 rpm for 2 hours. Cultures spread on LB agar were incubated at 28^{o}C for 2 days.

Transformed colonies were screened for luminescence by viewing the plate with the NightOWL LB 983 NC100 *in vivo* imaging system (Berthold Technologies).

4.2.7 Bactericidal action of liquid intervention treatments on pathogens *in vitro*

Overnight cultures of luminescent model pathogens (table 4.3) were centrifuged at 4000 x g for 6 minutes, washed with sterile distilled water once, resuspended in sterile distilled water equivalent to 0.5 x the original volume, and adjusted to OD_{600nm} 1 in sterile distilled water. 10 µl of each bacterium was then added to a 50 ml falcon tube containing 10 ml of sterile distilled water, ozonated tap water (0.7 - 1.0 ppm ozone), peracetic acid (80 ppm

peracetic acid) and sodium hypochlorite (100 ppm free chlorine), respectively. After 1 minute of bacterial addition, each solution was vortexed at a medium speed for several seconds with a Rotamixer Hati Vortex-Mixer before serial dilutions were completed in sterile distilled water. 3 x 20 µl spots for each serial dilution were dispensed onto LB agar, which were left to dry in a laminar flow cabinet. LB agar plates were incubated at 28^{o}C for 1 - 2 days until single colonies appeared which were subsequently counted. The mean count for 3 spots was used to calculate the experimental mean.

4.2.8 Inoculation of bioluminescent pathogens onto produce

An overnight culture of a model pathogen which expressed *luxCDABE* (or p_{gyrA}-GFP+ for confocal microscopy experiments) (table 4.3) was diluted into 3 x 200 ml fresh LB, each by a factor of 1:100, which were incubated at 28^{o}C, 220 rpm overnight (20 to 24 hours). Bacteria were centrifuged at 3214 x g for 6 minutes, washed in PBS once and resuspended in PBS equivalent to 0.5 x the original volume. Bacteria were diluted to OD_{600nm} 0.5 in 800 ml PBS, which was poured into a 1.5 L tub. Either 6 carrots or 6 tomatoes were added to the tub with the relevant model pathogen (table 4.1), which was placed on a Fisherbrand Multi-Platform Shaker for 30 minutes at 50 rpm. Produce was then dried for 1 hour on tissue in a laminar flow cabinet.

4.2.9 Delivery of intervention treatments

Intervention treatments and subsequent controls were assigned into one of three treatment sets. Set 1 treatments included 80 ppm peracetic acid ($C_2H_4O_3$), sodium hypochlorite (NaClO) with 100 ppm free chlorine, and a distilled water control (table 4.2). For all set 1 treatments, a 1 kg produce: 10 L treatment ratio was used because this had been done in previous studies (Suwimon *et al*., 2011: Singh *et al*., 2018). Produce was submerged in each treatment in a 3 L tub. The submersion time for all treatments was 1 minute, however after the application of sodium hypochlorite, produce was immediately submerged in a 3 L tub containing the same volume of distilled water for a further minute,

to represent a subsequent wash in potable water. Produce was dried for 1 hour on tissue in a laminar flow cabinet.

Set 2 treatments included ozonated tap water (aqueous O_3) (0.7 - 1.0 ppm) and a tap water control. Tap water was supplied to central Oxford, which was the site of the laboratory where experiments were completed, by Thames Water Utilities Limited. Parameter (organism, substance or physical property) levels that were in tap water in central Oxford, 2022 is available in appendix 14 (2022 was when relevant experiments were completed). For all set 2 treatments, a 1 kg produce: 40 L treatment ratio was used, because a large volume of aqueous ozone is typically applied to produce (Sarron *et al*., 2021) and this was the maximum volume that could be achieved with the laboratory set-up. Each treatment was delivered continuously from a 25 L tank over a time period of 2.57 - 3.66 minutes for carrots and 1.93 - 3.00 minutes for tomatoes. To deliver each treatment, a 19 L tub was used to catch overflow, and a 3 L tub, containing produce, was placed on top of a rack within this tub. Water from the tank flowed into the 3 L tub, which would eventually overflow into the 19 L tub, however, overflow never reached the contents of the 3 L tub. Overflow was treated with Virkon for safe pathogen disposal. Produce was dried for 1 hour on tissue in a laminar flow cabinet.

Set 3 treatments included gaseous ozone (gaseous O_3), which was generated for 3 seconds at a command voltage of 3.2 V by the in-pack ozone system (Anacail Ltd, UK, model: F250, serial no: 4) and a no treatment control. The ozone which was generated would have taken up to a few hours to completely decay (Potts and Diver, 2012) so bacteria would have remained exposed to ozone during this time. For set 3 treatments, produce colonised by bioluminescent bacteria was packed into punnets (DUNI, UK). All tomatoes for either treatment or no treatment were packed into the same punnet respectively, with each tomato resting on its flat cut edge, and also against each other. Carrots were packed into separate, individual punnets, due to their size. Punnets were sealed with 5-lane custom microperforated film (Coveris, UK) at 100^{o}C before being

ozone-treated or not. Before ozone treatments were performed on samples, 3 empty sealed punnets were used to record peak ozone concentrations produced by a 3 second ozone generation time because this could not be recorded in sample punnets without destruction of ozone (appendix 1.2). Peak ozone concentrations ranged from 663 - 827 ppm (appendix 1.2). Treated or non-treated produce was kept in sealed punnets for 1 hour at room temperature before punnets were opened in the fume hood.

4.2.10 Bioluminescence imaging

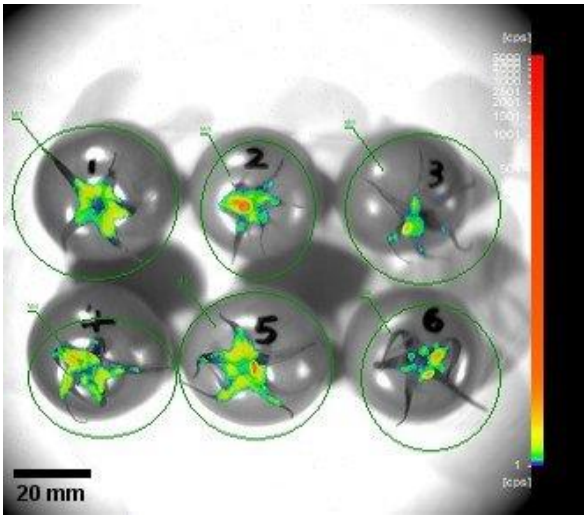
Produce was kept in the dark for 10 minutes before being imaged with a NightOWL LB 983 NC100 *in vivo* imaging system (Berthold Technologies) at a distance and resolution determined by the sample height and size. Luminescence was imaged with a high camera gain, 20 minute exposure time and 1 x 1 binning. A bright field image was then recorded with a low camera gain, 0.1 second exposure time and 10% illumination. IndiGO™ version 2.0.5.0 (Berthold Technologies) overlaid luminescent and bright field images and images were modified to only display luminescence within a specific range, defined on a scalebar. Ranges were selected to include maximum luminescence values but to avoid oversaturation. Luminescence (counts per second (cps)) was quantified in regions of the image that were outlined, and all luminescence detected was quantified, regardless of the luminescence range selected to be displayed on images.

4.2.11 Bioluminescence imaging for the effectiveness of different intervention treatments

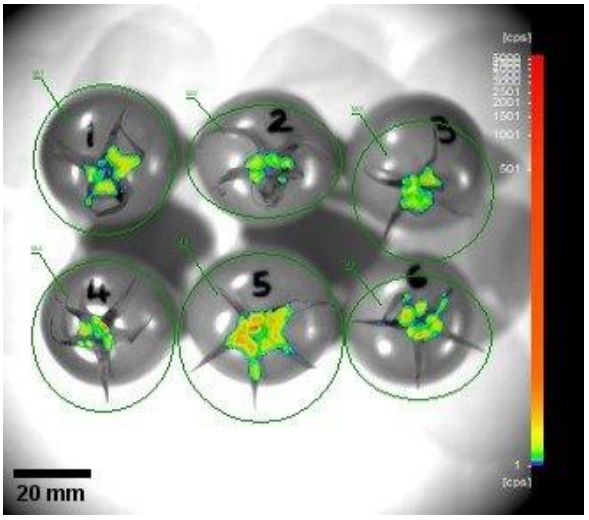
Produce colonised by bioluminescent model pathogens (tables 4.1 and 4.3) were imaged for luminescence before and after treatment. Tomatoes were imaged using a sample height and size of 50 mm and 150 mm, respectively, whereas carrots were imaged using a sample height and size of 25 mm and 230 mm, respectively. On each image, circles were manually drawn around the calyx and pedicel of each tomato because these were the only parts of tomatoes which model pathogens appeared to colonise, as seen in

bioluminescence imaging (figure 4.3). The outline of each carrot was also manually drawn around (figure 4.4), so that luminescence quantification data was obtained for the pathogens present on each tomato calyx and pedicel, and each carrot. To account for luminescence values of zero, one was added to all luminescence values before $\log_{10}$ transformation for data presentation and analysis.

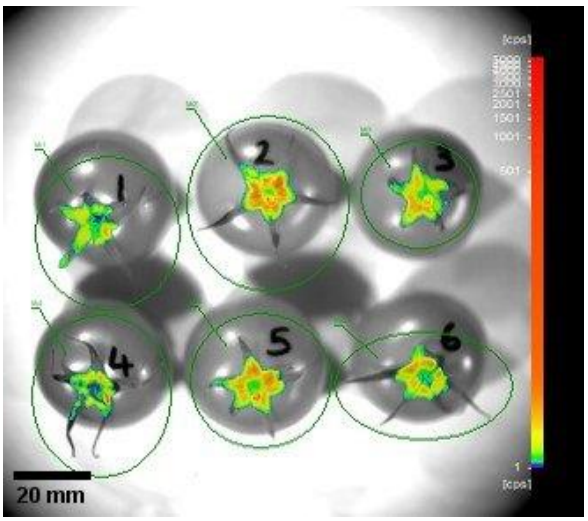
A. JHI-5025 (pIJ11282)



B. DC3000 p_{nptII}::lux



C. T1 p_{nptII}::lux



D. PC006 p_{nptII}::lux

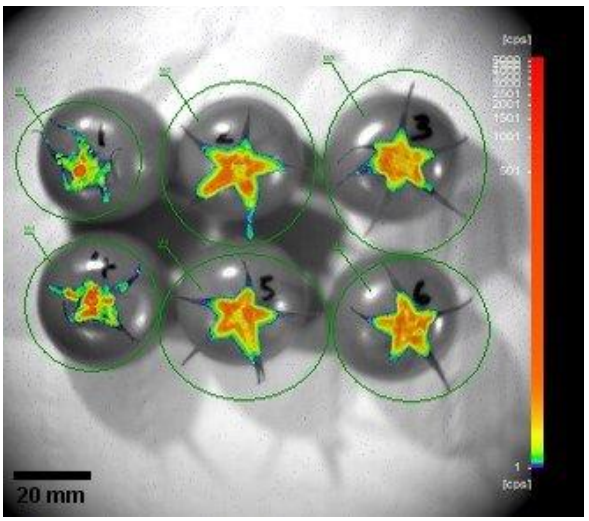


Figure 4.3: Example luminescent images of tomatoes colonised by bioluminescent bacteria: (A) *E. coli* JHI-5025 (pIJ11282), (B) *P. syringae* pv. tomato DC3000 p_{nptII}::lux, (C) *P. syringae* pv. tomato T1 p_{nptII}::lux and (D) *P. viridiflava* PC006 p_{nptII}::lux. Bacteria at OD_{600nm} 0.5 in PBS were inoculated onto tomatoes by submersion. Tomatoes were dried and imaged for luminescence with the NightOWL LB 983. Colour scales for luminescence counts per second (cps) are displayed.

A. EC16 (pIJ11282)

B. PC006 p_{nptII}::lux

C. JHI-5025 (pIJ11282)

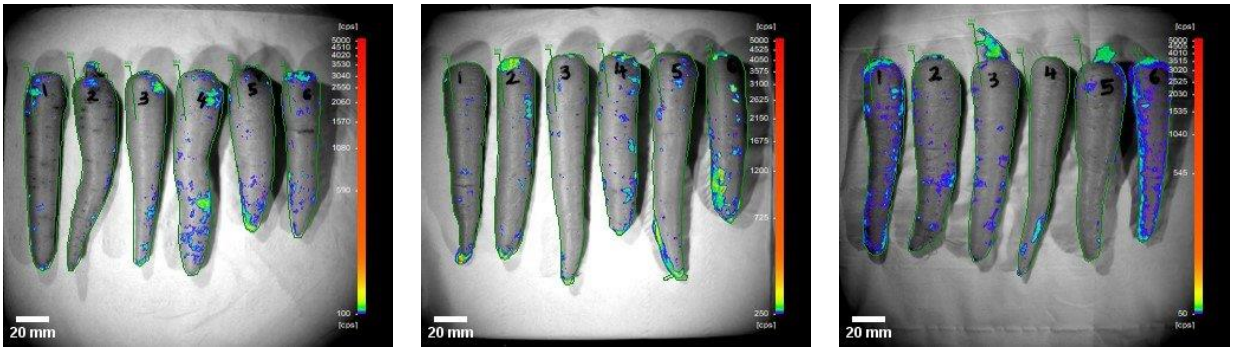


Figure 4.4: Example luminescent images of carrots colonised by bioluminescent bacteria: (A) *D. chrysanthemi* EC16 (pIJ11282), (B) *P. viridiflava* PC006 p_{nptII}::lux and (C) *E. coli* JHI-5025 (pIJ11282). Bacteria at OD_{600nm} 0.5 in PBS were inoculated onto carrots by submersion. Carrots were dried and imaged for luminescence with the NightOWL LB 983. Colour scales for luminescence counts per second (cps) have different minimum values to avoid oversaturation.

4.2.12 Bioluminescence imaging technique validation with colony counts

A single carrot model system, with *P. viridiflava* PC006 p_{nptII}::lux, and a single tomato model system, with *E. coli* JHI-5025 (pIJ11282) (tables 4.1 and 4.3), were used to validate bioluminescence imaging as a technique for determining the effectiveness of different intervention treatments. This involved the quantification of bioluminescent bacteria on either treated or untreated produce by both bioluminescence imaging and bacterial colony counting so that results from each of these measures could be compared.

Produce colonised by bioluminescent bacteria were either left untreated or were subjected to an intervention treatment or the relevant water control. For tomatoes, the calyx and pedicel (chapter 2, figure 2.1) were then removed because these were the only parts of tomatoes which bacteria colonised, as seen in bioluminescence imaging (figure 4.3), therefore they were the only parts that were subjected to bacterial quantification. The pedicel, which was detached from the calyx and held upright, was cut down the centre. For bioluminescence imaging, the two halves of each pedicel were arranged on their cut surface so that the outer portions of the pedicel were exposed for imaging, and each calyx was flattened as much as possible, with their tips being secured by micropore tape (figure 4.5: A). It is to be noted that bioluminescent bacteria generally adhered to the central area of calyxes and not calyx tips (figure 4.3 and 4.5: A, B), therefore the use of tape on calyx

tips was justified. For imaging, the sample height and size were set to 2 mm and 200 mm respectively. The NightOWL LB 983 NC100 *in vivo* imaging system (Berthold Technologies) does have some penetration depth, which is variable dependent upon the sample intensity (Berthold Technologies, personal communication), however luminescence on the underside of a calyx being imaged was not captured (appendix 15). Since it would have been possible for bacteria to adhere to either side of the calyx during inoculation, and since the entire calyx would be used for bacterial colony counting, the luminescence on the opposite side of each calyx was captured in a separate image, using the same sample height and sample size measurements (figure 4.5: B). After imaging, outlines were manually drawn around calyxes and pedicel halves for area and luminescence quantification (figures 4.5: A, B). The total area and luminescence from the two pedicel halves, upperside calyx and underside calyx from the same tomato were pooled together respectively to provide the total luminescence and total area for that replicate.

After carrots were exposed to an intervention treatment or not, 3 strips of epidermal surface were collected from each carrot using a vegetable peeler. Their luminescence was imaged using a sample height of 2 mm and a sample size of 275 mm, and an outline was manually drawn around each carrot peel for area and luminescence quantification (figure 4.5: C). The total area and luminescence from each peel from the same carrot were pooled together respectively to provide the total luminescence and total area for that replicate. Luminescence results from carrots and tomatoes were presented as $\log_{10}$(luminescence (cps mm^{-2})) for a measure of bacterial quantification.

A. JHI-5025 (pIJ11282) on upperside tomato calyxes and outer pedicel sections

B. JHI-5025 (pIJ11282) on underside tomato calyxes

C. PC006 p_{nptII}::lux on carrot epidermal surface strips

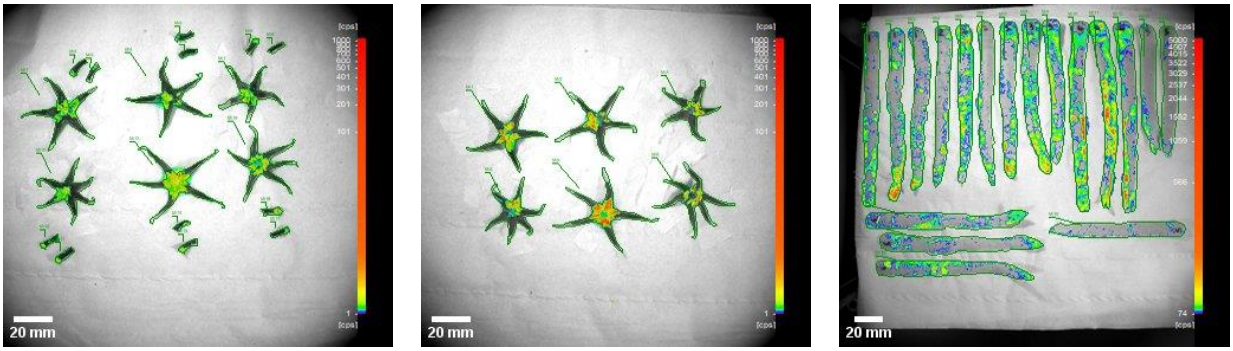


Figure 4.5: Example luminescent images of (A) *E. coli* JHI-5025 (pIJ11282) on upperside tomato calyxes and outer pedicel sections, (B) *E. coli* JHI-5025 (pIJ11282) on underside tomato calyxes and (C) *P. viridiflava* PC006 p_{nptII}::lux on carrot epidermal surface strips. Bacteria at OD_{600nm} 0.5 in PBS were inoculated onto tomatoes or carrots by submersion, which were then dried. For tomatoes, the upperside of tomato calyxes, and two halves of the pedicel, which were displayed to present the outer portions of the pedicel, were imaged for luminescence. The undersides of the same tomato calyxes were then imaged for luminescence. For carrots, 3 epidermal surface strips from each carrot were imaged for luminescence. All luminescence images were taken with the NightOWL LB 983. Colour scales for luminescence counts per second (cps) have different minimum and maximum values to avoid oversaturation.

The calyx and two pedicel halves from each tomato, or the 3 epidermal surface strips from each carrot, were then pooled, weighed, and placed in a Stomacher® 80 Biomaster 101 x 152 mm bag. 50 ml PBS was added to carrot samples and 20 ml PBS was added to tomato samples, before they were stomached for 1 minute on normal speed in a Stomacher® 80 Biomaster (Seward). The contents were serially diluted in PBS by a factor of 10, and 20 µl of each serial dilution was spotted onto LB agar with either nitrofurantoin and gentamicin for *P. viridiflava* PC006 p_{nptII}::lux selection from carrots, or carbenicillin for *E. coli* JHI-5025 (pIJ11282) selection from tomatoes. The antibiotic selection for bacteria from produce had previously been tested by imaging recovered colonies for luminescence, and in each case, all colonies recovered were luminescent. Agar plates were incubated at 28°C for 24 hours before colonies were counted. Results were presented as $\log_{10}(CFU\ mm^{-2})$ for a measure of bacterial quantification, which were compared against the $\log_{10}(luminescence\ (cps\ mm^{-2}))$ results.

4.2.13 Determining the detection limits for bioluminescent model pathogens

An overnight culture of a luminescent model pathogen (table 4.3) was diluted into 200 ml fresh LB by a factor of 1:100, which was incubated at 28ºC, 220 rpm overnight (20 - 24 hours). It was then centrifuged at 3214 x g for 6 minutes, washed in PBS once and resuspended in PBS equivalent to 0.2 x the original volume.

For luminescence measurements, all model pathogens, except *D. chrysanthemi* EC16 (pIJ11282) (table 4.3), were diluted to OD_{600nm} 5 in PBS, which underwent serial dilutions by a factor of 5 in PBS. *D. chrysanthemi* EC16 (pIJ11282) was instead diluted to OD_{600nm} 10, which underwent serial dilutions by a factor of 3. For each bacterium respectively, 3 x 50 µl aliquots of the culture at OD_{600nm} 5, or OD_{600nm} 10, were spotted onto a LB agar plate, which was dried for 1 hour in a laminar flow cabinet and imaged for luminescence using the settings previously described, however no pre-incubation in the dark was necessary. Luminescence and area quantification data were obtained for each spot to calculate luminescence mm^{-2}. This was repeated with subsequent serial dilutions until no luminescence could be detected. Every dilution which had luminescence detected in the complete area of the spots for at least one biological replicate was included in the analysis. To account for spots from biological replicates which did not present this at the same dilution, and therefore did not have a countable area, an average spot area from that bacterium was used, which was assigned a luminescence value of zero. To account for zero values, one was added to all luminescence values before log_{10} transformation for data presentation and analysis.

For colony counting, the cultures at OD_{600nm} 5, or OD_{600nm} 10, underwent serial dilutions by a factor of 10, which were plated in triplicate onto LB agar and incubated at 28ºC until single colonies appeared. The mean CFU/ml from each biological replicate was used to calculate the CFU/50 µl per serial dilution, which was used to calculate the CFU mm^{-2} for

each spot from that biological replicate. Colony counts were presented as $\log_{10}$(CFU mm^{-2}).

4.2.14 Confocal imaging of *E. coli* on the tomato calyx

Tomatoes colonised by *E. coli* JHI-5025 (p_{gyrA}-GFP+) (table 4.3) were either left untreated or submerged in water as previously described. Samples of tomato calyx were loaded onto glass slides with Carolina observation gel and a coverslip. Confocal microscope images of samples were taken by William Kay with a TCS Leica SP5 confocal microscope (objective used: HC PL APO CS2 63.0x1.20 WATER UV). GFP+ was excited with an argon laser (power = 20%) at 488 nm and emission for GFP+ was detected at 505 - 515 nm, whilst emission for chlorophyll autofluorescence was detected at 590 - 680 nm. Images were modified to have the following colour scales: green (GFP+); magenta (chlorophyll autofluorescence); grey (brightfield).

4.2.15 Presentation and statistical analysis of data

Data was processed using R version 4.3.1 (R Core Team, 2023) and charts were produced using the ggplot2 package version 3.4.2 (Wickham, 2016). Diagnostic plots were used to check that linear and mixed linear models produced met linear model requirements: linearity of data, homogeneity of residuals variance and normality of residuals (Kassambara, 2017). Statistical results with p-values < 0.05 were deemed significant, unless otherwise stated.

<u>Bioluminescence technique validation</u>

Linear models were built for each dataset, where results from individual produce were included as independent data points. Either $\log_{10}$(CFU mm^{-2}) or $\log_{10}$(luminescence (cps mm^{-2})) was the response variable and treatment and experimental replicate were fixed effects. ANOVAs were performed and where a significant result was generated, a post-hoc Tukeys HSD test was performed.

Bioluminescence imaging for the effectiveness of different intervention treatments

Linear mixed models were built for each dataset using the lme4 package in R (Bates *et al.*, 2015), where results from individual produce were included as independent data points. Log_{10}(luminescence + 1) was the response variable and the interaction between treatment and time were included as a fixed effect, alongside experimental replicate. The produce identification number was included as a random effect to account for the paired data. To determine if the treatments were better at reducing bacteria compared to the control, the emmeans package in R (Lenth *et al.*, 2023) was used to perform contrast analysis between the treatment effects by performing Tukeys HSD tests.

Differences in the pre-treatment log_{10}(luminescence + 1) means across treatment groups within each dataset were tested for. This was completed by building a linear model with data from the 'before treatment' time group only. Log_{10}(luminescence + 1) was the response variable, and treatment and experimental replicate were included as fixed effects. ANOVAs were performed.

Determining the detection limit for bioluminescent model pathogens

For each model pathogen, results from serial dilutions were used to generate a linear model where log_{10}(luminescence mm^{-2} + 1) was the response variable and log_{10}(CFU mm^{-2}) was a fixed effect. Linear model equations were used to calculate limits of detection for each model pathogen.

4.3 Results

4.3.1 Peracetic acid, sodium hypochlorite and aqueous ozone reduced model pathogens *in vitro*

The ability of each liquid intervention treatment (0.7 - 1.0 ppm aqueous ozone, 80 ppm peracetic acid and sodium hypochlorite with 100 ppm free chlorine) to reduce each model pathogen, which had been modified to express luminescence (Pst DC3000 p_{nptII}::lux, Pst

T1 p_{nptII}::lux, *P. viridiflava* PC006 p_{nptII}::lux, *E. coli* JHI-5025 (pIJ11282), *D. chrysanthemi* EC16 (pIJ11282) (table 4.3)), was tested. This involved a 1:1000 dilution of each luminescent model pathogen (OD_{600nm} = 1) into each liquid intervention treatment, and bacterial survival was subsequently tested for by colony counting.

Aqueous ozone, peracetic acid and sodium hypochlorite all caused complete inactivation of all model pathogens whereas all model pathogens survived in the water control (figure 4.6). Although all model pathogens were adjusted to the same OD_{600nm} for testing the bactericidal action of treatments, this did not represent the same number of cells, because *D. chrysanthemi* EC16 (pIJ11282) had a much lower cell count in the water control compared to the other model pathogens (figure 4.6).

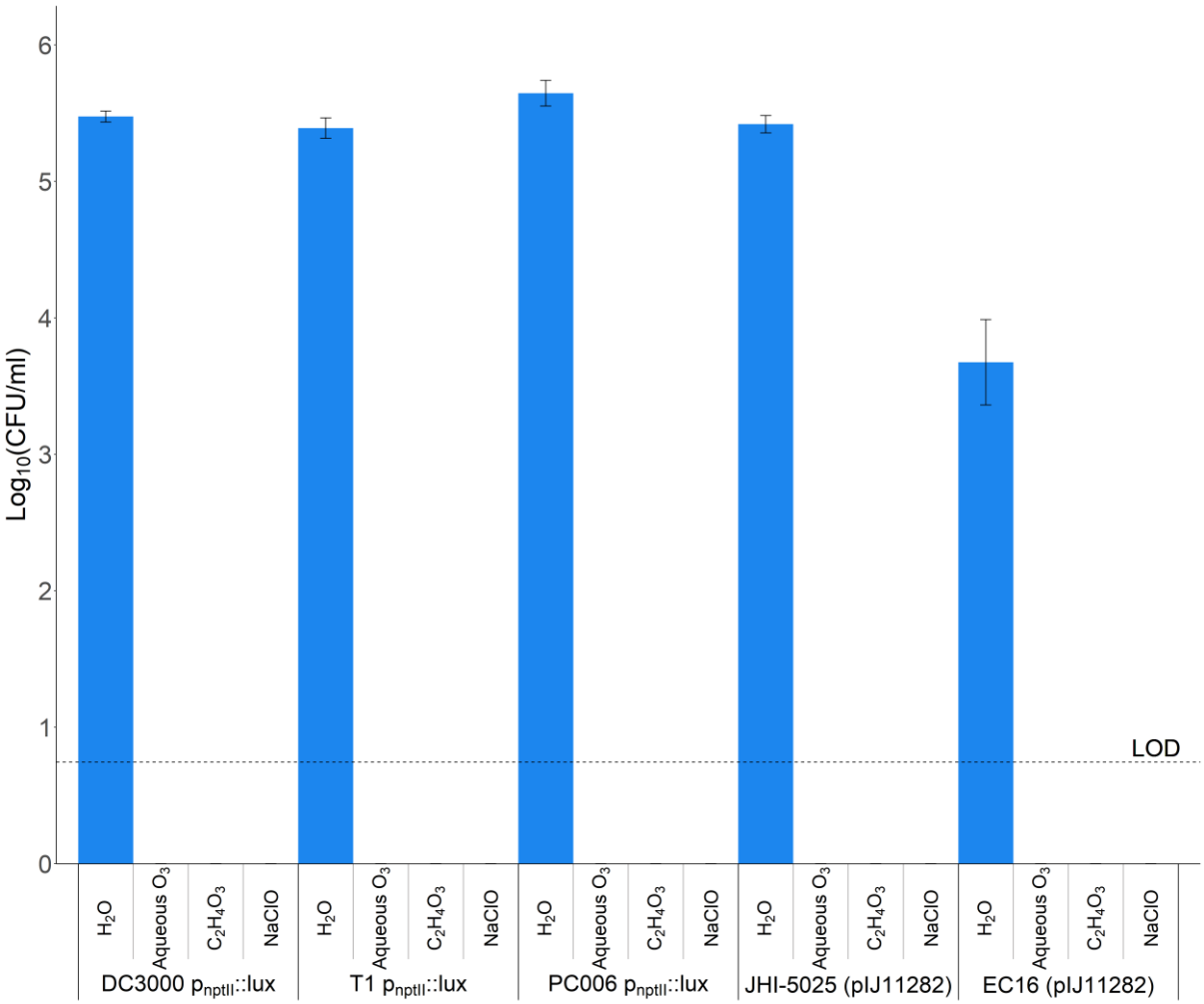


Figure 4.6: Aqueous ozone (O_3), peracetic acid ($C_2H_4O_3$) and sodium hypochlorite (NaClO) reduced *P. syringae* pv. tomato DC3000 p_{nptII}::lux, *P. syringae* pv. tomato T1 p_{nptII}::lux, *P. viridiflava* PC006 p_{nptII}::lux, *E. coli* JHI-5025 (pIJ11282) and *D. chrysanthemi* EC16 (pIJ11282). Bacteria (OD_{600nm} 1) were diluted into each treatment (0.7 - 1.0 ppm aqueous O_3, 80 ppm $C_2H_4O_3$, 100 ppm free chlorine NaClO) by 1:1000, serially diluted then plated onto LB agar, which was incubated at 28°C until single colonies appeared. Colony forming units (CFU)/ml were calculated. Mean and standard error are shown (n = 3). LOD = limit of detection.

Since each liquid intervention treatment could reduce each model pathogen *in vitro*, their ability to reduce each model pathogen, when they were presented on the surface of associated model produce, was later tested.

A gaseous ozone treatment (3 second ozone generation, ~663 - 827 peak ppm) was also included as an intervention treatment for work in this chapter, however it could not be

included in this experiment because it is applied to pathogens as a gas. The ability of gaseous ozone with a 3 second ozone generation time, to reduce Pst DC3000, Pst T1 and *E. coli* JHI-5025 *in vitro* was previously demonstrated in chapter 2, section 2.3.1, however no *in vitro* data was collected for *P. viridiflava* PC006 and *D. chrysanthemi* EC16 due to unforeseen circumstances (as a result of company (Anacail Ltd) failure) which halted the use of the in-pack ozone system.

Before the effect of each intervention treatment was tested on model pathogens *in planta*, it was first important to validate the bioluminescence imaging technique which would be used for this.

4.3.2 Bioluminescence imaging can be used to demonstrate the effectiveness of peracetic acid, sodium hypochlorite and aqueous ozone to control pathogens *in planta*

Experiments were set up to validate that bioluminescence imaging of luminescent model pathogens on associated produce (table 4.1) could be used as a bacterial quantification method for determining the effectiveness of peracetic acid, sodium hypochlorite and aqueous ozone against them. For the validations, a single carrot model system, with *P. viridiflava* PC006 p_{nptII}::lux, and a single tomato model system, with *E. coli* JHI-5025 (pIJ11282), were used (tables 4.1 and 4.3). Validations were completed by quantifying luminescent bacteria on produce, after an intervention treatment or not, by both *in planta* bioluminescence imaging and *in vitro* colony counting. This was so that results generated from data collected by each of these techniques could be compared for similarity. Colony counting was used for validations because this is the gold standard technique for determining the effectiveness of intervention treatments on pathogens (Selma *et al.*, 2006; Hassenberg *et al.*, 2008; Brilhante São José and Dantas Vanetti, 2012; Torlak *et al*., 2013; Wani *et al.*, 2015; Singh *et al*., 2018; Dharmarha *et al.*, 2019).

The bioluminescence imaging technique that was used to test treatment effects in this chapter, involved paired data where bacterial luminescence on each produce was quantified before and after treatment. Colony counting however could not be completed in a paired data set-up because it required sample destruction, so only bacteria on post-treatment produce were quantified by both *in planta* bioluminescence imaging and then *in vitro* colony counting. To account for the absence of 'before' data, an untreated control was included to investigate the impact of treatments and water-only controls. Also, since treatment effects were assessed by comparing data collected from different post-treatment produce, different sample sizes had to be accounted for, therefore both luminescence data and colony count data were presented per mm^{-2} of produce imaged. Although colony count data is typically presented as CFU/g (Selma *et al.*, 2006; Hassenberg *et al.*, 2008; Brilhante São José and Dantas Vanetti, 2012; Torlak *et al*., 2013; Wani *et al.*, 2015; Singh *et al*., 2018; Dharmarha *et al.*, 2019), it was presented as CFU mm^{-2} in this experiment so that any differences in results collected by bioluminescence imaging or colony counts, would not be due to differences in the metric used for sample size normalisation. All datasets where $\log_{10}$(CFU mm^{-2}) was used to assess treatment effects, were also analysed using $\log_{10}$(CFU/g) as the response variable, and all significant results identified within datasets by colony counting were the same, and at the same level (* = $p < 0.05$, ** = $p < 0.01$, *** = $p < 0.001$), regardless if $\log_{10}$(CFU mm^{-2}) or $\log_{10}$(CFU/g) was used as the response variable (data not shown).

The experiments involved the submersion of produce in a suspension of a luminescent model pathogen (OD_{600nm} = 0.5) before produce was dried and either subjected to a treatment or not. Treatments that were used for work in this chapter were applied to each model system, which included those applied by submersion (80 ppm peracetic acid, sodium hypochlorite with 100 ppm free chlorine and a water control) (table 4.2) and those applied by a continuous flow (0.7 - 1.0 ppm aqueous ozone and a water control). A gaseous ozone treatment, generated by the in-pack ozone system, was also included as

an intervention treatment for work in this chapter, however validations with this treatment were not completed due to unforeseen circumstances (as a result of company (Anacail Ltd) failure) which halted the use of the in-pack ozone system. After treatment, or no treatment, produce was dried before the quantity of luminescent bacteria on produce was determined by both *in planta* bioluminescence imaging and then *in vitro* colony counting. For colony counting, samples were stomached in buffer to release bacteria before being plated on antibiotics which selected for the luminescent model pathogen only.

For bacterial quantifications, only tomato calyxes and pedicels were used because *E. coli* only colonised the calyx and pedicel of tomatoes during inoculations, as seen in bioluminescence imaging (figure 4.3). *P. viridiflava* colonised any part of carrot surfaces during inoculations (figure 4.4), however since only a small sample of carrot could be processed in the stomacher for colony counting, epidermal surface strips from carrots were imaged for bioluminescence and then processed for colony counting.

Both bioluminescence imaging data and colony count data identified that submersion in water caused no significant reductions of *P. viridiflava* on carrots, but submersion in peracetic acid and sodium hypochlorite caused large, significant reductions (figure 4.7). Treatment (groups = untreated, water, peracetic acid, sodium hypochlorite) significantly affected Log_{10}(luminescence (cps mm^{-2})) [ANOVA, $F(3, 66) = 176.381$, $p < 2e\text{-}16$] and Log_{10}(CFU mm^{-2}) [ANOVA, $F(3, 66) = 260.368$, $p < 2e\text{-}16$], and post hoc Tukeys HSD tests identified that the significant differences ($p < 0.001$) were between the same treatments within each dataset (figure 4.7).

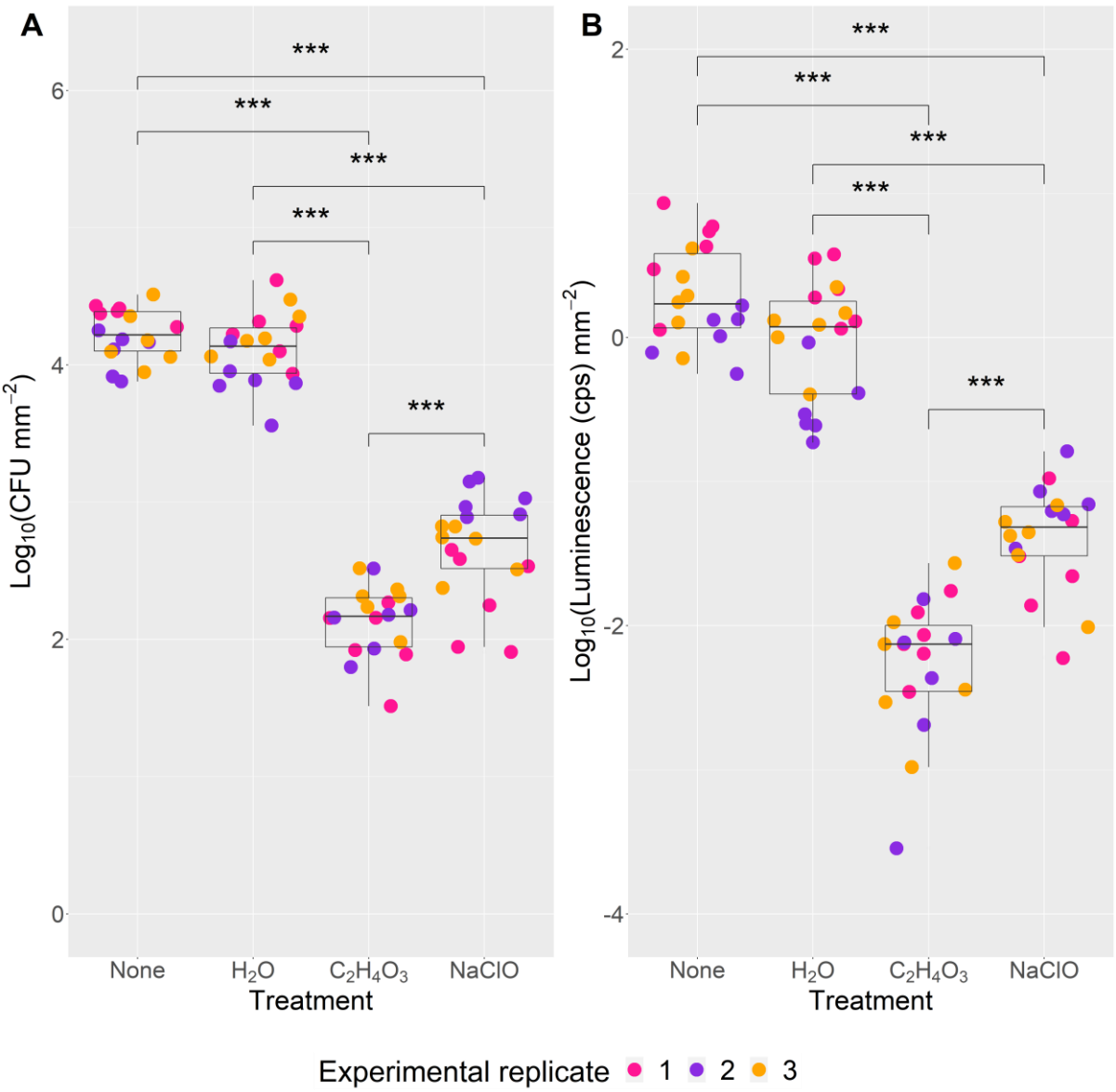


Figure 4.7: (A) Colony count data and (B) bioluminescence imaging data both showed that water caused no significant reductions of *P. viridiflava* on carrots, but peracetic acid ($C_2H_4O_3$) and sodium hypochlorite (NaClO) caused large, significant reductions. *P. viridiflava* PC006 p_{nptII}::lux at OD_{600nm} 0.5 in PBS was inoculated onto carrots by submersion. Carrots were dried, either submerged in a treatment (80 ppm $C_2H_4O_3$, 100 ppm free chlorine NaClO or water control) or not, then dried and peeled three times to collect epidermal surface strips, which were imaged for luminescence with the NightOWL LB 983. Area and luminescence counts per second (cps) quantifications were pooled from the epidermal surface strips from the same carrot, which were used to calculate luminescence per area, presented as log_{10}(luminescence (cps mm^{-2})). Epidermal surface strips from each carrot, were then pooled and stomached with PBS for 1 minute, normal speed. The contents were serially diluted, plated onto LB agar with nitrofurantoin and gentamicin and incubated at 28°C for 24 hours. Colony forming units (CFU) were presented as log_{10}(CFU mm^{-2}). Boxplots display the median, interquartile range, minimum and maximum values (n = 18). Asterisks indicate significant differences (*** = $p < 0.001$) from ANOVA and Tukeys HSD tests.

Both bioluminescence imaging data and colony count data showed that water and aqueous ozone did not cause large reductions of *P. viridiflava* on carrots (figure 4.8). However, statistical testing revealed slightly different results (figure 4.8). Treatment (groups = untreated, water, aqueous ozone) had a significant effect on Log_{10}(luminescence (cps mm^{-2})) [ANOVA, $F(2, 49) = 3.222$, $p = 0.0484$], however had a more significant effect on Log_{10}(CFU mm^{-2}) [ANOVA, $F(2, 49) = 10.793$, $p = 0.000131$]. Post-hoc Tukeys HSD tests identified no significant differences in Log_{10}(luminescence (cps mm^{-2})) between specific treatment groups, however identified a significant difference in Log_{10}(CFU mm^{-2}) between no treatment and water ($p < 0.01$) and water and ozone ($p < 0.001$) (figure 4.8).

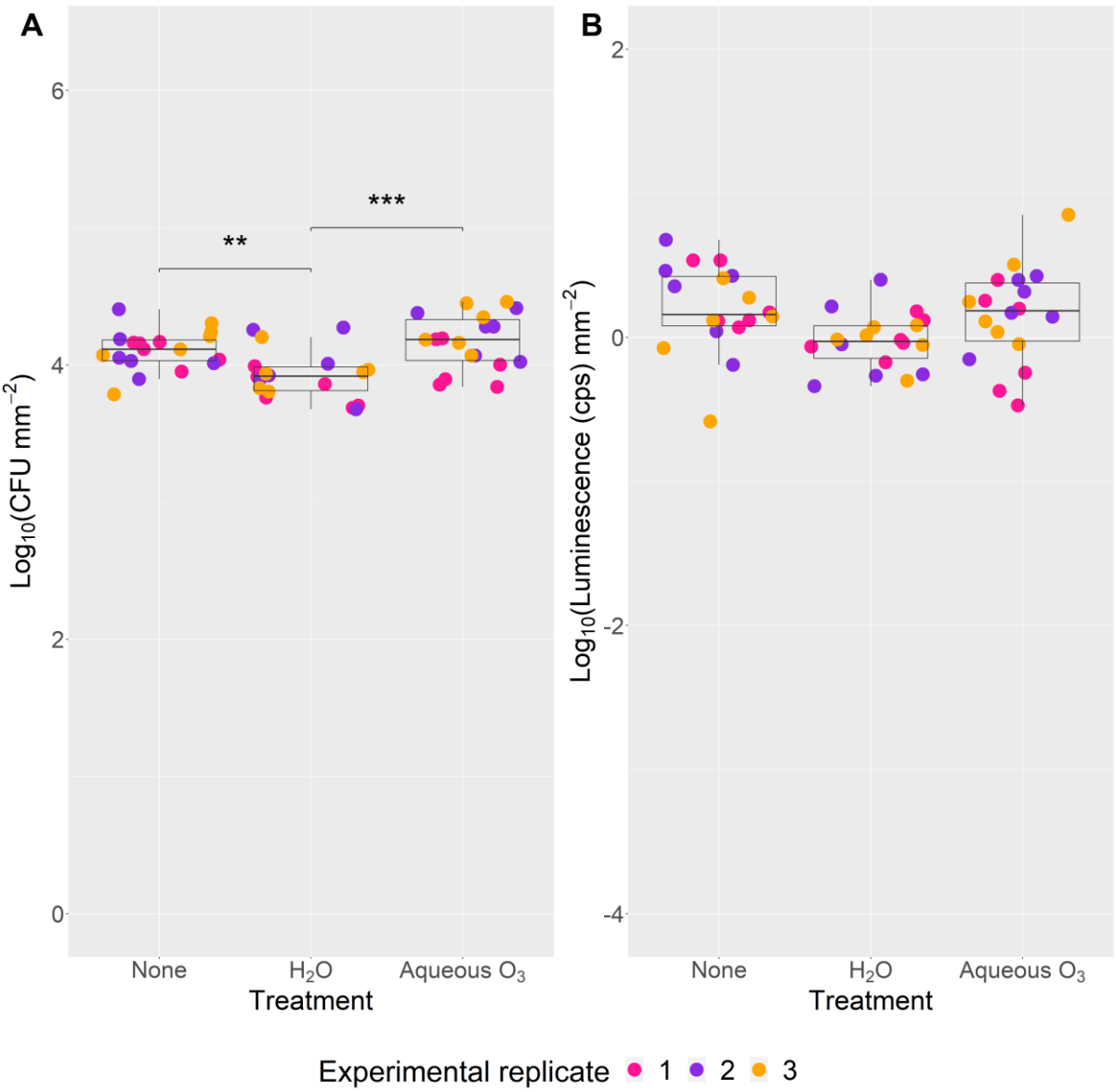


Figure 4.8: (A) Colony count data and (B) bioluminescence imaging data both showed that water and aqueous ozone (O_3) did not cause large reductions of *P. viridiflava* on carrots. *P. viridiflava* PC006 p_{nptII}::lux at OD_{600nm} 0.5 in PBS was inoculated onto carrots by submersion. Carrots were dried and either left untreated or subjected to a flow of water or aqueous ozone (0.7 - 1.0 ppm), then dried and peeled three times to collect epidermal surface strips, which were imaged for luminescence with the NightOWL LB 983. Area and luminescence counts per second (cps) quantifications were pooled from the epidermal surface strips from the same carrot, which were used to calculate luminescence per area, presented as $\log_{10}$(luminescence (cps mm^{-2})). Epidermal surface strips from each carrot, were then pooled and stomached with PBS for 1 minute, normal speed. The contents were serially diluted, plated onto LB agar with nitrofurantoin and gentamicin and incubated at 28°C for 24 hours. Colony forming units (CFU) were presented as $\log_{10}$(CFU mm^{-2}). Boxplots display the median, interquartile range, minimum and maximum values (n = 18). Asterisks indicate significant differences (*** = $p < 0.001$, ** = $p < 0.01$) from ANOVA and Tukeys HSD tests.

Both bioluminescence imaging data and colony count data showed that no treatments (applied by submersion or a continuous flow) caused large reductions of *E. coli* on

tomatoes (figures 4.9 and 4.10). However, statistical testing revealed slightly different results (figures 4.9 and 4.10). Treatment applied via submersion (groups = untreated, water, peracetic acid, sodium hypochlorite) did not significantly affect Log_{10}(luminescence (cps mm^{-2})) however it caused a slight significant effect on Log_{10}(CFU mm^{-2}) [ANOVA, $F(3, 66) = 2.798$, $p = 0.0469$], and a post hoc Tukeys HSD test identified that this significant difference was between the untreated control and peracetic acid ($p < 0.05$) (figure 4.9). Treatment applied via a continuous flow (groups = untreated, water, aqueous ozone) again did not significantly affect Log_{10}(luminescence (cps mm^{-2})) however caused a significant effect on Log_{10}(CFU mm^{-2}) [ANOVA, $F(2, 49) = 3.604$, $p = 0.0347$], of which the significant differences were between the water control and aqueous ozone ($p < 0.05$), as identified in a post hoc Tukeys HSD test (figure 4.10).

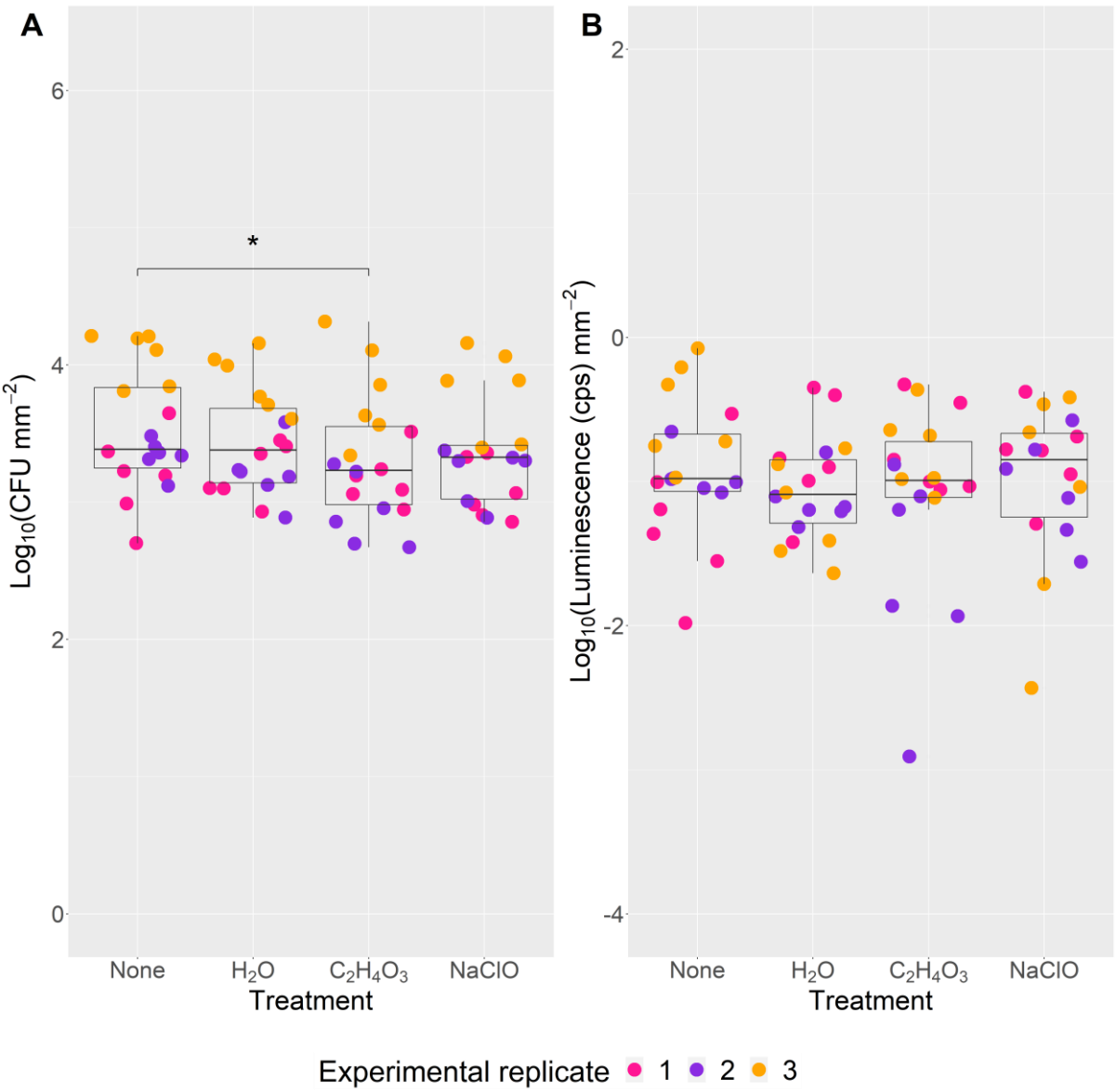


Figure 4.9: (A) Colony count data and (B) bioluminescence imaging data both showed that water, peracetic acid ($C_2H_4O_3$) and sodium hypochlorite (NaClO) did not cause large reductions of *E. coli* on tomatoes. *E. coli* JHI-5025 (pIJ11282) at OD_{600nm} 0.5 in PBS were inoculated onto tomatoes by submersion. Tomatoes were dried, either submerged in a treatment (80 ppm $C_2H_4O_3$, 100 ppm free chlorine NaClO or water control) or not, then dried. Tomato calyxes and pedicels were removed and imaged for luminescence with the NightOWL LB 983. Area and luminescence counts per second (cps), quantified from the calyx and pedicel of each tomato, were used to calculate luminescence per area, presented as $\log_{10}$(luminescence (cps mm^{-2})). The calyx and pedicel from each tomato were then stomached with PBS for 1 minute, normal speed. The contents were serially diluted, plated onto LB agar with carbenicillin and incubated at 28°C for 24 hours. Colony forming units (CFU) were presented as $\log_{10}$(CFU mm^{-2}). Boxplots display the median, interquartile range, minimum and maximum values (n = 18). Asterisk indicates a significant difference (* = $p < 0.05$) from ANOVA and Tukeys HSD tests.

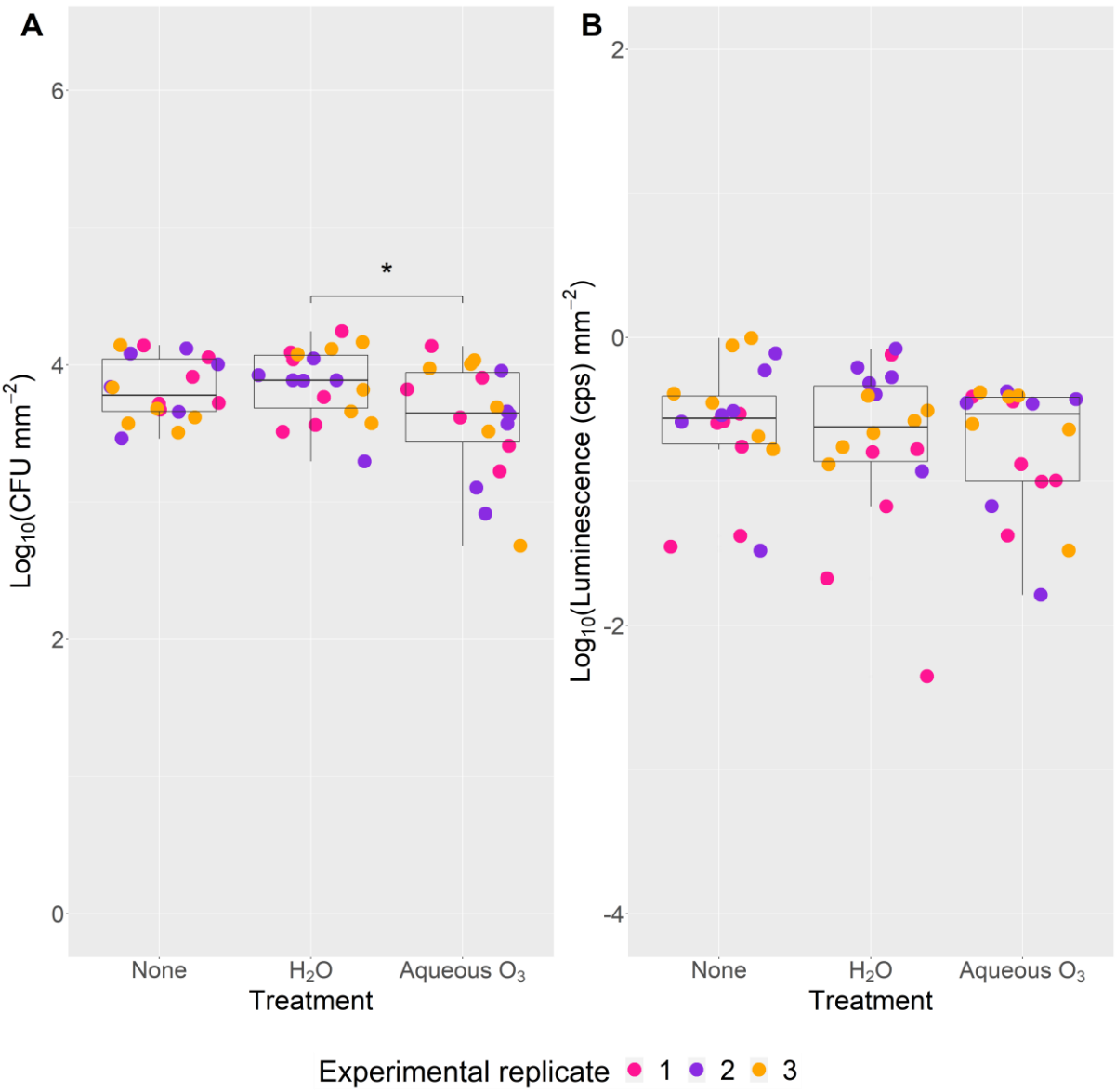


Figure 4.10: (A) Colony count data and (B) bioluminescence imaging data both showed that water and aqueous ozone (O_3) did not cause large reductions of *E. coli* on tomatoes. *E. coli* JHI-5025 (pIJ11282) at OD_{600nm} 0.5 in PBS were inoculated onto tomatoes by submersion. Tomatoes were dried and either left untreated or subjected to a flow of water or aqueous ozone (0.7 - 1.0 ppm), then dried. Tomato calyxes and pedicels were removed and imaged for luminescence with the NightOWL LB 983. Area and luminescence counts per second (cps), quantified from the calyx and pedicel of each tomato, were used to calculate luminescence per area, presented as log_{10}(luminescence (cps mm^{-2})). The calyx and pedicel from each tomato were then stomached with PBS for 1 minute, normal speed. The contents were serially diluted, plated onto LB agar with carbenicillin and incubated at 28°C for 24 hours. Colony forming units (CFU) were presented as log_{10}(CFU mm^{-2}). Boxplots display the median, interquartile range, minimum and maximum values (n = 18). Asterisk indicates a significant difference (* = $p < 0.05$) from ANOVA and Tukeys HSD tests.

In some datasets where colony counts were used to validate bioluminescence data,

colony counts identified significant differences where bioluminescence data did not,

however the significant differences detected were very small changes in bacterial quantifications so would not have a large impact on the overall interpretation of results. *In planta* bioluminescence imaging was therefore used as a bacterial quantification technique for investigating the effectiveness of different intervention treatments in this chapter. Before bioluminescence imaging was used for this, it was used to identify detection limits for each model pathogen, which would be an important consideration during result interpretation.

4.3.3 Detection limits are variable for bioluminescent model pathogens on LB agar plates

The bioluminescence detection limit, in the form of the number of cells detectable per unit area (mm^{-2}), was calculated for each model pathogen on LB agar. Briefly, luminescent model pathogens (Pst DC3000 p_{nptII}::lux, Pst T1 p_{nptII}::lux, *P. viridiflava* PC006 p_{nptII}::lux, *E. coli* JHI-5025 (pIJ11282), *D. chrysanthemi* EC16 (pIJ11282) (table 4.3)) were serially diluted in PBS, and aliquots of each serial dilution were spotted and dried onto LB agar for bioluminescence imaging and subsequent luminescence quantification per mm^{-2}. Colony counts on LB agar were measured from the same cultures which were serially diluted so that the CFU per mm^{-2} could be estimated for spots from which luminescence per mm^{-2} was measured. Linear models were then generated to present the relationship between luminescence and colony counts per mm^{-2}.

Detection limits varied from approximately 250 - 5000 CFU mm^{-2}: 277 for *D. chrysanthemi* EC16 (pIJ11282), 1153 for Pst T1 p_{nptII}::lux, 2384 for Pst DC3000 p_{nptII}::lux, 2419 for *P. viridiflava* PC006 p_{nptII}::lux and 4916 for *E. coli* JHI-5025 (pIJ11282) (figure 4.11). High correlations (>0.97) between luminescence and CFU were also observed (figure 4.11). A good correlation between luminescence and CFU was also previously observed in figures 4.7, 4.8, 4.9 and 4.10, since data collected by bioluminescence imaging and colony counting was similar.

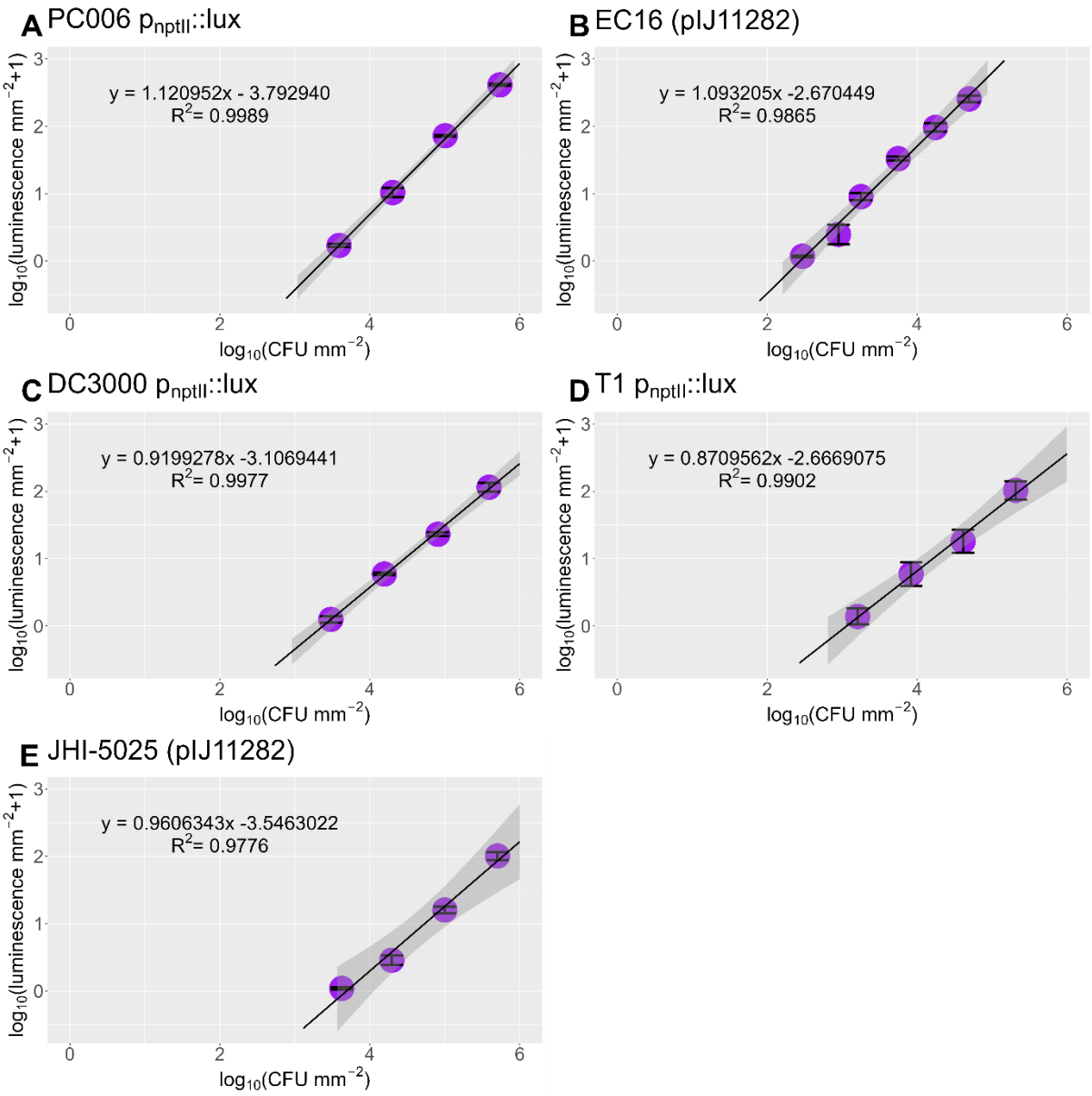


Figure 4.11: Detection limit for bioluminescent model pathogens on LB agar plates.
(A) *P. viridiflava* PC006 p_{nptII}::lux. 2419 CFU mm^{-2}.
(B) *D. chrysanthemi* EC16 (pIJ11282). 277 CFU mm^{-2}.
(C) *P. syringae* pv. tomato DC3000 p_{nptII}::lux. 2384 CFU mm^{-2}.
(D) *P. syringae* pv. tomato T1 p_{nptII}::lux. 1153 CFU mm^{-2}.
(E) *E. coli* JHI-5025 (pIJ11282). 4916 CFU mm^{-2}.
For each bacterium apart from EC16 (pIJ11282), suspensions at OD_{600nm} 5 in PBS were spotted in serial dilution by a factor of 5 on LB agar. For EC16 (pIJ12282), suspensions at OD_{600nm} 10 in PBS were spotted in serial dilution by a factor of 3 on LB agar. Images for bioluminescence were taken after 1 hour using the NightOWL LB 983 with a 20 minute exposure time. Luminescence counts per second (cps) were presented as $\log_{10}$(luminescence mm^{-2} + 1). Colony forming units (CFU), estimated by colony counting, were presented as $\log_{10}$(CFU mm^{-2}). Mean and standard error for data points are shown (n = 3). The shaded areas represent 95% confidence intervals of linear models.

4.3.4 Peracetic acid and sodium hypochlorite reduced model pathogens on carrots but not tomatoes, compared to water

Experiments were set up to investigate if peracetic acid and sodium hypochlorite could reduce luminescent model pathogens on associated post-harvest produce, compared to a water control: *P. viridiflava* PC006 p_{nptII}::lux and *D. chrysanthemi* EC16 (pIJ11282) on carrots, and Pst DC3000 p_{nptII}::lux, Pst T1 p_{nptII}::lux and *E. coli* JHI-5025 (pIJ11282) on tomatoes (tables 4.1 and 4.3).

The experiments involved the submersion of produce in a suspension of a luminescent model pathogen (OD_{600nm} = 0.5) before produce was dried and subjected to *in planta* bioluminescence imaging for bacterial quantification. Produce was then submerged in a treatment (80 ppm peracetic acid, sodium hypochlorite with 100 ppm free chlorine or a water control) before being dried and subjected to *in planta* bioluminescence imaging again for bacterial quantification. Model pathogens only colonised the calyx and pedicel of tomatoes, as seen in bioluminescence imaging (figure 4.3), therefore only tomato calyxes and pedicels were used for bacterial quantification. Model pathogens however colonised any part of carrot surfaces (figure 4.4), so bacterial quantification was not limited to specific areas of carrots. To ensure that the same part of each produce was captured in 'before' and 'after' images, produce was modified so that they had flat edges to sit against. Since paired data, in the form of luminescence quantifications on 'before' and 'after' images, was used to test for treatment effects, different sample sizes did not have to be accounted for.

Results showed that a water-only submersion caused an obvious reduction in *P. viridiflava* and *D. chrysanthemi* on carrots (figure 4.12: A, B). Compared to water, peracetic acid significantly reduced *P. viridiflava* ($p < 0.0001$) and *D. chrysanthemi* ($p = 0.0066$) on carrots, and sodium hypochlorite significantly reduced *P. viridiflava* ($p < 0.0001$) but not *D. chrysanthemi* on carrots (figure 4.12: A, B). In contrast to the carrot

model systems, water-only submersions did not visibly reduce any bacteria (Pst DC3000, Pst T1 or *E. coli* JHI-5025) on tomatoes, and compared to water, treatments with peracetic acid and sodium hypochlorite did not cause any significant bacterial reductions (figure 4.12: C, D, E).

Within each of the datasets presented in figure 4.12, there were no significant differences in bacterial luminescence (Log_{10}(luminescence (cps) + 1)) on pre-treatment produce, between different treatment groups, so there were no differences in the ’starting points’ for testing treatment effects.

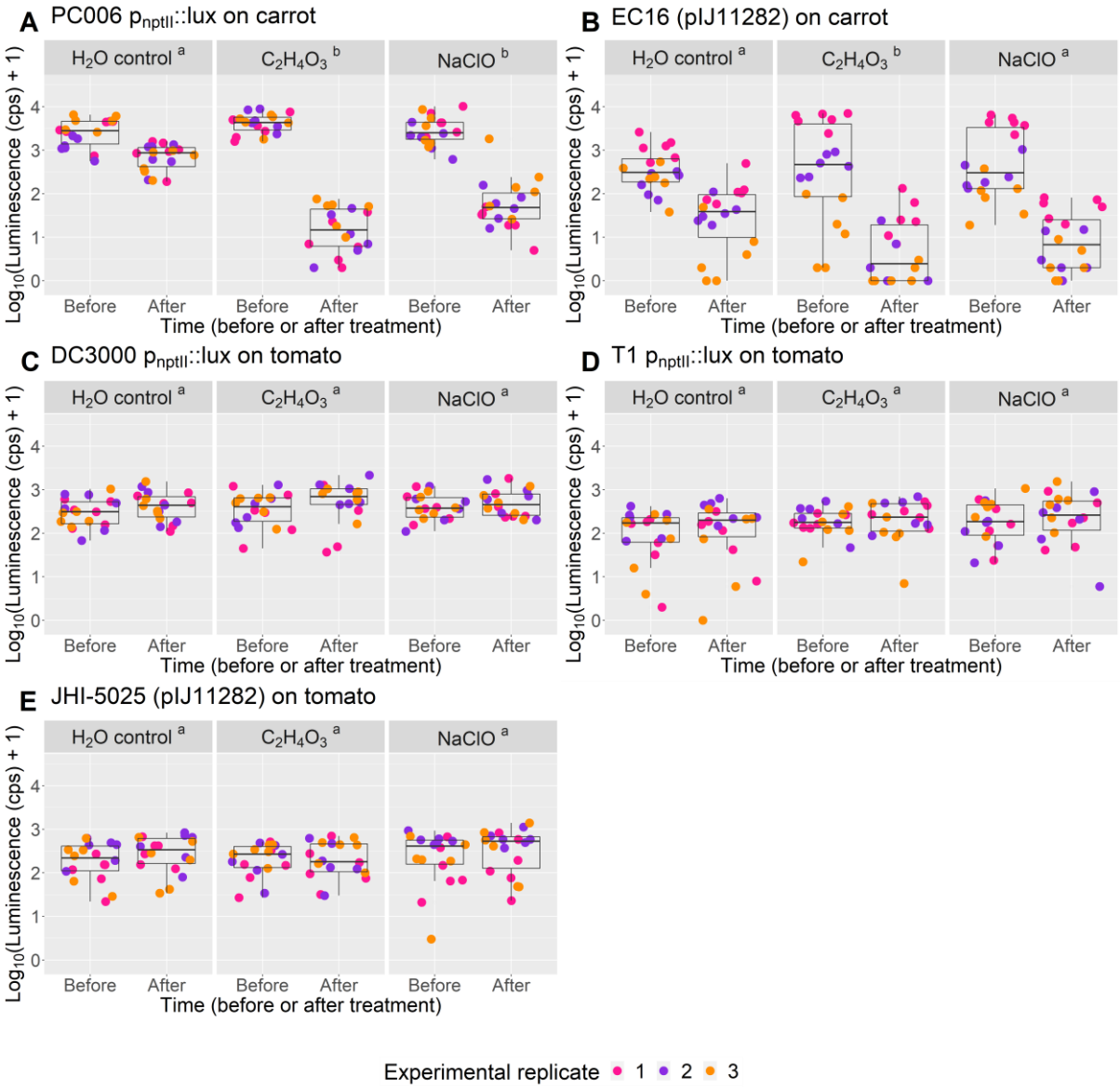


Figure 4.12: Peracetic acid ($C_2H_4O_3$) and sodium hypochlorite (NaClO) reduced model pathogens on carrots but not tomatoes, compared to water. Bacteria (**(A)** *P. viridiflava* PC006 p_{nptII}::lux, **(B)** *D. chrysanthemi* EC16 (pIJ11282), **(C)** *P. syringae* pv. tomato DC3000 p_{nptII}::lux, **(D)** *P. syringae* pv. tomato T1 p_{nptII}::lux, **(E)** *E. coli* JHI-5025 (pIJ11282)) at OD_{600nm} 0.5 in PBS were inoculated onto their associated model produce by submersion. Produce was dried, imaged for luminescence with the NightOWL LB 983, submerged in a treatment (80 ppm $C_2H_4O_3$, 100 ppm free chlorine NaClO or water control), dried and then imaged for luminescence again. Luminescence counts per second (cps) were quantified for each produce, before and after treatment, log_{10} transformed and presented as individual data points on the chart. Boxplots display the median, interquartile range, minimum and maximum values (n = 18). Different letters next to treatment titles indicate where treatments had a significantly different effect ($p < 0.05$) on the change in bacterial luminescence.

Since model pathogens on carrots responded to treatments very differently compared to model pathogens on tomatoes, another experiment was set up to test if these differences in response were primarily driven by the plant hosts' ability to provide, or not provide,

enhanced protection to pathogens against treatments. This involved selecting a single carrot model system, with *P. viridiflava* PC006, and a single tomato model system, with *E. coli* JHI-5025, and swapping the model produce, so that the effect of treatments against *P. viridiflava* PC006 on tomatoes and *E. coli* JHI-5025 on carrots was tested.

Results supported the hypothesis that tomatoes were able to provide enhanced protection to pathogens against treatments, whereas carrots were not. This was because a water-only submersion caused an obvious reduction in *E. coli* on carrots, and compared to water, more significant reductions of *E. coli* were caused by peracetic acid ($p = 0.0002$) and sodium hypochlorite ($p = 0.0055$) (figure 4.13: A). This contrasts previous results where water did not visibly reduce *E. coli* on tomatoes and peracetic acid and sodium hypochlorite had no significant effects compared to this (figure 4.12: E). Also, a water-only submersion did not cause any visible reductions in *P. viridiflava* on tomatoes, and compared to water, no more significant reductions of *P. viridiflava* were caused by peracetic acid or sodium hypochlorite (figure 4.13: B). This again contrasts previous results where water caused an obvious reduction in *P. viridiflava* on carrots, and peracetic acid and sodium hypochlorite caused significantly greater reductions (figure 4.12: A).

It is to be mentioned that the linear model that was generated for the *E. coli* dataset (figure 4.13: A) violated the normality of residuals and homogeneity of residuals assumptions that were required for linear models (which was indicated by a poor qqplot and histogram of residuals, respectively). Since the main issue with this violation would be an inflated type 1 error (which would cause rejection of a null hypothesis of no differences when it should not be rejected), we decided to complete the standard ANOVA but with a more conservative alpha significance threshold for result interpretation. Since p-values for the treatment effects were very small, it was concluded that peracetic acid and sodium hypochlorite significantly reduced *E. coli* on carrots, more than water alone did.

Within both of the datasets presented in figure 4.13, there were no significant differences in bacterial luminescence (Log_{10}(luminescence (cps) + 1)) on pre-treatment produce, between different treatment groups, so there were no differences in the ’starting points’ for testing treatment effects.

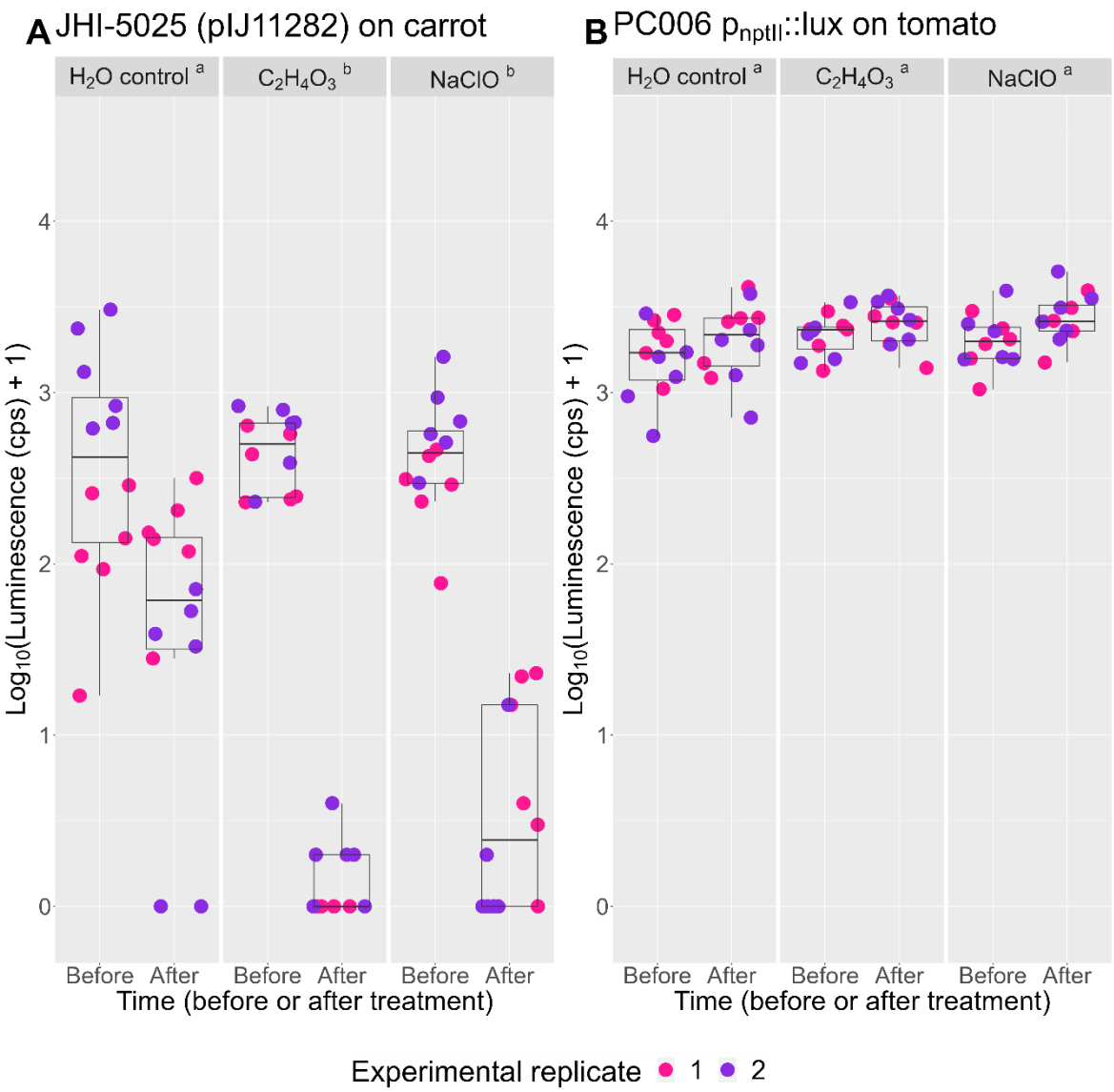


Figure 4.13: Peracetic acid ($C_2H_4O_3$) and sodium hypochlorite (NaClO) reduced model pathogens on carrots but not tomatoes, compared to water. Bacteria (**(A)** *P. viridiflava* PC006 p_{nptII}::lux, **(B)** *E. coli* JHI-5025 (pIJ11282)) at OD_{600nm} 0.5 in PBS were inoculated onto produce by submersion. Produce was dried, imaged for luminescence with the NightOWL LB 983, submerged in a treatment (80 ppm $C_2H_4O_3$, 100 ppm free chlorine NaClO or water control), dried and then imaged for luminescence again. Luminescence counts per second (cps) were quantified for each produce, before and after treatment, log_{10} transformed and presented as individual data points on the chart. Boxplots display the median, interquartile range, minimum and maximum values (n = 12). Different letters next to treatment titles indicate where treatments had a significantly different effect ($p < 0.05$) on the change in bacterial luminescence.

Since tomatoes, specifically tomato calyxes and pedicels, were able to provide enhanced protection to pathogens against water, peracetic acid and sodium hypochlorite, whereas carrots were not, the location of pathogens on the tomato calyx was investigated, to identify where they resided for this enhanced protection.

4.3.5 Bacteria mainly reside on trichomes but also in/around stomata and on the general surface of the tomato calyx

To provide insight as to how model pathogens were able to gain enhanced protection against water, peracetic acid and sodium hypochlorite when they were presented on the tomato calyx and pedicel, a representative model pathogen, namely *E. coli* JHI-5025, was used to investigate where pathogens resided on the tomato calyx. *E. coli* JHI-5025 (p_{gyrA}-GFP+) is a constitutive fluorescent reporter strain (table 4.3) which was used to investigate the location of *E. coli* JHI-5025 on the tomato calyx.

Tomatoes were submerged in a suspension of *E. coli* JHI-5025 (p_{gyrA}-GFP+) (OD_{600nm} = 0.5) before they were dried and subjected to confocal microscopy to identify the location of *E. coli* JHI-5025 on the tomato calyx and pedicel. The location of *E. coli* JHI-5025 on tomatoes colonised by *E. coli* JHI-5025 (p_{gyrA}-GFP+), which had then been submerged in water and dried, was also investigated because a water submersion caused bacterial reductions on carrots but not tomatoes (figures 4.12 and 4.13).

Confocal microscopy images of *E. coli* JHI-5025 (p_{gyrA}-GFP+) on the tomato calyx, after inoculation by submersion, are shown in figure 4.14. Dense populations of *E. coli* were mainly seen at trichomes (figure 4.14: A, B, C, D, E). *E. coli* mainly did not interact with stomata (figure 4.14: A), however cases of *E. coli* internalisation via stomata and *E. coli* surrounding stomata were seen (figure 4.14: B, F, G, H). *E. coli* were also seen on the general surface of the calyx (figure 4.14: I, J, K), however populations were not as dense as those typically seen around trichomes (figure 4.14: A, B, C, D, E).

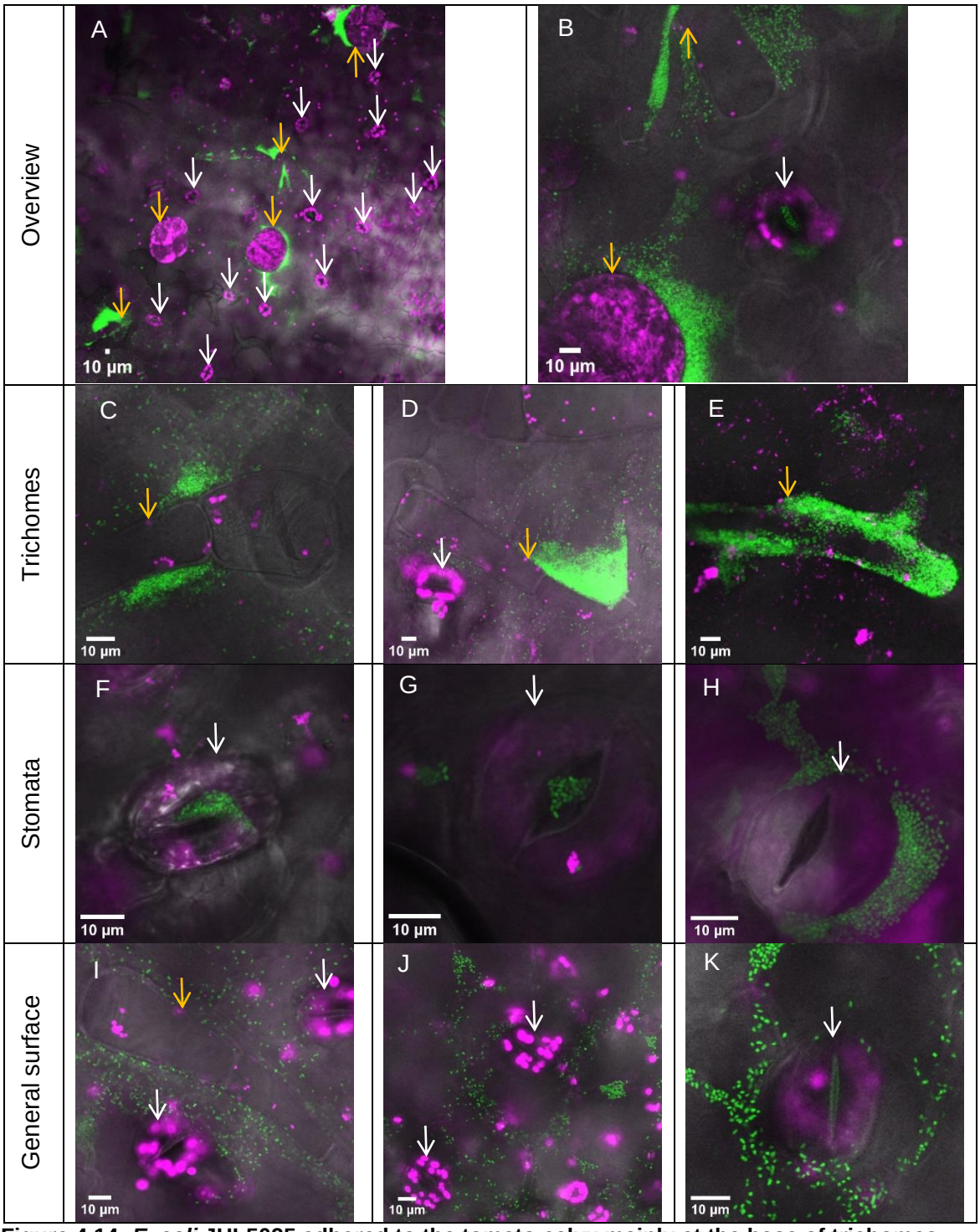


Figure 4.14: *E. coli* JHI-5025 adhered to the tomato calyx mainly at the base of trichomes, but also on the general surface and stomata. *E. coli* JHI-5025 (p_{gyrA}-GFP+) at OD_{600nm} 0.5 in PBS were inoculated onto tomatoes by submersion. Tomatoes were dried and samples of tomato calyx were imaged with a TCS Leica SP5 confocal microscope (GFP+ excitation = 488 nm, GFP+ emission = 505 - 515 nm, chlorophyll autofluorescence emission = 590 - 680 nm). The images show an overview of *E. coli* inoculations (**A**, **B**) and inoculations on trichomes (**C**, **D**, **E**), stomata (**F**, **G**, **H**) and the general surface (**I**, **J**, **K**). The white arrows indicate stomata and the orange arrows indicate trichomes. Colour scale: green (GFP+); magenta (chlorophyll autofluorescence); grey (brightfield).

Confocal microscopy images of *E. coli* JHI-5025 (p_{gyrA}-GFP+) on the tomato calyx, after tomatoes colonised by *E. coli* were submerged in water and dried, are shown in figure 4.15. A similar pattern of *E. coli* inoculation was shown, compared to the pattern previously seen when *E. coli* was first inoculated onto the calyx. *E. coli* mainly did not interact with stomata (figure 4.15: A, B) and dense populations of *E. coli* were associated with trichomes (figure 4.15: B, C, D, E). Evidence of *E. coli* internalisation via stomata was once again seen (figure 4.15: F) as well as evidence of *E. coli* surrounding stomata (figure 4.15: G, H). *E. coli* were also present on the general surface of the calyx in not very dense populations (figure 4.15: I, J, K).

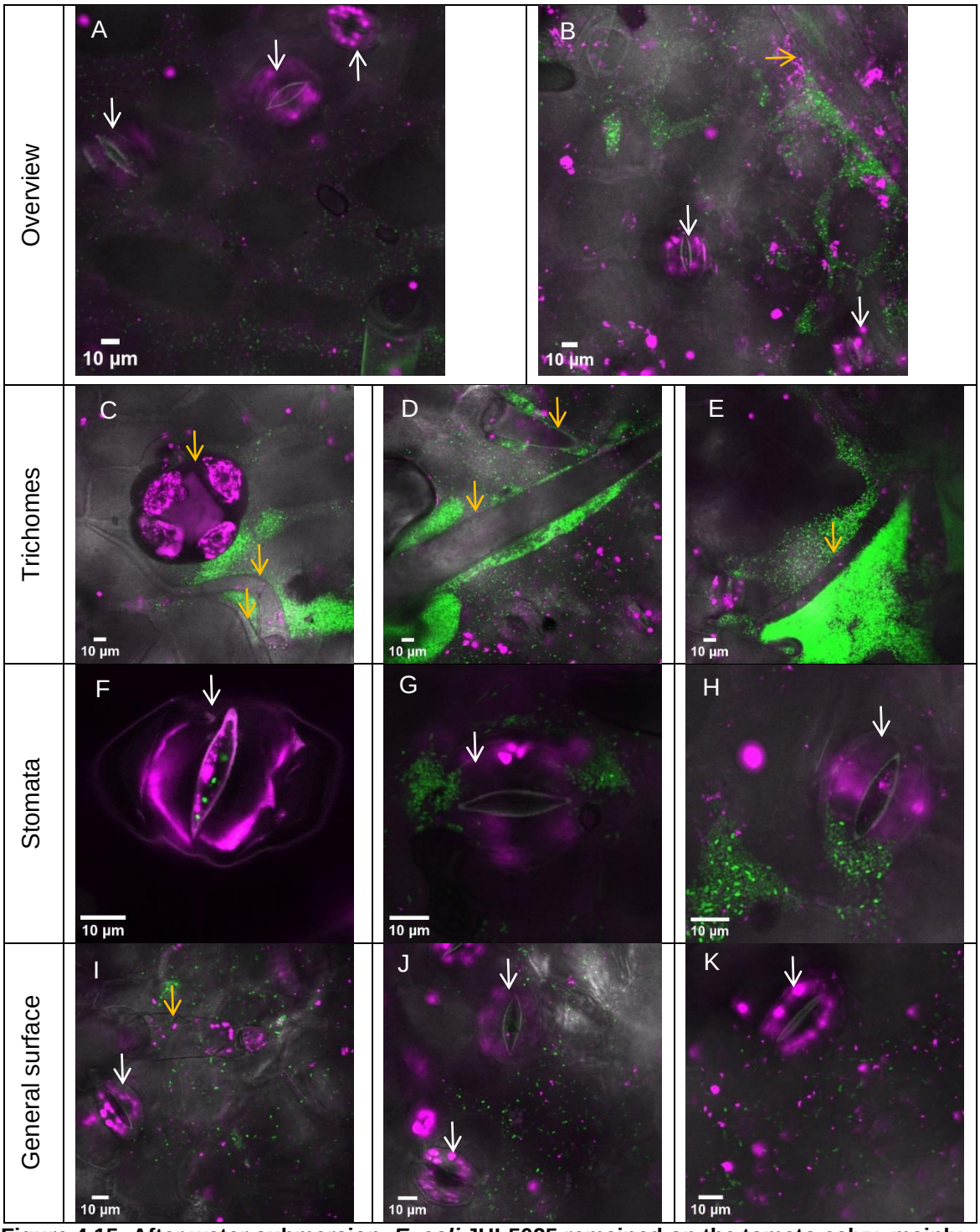


Figure 4.15: After water submersion, *E. coli* JHI-5025 remained on the tomato calyx, mainly at the base of trichomes, but also on the general surface and stomata. *E. coli* JHI-5025 (p_{gyrA}-GFP+) at OD_{600nm} 0.5 in PBS were inoculated onto tomatoes by submersion and then dried. Tomatoes were submerged in water, dried and samples of tomato calyx were imaged with a TCS Leica SP5 confocal microscope (GFP+ excitation = 488 nm, GFP+ emission = 505 - 515 nm, chlorophyll autofluorescence emission = 590 - 680 nm). The images show an overview of *E. coli* inoculations (**A**, **B**) and inoculations on trichomes (**C**, **D**, **E**), stomata (**F**, **G**, **H**) and the general surface (**I**, **J**, **K**). The white arrows indicate stomata and the orange arrows indicate trichomes. Colour scale: green (GFP+); magenta (chlorophyll autofluorescence); grey (brightfield).

To summarise, after tomato colonisation, *E. coli* were mainly present on trichomes but were also present on the general surface and in, or around, some stomata. After tomatoes colonised by *E. coli* were submerged in water, *E. coli* also showed this same pattern of presence.

4.3.6 Aqueous ozone did not reduce model pathogens on carrots or tomatoes compared to water

Experiments were set up to investigate if aqueous ozone could reduce luminescent model pathogens on associated post-harvest produce, compared to a water control: *P. viridiflava* PC006 p_{nptII}::lux and *D. chrysanthemi* EC16 (pIJ11282) on carrots, and Pst DC3000 p_{nptII}::lux, Pst T1 p_{nptII}::lux and *E. coli* JHI-5025 (pIJ1282) on tomatoes (tables 4.1 and 4.3). This was completed because ozone has advantages over peracetic acid and sodium hypochlorite for use in the food industry (chapter 1, section 1.7).

The experiments involved the submersion of produce in a suspension of a luminescent model pathogen (OD_{600nm} = 0.5) before produce was dried and subjected to *in planta* bioluminescence imaging for bacterial quantification. Produce was then subjected to a treatment applied via a continuous flow (0.7 - 1.0 ppm aqueous ozone or a water control) before being dried and subjected to *in planta* bioluminescence imaging again for bacterial quantification. Model pathogens only colonised the calyx and pedicel of tomatoes, as seen in bioluminescence imaging (figure 4.3), therefore only tomato calyxes and pedicels were used for bacterial quantification. Model pathogens however colonised any part of carrot surfaces (figure 4.4), so bacterial quantification was not limited to specific areas of carrots. To ensure that the same part of each produce was captured in ‘before’ and ‘after’ images, produce was modified so that they had flat edges to sit against. Since paired data, in the form of luminescence quantifications on ‘before’ and ‘after’ images, was used to test for treatment effects, different sample sizes did not have to be accounted for.

Results showed that a continuous flow of water-only caused an obvious reduction in *P. viridiflava* and *D. chrysanthemi* on carrots and compared to water, aqueous ozone did not cause any further significant reductions (figure 4.16: A, B). A continuous flow of water-only did not visibly reduce any bacteria (Pst DC3000, Pst T1 or *E. coli* JHI-5025) on tomatoes, and compared to water, aqueous ozone did not cause any further significant reductions (figure 4.16: C, D, E).

To ensure that there were no differences in the 'starting points' for testing treatment effects, differences in bacterial luminescence (Log_{10}(luminescence (cps) + 1)) on pre-treatment produce, between different treatment groups within each dataset shown in figure 4.16 were tested for. There were no significant differences in the pre-treatment log_{10}(luminescence (cps) + 1) means across treatment groups within each dataset, apart from the Pst T1 dataset [ANOVA, $F(1, 32) = 5.056$, $p = 0.0316$] (figure 4.16: D). When experimental replicate 2 was removed from this dataset, there were no significant differences in the pre-treatment log_{10}(luminescence (cps) + 1) means across treatment groups, however this experimental replicate was kept because overall results to determine if ozone was having a significant effect on model pathogens compared to the water control, were still the same with or without this experimental replicate.

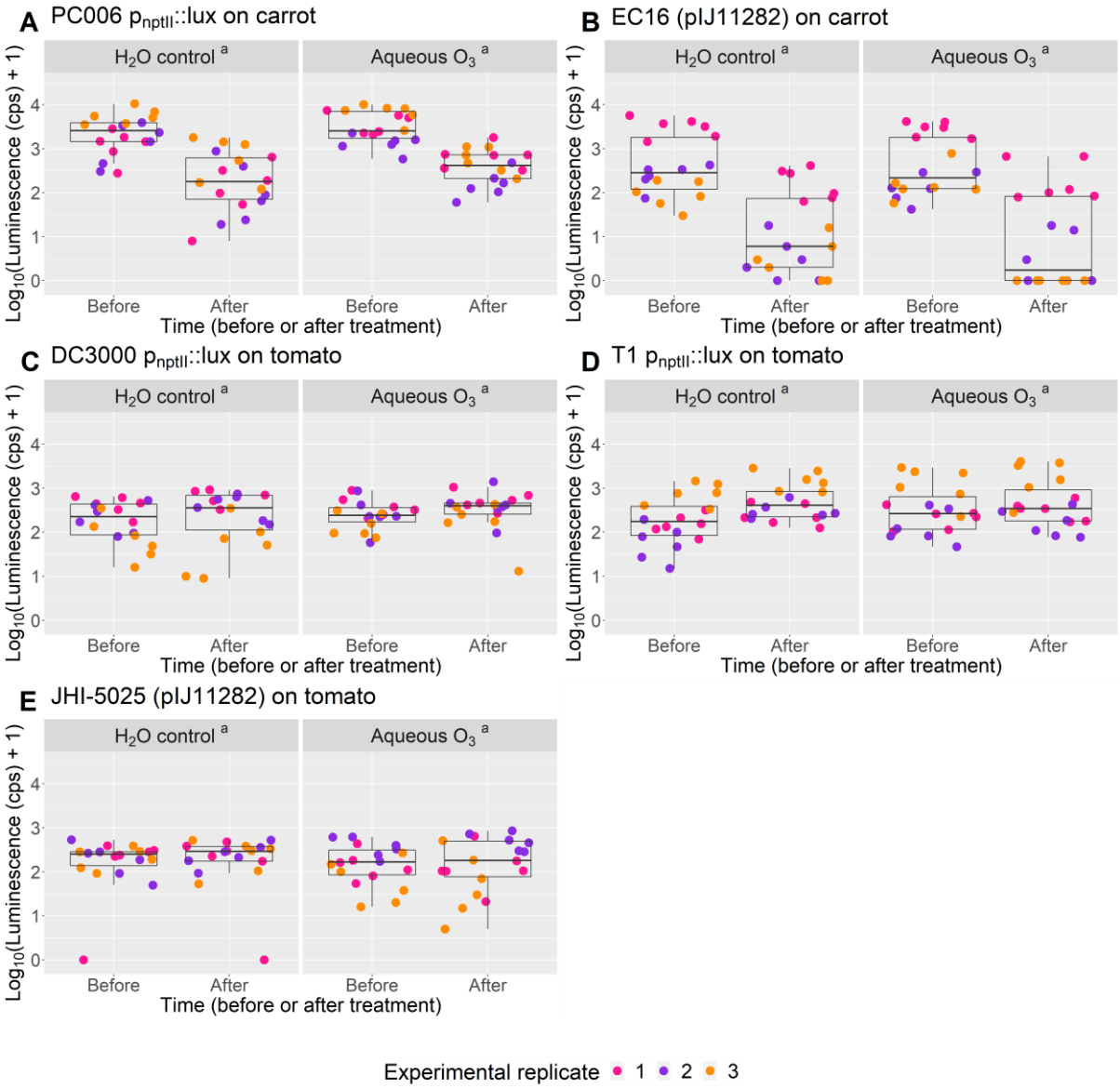


Figure 4.16: Aqueous ozone (O_3) did not reduce model pathogens on tomatoes or carrots, compared to water. Bacteria (**(A)** *P. viridiflava* PC006 p_{nptII}::lux, **(B)** *D. chrysanthemi* EC16 (pIJ11282), **(C)** *P. syringae* pv. tomato DC3000 p_{nptII}::lux, **(D)** *P. syringae* pv. tomato T1 p_{nptII}::lux, **(E)** *E. coli* JHI-5025 (pIJ11282)) at OD_{600nm} 0.5 in PBS were inoculated onto produce by submersion. Produce was dried, imaged for luminescence with the NightOWL LB 983, subjected to a flow of either aqueous ozone (0.7 - 1.0 ppm) or water, dried and then imaged for luminescence again. Luminescence counts per second (cps) were quantified for each produce, before and after treatment, log_{10} transformed and presented as individual data points on the chart. Boxplots display the median, interquartile range, minimum and maximum values (n = 18). Different letters next to treatment titles indicate where treatments had a significantly different effect ($p < 0.05$) on the change in bacterial luminescence.

Aqueous ozone was not able to significantly reduce model pathogens on carrots or tomatoes, compared to the water control, so the ability of gaseous ozone to reduce model pathogens on post-harvest produce was next tested.

4.3.7 Gaseous ozone reduced model pathogens on carrots but not tomatoes

Experiments were set up to investigate if gaseous ozone could reduce luminescent model pathogens on associated post-harvest produce, compared to a water control: *P. viridiflava* PC006 p_{nptII}::lux and *D. chrysanthemi* EC16 (pIJ11282) on carrots, and Pst DC3000 p_{nptII}::lux, Pst T1 p_{nptII}::lux and *E. coli* JHI-5025 (pIJ11282) on tomatoes (tables 4.1 and 4.3). Due to unforeseen circumstances (as a result of company (Anacail Ltd) failure) which halted the use of the in-pack ozone system, this experiment was not fully completed, therefore different numbers of experimental replicates were completed for each model system (figure 4.17).

The experiments involved the submersion of produce in a suspension of a luminescent model pathogen (OD_{600nm} = 0.5) before produce was dried and subjected to *in planta* bioluminescence imaging for bacterial quantification. Produce was then packed into punnets, either subjected to an ozone treatment (3 second ozone generation time, ~663 - 827 peak ppm) or not and subjected to *in planta* bioluminescence imaging again for bacterial quantification. Model pathogens only colonised the calyx and pedicel of tomatoes, as seen in bioluminescence imaging (figure 4.3), therefore only tomato calyxes and pedicels were used for bacterial quantification. Model pathogens however colonised any part of carrot surfaces (figure 4.4), so bacterial quantification was not limited to specific areas of carrots. To ensure that the same part of each produce was captured in ‘before’ and ‘after’ images, produce was modified so that they had flat edges to sit against. Since paired data, in the form of luminescence quantifications on ‘before’ and ‘after’ images, was used to test for treatment effects, different sample sizes did not have to be accounted for.

Results showed that gaseous ozone significantly reduced *P. viridiflava* ($p = 0.0260$) and *D. chrysanthemi* ($p = 0.0310$) on carrots (figure 4.17: A, B) but did not significantly reduce Pst DC3000, Pst T1 or *E. coli* on tomatoes (figure 4.17: C, D, E), compared to changes in

bacterial quantifications on no treatment controls. It is to be mentioned that the linear model that was generated for the *P. viridiflava* dataset violated the normality of residuals assumption that was required for a linear model (which was indicated by a poor histogram of residuals). Since the main issue with this violation would be an inflated type 1 error (which would cause rejection of a null hypothesis of no differences when it should not be rejected), the standard ANOVA was completed, but with a more conservative alpha significance threshold for result interpretation. Since the p-value was 0.0274, it was concluded that gaseous ozone significantly reduced *P. viridiflava*, however more experimental replication would be required for more robust statistical testing.

To ensure that there were no differences in the 'starting points' for testing treatment effects, differences in bacterial luminescence (Log_{10}(luminescence (cps) + 1)) on pre-treatment produce, between different treatment groups within each dataset shown in figure 4.17 were tested for. There were no significant differences in the pre-treatment Log_{10}(luminescence (cps) + 1) means across treatment groups within each dataset apart from the *P. viridiflava* dataset [ANOVA, $F(1, 10) = 6.661$, $p = 0.0274$] (figure 4.17: A). This meant that tomatoes which were treated with ozone had significantly more bacteria to begin with, compared to the tomatoes which were not treated.

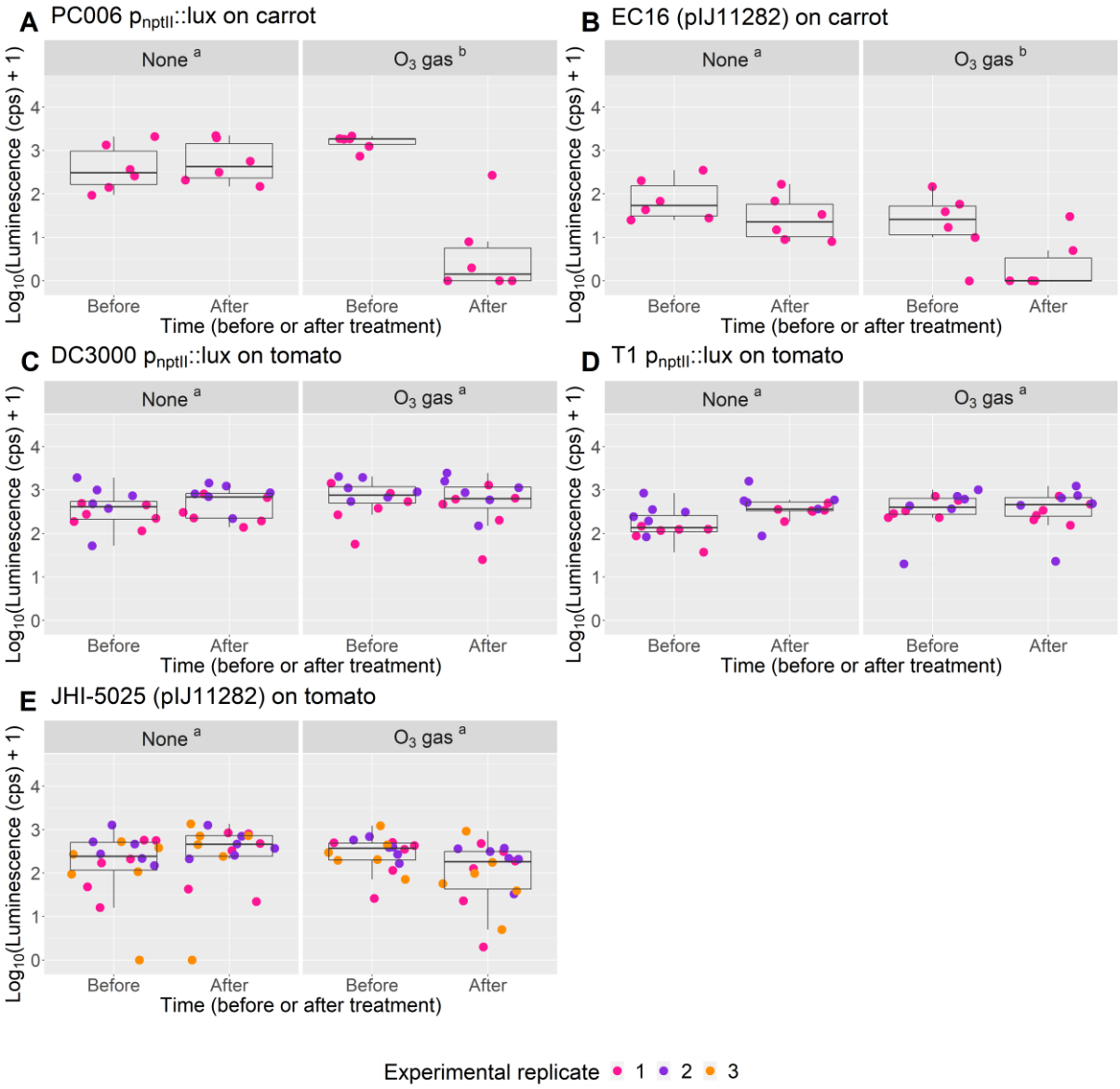


Figure 4.17: Gaseous ozone (O_3) reduced model pathogens on carrots but not tomatoes. Bacteria (**(A)** *P. viridiflava* PC006 p_{nptII}::lux, **(B)** *D. chrysanthemi* EC16 (pIJ11282), **(C)** *P. syringae* pv. tomato DC3000 p_{nptII}::lux, **(D)** *P. syringae* pv. tomato T1 p_{nptII}::lux, **(E)** *E. coli* JHI-5025 (pIJ11282)) at OD_{600nm} 0.5 in PBS were inoculated onto produce by submersion. Produce was dried, imaged for luminescence with the NightOWL LB 983, packed into punnets, either subjected to an ozone treatment (3 second ozone generation time, ~663 - 827 peak ppm) or not and then imaged for luminescence again. Luminescence counts per second (cps) were quantified for each produce, before and after treatment, log_{10} transformed and presented as individual data points on the chart. Boxplots display the median, interquartile range, minimum and maximum values. Different letters next to treatment titles indicate where treatments had a significantly different effect ($p < 0.05$) on the change in bacterial luminescence.

To summarise, gaseous ozone was effective against model pathogens on carrots but not model pathogens on tomatoes, which suggests the tomato calyx provides an enhanced protection to pathogens against intervention treatments.

4.4 Discussion

The validity of *in planta* bioluminescence imaging as a bacterial quantification method, to investigate the effectiveness of peracetic acid, sodium hypochlorite and ozone against *luxCDABE* tagged pathogens on post-harvest produce was confirmed. The effectiveness of peracetic acid, sodium hypochlorite and ozone were then tested against selected pathogen-produce model systems by imaging, and quantifying *luxCDABE* tagged pathogens directly on the surface of produce, before and after the application of an intervention treatment.

4.4.1 Bioluminescence imaging can be used to demonstrate the effectiveness of peracetic acid, sodium hypochlorite and aqueous ozone to control pathogens *in planta*

The validity of *in planta* bioluminescence imaging as a method to determine the effectiveness of peracetic acid, sodium hypochlorite and aqueous ozone against *luxCDABE*-tagged pathogens on the surface of carrots and tomatoes, was confirmed by results obtained from bacterial colony counts. As expected, based on previous studies (Karsi *et al.*, 2008; Nyhan *et al.*, 2020; Soldan *et al.*, 2021), strong correlations between luminescence and colony counts were observed (> 0.97).

Within the dataset which investigated the effect of peracetic acid and sodium hypochlorite against *P. viridiflava* on carrots, the same significant differences were identified by the results obtained from bioluminescence imaging and colony counting, and all of the significant differences identified were large bacterial reductions. In the other datasets where colony count data was used to validate bioluminescence data, colony count data identified significant differences where bioluminescence data did not. However, the

significant differences detected were very small changes in bacterial quantifications so would not be used to generate conclusions for strong treatment effects.

One of the major advantages of using bioluminescence imaging for quantifying bacterial viability is that since results are provided *in situ*, spatial data is collected without the requirement for sample destruction, therefore multiple bacterial viability measurements could be taken from the same sample, over a time course (Morrissey *et al*., 2013). This allowed bacteria on the same produce to be quantified before and after the application of an intervention treatment, so that paired data could be used to assess treatment effects. This was a large benefit because the quantity of bacteria that initially colonised each produce was very variable, so the use of paired data in result analysis allowed this variation to be accounted for, which provided more statistical power.

Conclusions made from paired data results were generally the same as those made from results which were collected from post-treated produce only (during validation experiments). This was because both sets of results showed that peracetic acid and sodium hypochlorite reduced *P. viridiflava* on carrots more than the water control did, and that peracetic acid, sodium hypochlorite and aqueous ozone did not visibly cause a large reduction of *E. coli* on tomatoes. Paired data however showed that both aqueous ozone and the water control reduced *P. viridiflava* on carrots by the same amount, and although results, which were collected from post-treated produce only, also showed that there were no large, obvious differences in effects caused by aqueous ozone or water, they did not show the obvious reduction caused by water and aqueous ozone that was seen in paired data. This could have been due to the differences in the data analysis approach.

In addition to allowing for multiple bacterial viability measurements to be taken from the same sample, *in planta* bioluminescence imaging has many other benefits (but also some limitations) over bacterial colony counting as a method for bacterial quantification (section 4.1.3). Due to its many benefits over bacterial colony counting, and since it has been

validated as a technique to investigate the effectiveness of peracetic acid, sodium hypochlorite and ozone against pathogens inoculated onto post-harvest produce, it could be used as an alternative to colony counting in future studies.

All of the pathogens that were present on produce might not have been detected by bioluminescence imaging. This is because bacteria have a limit of detection for bioluminescence imaging, therefore some areas of produce may have been colonised by pathogens, but at too low of a density to be detected. Model pathogens used for this project had detection limits between 250 - 5000 CFU mm^{-2} and different factors can affect this, for example the *luxCDABE* location and expression levels in bacteria, the media bacteria are presented in, the image exposure time, and the image resolution (Chen *et al*., 1996; Luker and Luker, 2009). The plant tissue that bacteria are presented on might also affect bacterial detection because the detection of bioluminescence from internalised bacteria may be limited by the passage of light through the plant tissue. For example, leaf-internalised bacteria have previously been imaged by bioluminescence imaging (Soldan *et al.*, 2021) however bacteria on the underside of a calyx were not detected by bioluminescence imaging in this work.

Pathogens have different infective doses for causing disease, for example enterotoxigenic *E. coli* (which causes gastroenteritis in humans) has an infective dose from 10 million - 10 billion cells whereas the infective dose of enterohemorrhagic *E. coli* O157:H7 (which can cause haemorrhagic colitis and life-threatening complications in humans), is 10 - 100 cells (U.S. Food and Drug Administration, 2012). The use of *in planta* bioluminescence imaging to determine if pathogens can be reduced to safe levels on produce may therefore need to undergo pathogen-specific modifications to ensure limits of detection are suitable, or to be validated using orthogonal methods such as colony counts.

4.4.2 Intervention treatment effects against pathogens on carrots and tomatoes

For work in this chapter, pathogens were inoculated onto produce by submerging produce into a pathogen inoculum, which was relevant because this could represent inoculations from water dunk tanks, which can be a source of post-harvest contamination (Godfrey and Marshall, 2002; Toth *et al.*, 2011; Zheng *et al.*, 2017; Lipps and Samac, 2022). Pathogens were inoculated onto produce at a high-density (OD_{600nm} = 0.5), so the quantity of pathogens on produce could be greater than what naturally may be found, however high-density bacterial inoculations were completed in other studies which investigated the effect of intervention treatments against pathogens on produce (Lang *et al*., 2004; Chaidez *et al.*, 2007; Keeratipibul *et al*., 2011; Brilhante São José and Dantas Vanetti, 2012; Wang *et al.*, 2023). Pathogens colonised any part of the carrot surface, whereas pathogens only colonised the tomato calyx and pedicel, according to bioluminescence imaging. The tomato calyx has previously been reported as the site where most bacteria adhered to, or where most bacteria were recovered from, in comparison to the tomato fruit body (Barak *et al*., 2011; Ukuku *et al.*, 2022). Since bacterial colonisation has previously been reported on the tomato fruit body (Barak *et al*., 2011; Ukuku *et al.*, 2022), it is possible that pathogens were present on the tomato fruit body during experiments, but they could have been below the limit for detection.

The data obtained from *in planta* bioluminescence imaging showed that 80 ppm peracetic acid and sodium hypochlorite with 100 ppm free chlorine provided further antimicrobial benefits than using water alone did against pathogens on carrots, however 0.7 - 1.0 ppm aqueous ozone did not. ~ 663 - 827 peak ppm gaseous ozone was however able to reduce pathogens on carrots. Pathogens on tomatoes were not reduced by any treatment tested; peracetic acid, sodium hypochlorite, aqueous ozone, or gaseous ozone, in comparison to either the water-only control for aqueous treatments or the no treatment control for gaseous ozone.

Many factors can contribute to the ability of an intervention treatment to reduce micro-organisms on produce, including produce type (produce surface area, produce surface characteristics, native microflora), density and age of the treated microbial population, treatment application method, treatment concentration, treatment contact time and measurement methods (Khadre *et al*., 2001; Vandekinderen *et al.*, 2009; Sarron *et al*., 2021). Due to this, it is difficult to make comparisons between results of different studies (Khadre *et al*., 2001).

Studies that investigated the effects of intervention treatments against bacteria on raw, whole carrots were limited, because they were typically completed on cut, peeled, or shredded carrots (Gonzalez *et al.*, 2004; Ruiz-Cruz *et al.*, 2007; Dharmarha *et al.*, 2019). Nevertheless, peracetic acid (40 ppm, 1.5 minute contact time) and sodium hypochlorite (50 ppm free chlorine, 2 minute contact time) have previously been shown to significantly reduce *E. coli* and *Pseudomonas* on peeled carrots, compared to tap water (Dharmarha *et al.*, 2019), which supports results demonstrated from this study. Studies that investigated the effects of intervention treatments on tomatoes, typically reported effects on ‘tomatoes’ or ‘tomato fruits’ (Lang *et al*., 2004; Alvaro *et al.*, 2009; Singh *et al*., 2018), therefore it was difficult to find reported effects of intervention treatments against bacteria specifically on the tomato calyx and pedicel. Ukuku *et al*., 2022 however reported that sodium hypochlorite (200 ppm free chlorine, 3 minute contact time), significantly reduced *Salmonella* on tomatoes by 2.5 log CFU/g, whereas water only caused a 0.6 log CFU/g reduction, and they reported that most of the bacteria recovered were from the calyx rather than the fruit body. Since results from this study showed that sodium hypochlorite (100 ppm free chlorine, 1 minute contact time) was not sufficient to reduce any bacteria tested on the tomato calyx, perhaps testing different species of bacteria such as *Salmonella*, or increasing the chlorine concentration or contact time would have demonstrated significant reductions, so this could be tested in future work.

Gaseous ozone treatments have previously been tested against bacteria on carrots and tomatoes however this typically involved much lower concentrations of ozone, and much longer treatment times than those used in this study (Sarron *et al*., 2021), therefore it is difficult to compare results generated from other studies to this study. The only similar gaseous ozone treatment application that could be found, in comparison to the one used in this study, involved an in-pack ozone treatment which generated >1000 ppm ozone within 1 minute of activation, which caused significant reductions of *E. coli, Salmonella* and *Listeria* on the tomato fruit surface and tomato stem scar areas (Fan *et al.*, 2012). For work in this chapter, gaseous ozone was generated for 3 seconds by the in-pack ozone system, which produced ~ 663 - 827 peak ppm ozone, and since this ozone would have taken up to a few hours to completely decay (Potts and Diver, 2012), bacteria would have remained exposed to it during this time. Since this was not sufficient enough to reduce any bacteria tested on the tomato calyx in this study, perhaps increasing the treatment time to increase the peak concentration of ozone would have demonstrated significant reductions, so this could be tested in future work.

Results from this study showed that 0.7 - 1.0 ppm aqueous ozone did not provide any further antimicrobial benefits than using water alone did, for any pathogen-produce model system tested. The antimicrobial effect of aqueous ozone, in comparison to water, against model pathogens used for work in this chapter was demonstrated *in vitro*, therefore aqueous ozone had the potential to reduce them. A reason why aqueous ozone may have been ineffective on pathogens *in planta*, in comparison to water alone, may have been that the set-up for aqueous ozone delivery was not optimal. Aqueous ozone has previously been applied to pathogens on carrots and tomatoes with different concentrations and treatment times (Sarron *et al*., 2021). One study identified no significant changes in the quantity of *E. coli* inoculated on baby carrots after 5.2 ppm aqueous ozone was applied for 15 minutes, however a significant reduction was detected with an application of 9.7 ppm ozone for 10 minutes, in comparison to water controls

(Singh *et al.*, 2002). This highlights that aqueous ozone concentration and exposure time are very important factors for ozone's efficiency against pathogens. Optimum conditions for aqueous ozone to treat pathogens on produce, could be tested in future work. Aqueous ozone may also be more efficient against pathogens colonised on specific types of produce because studies have shown that aqueous ozone was more effective against *E. coli* on the surface of tomatoes and lettuce, in comparison to baby carrots (Singh *et al.*, 2002; Bermúdez-Aguirre and Barbosa-Cánovas, 2013). This could be because different produce surfaces offer bacteria different levels of protection against ozone (Vandekinderen *et al.*, 2009) or because different produce surfaces have more organic materials for ozone to react with, which would subsequently deplete the amount of active ozone to react with bacteria. It would therefore be interesting to test the efficiency of aqueous ozone against pathogens on other model produce, to investigate if antimicrobial effects could be seen.

Since peracetic acid and sodium hypochlorite, which were applied at concentrations and treatment times relevant to the food industry (Chilled Food Association, 2010; Hadad, 2018; Food Standards Scotland, personal communication; 21 C.F.R. §173.315), provided more antimicrobial benefits against pathogens on carrots than water did, results from this study support their use in the food industry to treat potential contaminants on post-harvest produce such as carrots. Ozone has benefits over sodium hypochlorite and peracetic acid since it does not produce toxic residues and eliminates the need for chemical transportation and storage (Karaca and Velioglu, 2007; Goodburn and Wallace, 2013; Deng *et al.*, 2020), therefore it would be ideal to use ozone to treat potential contaminants on post-harvest produce instead of peracetic acid and sodium hypochlorite. Results from this study however do not support that 0.7 - 1 ppm aqueous ozone would be a good alternative to peracetic acid and sodium hypochlorite, because no antimicrobial effects on pathogens *in planta* were demonstrated, however increased concentrations and treatment times could be tested to determine more suitable treatment conditions. A gaseous ozone

treatment, which involved a 3 second ozone generation time (~ 663 - 827 peak ppm), may however be a suitable alternative to peracetic acid and sodium hypochlorite since it significantly reduced model pathogens on carrots.

Since no treatments were able to reduce pathogens on tomato calyxes and pedicels, future work should investigate if greater concentrations or treatment times are more effective. It is important that pathogens are effectively controlled on the tomato calyx and pedicel because although they are not for direct consumer consumption, they may serve as a risk factor for cross contamination in food preparation areas (Barak *et al*., 2011). They could also contribute to post-harvest tomato fruit decay (Khaleghi *et al.*, 2013).

4.4.3 The tomato calyx provided a protective environment for bacteria against intervention treatments

The ability of pathogens to survive treatments on the tomato calyx and pedicel was a host-dependent response since sodium hypochlorite and peracetic acid reduced both *P. viridiflava* and *E. coli* on carrots but not tomato calyxes and pedicels. The efficiency of intervention treatments to reduce micro-organisms on produce is highly dependent on the produce surface (Vandekinderen *et al.*, 2009; Sarron *et al*., 2021). Produce may provide enhanced protection to micro-organisms against intervention treatments if, for example, it is abundant in cavities where bacteria could reside, or if it provides an easy route for micro-organism internalisation into the hosts' cells, each of which could subsequently shelter bacteria so that they are out of reach from treatments. The degree of produce hydrophobicity may affect the ability of treatments to reach micro-organisms in cavities, because hydrophilic treatments may reach cavities on a hydrophilic surface more easily than on a hydrophobic surface (Vandekinderen *et al.*, 2009). The produce surface area and native microflora might also affect the efficiency of the treatment to reduce micro-organisms (Sarron *et al*., 2021) because peracetic acid, sodium hypochlorite and ozone are all oxidants so may oxidise other organic materials that are present (McKenna and

Davies, 1988; Karaca and Velioglu, 2007; Zhao *et al.*, 2008). The produce surface area and native microflora could act as other sources of organic material for the active substance of the treatment to oxidise, which could reduce the amount of active substance available to react with micro-organisms.

Strong attachment of enteric bacteria, such as *Salmonella*, to the tomato calyx have previously been reported (Ukuku *et al.*, 2022). Results from this study showed that *E. coli* attached to the tomato calyx, mainly on trichomes, and *E. coli* mainly did not interact with stomata, however cases of *E. coli* internalisation via stomata and *E. coli* surrounding stomata were seen. It was previously reported that *Salmonella* preferentially colonised trichomes, and was rarely found near stomata, on tomato leaves (Barak *et al*., 2011), which supports results from this study. In this study, *E. coli* were also seen on the general surface of the calyx.

4.4.4 Conclusion

Bacterial quantification via *in planta* bioluminescence imaging is just as effective as bacterial colony counts, however results are generated more rapidly and detail about the location of viable bacteria is provided. It could be used as an alternative to colony counting in future studies.

On carrots, peracetic acid, sodium hypochlorite and gaseous ozone were effective antimicrobials, whereas aqueous ozone was not. Gaseous ozone could therefore be a promising alternative intervention treatment to sodium hypochlorite and peracetic acid.

On tomatoes, no treatment that was tested provided effective antimicrobial activity, likely because the bacteria were located on the tomato calyx and pedicel, which provided a protective environment. More effective treatments would therefore be required to limit pathogens on the tomato calyx and pedicel.

Chapter 5: General discussion

This work aimed to investigate if ozone could be used as an alternative treatment to effectively control pathogens on post-harvest produce in the food industry. This was because ozone has benefits over treatments which are currently being used for this, such as sodium hypochlorite and peracetic acid. For example, it does not form toxic residues and eliminates the requirement for chemical transportation and storage (Karaca and Velioglu, 2007; Goodburn and Wallace, 2013; Deng *et al.*, 2020). With consideration given to all of the work that has been presented in this thesis, this section will discuss whether ozone is a promising alternative treatment for the food industry, in addition to other key findings from this work.

5.1 Gaseous ozone is a promising alternative treatment for controlling pathogens in the food industry

Gaseous ozone, delivered by the in-pack ozone system, is a promising alternative to current treatments used for pathogen control in the food industry, such as sodium hypochlorite and peracetic acid. This is because gaseous ozone demonstrated comparable efficacy to sodium hypochlorite and peracetic acid against pathogens on fruits and vegetables: all treatments successfully reduced pathogens on carrots but had no effect against pathogens that resided on the tomato calyx and pedicel. To further validate the suitability of gaseous ozone as an alternative treatment, it would be beneficial to compare the efficacy of these treatments against pathogens on a broader range of produce, and this could be addressed in future work. This is because the type of plant tissue on which pathogens were present impacted the effectiveness of treatments against pathogens.

5.2 More work is required to investigate the impact of gaseous ozone on pathogen presence over time

While gaseous ozone demonstrated the capability to reduce pathogens on produce, more work is required to investigate if the presence of pathogens on ozone-treated produce remains reduced over time.

Results from this study identified that gaseous ozone treatment induced changes in the native microbiota of produce, which included a reduction in the diversity of the bacterial community. Since reduced microbial community diversities have been reported to be more invasible by pathogens (Matos *et al*, 2005; van Elsas *et al.*, 2012), treated produce may be at an increased risk of pathogen colonisation. Nevertheless, sodium hypochlorite and peracetic acid have also reduced the diversity of bacterial communities (Gu *et al.*, 2020) so produce treated with these chemicals may also be more invasible by pathogens post-treatment. An advantage that the in-pack ozone system has over peracetic acid and sodium hypochlorite, is that it treats produce within a pack, in which it can remain in until the point of consumption. This would protect produce from being exposed to sources of pathogens post-treatment such as personnel, insects or transportation equipment (Balali *et al.*, 2020). However, in scenarios where gaseous ozone is employed to treat produce, and subsequent exposure to potential pathogen sources is unavoidable, measures may have to be put into place to account for the heightened risk of post-treatment pathogen colonisation. Future work could aim to confirm if ozone-treated produce is more invasible by pathogens, in comparison to non-treated produce. This could be completed by spiking ozone-treated or non-treated produce with a pathogen and monitoring the survival and growth of the pathogen over time, for example by bioluminescence imaging, quantitative PCR or colony counting on selective agar.

Since reduced microbial community diversities have been reported to be more invasible by pathogens (Matos *et al*, 2005; van Elsas *et al.*, 2012), the reduced bacterial community

diversity resulting from ozone treatment may create conditions to support the proliferation of ozone-surviving pathogens already present in the community. Therefore, although this study has demonstrated that gaseous ozone is effective against pathogens on produce, future work should investigate the ability of surviving pathogens to remain at decreased levels in an ozone-altered microbiota. This could be investigated by spiking the native microbiota of produce with a pathogen, applying ozone treatment, and then monitoring the survival and growth of the pathogen over time.

5.3 Better treatments are needed to effectively control pathogens on the tomato calyx and pedicel

Better treatments are needed in the food industry to effectively control pathogens on the tomato calyx and pedicel. This is because food industry-relevant concentrations of gaseous ozone, aqueous ozone, sodium hypochlorite and peracetic acid did not reduce bacterial pathogens on the tomato calyx and pedicel in this study, which was likely because the tomato calyx and pedicel provided a particularly protective environment for bacteria. This problem needs to be addressed in the food industry because bacterial pathogens on the tomato calyx and pedicel could be problematic: they could contribute to post-harvest fruit decay (Khaleghi *et al.*, 2013) or could be transferred to food preparation areas via cross-contamination (Barak *et al*., 2011) which could cause food-borne illness in consumers (U.S. Food and Drug Administration, 2012). Tomatoes are one of the most common fruits and vegetables associated with food-borne outbreaks (Callejón *et al.*, 2015) and since more micro-organisms reside on the calyx and pedicel than on the fruit surface (Smid *et al.*, 1996; Barak *et al.*, 2011), ineffective control of pathogens on the calyx and pedicel could be a contributor to this. Therefore, more effective treatments are required to be used in the food industry to limit pathogens on the tomato calyx and pedicel. These could be identified in future work, which could be used to provide guidance to the food industry.

5.4 Aqueous ozone, in the set-up which was used, is not a promising alternative treatment for controlling pathogens in the food industry

Aqueous ozone, in the set-up which was utilised, is not a promising alternative to current treatments used for pathogen control in the food industry, such as sodium hypochlorite and peracetic acid. This is because aqueous ozone did not decrease pathogens on post-harvest produce any more than water alone did. Therefore, the incorporation of ozone into water failed to confer additional antimicrobial benefits against pathogens on produce. In contrast, sodium hypochlorite and peracetic acid did provide greater antimicrobial benefits than water alone. Also, in experiments which were set up to measure phenotypic changes in bacteria that were associated with an oxidative stress response, which included an extended 'apparent' lag phase and an increased intracellular redox state, aqueous ozone did not induce these changes, whereas sodium hypochlorite and peracetic acid did. It was speculated that the reason for the ineffectiveness of aqueous ozone against bacteria in these experiments was that the instantaneous ozone demand would have depleted the ozone available to stress bacteria, for example, due to the initial reactions of ozone with post-harvest produce hosts, media or high bacterial densities. This was because in an experimental set-up which would have had a much lower instantaneous ozone demand, aqueous ozone reduced pathogens *in vitro* to below the limit of detection. Nevertheless, it is crucial to consider the instantaneous ozone demand that would occur when produce is treated in the food industry, for example, due to ozone reacting with the host, the host's microbiota, and residual pesticides. Future work could involve modifying the set-up of the aqueous ozone system to try to increase its maximum ozone concentration, or testing different aqueous ozone systems, to determine if they are more effective.

5.5 Hydrogen peroxide tolerance is not correlated with sodium hypochlorite or peracetic acid tolerance

In this study, it was demonstrated that hydrogen peroxide tolerance was not completely correlated with sodium hypochlorite or peracetic acid tolerance. This was because bacteria which were the most tolerant to hydrogen peroxide were not always the most tolerant to sodium hypochlorite or peracetic acid. Therefore, pathogens which may have evolved a strong oxidative stress response to cope with the oxidative burst from eukaryotic hosts, which is mainly hydrogen peroxide (Lamb and Dixon, 1997; O'Brien *et al.*, 2012), may not necessarily be more tolerant to sodium hypochlorite and peracetic acid, which are used as treatments used in the food industry.

Similarities and differences in the response of bacteria to hydrogen peroxide, sodium hypochlorite and peracetic acid were identified, which provided a deeper understanding of the mechanisms that bacteria use to tolerate each treatment. Similarities included that they all caused an increased 'apparent' lag growth phase, reduced culturability, and an increased intracellular redox state in bacteria. They all also induced genes involved in the oxidative stress and DNA damage response in enterics. A clear difference in the response of Pst DC3000 to these chemicals was however identified since *oxyR* and catalases were required for hydrogen peroxide tolerance, but not always peracetic acid or sodium hypochlorite tolerance.

It is to be mentioned that the investigation of a correlation between hydrogen peroxide and ozone tolerance, and comparisons between the mechanisms which bacteria used to respond to each of these treatments could not be completed. This was because, as previously mentioned, in experiments which were set up to measure phenotypic changes in bacteria that were associated with an oxidative stress response, aqueous ozone did not induce oxidative stress. Also, gaseous ozone could not be used for these experiments since the use of the in-pack ozone system was halted. Future work could involve

modifying the experiments which aimed to determine the impact of aqueous ozone on bacterial responses, to reduce the instantaneous ozone demand so that more ozone would be available to induce bacterial stress. For example, this could be achieved by reducing the density of bacteria in experiments (Selma *et al.*, 2007). However, roGFP biosensors were used to measure the intracellular redox state of bacteria and a large density of bacteria was required for sufficient signal from the biosensors at whole population levels (van der Heijden and Finlay, 2015). Nevertheless, in experiments with a low bacterial density, signals from roGFP biosensors could be measured at the single-cell level, for example by flow cytometry. This would be beneficial because it could identify any heterogeneity within the population response, and the extent of this. Alternatively, future work could involve modifying the set-up of the aqueous ozone system or testing different aqueous ozone systems to establish conditions which sufficiently stress bacteria.

Future work could aim to further explore the differences in the response of bacteria to hydrogen peroxide and treatments used in the food industry. For example, the effects of treatments on protein oxidation in the proteome of model pathogens could be compared using cysteine reactivity profiling (Weerapana *et al.*, 2010; Morimoto *et al.*, 2022). Cysteine is the most intrinsically nucleophilic amino acid and, depending on its position within the polypeptide chain, it can have a heightened nucleophilicity, making it highly prone to oxidation under oxidative stress conditions (Weerapana *et al.*, 2010). These cysteines are termed hyper-reactive and they can serve as a regulatory switch on proteins that are required in the oxidative stress response, such as OxyR (Weerapana *et al.*, 2010). Cysteine reactivity profiling identifies reactive cysteines within the bacterial proteome by using isotopically labelled electrophiles for quantitative profiling (Weerapana *et al.*, 2010; Morimoto *et al.*, 2022). It has previously been used to identify cysteines in Pst DC3000 which became more and less reactive in response to hydrogen peroxide (Morimoto *et al.*, 2022). Hence, the technique could identify hyper-reactive cysteines which could be involved in the bacterial stress response to treatments, and it could

simultaneously identify cysteines which are damaged by treatments. It would be beneficial to use this technique to compare the response of bacteria to hydrogen peroxide, ozone, sodium hypochlorite and peracetic acid to gain further insight into the similarities and differences in the bacterial response to each of these treatments.

5.5 Conclusion

Gaseous ozone, but not aqueous ozone, was as effective as sodium hypochlorite and peracetic acid against pathogens on post-harvest produce, therefore it is a promising alternative intervention treatment for the food industry. This would be beneficial because ozone does not form toxic residues and eliminates the requirement for chemical transportation and storage. However, since it was identified that the plant tissue affected the ability of treatments to reduce pathogens on them, it would be useful to generate more results with a broader range of produce to further validate the suitability of ozone as an alternative treatment. One key finding from this study was that no treatment was effective at controlling bacterial pathogens on the tomato calyx and pedicel, so better treatments are needed for this.

More work is required to investigate the impact of gaseous ozone on pathogen presence over time. This is because gaseous ozone reduced the bacterial community diversity of the native microbiota of post-harvest produce, which could make produce more invasible to pathogens post-treatment or could create conditions to support the proliferation of ozone-surviving pathogens already present in the community.

The survival of pathogens during intervention treatments which were strong oxidants (peracetic acid and sodium hypochlorite) does not completely correlate with their hydrogen peroxide tolerance. Therefore, pathogens which could have evolved a strong response against hydrogen peroxide due to host defences, may not be any more tolerant to treatments which are strong oxidants, than any other bacteria.

Bibliography

Agathokleous, E. *et al.* (2020) ‘Ozone affects plant, insect, and soil microbial communities: A threat to terrestrial ecosystems and biodiversity.’, *Science advances*. United States, 6(33). doi: 10.1126/sciadv.abc1176.

Ali, G. A. *et al.* (2022) ‘Massilia timonae bacteremia: An unusual pathogen of septic abortion’, *IDCases*, 29. doi: https://doi.org/10.1016/j.idcr.2022.e01592.

Aller, I. *et al*. (2013) ‘Development of roGFP2-derived redox probes for measurement of the glutathione redox potential in the cytosol of severely glutathione-deficient rml1 seedlings’, *Frontiers in Plant Science*, 4. doi: 10.3389/fpls.2013.00506.

Almeida, N. F. *et al.* (2009) ‘A draft genome sequence of Pseudomonas syringae pv. tomato T1 reveals a type III effector repertoire significantly divergent from that of Pseudomonas syringae pv. tomato DC3000.’, *Molecular plant-microbe interactions : MPMI*. United States, 22(1), pp. 52–62. doi: 10.1094/MPMI-22-1-0052.

Alton GG, F. J. (1996) ‘Brucella’, in Baron, S. (ed.) *Medical microbiology*. 4th edn.

Altshuller, A. P. *et al*. (1961) ‘The interaction of ozone with plastic and metallic materials in a dynamic flow system.’, *International journal of air and water pollution*. United States, 4, pp. 70–78.

Alvaro, J. E. *et al.* (2009) ‘Effects of peracetic acid disinfectant on the postharvest of some fresh vegetables’, *Journal of Food Engineering*, 95(1), pp. 11–15. doi: https://doi.org/10.1016/j.jfoodeng.2009.05.003.

Alwi, N. A. and Ali, A. (2014) ‘Reduction of Escherichia coli O157, Listeria monocytogenes and Salmonella enterica sv. Typhimurium populations on fresh-cut bell pepper using gaseous ozone’, *Food Control*, 46, pp. 304–311. doi: https://doi.org/10.1016/j.foodcont.2014.05.037.

Anderson, C. J. and Kendall, M. M. (2017) ‘Salmonella enterica Serovar Typhimurium Strategies for Host Adaptation’, *Frontiers in Microbiology*, 8. doi: 10.3389/fmicb.2017.01983.

Anderson, M. J. (2017) ‘Permutational Multivariate Analysis of Variance (PERMANOVA)’, in *Wiley StatsRef: Statistics Reference Online*. John Wiley & Sons, Ltd, pp. 1–15. doi: https://doi.org/10.1002/9781118445112.stat07841.

Antunes, L. C. S. *et al.* (2011) ‘Deciphering the multifactorial nature of Acinetobacter baumannii pathogenicity.’, *PloS one*. United States, 6(8). doi: 10.1371/journal.pone.0022674.

Ao, X. *et al.* (2021) ‘Peracetic acid-based advanced oxidation processes for decontamination and disinfection of water: A review’, *Water Research*, 188. doi: https://doi.org/10.1016/j.watres.2020.116479.

Apprill, A. *et al.* (2015) ‘Minor revision to V4 region SSU rRNA 806R gene primer greatly increases detection of SAR11 bacterioplankton’, *Aquatic Microbial Ecology*, 75, pp. 129–137.

Aslam, R. *et al*. (2020) ‘Sanitization Potential of Ozone and Its Role in Postharvest Quality Management of Fruits and Vegetables’, *Food Engineering Reviews*, 12(1), pp. 48–67. doi: 10.1007/s12393-019-09204-0.

Aussel, L. *et al.* (2011) ‘Salmonella detoxifying enzymes are sufficient to cope with the host oxidative burst.’, *Molecular microbiology*. England, 80(3), pp. 628–640. doi: 10.1111/j.1365-2958.2011.07611.x.

Bagley, S. T. (1985) ‘Habitat association of Klebsiella species.’, *Infection control : IC*. United States, 6(2), pp. 52–58. doi: 10.1017/s0195941700062603.

Bailey, A. M. *et al.* (2010) ‘RamA, a Member of the AraC/XylS Family, Influences Both Virulence and Efflux in Salmonella enterica Serovar Typhimurium’, *Journal of Bacteriology*, 192(6), pp. 1607. doi: 10.1128/JB.01517-09.

Balali, G. I. *et al.* (2020) ‘Microbial Contamination, an Increasing Threat to the Consumption of Fresh Fruits and Vegetables in Today’s World.’, *International journal of microbiology*. Egypt, 2020. doi: 10.1155/2020/3029295.

Balleza, E. *et al*. (2018) ‘Systematic characterization of maturation time of fluorescent proteins in living cells.’, *Nature methods*. United States, 15(1), pp. 47–51. doi: 10.1038/nmeth.4509.

Barak, J. D. *et al*. (2011) ‘Colonization of tomato plants by Salmonella enterica is cultivar dependent, and type 1 trichomes are preferred colonization sites.’, *Applied and environmental microbiology*. United States, 77(2), pp. 498–504. doi: 10.1128/AEM.01661-10.

Barnard, R. L. *et al*. (2013) ‘Responses of soil bacterial and fungal communities to extreme desiccation and rewetting’, *The ISME Journal*, 7(11), pp. 2229–2241. doi: 10.1038/ismej.2013.104.

Basim, H. *et al.* (2004) ‘An Outbreak of Bacterial Speck Caused by Pseudomonas syringae pv. tomato on Tomato Transplants Grown in Commercial Seedling Companies Located in the Western Mediterranean Region of Turkey.’, *Plant disease*. United States, 88(9). doi: 10.1094/PDIS.2004.88.9.1050A.

Bates, D. *et al.* (2015) ‘Fitting Linear Mixed-Effects Models Using lme4’, *Journal of Statistical Software*, 67(1), pp. 1–48. doi: 10.18637/jss.v067.i01.

Bayir, H. (2005) ‘Reactive oxygen species.’, *Critical care medicine*. United States, 33(12 Suppl), pp. S498-501. doi: 10.1097/01.ccm.0000186787.64500.12.

Beer, S. M. *et al.* (2004) ‘Glutaredoxin 2 Catalyzes the Reversible Oxidation and Glutathionylation of Mitochondrial Membrane Thiol Proteins: Implications for mitochondrial redox regulation and antioxidant defense*’, *Journal of Biological Chemistry*, 279(46), pp. 47939–47951. doi: https://doi.org/10.1074/jbc.M408011200.

Bennur, T. *et al.* (2015) ‘Nocardiopsis species: Incidence, ecological roles and adaptations’, *Microbiological Research*, 174, pp. 33–47. doi: https://doi.org/10.1016/j.micres.2015.03.010.

Berger, C. N. *et al.* (2009) ‘Interaction of Salmonella enterica with basil and other salad leaves.’, *The ISME journal*. England, 3(2), pp. 261–265. doi: 10.1038/ismej.2008.95.

Bergogne-Bérézin, E. (2014) ‘Bacteria: Acinetobacter’, in Motarjemi, Y. (ed.) *Encyclopedia of Food Safety*. Waltham: Academic Press, pp. 337–341. doi: https://doi.org/10.1016/B978-0-12-378612-8.00084-6.

Bermúdez-Aguirre, D. and Barbosa-Cánovas, G. V (2013) ‘Disinfection of selected vegetables under nonthermal treatments: Chlorine, acid citric, ultraviolet light and ozone’, *Food Control*, 29(1), pp. 82–90. doi: https://doi.org/10.1016/j.foodcont.2012.05.073.

Bernardet, J.-F. and Bowman, J. P. (2006) ‘The Genus Flavobacterium’, in Dworkin, M. et al. (eds) *The Prokaryotes: Volume 7: Proteobacteria: Delta, Epsilon Subclass*. New York, NY: Springer New York, pp. 481–531. doi: 10.1007/0-387-30747-8_17.

Bhandari, R. *et al.* (2023) ‘Xanthomonas infection and ozone stress distinctly influence the microbial community structure and interactions in the pepper phyllosphere’, *ISME Communications*, 3(1). doi: 10.1038/s43705-023-00232-w.

Bienert, G. P. *et al*. (2006) ‘Membrane transport of hydrogen peroxide’, *Biochimica et Biophysica Acta (BBA) - Biomembranes*, 1758(8), pp. 994–1003. doi: https://doi.org/10.1016/j.bbamem.2006.02.015.

Blomfield, I. C. *et al.* (1991) ‘Allelic exchange in Escherichia coli using the Bacillus subtilis sacB gene and a temperature-sensitive pSC101 replicon’, *Molecular Microbiology*, 5(6), pp. 1447–1457. doi: https://doi.org/10.1111/j.1365-2958.1991.tb00791.x.

Bor, B. *et al.* (2019) ‘Saccharibacteria (TM7) in the Human Oral Microbiome.’, *Journal of dental research*. United States, 98(5), pp. 500–509. doi: 10.1177/0022034519831671.

Braun, T. F. *et al.* (2005) ‘Flavobacterium johnsoniae gliding motility genes identified by mariner mutagenesis.’, *Journal of bacteriology*. United States, 187(20), pp. 6943–6952. doi: 10.1128/JB.187.20.6943-6952.2005.

Brilhante São José, J. F. and Dantas Vanetti, M. C. (2012) ‘Effect of ultrasound and commercial sanitizers in removing natural contaminants and Salmonella enterica Typhimurium on cherry tomatoes’, *Food Control*, 24(1), pp. 95–99. doi: https://doi.org/10.1016/j.foodcont.2011.09.008.

British Tomato Growers’ Association (2023) *Tomato Facts*. Available at: https://www.britishtomatoes.co.uk/tomato-facts (Accessed: 5 June 2023).

Brooke, J. S. *et al.* (2008) ‘Mutation of a lipopolysaccharide synthesis gene results in increased biofilm of Stenotrophomonas maltophilia on plastic and glass surfaces’, *Annals of Microbiology*, 58(1), pp. 35–40. doi: 10.1007/BF03179442.

Brown, S. H. J. *et al*. (2011) ‘Analysis of unsaturated lipids by ozone-induced dissociation’, *Biochimica et Biophysica Acta (BBA) - Molecular and Cell Biology of Lipids*, 1811(11), pp. 807–817. doi: https://doi.org/10.1016/j.bbalip.2011.04.015.

Burkholder, W. R. *et al*. (1953) ‘A bacterial blight ol Chrysanthemums.’, *Phytopathology*, 43(9), pp. 522–526.

Butcher, B. G. *et al.* (2011) ‘Characterization of the Fur regulon in Pseudomonas syringae pv. tomato DC3000.’, *Journal of bacteriology*, 193(18), pp. 4598–4611. doi: 10.1128/JB.00340-11.

Callahan, B. J. *et al.* (2016) ‘DADA2: High-resolution sample inference from Illumina amplicon data.’, *Nature methods*. United States, 13(7), pp. 581–583. doi: 10.1038/nmeth.3869.

Callejón, R. *et al.* (2015) ‘Reported Foodborne Outbreaks Due to Fresh Produce in the United States and European Union: Trends and Causes’, *Foodborne pathogens and disease*, 12, pp. 32–38. doi: 10.1089/fpd.2014.1821.

Carmel-Harel, O. and Storz, G. (2000) ‘Roles of the Glutathione- and Thioredoxin-Dependent Reduction Systems in the Escherichia Coli and Saccharomyces Cerevisiae Responses to Oxidative Stress’, *Annual Review of Microbiology*, 54(1), pp. 439–461. doi: 10.1146/annurev.micro.54.1.439.

de Castro Medeiros, L. *et al.* (2019) 'Toxicological aspects of trihalomethanes: a systematic review', *Environmental Science and Pollution Research*, 26(6), pp. 5316–5332. doi: 10.1007/s11356-018-3949-z.

Centre for Agriculture and Bioscience International (2022) *Dickeya chrysanthemi (bacterial wilt of chrysanthemum and other ornamentals)*. Available at: https://www.plantwise.org/knowledgebank/datasheet/21912#HostPlantsSection (Accessed: 18 August 2022).

Ceragioli, M. *et al.* (2010) 'Comparative transcriptomic and phenotypic analysis of the responses of Bacillus cereus to various disinfectant treatments.', *Applied and environmental microbiology*. United States, 76(10), pp. 3352–3360. doi: 10.1128/AEM.03003-09.

Chaidez, C. *et al.* (2007) 'Efficacy of chlorinated and ozonated water in reducing Salmonella typhimurium attached to tomato surfaces', *International Journal of Environmental Health Research*. Taylor & Francis, 17(4), pp. 311–318. doi: 10.1080/09603120701417063.

Chalfie, M. *et al.* (1994) 'Green fluorescent protein as a marker for gene expression.', *Science (New York, N.Y.)*. United States, 263(5148), pp. 802–805. doi: 10.1126/science.8303295.

Chandra, S. *et al*. (1996) 'The Pto kinase mediates a signaling pathway leading to the oxidative burst in tomato', *Proceedings of the National Academy of Sciences*. National Academy of Sciences, 93(23), pp. 13393–13397. doi: 10.1073/pnas.93.23.13393.

Chen, J. *et al*. (1996) 'Use of Luminescent Strains of Salmonella enteritidis To Monitor Contamination and Survival in Eggs', *Journal of Food Protection*, 59(9), pp. 915–921. doi: https://doi.org/10.4315/0362-028X-59.9.915.

Chen, J. Y. *et al*. (2013) 'Pesticide residue removal from vegetables by ozonation', *Journal of Food Engineering*, 114(3), pp. 404–411. doi: https://doi.org/10.1016/j.jfoodeng.2012.08.033.

Cheng, Z. *et al.* (2020) 'Revealing the Variation and Stability of Bacterial Communities in Tomato Rhizosphere Microbiota.', *Microorganisms*. Switzerland, 8(2). doi: 10.3390/microorganisms8020170.

Chilled Food Association (2010) *Protocol for produce washing*. Available at: https://www.chilledfood.org/wp-content/uploads/2015/09/CFA-56-10-Produce-Wash-Protocol-revised-11-5-10-final.pdf.

Chinchkar, A. V *et al.* (2022) 'Potential sanitizers and disinfectants for fresh fruits and vegetables: A comprehensive review', *Journal of Food Processing and Preservation*, n/a(n/a). doi: https://doi.org/10.1111/jfpp.16495.

Cho, M. *et al.* (2010) 'Mechanisms of Escherichia coli inactivation by several disinfectants', *Water Research*, 44(11), pp. 3410–3418. doi: https://doi.org/10.1016/j.watres.2010.03.017.

Choi, K.-H. *et al.* (2005) 'A Tn7-based broad-range bacterial cloning and expression system', *Nature Methods*, 2(6), pp. 443–448. doi: 10.1038/nmeth765.

Choi, K.-H. and Schweizer, H. P. (2006) 'mini-Tn7 insertion in bacteria with single attTn7 sites: example Pseudomonas aeruginosa', *Nature Protocols*, 1(1), pp. 153–161. doi: 10.1038/nprot.2006.24.

Collmer, A. *et al*. (1994) ‘Molecular Biology of Pathogenicity in Erwinia Chrysanthemi EC16’, in Bills, D. D. and Kung, S.-D. (eds) *Biotechnology and Plant Protection*. World Scientific Publishing Co. Pte. Ltd., pp. 73–84.

Committee on Toxicity of Chemicals in Food Consumer Products and the Environment (2006) *COT statement on a commercial survey investigating the occurence of disinfectants and disinfection by-products in prepared salads*. Available at: https://cot.food.gov.uk/sites/default/files/cot/cotstatementwashaids200614.pdf.

Cousin, M. A. (1999) ‘PSEUDOMONAS | Introduction’, in Robinson, R. K. (ed.) *Encyclopedia of Food Microbiology*. Oxford: Elsevier, pp. 1864–1867. doi: https://doi.org/10.1006/rwfm.1999.1290.

Coyle, E. E. *et al*. (2014) ‘Peracetic acid as an alternative disinfection technology for wet weather flows.’, *Water environment research : a research publication of the Water Environment Federation*. United States, 86(8), pp. 687–697. doi: 10.2175/106143014x13975035525663.

Cruz-Alcalde, A. *et al*. (2019) ‘Abatement of ozone-recalcitrant micropollutants during municipal wastewater ozonation: Kinetic modelling and surrogate-based control strategies’, *Chemical Engineering Journal*, 360, pp. 1092–1100. doi: https://doi.org/10.1016/j.cej.2018.10.206.

da Cruz Nizer, W. S. *et al*. (2020) ‘Surviving Reactive Chlorine Stress: Responses of Gram-Negative Bacteria to Hypochlorous Acid’, *Microorganisms*, 8(8). doi: 10.3390/microorganisms8081220.

Cuppels, D. A. (1986) ‘Generation and Characterization of Tn5 Insertion Mutations in Pseudomonas syringae pv. tomato.’, *Applied and environmental microbiology*, 51(2), pp. 323–327.

Dahal, R. H. *et al*. (2021) ‘Genome insight and description of antibiotic producing Massilia antibiotica sp. nov., isolated from oil-contaminated soil.’, *Scientific reports*. England, 11(1). doi: 10.1038/s41598-021-86232-z.

Daniel, N. *et al.* (2020) *The Burden of Foodborne Disease in the UK 2018*. Available at: https://www.food.gov.uk/sites/default/files/media/document/the-burden-of-foodborne-disease-in-the-uk_0.pdf.

Daudi, A. *et al.* (2012) ‘The Apoplastic Oxidative Burst Peroxidase in Arabidopsis Is a Major Component of Pattern-Triggered Immunity ’, *The Plant Cell*, 24(1), pp. 275–287. doi: 10.1105/tpc.111.093039.

Davey, H. M. (2011) ‘Life, death, and in-between: meanings and methods in microbiology.’, *Applied and environmental microbiology*, 77(16), pp. 5571–5576. doi: 10.1128/AEM.00744-11.

Dedysh, S. N. *et al.* (2020) ‘Lacipirellula parvula gen. nov., sp. nov., representing a lineage of planctomycetes widespread in low-oxygen habitats, description of the family Lacipirellulaceae fam. nov. and proposal of the orders Pirellulales ord. nov., Gemmatales ord. nov. and Isosph’, *Systematic and Applied Microbiology*, 43(1). doi: https://doi.org/10.1016/j.syapm.2019.126050.

Delport, J. *et al.* (2014) ‘Cellulosmicrobium cellulans isolated from a patient with acute renal failure’, *JMM Case Reports*. Microbiology Society, 1(2). doi: https://doi.org/10.1099/jmmcr.0.000976.

Deng, L.-Z. *et al.* (2020) 'Emerging chemical and physical disinfection technologies of fruits and vegetables: a comprehensive review.', *Critical reviews in food science and nutrition*. United States, 60(15), pp. 2481–2508. doi: 10.1080/10408398.2019.1649633.

Dharmarha, V. *et al.* (2019) 'Effect of post-harvest interventions on surficial carrot bacterial community dynamics, pathogen survival, and antibiotic resistance.', *International journal of food microbiology*. Netherlands, 291, pp. 25–34. doi: 10.1016/j.ijfoodmicro.2018.11.006.

Díaz-López, M. *et al.* (2022) 'The effects of ozone treatments on the agro-physiological parameters of tomato plants and the soil microbial community.', *The Science of the total environment*. Netherlands, 812. doi: 10.1016/j.scitotenv.2021.151429.

Diaz-Ochoa, V. E. *et al.* (2016) 'Salmonella Mitigates Oxidative Stress and Thrives in the Inflamed Gut by Evading Calprotectin-Mediated Manganese Sequestration', *Cell Host & Microbe*, 19(6), pp. 814–825. doi: https://doi.org/10.1016/j.chom.2016.05.005.

Dodd, C. E. R. (2014) 'PSEUDOMONAS | Introduction', in Batt, C. A. and Tortorello, M. Lou (eds) *Encyclopedia of Food Microbiology (Second Edition)*. Second Edi. Oxford: Academic Press, pp. 244–247. doi: https://doi.org/10.1016/B978-0-12-384730-0.00282-2.

Dodds, P. N. and Rathjen, J. P. (2010) 'Plant immunity: towards an integrated view of plant-pathogen interactions.', *Nature reviews. Genetics*. England, 11(8), pp. 539–548. doi: 10.1038/nrg2812.

Dong, C.-J. *et al.* (2019) 'Bacterial communities in the rhizosphere, phyllosphere and endosphere of tomato plants.', *PloS one*, 14(11). doi: 10.1371/journal.pone.0223847.

Dong, N. *et al.* (2022) 'Klebsiella species: Taxonomy, hypervirulence and multidrug resistance.', *EBioMedicine*. Netherlands, 79. doi: 10.1016/j.ebiom.2022.103998.

Duan, Y. *et al.* (2020) 'Limnobacter alexandrii sp. nov., a thiosulfate-oxidizing, heterotrophic and EPS-bearing Burkholderiaceae isolated from cultivable phycosphere microbiota of toxic Alexandrium catenella LZT09', *Antonie van Leeuwenhoek*, 113(11), pp. 1689–1698. doi: 10.1007/s10482-020-01473-8.

Dublan, M. de los A. *et al.* (2014) 'Plant-adapted Escherichia coli show increased lettuce colonizing ability, resistance to oxidative stress and chemotactic response.', *PloS one*. United States, 9(10). doi: 10.1371/journal.pone.0110416.

Dul'neva, L. V and Moskvin, A. V (2005) 'Kinetics of Formation of Peroxyacetic Acid', *Russian Journal of General Chemistry*, 75(7), pp. 1125–1130. doi: 10.1007/s11176-005-0378-8.

Duncan, S. *et al.* (1994) 'Luminescence-based detection of activity of starved and viable but nonculturable bacteria.', *Applied and environmental microbiology*, 60(4), pp. 1308–1316. doi: 10.1128/aem.60.4.1308-1316.1994.

van Elsas, J. D. *et al.* (2012) 'Microbial diversity determines the invasion of soil by a bacterial pathogen.', *Proceedings of the National Academy of Sciences of the United States of America*. United States, 109(4), pp. 1159–1164. doi: 10.1073/pnas.1109326109.

Elviss, N. C. *et al.* (2009) 'Microbiological study of fresh herbs from retail premises uncovers an international outbreak of salmonellosis', *International Journal of Food Microbiology*, 134, pp. 83–8. doi: 10.1016/j.ijfoodmicro.2009.01.015.

Emerson, J. B. *et al.* (2017) 'Schrödinger's microbes: Tools for distinguishing the living from the dead in microbial ecosystems', *Microbiome*, 5(1). doi: 10.1186/s40168-017-0285-3.

Environmental Protection Agency (2000) ‘Peroxyacetic Acid; Exemption From the Requirement of a Tolerance’, *Federal Register*, 65(232).

Epelle, E. I. *et al.* (2023) ‘Ozone application in different industries: A review of recent developments.’, *Chemical engineering journal (Lausanne, Switzerland : 1996)*. Switzerland, 454. doi: 10.1016/j.cej.2022.140188.

Ersoy, Z. *et al*. (2019) ‘Mechanisms of the Escherichia coli and Enterococcus faecalis inactivation by ozone’, *LWT*, 100, pp. 306–313. doi: https://doi.org/10.1016/j.lwt.2018.10.095.

Escobar Rodríguez, C. *et al.* (2021) ‘The Bacterial Microbiome of the Tomato Fruit Is Highly Dependent on the Cultivation Approach and Correlates With Flavor Chemistry’, *Frontiers in Plant Science*, 12. doi: 10.3389/fpls.2021.775722.

European Food Safety Authority; European Centre for Disease Prevention and Control. (2022) ‘The European Union One Health 2021 Zoonoses Report.’, *EFSA journal. European Food Safety Authority*. United States, 20(12). doi: 10.2903/j.efsa.2022.7666.

Fan, X. *et al.* (2012) ‘Inactivation of Listeria innocua, Salmonella Typhimurium, and Escherichia coli O157:H7 on Surface and Stem Scar Areas of Tomatoes Using In-Package Ozonation’, *Journal of Food Protection*, 75(9), pp. 1611–1618. doi: https://doi.org/10.4315/0362-028x.jfp-12-103.

Farrar, J. J. *et al*. (2000) ‘Influence of Soil Saturation and Temperature on Erwinia chrysanthemi Soft Rot of Carrot.’, *Plant disease*. United States, 84(6), pp. 665–668. doi: 10.1094/PDIS.2000.84.6.665.

Farvardin, A. *et al.* (2020) ‘The Apoplast: A Key Player in Plant Survival.’, *Antioxidants (Basel, Switzerland)*. Switzerland, 9(7). doi: 10.3390/antiox9070604.

Fathi-Najafabadi, A. *et al.* (2021) ‘Chlorophyll fluorescence imaging as a tool to evaluate calyx senescence during the ripening of persimmon fruit treated with gibberellic acid’, *Postharvest Biology and Technology*, 179. doi: https://doi.org/10.1016/j.postharvbio.2021.111582.

Ferrer-Navarro, M. *et al.* (2013) ‘Abundance of the Quorum-Sensing Factor Ax21 in Four Strains of Stenotrophomonas maltophilia Correlates with Mortality Rate in a New Zebrafish Model of Infection’, *PLOS ONE*. Public Library of Science, 8(6), pp. 1–10. doi: 10.1371/journal.pone.0067207.

Figurski, D. H. and Helinski, D. R. (1979) ‘Replication of an origin-containing derivative of plasmid RK2 dependent on a plasmid function provided in trans.’, *Proceedings of the National Academy of Sciences of the United States of America*, 76(4), pp. 1648–1652. doi: 10.1073/pnas.76.4.1648.

Floc’h, K. *et al.* (2019) ‘Cell morphology and nucleoid dynamics in dividing Deinococcus radiodurans’, *Nature Communications*, 10(1). doi: 10.1038/s41467-019-11725-5.

Food Standards Scotland (2023) *Chlorate*. Available at: https://www.foodstandards.gov.scot/self-assessment-resources/chlorate (Accessed: 21 May 2023).

Frederix, M. *et al.* (2014) ‘Mutation of praR in Rhizobium leguminosarum enhances root biofilms, improving nodulation competitiveness by increased expression of attachment proteins.’, *Molecular microbiology*, 93(3), pp. 464–478. doi: 10.1111/mmi.12670.

Fukuzaki, S. (2006) ‘Mechanisms of actions of sodium hypochlorite in cleaning and disinfection processes.’, *Biocontrol science*. Japan, 11(4), pp. 147–157. doi: 10.4265/bio.11.147.

Gardoni, D. *et al*. (2012) ‘Decay of Ozone in Water: A Review’, *Ozone: Science \& Engineering*. Taylor & Francis, 34(4), pp. 233–242. doi: 10.1080/01919512.2012.686354.

Getz, S. *et al*. (1983) ‘Scanning electron microscopy of infection sites and lesion development on tomato fruit infected with Pseudomonas syringae pv. tomato’, *Phytopathology*, 73(1). doi: 10.1094/phyto-73-39.

Gibalov, V. I. and Pietsch, G. J. (2006) ‘On the Performance of Ozone Generators Working with Dielectric Barrier Discharges’, *Ozone: Science \& Engineering*. Taylor & Francis, 28(2), pp. 119–124. doi: 10.1080/01919510600559419.

Gibbs-Flournoy, E. A. *et al.* (2013) ‘Monitoring Intracellular Redox Changes in Ozone-Exposed Airway Epithelial Cells’, *Environmental Health Perspectives*, 121(3), pp. 312–317. doi: 10.1289/ehp.1206039.

Gibson, D. G. *et al.* (2009) ‘Enzymatic assembly of DNA molecules up to several hundred kilobases’, *Nature Methods*, 6(5), pp. 343–345. doi: 10.1038/nmeth.1318.

Gloor, G. B. *et al.* (2017) ‘Microbiome Datasets Are Compositional: And This Is Not Optional’, *Frontiers in Microbiology*, 8. doi: 10.3389/fmicb.2017.02224.

Godfrey, S. A. C. and Marshall, J. (2002) ‘Identification of cold_tolerant Pseudomonas viridiflava and P. marginalis causing severe carrot postharvest bacterial soft rot during refrigerated export from New Zealand’, *Plant Pathology*, 51, pp. 155–162.

Gonzalez, R. J. *et al.* (2004) ‘Efficacy of Sanitizers To Inactivate Escherichia coli O157:H7 on Fresh-Cut Carrot Shreds under Simulated Process Water Conditions’, *Journal of Food Protection*, 67(11), pp. 2375–2380. doi: https://doi.org/10.4315/0362-028X-67.11.2375.

Goodburn, C. and Wallace, C. A. (2013) ‘The microbiological efficacy of decontamination methodologies for fresh produce: A review’, *Food Control*, 32(2), pp. 418–427. doi: https://doi.org/10.1016/j.foodcont.2012.12.012.

Gordon, M. A. (2011) ‘Invasive nontyphoidal Salmonella disease: epidemiology, pathogenesis and diagnosis.’, *Current opinion in infectious diseases*. United States, 24(5), pp. 484–489. doi: 10.1097/QCO.0b013e32834a9980.

Gregor, C. *et al.* (2018) ‘Strongly enhanced bacterial bioluminescence with the ilux operon for single-cell imaging.’, *Proceedings of the National Academy of Sciences of the United States of America*. United States, 115(5), pp. 962–967. doi: 10.1073/pnas.1715946115.

Gu, G. *et al.* (2020) ‘Microbiome convergence following sanitizer treatment and identification of sanitizer resistant species from spinach and lettuce rinse water’, *International Journal of Food Microbiology*, 318. doi: https://doi.org/10.1016/j.ijfoodmicro.2019.108458.

Gu, M. and Imlay, J. A. (2011) ‘The SoxRS response of Escherichia coli is directly activated by redox-cycling drugs rather than by superoxide’, *Molecular Microbiology*, 79(5), pp. 1136–1150. doi: https://doi.org/10.1111/j.1365-2958.2010.07520.x.

Guo, M. *et al.* (2012) ‘Pseudomonas syringae Catalases Are Collectively Required for Plant Pathogenesis’, *Journal of Bacteriology*, 194(18). doi: 10.1128/JB.00999-12.

Hadad, R. (2018) *How to Wash Produce Using a Peracetic Acid (PAA) Solution*. Available at: https://cvp.cce.cornell.edu/submission.php?id=298.

Hahn, M. M. *et al*. (2021) ‘Salmonella Biofilms Tolerate Hydrogen Peroxide by a Combination of Extracellular Polymeric Substance Barrier Function and Catalase Enzymes.’, *Frontiers in cellular and infection microbiology*. Switzerland, 11. doi: 10.3389/fcimb.2021.683081.

Hamelin, C. (1985) ‘Production of single- and double-strand breaks in plasmid DNA by ozone.’, *International journal of radiation oncology, biology, physics*. United States, 11(2), pp. 253–257. doi: 10.1016/0360-3016(85)90146-4.

Hanson, G. T. *et al.* (2004) ‘Investigating Mitochondrial Redox Potential with Redox-sensitive Green Fluorescent Protein Indicators’, *Journal of Biological Chemistry*. Elsevier, 279(13), pp. 13044–13053. doi: 10.1074/jbc.M312846200.

Hassenberg, K. *et al.* (2008) ‘Ozonated Wash Water for Inhibition of Pectobacterium carotovorum on Carrots and the Effect on the Physiological Behaviour of Produce’, *European Journal of Horticultural Science*, 73, pp. 37–42.

Hauben, L. *et al.* (1998) ‘Phylogenetic Position of Phytopathogens within the Enterobacteriaceae’, *Systematic and Applied Microbiology*, 21(3), pp. 384–397. doi: https://doi.org/10.1016/S0723-2020(98)80048-9.

Hautefort, I. *et al*. (2003) ‘Single-copy green fluorescent protein gene fusions allow accurate measurement of Salmonella gene expression in vitro and during infection of mammalian cells.’, *Applied and environmental microbiology*. United States, 69(12), pp. 7480–7491. doi: 10.1128/AEM.69.12.7480-7491.2003.

Health and Safety Executive (2014) *UK HSE Ozone: Health hazards and control measures. Guidance Note EH38.* Available at: https://www.hse.gov.uk/pubns/eh38.pdf.

Health and Safety Executive (2023) *Maximum residue levels (MRLs) and import tolerances*. Available at: https://www.hse.gov.uk/pesticides/mrls/index.htm (Accessed: 21 May 2023).

Hebisch, E. *et al.* (2013) ‘High variation of fluorescence protein maturation times in closely related Escherichia coli strains.’, *PloS one*. United States, 8(10). doi: 10.1371/journal.pone.0075991.

van der Heijden, J. and Finlay, B. B. (2015) ‘In vitro Real-time Measurement of the Intra-bacterial Redox Potential.’, *Bio-protocol*. United States, 5(17), pp. 1–9. doi: 10.21769/bioprotoc.1579.

Heim, R. *et al*. (1994) ‘Wavelength mutations and posttranslational autoxidation of green fluorescent protein.’, *Proceedings of the National Academy of Sciences of the United States of America*. United States, 91(26), pp. 12501–12504. doi: 10.1073/pnas.91.26.12501.

Hillar, A. *et al*. (1999) ‘Intracellular location of catalase-peroxidase hydroperoxidase I of Escherichia coli.’, *FEMS microbiology letters*. England, 170(2), pp. 307–312. doi: 10.1111/j.1574-6968.1999.tb13388.x.

Höfte, M. and De Vos, P. (2006) ‘Plant pathogenic Pseudomonas species’, in Gnanamanickam, S. S. (ed.) *Plant-Associated Bacteria*. Dordrecht: Springer Netherlands, pp. 507–533. doi: 10.1007/978-1-4020-4538-7_14.

Hoiseth, S. K. and Stocker, B. A. D. (1981) ‘Aromatic-dependent Salmonella typhimurium are non-virulent and effective as live vaccines’, *Nature*, 291(5812), pp. 238–239. doi: 10.1038/291238a0.

Holden, N. *et al.* (2007) ‘Regulation of P-fimbrial phase variation frequencies in Escherichia coli CFT073.’, *Infection and immunity*. United States, 75(7), pp. 3325–3334. doi: 10.1128/IAI.01989-06.

Holden, N. (2021) ‘Genomic data of an environmental Escherichia coli isolate shows high resemblance to E. coli K-12 reference strain MG1655’, *Data in Brief*, 39. doi: https://doi.org/10.1016/j.dib.2021.107586.

Holden, N. J. *et al.* (2006) ‘Demonstration of regulatory cross-talk between P fimbriae and type 1 fimbriae in uropathogenic Escherichia coli.’, *Microbiology (Reading, England)*. England, 152(Pt 4), pp. 1143–1153. doi: 10.1099/mic.0.28677-0.

Horvitz, S. and Cantalejo, M. J. (2014) ‘Application of ozone for the postharvest treatment of fruits and vegetables.’, *Critical reviews in food science and nutrition*. United States, 54(3), pp. 312–339. doi: 10.1080/10408398.2011.584353.

Huang, K. and Nitin, N. (2017) ‘Enhanced removal of Escherichia coli O157:H7 and Listeria innocua from fresh lettuce leaves using surfactants during simulated washing’, *Food Control*, 79, pp. 207–217. doi: https://doi.org/10.1016/j.foodcont.2017.03.032.

Huang, Z. *et al.* (2022) ‘Comparative Genomic Analysis Reveals Potential Pathogenicity and Slow-Growth Characteristics of Genus Brevundimonas and Description of Brevundimonas pishanensis sp. nov.’, *Microbiology spectrum*. United States, 10(2). doi: 10.1128/spectrum.02468-21.

Hudson, J. B. and Sharma, M. (2009) ‘The Practical Application of Ozone Gas as an Anti-fungal (Anti-mold) Agent’, *Ozone: Science \& Engineering*. Taylor & Francis, 31(4), pp. 326–332. doi: 10.1080/01919510903043996.

Humphrey, P. T. and Whiteman, N. K. (2020) ‘Insect herbivory reshapes a native leaf microbiome’, *Nature Ecology & Evolution*, 4(2), pp. 221–229. doi: 10.1038/s41559-019-1085-x.

Iglewski, B. H. (1996) ‘Pseudomonas’, in Baron, S. (ed.) *Medical Microbiology.* 4th edn.

Iizuka, R. *et al*. (2011) ‘Kinetic study of de novo chromophore maturation of fluorescent proteins’, *Analytical Biochemistry*, 414(2), pp. 173–178. doi: https://doi.org/10.1016/j.ab.2011.03.036.

Imlay, J. A. (2008) ‘Cellular defenses against superoxide and hydrogen peroxide.’, *Annual review of biochemistry*. United States, 77, pp. 755–776. doi: 10.1146/annurev.biochem.77.061606.161055.

Imlay, J. A. (2009) ‘Oxidative Stress’, in *EcoSal Plus*. Available at: https://www.asmscience.org/content/journal/ecosalplus/10.1128/ecosalplus.5.4.4.

Imlay, J. A. (2015) ‘Transcription Factors That Defend Bacteria Against Reactive Oxygen Species.’, *Annual review of microbiology*, 69, pp. 93–108. doi: 10.1146/annurev-micro-091014-104322.

Ishiga, Y. and Ichinose, Y. (2015) ‘Pseudomonas syringae pv. tomato OxyR Is Required for Virulence in Tomato and Arabidopsis’, *Molecular Plant-Microbe Interactions*. Scientific Societies, 29(2), pp. 119–131. doi: 10.1094/MPMI-09-15-0204-R.

Ishizaki, K. *et al.* (1987) ‘Effect of ozone on plasmid DNA of Escherichia coli in situ’, *Water Research*, 21(7), pp. 823–827. doi: https://doi.org/10.1016/0043-1354(87)90158-8.

Isler, B. *et al.* (2020) ‘Achromobacter Infections and Treatment Options.’, *Antimicrobial agents and chemotherapy*. United States, 64(11). doi: 10.1128/AAC.01025-20.

Ito, Y. and Nakano, T. (2015) ‘Development and regulation of pedicel abscission in tomato’, *Frontiers in Plant Science*, 6. doi: 10.3389/fpls.2015.00442.

Iwase, T. *et al.* (2013) ‘A simple assay for measuring catalase activity: a visual approach.’, *Scientific reports*. England, 3. doi: 10.1038/srep03081.

Jasson, V. *et al.* (2010) ‘Alternative microbial methods: An overview and selection criteria’, *Food Microbiology*, 27(6), pp. 710–730. doi: https://doi.org/10.1016/j.fm.2010.04.008.

Jin, L. *et al.* (2021) ‘Genomic Insights into Denitrifying Methane-Oxidizing Bacteria Gemmobacter fulva sp. Nov., Isolated from an Anabaena Culture.’, *Microorganisms*. Switzerland, 9(12). doi: 10.3390/microorganisms9122423.

Jin, M. *et al.* (2019) ‘The diversity and commonalities of the radiation-resistance mechanisms of Deinococcus and its up-to-date applications’, *AMB Express*, 9(1). doi: 10.1186/s13568-019-0862-x.

Jones, L. A. *et al.* (2015) ‘Genome-Assisted Development of a Diagnostic Protocol for Distinguishing High Virulence Pseudomonas syringae pv. tomato Strains’, *Plant Disease*, 99(4), pp. 527–534. doi: 10.1094/PDIS-08-14-0833-RE.

Jwa, N.-S. and Hwang, B. K. (2017) ‘Convergent Evolution of Pathogen Effectors toward Reactive Oxygen Species Signaling Networks in Plants.’, *Frontiers in plant science*, 8. doi: 10.3389/fpls.2017.01687.

Kämpfer, P. (2014) ‘Acinetobacter’, in Batt, C. A. and Tortorello, M. Lou (eds) *Encyclopedia of Food Microbiology (Second Edition)*. Second Edi. Oxford: Academic Press, pp. 11–17. doi: https://doi.org/10.1016/B978-0-12-384730-0.00002-1.

Kaplan, J. B. (2011) ‘Antibiotic-induced biofilm formation.’, *The International journal of artificial organs*. United States, 34(9), pp. 737–751. doi: 10.5301/ijao.5000027.

Karaca, H. and Velioglu, Y. S. (2007) ‘Ozone Applications in Fruit and Vegetable Processing’, *Food Reviews International*. Taylor & Francis, 23(1), pp. 91–106. doi: 10.1080/87559120600998221.

Karsi, A. *et al.* (2008) ‘Development of bioluminescent Salmonella strains for use in food safety’, *BMC Microbiology*, 8(1). doi: 10.1186/1471-2180-8-10.

Karstens, L. *et al.* (2019) ‘Controlling for Contaminants in Low-Biomass 16S rRNA Gene Sequencing Experiments.’, *mSystems*. United States, 4(4). doi: 10.1128/mSystems.00290-19.

Kassambara, A. (2017) ‘Chapter 3: Linear regression’, in *Machine Learning Essesntials: Practical Guide in R*. STHDA, pp. 10–20.

Keen, N. T. *et al.* (1988) ‘Improved broad-host-range plasmids for DNA cloning in Gram-negative bacteria’, *Gene*, 70(1), pp. 191–197. doi: https://doi.org/10.1016/0378-1119(88)90117-5.

Keeratipibul, S. *et al*. (2011) ‘Prediction of coliforms and Escherichia coli on tomato fruits and lettuce leaves after sanitizing by using Artificial Neural Networks’, *LWT - Food Science and Technology*, 44, pp. 130–138. doi: 10.1016/j.lwt.2010.05.015.

Keith, L. M. *et al*. (1999) ‘dnaK and the heat stress response of Pseudomonas syringae pv. glycinea.’, *Molecular plant-microbe interactions : MPMI*. United States, 12(7), pp. 563–574. doi: 10.1094/MPMI.1999.12.7.563.

van Keulen, G. *et al.* (2007) ‘The obligate aerobic actinomycete Streptomyces coelicolor A3(2) survives extended periods of anaerobic stress.’, *Environmental microbiology*. England, 9(12), pp. 3143–3149. doi: 10.1111/j.1462-2920.2007.01433.x.

Khademi, S. M. H. *et al.* (2021) ‘Genomic and Phenotypic Evolution of Achromobacter xylosoxidans during Chronic Airway Infections of Patients with Cystic Fibrosis.’, *mSystems*. United States, 6(3). doi: 10.1128/mSystems.00523-21.

Khadre, M. A. *et al*. (2001) ‘Microbiological Aspects of Ozone Applications in Food: A Review’, *Journal of Food Science*, 66(9), pp. 1242–1252. doi: 10.1111/j.1365-2621.2001.tb15196.x.

Khaleghi, S. S. *et al.* (2013) ‘Effect of calyx removal and disinfection on ripening rate and control of postharvest decay in tomato fruit’, in.

Kim, J.-G. *et al*. (2003) ‘Ozone and its current and future application in the food industry.’, *Advances in Food and Nutrition Research*, 45, pp. 167–218.

Kim, J. and Park, W. (2014) ‘Oxidative stress response in Pseudomonas putida’, *Applied Microbiology and Biotechnology*, 98(16), pp. 6933–6946. doi: 10.1007/s00253-014-5883-4.

Koivunen, J. and Heinonen-Tanski, H. (2005) ‘Inactivation of enteric microorganisms with chemical disinfectants, UV irradiation and combined chemical/UV treatments.’, *Water research*. England, 39(8), pp. 1519–1526. doi: 10.1016/j.watres.2005.01.021.

Komanapalli, I. R. and Lau, B. H. S. (1996) ‘Ozone-induced damage of Escherichia coli K-12’, *Applied Microbiology and Biotechnology*, 46(5), pp. 610–614. doi: 10.1007/s002530050869.

Komanapalli, I. R. *et al*. (1997) ‘Effect of ozone on metabolic activities of Escherichia coli K-12’, *Toxicology Letters*, 90(1), pp. 61–66. doi: https://doi.org/10.1016/S0378-4274(96)03830-1.

Kröger, C. *et al.* (2013) ‘An infection-relevant transcriptomic compendium for salmonella enterica serovar typhimurium’, *Cell Host and Microbe*, 14(6), pp. 683–95. doi: 10.1016/j.chom.2013.11.010.

Kunadiya, M. B. *et al.* (2021) ‘Persistence and degradation of Phytophthora cinnamomi DNA and RNA in different soil types’, *Environmental DNA*, 3(1), pp. 92–104. doi: https://doi.org/10.1002/edn3.127.

LaBauve, A. E. and Wargo, M. J. (2012) ‘Growth and laboratory maintenance of Pseudomonas aeruginosa.’, *Current protocols in microbiology*. United States, Chapter 6. doi: 10.1002/9780471729259.mc06e01s25.

Lahti, L. and Sudarshan, S. (2019) ‘Microbiome R package’.

Lamb, C. and Dixon, R. A. (1997) ‘The Oxidative Burst in Plant Disease Resistance.’, *Annual review of plant physiology and plant molecular biology*. United States, 48, pp. 251–275. doi: 10.1146/annurev.arplant.48.1.251.

Land, M. M. *et al*. (2004) ‘Evaluation of Inoculation Method and Inoculum Drying Time for Their Effects on Survival and Efficiency of Recovery of Escherichia coli O157:H7, Salmonella, and Listeria monocytogenes Inoculated on the Surface of Tomatoes’, *Journal of Food Protection*, 67(4), pp. 732–741. doi: 10.4315/0362-028X-67.4.732.

Laroussi, M. and Leipold, F. (2004) ‘Evaluation of the roles of reactive species, heat, and UV radiation in the inactivation of bacterial cells by air plasmas at atmospheric pressure’, *International Journal of Mass Spectrometry*, 233(1), pp. 81–86. doi: https://doi.org/10.1016/j.ijms.2003.11.016.

Layton, A. C. *et al.* (2000) ‘Quantification of Hyphomicrobium populations in activated sludge from an industrial wastewater treatment system as determined by 16S rRNA analysis.’, *Applied and environmental microbiology*. United States, 66(3), pp. 1167–1174. doi: 10.1128/AEM.66.3.1167-1174.2000.

Lenth, R. *et al.* (2023) ‘emmeans: Estimated Marginal Means, aka Least-Squares Means’. R package.

Lewis, R. J. *et al.* (2006) ‘Use of Salmonella enterica serovar Typhimurium DT104 expressing lux genes to assess, in real time and in situ, heat inactivation and recovery on a range of contaminated food surfaces’, *Journal of Food Engineering*, 76(1), pp. 41–48. doi: https://doi.org/10.1016/j.jfoodeng.2005.05.023.

Li, J. *et al.* (2020) ‘Effect of ozone stress on the intracellular metabolites from Cobetia marina.’, *Analytical and bioanalytical chemistry*. Germany, 412(23), pp. 5853–5861. doi: 10.1007/s00216-020-02810-6.

Li, K. *et al.* (2022) ‘Changes in microbial community composition drive the response of ecosystem multifunctionality to elevated ozone’, *Environmental Research*, 214. doi: https://doi.org/10.1016/j.envres.2022.114142.

Lin, H. and Peddada, S. Das (2020) ‘Analysis of microbial compositions: a review of normalization and differential abundance analysis’, *npj Biofilms and Microbiomes*, 6(1). doi: 10.1038/s41522-020-00160-w.

Lipps, S. M. and Samac, D. A. (2022) ‘Pseudomonas viridiflava: An internal outsider of the Pseudomonas syringae species complex.’, *Molecular plant pathology*, 23(1), pp. 3–15. doi: 10.1111/mpp.13133.

Liu, W. and Yang, S. S. (2014) ‘Oceanobacillus aidingensis sp. nov., a moderately halophilic bacterium.’, *Antonie van Leeuwenhoek*. Netherlands, 105(5), pp. 801–808. doi: 10.1007/s10482-014-0128-1.

Liu, X. *et al.* (2020) ‘Pichia kudriavzevii retards fungal decay by influencing the fungal community succession during cherry tomato fruit storage’, *Food Microbiology*, 88. doi: https://doi.org/10.1016/j.fm.2019.103404.

Löber, S. *et al.* (2006) ‘Regulation of Salmonella pathogenicity island 2 genes by independent environmental signals’, *International Journal of Medical Microbiology*, 296(7), pp. 435–447. doi: https://doi.org/10.1016/j.ijmm.2006.05.001.

López-Goñi, I. *et al*. (1992) ‘Identification of 2,3-dihydroxybenzoic acid as a Brucella abortus siderophore.’, *Infection and immunity*. United States, 60(11), pp. 4496–4503. doi: 10.1128/iai.60.11.4496-4503.1992.

López, S. M. Y. *et al.* (2020) ‘The endosphere bacteriome of diseased and healthy tomato plants’, *Archives of Microbiology*, 202(10), pp. 2629–2642. doi: 10.1007/s00203-020-01987-9.

Loria, R. *et al.* (1997) ‘Plant Pathogenicity in the Genus Streptomyces.’, *Plant disease*. United States, 81(8), pp. 836–846. doi: 10.1094/PDIS.1997.81.8.836.

Love, M. I. *et al*. (2014) ‘Moderated estimation of fold change and dispersion for RNA-seq data with DESeq2’, *Genome Biology*, 15(12). doi: 10.1186/s13059-014-0550-8.

Luker, K. E. and Luker, G. D. (2009) ‘Real-time bioluminescence imaging of viral pathogenesis.’, *Methods in molecular biology (Clifton, N.J.)*. United States, 574, pp. 125–135. doi: 10.1007/978-1-60327-321-3_11.

Lyle, S. (2006) *Discovering Fruit & Nuts: A Comprehensive Guide to the Cultivation, Uses and Health Benefits of Over 300 Food-producing Plants*. 1st edn. Landlinks Press.

Macdonald, P. J. *et al*. (2012) ‘Chromophore maturation and fluorescence fluctuation spectroscopy of fluorescent proteins in a cell-free expression system.’, *Analytical biochemistry*. United States, 421(1), pp. 291–298. doi: 10.1016/j.ab.2011.10.040.

Martínez-Romero, D. *et al.* (2007) ‘Tools to maintain postharvest fruit and vegetable quality through the inhibition of ethylene action: a review.’, *Critical reviews in food science and nutrition*. United States, 47(6), pp. 543–560. doi: 10.1080/10408390600846390.

Martinez Arbizu, P. (2020) ‘pairwiseAdonis: Pairwise multilevel comparison using adonis.’

Maslowska, K. H. *et al*. (2019) ‘The SOS system: A complex and tightly regulated response to DNA damage.’, *Environmental and molecular mutagenesis*. United States, 60(4), pp. 368–384. doi: 10.1002/em.22267.

Matos, A. *et al*. (2005) ‘Effects of microbial community diversity on the survival of Pseudomonas aeruginosa in the wheat rhizosphere.’, *Microbial ecology*. United States, 49(2), pp. 257–264. doi: 10.1007/s00248-004-0179-3.

McKenna, S. M. and Davies, K. J. (1988) ‘The inhibition of bacterial growth by hypochlorous acid. Possible role in the bactericidal activity of phagocytes.’, *The Biochemical journal*, 254(3), pp. 685–692. doi: 10.1042/bj2540685.

McMurdie, P. J. and Holmes, S. (2013) ‘phyloseq: an R package for reproducible interactive analysis and graphics of microbiome census data.’, *PloS one*. United States, 8(4). doi: 10.1371/journal.pone.0061217.

Mehdy, M. C. (1994) ‘Active Oxygen Species in Plant Defense against Pathogens.’, *Plant physiology*, 105(2), pp. 467–472. doi: 10.1104/pp.105.2.467.

Mendoza-Suárez, M. A. *et al.* (2020) ‘Optimizing Rhizobium-legume symbioses by simultaneous measurement of rhizobial competitiveness and N(2) fixation in nodules.’, *Proceedings of the National Academy of Sciences of the United States of America*. United States, 117(18), pp. 9822–9831. doi: 10.1073/pnas.1921225117.

Meng, F. *et al*. (2013) ‘Salmonella colonization activates the plant immune system and benefits from association with plant pathogenic bacteria.’, *Environmental microbiology*. England, 15(9), pp. 2418–2430. doi: 10.1111/1462-2920.12113.

Mérida-Floriano, A. *et al*. (2021) ‘Genome-Wide Identification and Expression Analysis of SOS Response Genes in Salmonella enterica Serovar Typhimurium.’, *Cells*. Switzerland, 10(4). doi: 10.3390/cells10040943.

Meyer, A. J. *et al.* (2007) ‘Redox-sensitive GFP in Arabidopsis thaliana is a quantitative biosensor for the redox potential of the cellular glutathione redox buffer.’, *The Plant journal : for cell and molecular biology*. England, 52(5), pp. 973–986. doi: 10.1111/j.1365-313X.2007.03280.x.

Microbiological Advisory Committee on the Safety of Food (2005) *Information Paper ACM/745: Microbiological status of ready to eat fruit and vegetables*. Available at: https://acmsf.food.gov.uk/sites/default/files/mnt/drupal_data/sources/files/multimedia/pdfs/acm745amended.pdf.

Miller, V. L. and Mekalanos, J. J. (1988) ‘A novel suicide vector and its use in construction of insertion mutations: osmoregulation of outer membrane proteins and virulence determinants in Vibrio cholerae requires toxR.’, *Journal of bacteriology*, 170(6), pp. 2575–2583. doi: 10.1128/jb.170.6.2575-2583.1988.

Morimoto, K. *et al.* (2022) ‘Cysteine Reactivity Profiling to Unveil Redox Regulation in Phytopathogens.’, *Methods in molecular biology (Clifton, N.J.)*. United States, 2447, pp. 105–117. doi: 10.1007/978-1-0716-2079-3_9.

Morrissey, R. *et al*. (2013) ‘Shining light on food microbiology; applications of Lux-tagged microorganisms in the food industry’, *Trends in Food Science & Technology*, 32(1), pp. 4–15. doi: https://doi.org/10.1016/j.tifs.2013.05.001.

Mudd, J. B. *et al.* (1969) ‘Reaction of ozone with amino acids and proteins’, *Atmospheric Environment (1967)*, 3(6), pp. 669–681. doi: https://doi.org/10.1016/0004-6981(69)90024-9.

Mur, L. A. *et al*. (2005) ‘In planta measurements of oxidative bursts elicited by avirulent and virulent bacterial pathogens suggests that H2O2 is insufficient to elicit cell death in tobacco’, *Plant, Cell \& Environment*, 28(4), pp. 548–561. doi: https://doi.org/10.1111/j.1365-3040.2005.01301.x.

Do Nascimento Nunes, M. C. (2008) ‘Solanaceous and Other Fruit Vegetables’, in *Color Atlas of Postharvest Quality of Fruits and Vegetables*. John Wiley & Sons, Ltd, pp. 237–309. doi: 10.1002/9780813802947.ch5.

Nielsen, K. M. *et al.* (2007) ‘Release and persistence of extracellular DNA in the environment.’, *Environmental biosafety research*. France, 6(1–2), pp. 37–53. doi: 10.1051/ebr:2007031.

Nyhan, L. *et al.* (2020) ‘An evaluation of Lux technology as an alternative methodology to determine growth rates of Listeria in laboratory media and complex food matrices’, *International Journal of Food Microbiology*, 317. doi: https://doi.org/10.1016/j.ijfoodmicro.2019.108442.

O’Brien, J. A. *et al.* (2012) ‘Reactive oxygen species and their role in plant defence and cell wall metabolism.’, *Planta*. Germany, 236(3), pp. 765–779. doi: 10.1007/s00425-012-1696-9.

Oblessuc, P. R. *et al*. (2020) ‘Novel molecular components involved in callose-mediated Arabidopsis defense against Salmonella enterica and Escherichia coli O157:H7’, *BMC Plant Biology*, 20(1). doi: 10.1186/s12870-019-2232-x.

Okada, F. and Naya, K. (2012) ‘Electrolysis for Ozone Water Production’, in Linkov, V. and Kleperis, J. (eds) *Electrolysis*. IntechOpen. doi: 10.5772/51945.

Oksanen, J. *et al.* (2015) ‘Vegan: Community Ecology Package’, *R Package Version 2.2-1*, 2, pp. 1–2.

Oliver, J. C. *et al.* (2019) ‘Ozone against Pseudomonas aeruginosa biofilms in contact lenses storage cases’, *Journal of the Institute of Tropical Medicine of São Paulo*, 61, pp. 19–23.

Ölmez, H. and Temur, S. D. (2010) ‘Effects of different sanitizing treatments on biofilms and attachment of Escherichia coli and Listeria monocytogenes on green leaf lettuce’, *LWT - Food Science and Technology*, 43(6), pp. 964–970. doi: https://doi.org/10.1016/j.lwt.2010.02.005.

Omoregie, A. I. *et al.* (2019) ‘Low-cost cultivation of Sporosarcina pasteurii strain in food-grade yeast extract medium for microbially induced carbonate precipitation (MICP) application’, *Biocatalysis and Agricultural Biotechnology*, 17, pp. 247–255. doi: https://doi.org/10.1016/j.bcab.2018.11.030.

Ottesen, A. R. *et al.* (2013) ‘Baseline survey of the anatomical microbial ecology of an important food plant: Solanum lycopersicum (tomato).’, *BMC microbiology*, 13. doi: 10.1186/1471-2180-13-114.

Panebianco, F. *et al.* (2021) ‘Effect of Gaseous Ozone on Listeria monocytogenes Planktonic Cells and Biofilm: An In Vitro Study’, *Foods*, 10(7). doi: 10.3390/foods10071484.

Pappas, G. (2014) ‘Bacteria: Brucella’, in Motarjemi, Y. (ed.) *Encyclopedia of Food Safety*. Waltham: Academic Press, pp. 364–368. doi: https://doi.org/10.1016/B978-0-12-378612-8.00088-3.

Parada, A. E. *et al*. (2016) ‘Every base matters: assessing small subunit rRNA primers for marine microbiomes with mock communities, time series and global field samples.’, *Environmental microbiology*. England, 18(5), pp. 1403–1414. doi: 10.1111/1462-2920.13023.

Parnell, T. L. *et al*. (2004) *Tomatoes: Safe Methods to Store, Preserve, and Enjoy*.

Parte, A. C. *et al.* (2020) ‘List of Prokaryotic names with Standing in Nomenclature (LPSN) moves to the DSMZ.’, *International journal of systematic and evolutionary microbiology*. England, 70(11), pp. 5607–5612. doi: 10.1099/ijsem.0.004332.

Patil, S. *et al.* (2011) ‘Assessing the microbial oxidative stress mechanism of ozone treatment through the responses of Escherichia coli mutants.’, *Journal of applied microbiology*. England, 111(1), pp. 136–144. doi: 10.1111/j.1365-2672.2011.05021.x.

Peleg, A. Y. *et al*. (2010) ‘Medically important bacterial–fungal interactions’, *Nature Reviews Microbiology*, 8(5), pp. 340–349. doi: 10.1038/nrmicro2313.

Penetrante, B. M. *et al*. (1997) ‘Kinetic Analysis of Non-Thermal Plasmas Used for Pollution Control’, *Japanese Journal of Applied Physics*, 36(7S). doi: 10.1143/JJAP.36.5007.

Pitt, J. I. and Hocking, A. D. (2022) ‘Fresh and Perishable Foods’, in *Fungi and Food Spoilage*. 4th edn. Springer Link, pp. 505–536.

de Poel, B. *et al.* (2012) ‘Targeted Systems Biology Profiling of Tomato Fruit Reveals Coordination of the Yang Cycle and a Distinct Regulation of Ethylene Biosynthesis during Postclimacteric Ripening ’, *Plant Physiology*, 160(3), pp. 1498–1514. doi: 10.1104/pp.112.206086.

Potts, H. E. and Diver, D. A. (2012) ‘Plasma decontamination of sealed packages’, in *IEEE International Conference on Plasma Science*. doi: 10.1109/PLASMA.2012.6383484.

Preston, G. M. (2000) ‘Pseudomonas syringae pv. tomato: the right pathogen, of the right plant, at the right time’, *Molecular Plant Pathology*, 1(5), pp. 263–275. doi: 10.1046/j.1364-3703.2000.00036.x.

Pryor, W. A. *et al*. (1991) ‘The ozonation of unsaturated fatty acids: aldehydes and hydrogen peroxide as products and possible mediators of ozone toxicity.’, *Chemical research in toxicology*. United States, 4(3), pp. 341–348. doi: 10.1021/tx00021a014.

Qian, Y.-F. *et al.* (2022) 'Effects of gaseous ozone treatment on the quality and microbial community of salmon (Salmo salar) during cold storage', *Food Control*, 142. doi: https://doi.org/10.1016/j.foodcont.2022.109217.

Quast, C. *et al.* (2013) 'The SILVA ribosomal RNA gene database project: improved data processing and web-based tools.', *Nucleic acids research*. England, 41(Database issue), pp. D590-6. doi: 10.1093/nar/gks1219.

Quinet, M. *et al.* (2019) 'Tomato Fruit Development and Metabolism', *Frontiers in Plant Science*, 10. doi: 10.3389/fpls.2019.01554.

Quinn, T. P. *et al.* (2018) 'Understanding sequencing data as compositions: an outlook and review', *Bioinformatics*, 34(16), pp. 2870–2878. doi: 10.1093/bioinformatics/bty175.

R Core Team (2023) 'R: A Language and Environment for Statistical Computing'. Vienna, Austria. Available at: https://www.r-project.org/.

Rahman, M. *et al.* (2023) 'Hydrogen Peroxide Measurement Can Be Used to Monitor Plant Oxidative Stress Rapidly Using Modified Ferrous Oxidation Xylenol Orange and Titanium Sulfate Assay Correlation', *International Journal of Plant Biology*, 14(3), pp. 546–557. doi: 10.3390/ijpb14030043.

Raja, V. *et al.* (2017) 'Abiotic stress: Interplay between ROS, hormones and MAPKs', *Environmental and Experimental Botany*, 137, pp. 142–157. doi: https://doi.org/10.1016/j.envexpbot.2017.02.010.

Ramos, B. *et al.* (2013) 'Fresh fruits and vegetables—An overview on applied methodologies to improve its quality and safety', *Innovative Food Science & Emerging Technologies*, 20, pp. 1–15. doi: https://doi.org/10.1016/j.ifset.2013.07.002.

Rangel, K. *et al.* (2021) 'Detrimental Effect of Ozone on Pathogenic Bacteria.', *Microorganisms*. Switzerland, 10(1). doi: 10.3390/microorganisms10010040.

Regué, M. *et al.* (2004) 'A gene, uge, is essential for Klebsiella pneumoniae virulence.', *Infection and immunity*. United States, 72(1), pp. 54–61. doi: 10.1128/IAI.72.1.54-61.2004.

Reinecke, F. *et al.* (2000) 'Isolation and characterization of an Achromobacter xylosoxidans strain B3 and other bacteria capable to degrade the synthetic chelating agent iminodisuccinate', *FEMS Microbiology Letters*, 188(1), pp. 41–46. doi: 10.1111/j.1574-6968.2000.tb09166.x.

Rest, R. F. and Robertson, D. C. (1975) 'Characterization of the electron transport system in Brucella abortus.', *Journal of bacteriology*. United States, 122(1), pp. 139–144. doi: 10.1128/jb.122.1.139-144.1975.

Riahi, H. S. *et al*. (2022) 'Genus Pseudonocardia: What we know about its biological properties, abilities and current application in biotechnology', *Journal of Applied Microbiology*, 132(2), pp. 890–906. doi: 10.1111/jam.15271.

Ricci, V. *et al*. (2012) 'Regulation of RamA by RamR in Salmonella enterica serovar Typhimurium: isolation of a RamR superrepressor.', *Antimicrobial agents and chemotherapy*, 56(11), pp. 6037–6040. doi: 10.1128/AAC.01320-12.

Rico, D. *et al.* (2007) 'Extending and measuring the quality of fresh-cut fruit and vegetables: a review', *Trends in Food Science & Technology*, 18(7), pp. 373–386. doi: https://doi.org/10.1016/j.tifs.2007.03.011.

Rijk Zwaan (2021) *Brioso RZ F1*. Available at: https://www.rijkzwaanusa.com/sites/default/files/varieties/SL11061_Brioso %2872-130%29 leaflet 2021.pdf.

Riviere, E. *et al.* (2012) 'Pulmonary streptomyces infection in patient with sarcoidosis, France, 2012.', *Emerging infectious diseases*. United States, pp. 1907–1909. doi: 10.3201/eid1811.120797.

Robbe-Saule, V. *et al.* (2001) 'Identification of a non-haem catalase in Salmonella and its regulation by RpoS (sigmaS).', *Molecular microbiology*. England, 39(6), pp. 1533–1545. doi: 10.1046/j.1365-2958.2001.02340.x.

Roberts, R. *et al.* (2019) 'Natural variation for unusual host responses and flagellin-mediated immunity against Pseudomonas syringae in genetically diverse tomato accessions', *New Phytologist*, 223(1), pp. 447–461. doi: 10.1111/nph.15788.

Robinson, M. D. and Oshlack, A. (2010) 'A scaling normalization method for differential expression analysis of RNA-seq data', *Genome Biology*, 11(3). doi: 10.1186/gb-2010-11-3-r25.

Rodrigues, M. H. P. and Furlong, E. B. (2022) 'Fungal diseases and natural defense mechanisms of tomatoes (Solanum lycopersicum): A review', *Physiological and Molecular Plant Pathology*, 122. doi: https://doi.org/10.1016/j.pmpp.2022.101906.

Rodríguez-Rojas, A. *et al.* (2020) 'Non-lethal exposure to H2O2 boosts bacterial survival and evolvability against oxidative stress', *PLOS Genetics*. Public Library of Science, 16(3), pp. 1–33. doi: 10.1371/journal.pgen.1008649.

Roldán, M. *et al.* (2013) 'Chalicogloea cavernicola gen. nov., sp. nov. (Chroococcales, Cyanobacteria), from low-light aerophytic environments: combined molecular, phenotypic and ecological criteria.', *International journal of systematic and evolutionary microbiology*. England, 63(Pt 6), pp. 2326–2333. doi: 10.1099/ijs.0.045468-0.

Rolfe, M. D. *et al.* (2012) 'Lag phase is a distinct growth phase that prepares bacteria for exponential growth and involves transient metal accumulation.', *Journal of bacteriology*. United States, 194(3), pp. 686–701. doi: 10.1128/JB.06112-11.

Romsang, A. *et al.* (2015) 'Pseudomonas aeruginosa IscR-Regulated Ferredoxin NADP(+) Reductase Gene (fprB) Functions in Iron-Sulfur Cluster Biogenesis and Multiple Stress Response', *PLOS ONE*. Public Library of Science, 10(7), pp. 1–23. doi: 10.1371/journal.pone.0134374.

Roux, V. *et al.* (2013) 'Non-contiguous finished genome sequence and description of Oceanobacillus massiliensis sp. nov.', *Standards in genomic sciences*. England, 9(2), pp. 370–384. doi: 10.4056/sigs.4267953.

Rowe, M. T. (2014) 'BRUCELLA | Problems with Dairy Products', in Batt, C. A. and Tortorello, M. Lou (eds) *Encyclopedia of Food Microbiology (Second Edition)*. Second Edi. Oxford: Academic Press, pp. 340–343. doi: https://doi.org/10.1016/B978-0-12-384730-0.00050-1.

Rowlinson, M.-C. *et al.* (2006) 'Clearance of Cellulosimicrobium cellulans bacteremia in a child without central venous catheter removal.', *Journal of clinical microbiology*. United States, 44(7), pp. 2650–2654. doi: 10.1128/JCM.02485-05.

Ruiz-Cruz, S. *et al.* (2007) 'Efficacy of sanitizers in reducing Escherichia coli O157:H7, Salmonella spp. and Listeria monocytogenes populations on fresh-cut carrots', *Food Control*, 18(11), pp. 1383–1390. doi: https://doi.org/10.1016/j.foodcont.2006.09.008.

Ryan, M. P. and Pembroke, J. T. (2018) ‘Brevundimonas spp: Emerging global opportunistic pathogens.’, *Virulence*. United States, 9(1), pp. 480–493. doi: 10.1080/21505594.2017.1419116.

Ryan, R. P. *et al.* (2009) ‘The versatility and adaptation of bacteria from the genus Stenotrophomonas’, *Nature Reviews Microbiology*, 7(7), pp. 514–525. doi: 10.1038/nrmicro2163.

Samson, R. *et al.* (2005) ‘Transfer of Pectobacterium chrysanthemi (Burkholder et al. 1953) Brenner et al. 1973 and Brenneria paradisiaca to the genus Dickeya gen. nov. as Dickeya chrysanthemi comb. nov. and Dickeya paradisiaca comb. nov. and delineation of four novel species, Dick’, *International Journal of Systematic and Evolutionary Microbiology*. Microbiology Society, 55(4), pp. 1415–1427. doi: https://doi.org/10.1099/ijs.0.02791-0.

Sarron, E. *et al*. (2021) ‘Ozone Treatments for Preserving Fresh Vegetables Quality: A Critical Review.’, *Foods (Basel, Switzerland)*, 10(3). doi: 10.3390/foods10030605.

Schäfer, A. *et al.* (1994) ‘Small mobilizable multi-purpose cloning vectors derived from the Escherichia coli plasmids pK18 and pK19: selection of defined deletions in the chromosome of Corynebacterium glutamicum.’, *Gene*. Netherlands, 145(1), pp. 69–73. doi: 10.1016/0378-1119(94)90324-7.

Schwarzländer, M. *et al.* (2008) ‘Confocal imaging of glutathione redox potential in living plant cells’, in *Journal of Microscopy*, pp. 299–316. doi: 10.1111/j.1365-2818.2008.02030.x.

La Scola, B. *et al.* (1998) ‘Massilia timonae gen. nov., sp. nov., isolated from blood of an immunocompromised patient with cerebellar lesions.’, *Journal of clinical microbiology*. United States, 36(10), pp. 2847–2852. doi: 10.1128/JCM.36.10.2847-2852.1998.

Scott, D. B. and Lesher, E. C. (1963) ‘Effect of ozone on survival and permeability of E. coli.’, *Journal of bacteriology*, 85(3), pp. 567–576. doi: 10.1002/path.1700850242.

Selma, M. V. *et al.* (2006) ‘Effect of ozone on the inactivation of Yersinia enterocolitica and the reduction of natural flora on potatoes.’, *Journal of food protection*. United States, 69(10), pp. 2357–2363.

Selma, M. V. *et al.* (2007) ‘Elimination by ozone of Shigella sonnei in shredded lettuce and water.’, *Food microbiology*. England, 24(5), pp. 492–499. doi: 10.1016/j.fm.2006.09.005.

Selvarajan, E. *et al*. (2018) ‘Polyphenol Oxidase, Beyond Enzyme Browning’, in Singh, J. et al. (eds) *Microbial Bioprospecting for Sustainable Development*. Singapore: Springer Singapore, pp. 203–222. doi: 10.1007/978-981-13-0053-0_10.

Sen, A. and Imlay, J. A. (2021) ‘How Microbes Defend Themselves From Incoming Hydrogen Peroxide’, *Frontiers in Immunology*, 12. doi: 10.3389/fimmu.2021.667343.

Seo, S. W. *et al.* (2015) ‘Genome-wide Reconstruction of OxyR and SoxRS Transcriptional Regulatory Networks under Oxidative Stress in Escherichia coli K-12 MG1655.’, *Cell reports*. United States, 12(8), pp. 1289–1299. doi: 10.1016/j.celrep.2015.07.043.

Shannon, C. E. (1948) ‘A Mathematical Theory of Communication’, *Bell System Technical Journal*, 27(3), pp. 379–423. doi: https://doi.org/10.1002/j.1538-7305.1948.tb01338.x.

Sharma, V. K. and Graham, N. J. D. (2010) 'Oxidation of Amino Acids, Peptides and Proteins by Ozone: A Review', *Ozone: Science & Engineering*. Taylor & Francis, 32(2), pp. 81–90. doi: 10.1080/01919510903510507.

Shenge, K. C. *et al.* (2007) 'First Report of Bacterial Speck of Tomato Caused by Pseudomonas syringae pv. tomato in Tanzania', *Plant Disease*, 91(4). doi: 10.1094/PDIS-91-4-0462C.

Shepherd, M. D. *et al.* (2010) 'Laboratory maintenance of Streptomyces species.', *Current protocols in microbiology*. United States, Chapter 10. doi: 10.1002/9780471729259.mc10e01s18.

Shi, Y. *et al.* (2022) 'Aureobasidium pullulans S-2 reduced the disease incidence of tomato by influencing the postharvest microbiome during storage', *Postharvest Biology and Technology*, 185. doi: https://doi.org/10.1016/j.postharvbio.2021.111809.

Shields, H. J., Traa, A. and Van Raamsdonk, J. M. (2021) 'Beneficial and Detrimental Effects of Reactive Oxygen Species on Lifespan: A Comprehensive Review of Comparative and Experimental Studies.', *Frontiers in cell and developmental biology*. Switzerland, 9. doi: 10.3389/fcell.2021.628157.

Simmons, L. A. *et al.* (2008) 'The SOS Regulatory Network.', *EcoSal Plus*, 2008. doi: 10.1128/ecosalplus.5.4.3.

Singh, N. *et al.* (2002) 'Efficacy of Chlorine Dioxide, Ozone, and Thyme Essential Oil or a Sequential Washing in Killing Escherichia coli O157:H7 on Lettuce and Baby Carrots', *LWT*, 35(8), pp. 720–729. doi: https://doi.org/10.1006/fstl.2002.0933.

Singh, P., Hung, Y.-C. and Qi, H. (2018) 'Efficacy of Peracetic Acid in Inactivating Foodborne Pathogens on Fresh Produce Surface.', *Journal of food science*. United States, 83(2), pp. 432–439. doi: 10.1111/1750-3841.14028.

Sinha, S. R. *et al.* (2019) 'Post-harvest assessment of fruit quality and shelf life of two elite tomato varieties cultivated in Bangladesh', *Bulletin of the National Research Centre*, 43(1). doi: 10.1186/s42269-019-0232-5.

Small, D. A. *et al.* (2007) 'Comparative global transcription analysis of sodium hypochlorite, peracetic acid, and hydrogen peroxide on Pseudomonas aeruginosa.', *Applied microbiology and biotechnology*. Germany, 76(5), pp. 1093–1105. doi: 10.1007/s00253-007-1072-z.

Smid, E. J. *et al.* (1996) 'Surface disinfection of tomatoes using the natural plant compound trans-cinnamaldehyde', *Postharvest Biology and Technology*, 9(3), pp. 343–350. doi: https://doi.org/10.1016/S0925-5214(96)00033-6.

Soldan, R. *et al.* (2021) 'From macro to micro: a combined bioluminescence-fluorescence approach to monitor bacterial localization.', *Environmental microbiology*, 23(4), pp. 2070–2085. doi: 10.1111/1462-2920.15296.

Solmi, L. *et al.* (2023) 'Polyamine-mediated mechanisms contribute to oxidative stress tolerance in Pseudomonas syringae', *Scientific Reports*, 13(1). doi: 10.1038/s41598-023-31239-x.

Soo, R. M. *et al.* (2015) 'Back from the dead; the curious tale of the predatory cyanobacterium Vampirovibrio chlorellavorus.', *PeerJ*. United States, 3. doi: 10.7717/peerj.968.

Soto-Giron, M. J. *et al.* (2021) 'The Edible Plant Microbiome represents a diverse genetic reservoir with functional potential in the human host', *Scientific Reports*, 11(1). doi: 10.1038/s41598-021-03334-4.

de Souza, L. P. *et al.* (2018) 'Ozone treatment for pesticide removal from carrots: Optimization by response surface methodology', *Food Chemistry*, 243, pp. 435–441. doi: https://doi.org/10.1016/j.foodchem.2017.09.134.

van der Straaten, T. *et al.* (2004) 'Salmonella enterica serovar Typhimurium RamA, intracellular oxidative stress response, and bacterial virulence.', *Infection and immunity*, 72(2), pp. 996–1003. doi: 10.1128/IAI.72.2.996-1003.2004.

Sunberg, R. J. (1986) 'A simple procedure to convert parts per million (ppm) to molarity (m)', *Journal of Chemical Education*, 63(8). doi: 10.1021/ed063p714.

Suslow, T. V (2004) *Ozone applications for postharvest disinfection of edible horticultural crops*. Available at: https://anrcatalog.ucanr.edu/pdf/8133.pdf.

Syromyatnikov, M. Y. *et al.* (2022) 'High-Throughput Sequencing as a Tool for the Quality Control of Microbial Bioformulations for Agriculture', *Processes*, 10(11). doi: 10.3390/pr10112243.

The Food and Agricultural Organisation of the United Nations and The World Health Organisation (2008) *Microbiological hazards in fresh leafy vegetables and herbs meeting report*. Available at: https://www.fao.org/3/i0452e/i0452e.pdf.

Torlak, E. *et al*. (2013) 'Efficacy of gaseous ozone against Salmonella and microbial population on dried oregano.', *International journal of food microbiology*. Netherlands, 165(3), pp. 276–280. doi: 10.1016/j.ijfoodmicro.2013.05.030.

Torres, M. A. *et al*. (2006) 'Reactive oxygen species signaling in response to pathogens.', *Plant physiology*, 141(2), pp. 373–378. doi: 10.1104/pp.106.079467.

Toth, I. K. *et al.* (2011) 'Dickeya species: an emerging problem for potato production in Europe', *Plant Pathology*, 60(3), pp. 385–399. doi: https://doi.org/10.1111/j.1365-3059.2011.02427.x.

Tournas, V. H. (2005) 'Spoilage of Vegetable Crops by Bacteria and Fungi and Related Health Hazards', *Critical Reviews in Microbiology*. Taylor & Francis, 31(1), pp. 33–44. doi: 10.1080/10408410590886024.

Tzortzakis, N. and Chrysargyris, A. (2017) 'Postharvest ozone application for the preservation of fruits and vegetables', *Food Reviews International*. Taylor & Francis, 33(3), pp. 270–315. doi: 10.1080/87559129.2016.1175015.

Tzortzakis, N. *et al*. (2008) 'Impact of low-level atmospheric ozone-enrichment on black spot and anthracnose rot of tomato fruit', *Postharvest Biology and Technology*, 47(1), pp. 1–9. doi: https://doi.org/10.1016/j.postharvbio.2007.06.004.

U.S. Food and Drug Administration (1999) *CFR - Code of Federal Regulations Title 21*. Available at: https://www.accessdata.fda.gov/scripts/cdrh/cfdocs/cfcfr/cfrsearch.cfm?fr=173.315.

U.S. Food and Drug Administration (2012) *Bad Bug Book*. 2nd edn. Edited by K. A. Lampel, S. Al-Khaldi, and S. M. Cahill. Center for Food Safety and Applied Nutrition (CFSAN) of the Food and Drug Administration (FDA), U.S. Department of Health and Human Services.

Ukuku, D. O. *et al.* (2022) ‘Strength of Salmonella attachment on apple and tomato surfaces: Effect of antimicrobial treatments on population reduction and inactivation’, *LWT*, 164. doi: https://doi.org/10.1016/j.lwt.2022.113605.

Uppalapati, S. R. and Vazquez-Torres, A. (2022) ‘Manganese Utilization in Salmonella Pathogenesis: Beyond the Canonical Antioxidant Response’, *Frontiers in Cell and Developmental Biology*, 10. doi: 10.3389/fcell.2022.924925.

Urakami, T. *et al.* (1995) ‘Characterization and Description of Hyphomicrobium denitrificans sp. nov.’, *International Journal of Systematic and Evolutionary Microbiology*. Microbiology Society, 45(3), pp. 528–532. doi: https://doi.org/10.1099/00207713-45-3-528.

Vainonen, J. P. and Kangasjarvi, J. (2015) ‘Plant signalling in acute ozone exposure’, *Plant, Cell \& Environment*, 38(2), pp. 240–252. doi: https://doi.org/10.1111/pce.12273.

Vaishampayan, A. and Grohmann, E. (2021) ‘Antimicrobials Functioning through ROS-Mediated Mechanisms: Current Insights.’, *Microorganisms*. Switzerland, 10(1). doi: 10.3390/microorganisms10010061.

Vandekinderen, I. *et al.* (2009) ‘Optimization and evaluation of a decontamination step with peroxyacetic acid for fresh-cut produce’, *Food Microbiology*, 26(8), pp. 882–888. doi: https://doi.org/10.1016/j.fm.2009.06.004.

Vassallo, A. *et al.* (2023) ‘Adaptation of Commensal Escherichia coli in Tomato Fruits: Motility, Stress, Virulence.’, *Biology*. Switzerland, 12(4). doi: 10.3390/biology12040633.

Veluchamy, S. *et al.* (2014) ‘Natural Variation for Responsiveness to flg22, flgII-28, and csp22 and Pseudomonas syringae pv. tomato in Heirloom Tomatoes’, *PLOS ONE*. Public Library of Science, 9(9), pp. 1–12. doi: 10.1371/journal.pone.0106119.

Vevea, J. D. *et al.* (2013) ‘Ratiometric biosensors that measure mitochondrial redox state and ATP in living yeast cells.’, *Journal of visualized experiments : JoVE*. United States, (77). doi: 10.3791/50633.

Victorin, K. (1992) ‘Review of the genotoxicity of ozone.’, *Mutation research*. Netherlands, 277(3), pp. 221–238.

Vos, P. *et al.* (2009) ‘Volume 3: The Firmicutes’, in *Bergey’s Manual of Systematic Bacteriology*. Springer Link.

Wagner, B. D. *et al*. (2011) ‘Application of Two-Part Statistics for Comparison of Sequence Variant Counts’, *PLOS ONE*. Public Library of Science, 6(5), pp. 1–8. doi: 10.1371/journal.pone.0020296.

Wang, J. *et al.* (2023) ‘The Impact of Storage Temperature on the Development of Microbial Communities on the Surface of Blueberry Fruit’, *Foods*, 12(8). doi: 10.3390/foods12081611.

Wang, R. Y. *et al.* (2023) ‘Chlorine and peroxyacetic acid inactivation of Listeria monocytogenes in simulated apple dump tank water’, *Food Control*, 144. doi: https://doi.org/10.1016/j.foodcont.2022.109314.

Wani, S. *et al.* (2015) ‘Effect of Ozone Treatment on Inactivation of Escherichia coli and Listeria sp. on Spinach’, *Agriculture*, 5, pp. 155–169. doi: 10.3390/agriculture5020155.

Wani, S. *et al*. (2016) ‘Investigation of potential reasons for bacterial survival on “ready-to-eat” leafy produce during exposure to gaseous ozone’, *Postharvest Biology and Technology*, 111, pp. 185–190. doi: https://doi.org/10.1016/j.postharvbio.2015.08.007.

Waśkiewicz, A. and Irzykowska, L. (2014) ‘Flavobacterium spp. – Characteristics, Occurrence, and Toxicity’, in Batt, C. A. and Tortorello, M. Lou (eds) *Encyclopedia of Food Microbiology (Second Edition)*. Second Edi. Oxford: Academic Press, pp. 938–942. doi: https://doi.org/10.1016/B978-0-12-384730-0.00126-9.

Watson, J. A. and Schubert, J. (1969) ‘Action of Hydrogen Peroxide on Growth Inhibition of Salmonella typhimurium’, *Journal of General Microbiology*. Microbiology Society, 57(1), pp. 25–34. doi: 10.1099/00221287-57-1-25.

Weerapana, E. *et al.* (2010) ‘Quantitative reactivity profiling predicts functional cysteines in proteomes.’, *Nature*. England, 468(7325), pp. 790–795. doi: 10.1038/nature09472.

Wei, H.-L. *et al*. (2018) ‘Modular Study of the Type III Effector Repertoire in Pseudomonas syringae pv. tomato DC3000 Reveals a Matrix of Effector Interplay in Pathogenesis.’, *Cell reports*. United States, 23(6), pp. 1630–1638. doi: 10.1016/j.celrep.2018.04.037.

Weinstein-Fischer, D. *et al*. (2000) ‘Escherichia coli response to hydrogen peroxide: a role for DNA supercoiling, topoisomerase I and Fis.’, *Molecular microbiology*. England, 35(6), pp. 1413–1420. doi: 10.1046/j.1365-2958.2000.01805.x.

Westover, C. *et al.* (2022) ‘Ozone Disinfection for Elimination of Bacteria and Degradation of SARS-CoV2 RNA for Medical Environments.’, *Genes*. Switzerland, 14(1). doi: 10.3390/genes14010085.

Whitehead, J. C. (2016) ‘Chapter 3 - The Chemistry of Cold Plasma’, in Misra, N. N., Schlüter, O., and Cullen, P. J. (eds) *Cold Plasma in Food and Agriculture*. San Diego: Academic Press, pp. 53–81. doi: https://doi.org/10.1016/B978-0-12-801365-6.00003-2.

Wickham, H. (2016) *ggplot2: Elegant Graphics for Data Analysis*. Springer-Verlag New York. Available at: https://ggplot2.tidyverse.org.

Willis, A. D. (2019) ‘Rarefaction, Alpha Diversity, and Statistics’, *Frontiers in Microbiology*, 10. doi: 10.3389/fmicb.2019.02407.

Wright, K. M. *et al.* (2017) ‘Differences in internalization and growth of Escherichia coli O157:H7 within the apoplast of edible plants, spinach and lettuce, compared with the model species Nicotiana benthamiana.’, *Microbial biotechnology*. United States, 10(3), pp. 555–569. doi: 10.1111/1751-7915.12596.

Wu, L. *et al.* (2014) ‘Go in for the kill: How plants deploy effector-triggered immunity to combat pathogens. [Corrected].’, *Virulence*, 5(7), pp. 710–721. doi: 10.4161/viru.29755.

Wu, Y.-R. and He, J. (2015) ‘Characterization of a xylanase-producing Cellvibrio mixtus strain J3-8 and its genome analysis’, *Scientific Reports*, 5(1). doi: 10.1038/srep10521.

Xin, X.-F. and He, S. Y. (2013) ‘Pseudomonas syringae pv. tomato DC3000: A Model Pathogen for Probing Disease Susceptibility and Hormone Signaling in Plants’, *Annual Review of Phytopathology*, 51(1), pp. 473–498. doi: 10.1146/annurev-phyto-082712-102321.

Youssef, K. *et al.* (2023) ‘Editorial: Advances in detection and control of post-harvest pathogens’, *Frontiers in Microbiology*, 14. doi: 10.3389/fmicb.2023.1184039.

Yu, Z. *et al.* (2023) ‘Phylogenetic Conservation of Soil Microbial Responses to Elevated Tropospheric Ozone and Nitrogen Fertilization.’, *mSystems*. United States, 8(1). doi: 10.1128/msystems.00721-22.

Zhang, C. *et al.* (2019) ‘Inhibition of regrowth of planktonic and biofilm bacteria after peracetic acid disinfection’, *Water Research*, 149, pp. 640–649. doi: https://doi.org/10.1016/j.watres.2018.10.062.

Zhang, J. *et al.* (2019) ‘Effects of elevated ground-level ozone on paddy soil bacterial community and assembly mechanisms across four years.’, *The Science of the total environment*. Netherlands, 654, pp. 505–513. doi: 10.1016/j.scitotenv.2018.11.130.

Zhang, K. *et al.* (2023) ‘Microbial community dynamics responding to nutrient allocation associated with soybean cultivar “Jake” ozone adaptation’, *Science of The Total Environment*, 864. doi: https://doi.org/10.1016/j.scitotenv.2022.161008.

Zhang, X.-H. *et al.* (2021) ‘Viable but nonculturable bacteria and their resuscitation: implications for cultivating uncultured marine microorganisms’, *Marine Life Science & Technology*, 3(2), pp. 189–203. doi: 10.1007/s42995-020-00041-3.

Zhang, Y. *et al.* (2015) ‘Effects of ozone on the cytomembrane and ultrastructure of Pseudomonas aeruginosa’, *Food Science and Biotechnology*, 24(3), pp. 987–993. doi: 10.1007/s10068-015-0126-8.

Zhang, Y. *et al.* (2018) ‘Petrol and diesel exhaust particles accelerate the horizontal transfer of plasmid-mediated antimicrobial resistance genes’, *Environment International*, 114, pp. 280–287. doi: https://doi.org/10.1016/j.envint.2018.02.038.

Zhang, Y. *et al.* (2022) ‘Ozone reduces the fruit decay of postharvest winter jujube by altering the microbial community structure on fruit surface’, *Microbiological Research*, 262. doi: https://doi.org/10.1016/j.micres.2022.127110.

Zhang, Y. Q. *et al.* (2011) ‘Effects of ozone on membrane permeability and ultrastructure in Pseudomonas aeruginosa.’, *Journal of applied microbiology*. England, 111(4), pp. 1006–1015. doi: 10.1111/j.1365-2672.2011.05113.x.

Zhao, X. *et al.* (2008) ‘Preparation of Peracetic Acid from Acetic Acid and Hydrogen Peroxide: Experimentation and Modeling’, *The Chinese Journal of Process Engineering*, 8, pp. 35–41.

Zhao, X. *et al.* (2017) ‘Current Perspectives on Viable but Non-culturable State in Foodborne Pathogens.’, *Frontiers in microbiology*, 8. doi: 10.3389/fmicb.2017.00580.

Zheng, J. *et al.* (2011) ‘Differential Gene Expression by RamA in Ciprofloxacin-Resistant Salmonella Typhimurium’, *PLOS ONE*. Public Library of Science, 6(7), pp. 1–8. doi: 10.1371/journal.pone.0022161.

Zheng, J. *et al.* (2017) ‘Microbial ecology of fresh vegetables’, in *Quantitative Microbiology in Food Processing*. John Wiley & Sons, Ltd, pp. 339–357. doi: https://doi.org/10.1002/9781118823071.ch17.

Zheng, M. *et al.* (2001) ‘DNA microarray-mediated transcriptional profiling of the Escherichia coli response to hydrogen peroxide.’, *Journal of bacteriology*. United States, 183(15), pp. 4562–4570. doi: 10.1128/JB.183.15.4562-4570.2001.

Appendices

Appendix 1

Appendix 1.1: Ozone concentrations generated by the in-pack ozone system which was assigned serial number 6

Treatment time (secs)	Calibration number	Peak ozone concentration detected in punnet (ppm)
Before treating *E. coli* JHI-5025 with ozone (figure 2.4)		
1	1	345.3
1	2	108.0
1	3	149.3
1	4	109.0
1	5	316.6
3	1	625.0
3	2	544.6
3	3	469.1
3	4	501.2
3	5	600.2
Before treating Pst DC3000 with ozone (figure 2.5)		
1	1	183.8
1	2	73.5
1	3	14.5
1	4	117.7
1	5	37.5
3	1	637.1
3	2	562.7
3	3	573.7
3	4	634.3
3	5	474.6
Before treating Pst T1 with ozone (figure 2.5)		
1	1	95.3
1	2	263.2
1	3	14.7
1	4	266.5
1	5	81
3	1	278.4
3	2	68.6
3	3	560.6
3	4	679.7
3	5	31.6
Before testing for the effect of ozone on the tomato calyx and pedicel culturable microbiota (figure 2.6)		
3	1	630.7
3	2	677.4
3	3	580.5
3	4	421.2
3	5	608.1
Before testing for the effect of ozone on the tomato calyx and pedicel bacterial community (figures 2.7 - 2.17): tomato collection date 1		
3	1	493.8
3	2	401.5

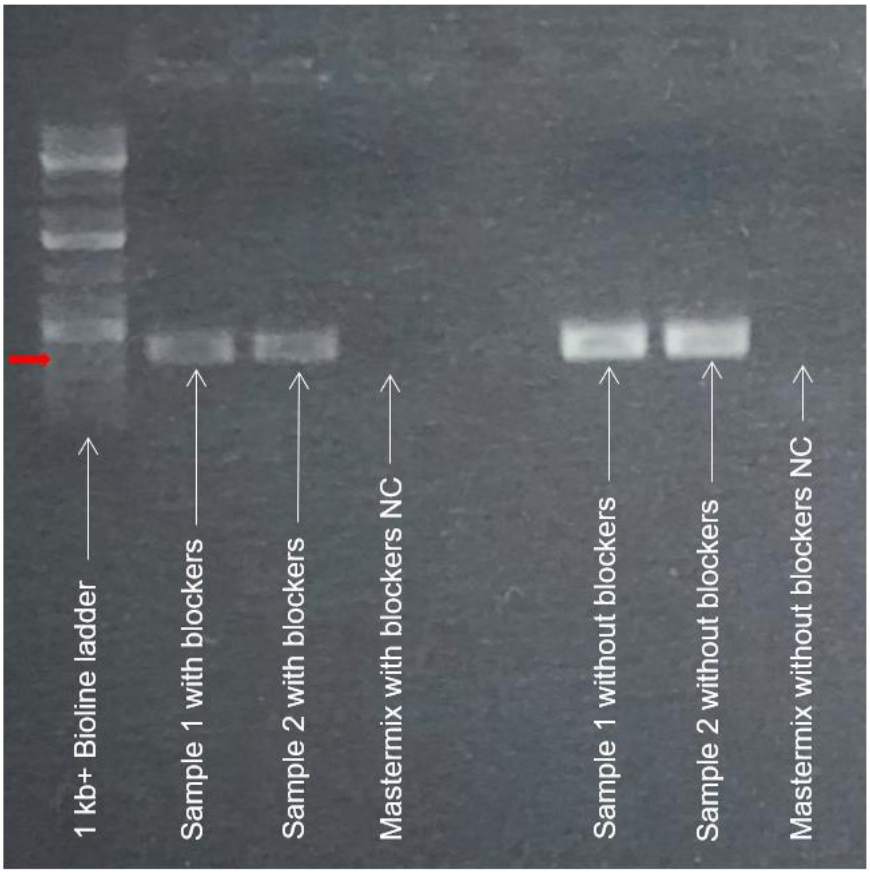
3	3	345.2
3	4	424.9
3	5	255.8
Before testing for the effect of ozone on the tomato calyx and pedicel bacterial community (figures 2.7 - 2.17): tomato collection date 2		
3	1	619.5
3	2	302.4
3	3	111.1
3	4	482.9
3	5	315
Before testing for the effect of ozone on the tomato calyx and pedicel bacterial community (figures 2.7 - 2.17): tomato collection date 3		
3	1	682.4
3	2	692.7
3	3	407.6
3	4	602.5
3	5	643.2
Before testing for the effect of ozone on the tomato calyx and pedicel bacterial community (figures 2.7 - 2.17): tomato collection date 4		
3	1	758.3
3	2	543.7
3	3	280.7
3	4	482.6
3	5	623.1
Before testing for the effect of ozone on the tomato calyx and pedicel bacterial community (figures 2.7 - 2.17): tomato collection date 5		
3	1	707.5
3	2	702.6
3	3	333.4
3	4	320.8
3	5	239
Before testing for the effect of ozone on the tomato calyx and pedicel bacterial community (figures 2.7 - 2.17): tomato collection date 6		
3	1	298.7
3	2	251.5
3	3	223.6
3	4	221.2
3	5	222.7
Before testing for the effect of ozone on the tomato calyx and pedicel bacterial community (figures 2.7 - 2.17): tomato collection date 7		
3	1	487.5
3	2	460.4
3	3	626.9
3	4	572.2
3	5	579.7

Table rows highlighted in red indicate cases where much lower ozone concentrations were generated than was expected for the treatment time. This was due to issues with the in-pack ozone system.

Appendix 1.2: Ozone concentrations generated by the in-pack ozone system which was assigned serial number 4

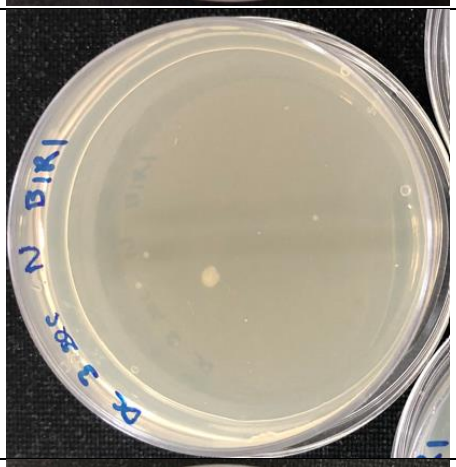
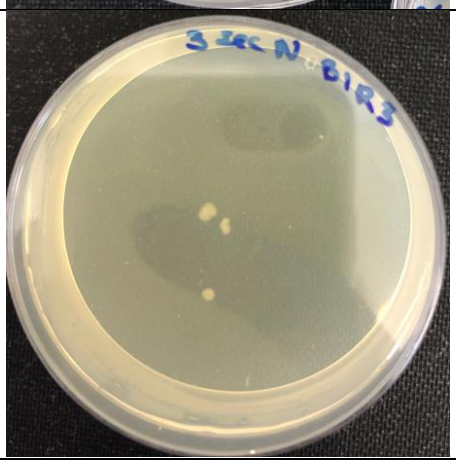
Treatment time (secs)	Calibration number	Peak ozone concentration detected in punnet (ppm)
Before treating carrots colonised by *P. viridiflava* PC006 (experimental replicate 1) (figure 4.17)		
3	1	663.6
3	2	681.5
3	3	727.6
Before treating carrots colonised by *D. chrysanthemi* EC16 (experimental replicate 1) (figure 4.17)		
3	1	793.3
3	2	755.7
3	3	826.5
Before treating tomatoes colonised by Pst DC3000 (experimental replicate 1) (figure 4.17)		
3	1	765.4
3	2	715.5
3	3	702.5
Before treating tomatoes colonised by Pst DC3000 (experimental replicate 2) (figure 4.17)		
3	1	729.2
3	2	729.7
3	3	772.8
Before treating tomatoes colonised by Pst T1 (experimental replicate 1) (figure 4.17)		
3	1	763.9
3	2	708.5
3	3	731.3
Before treating tomatoes colonised by Pst T1 (experimental replicate 2) (figure 4.17)		
3	1	743.1
3	2	768.9
3	3	751.7
Before treating tomatoes colonised by *E. coli* JHI-5025 (experimental replicate 1) (figure 4.17)		
3	1	722.8
3	2	707
3	3	700.8
Before treating tomatoes colonised by *E. coli* JHI-5025 (experimental replicate 2) (figure 4.17)		
3	1	724.3
3	2	715.5
3	3	744.3
Before treating tomatoes colonised by *E. coli* JHI-5025 (experimental replicate 3) (figure 4.17)		
3	1	698.2
3	2	781.8
3	3	749.4

Appendix 2



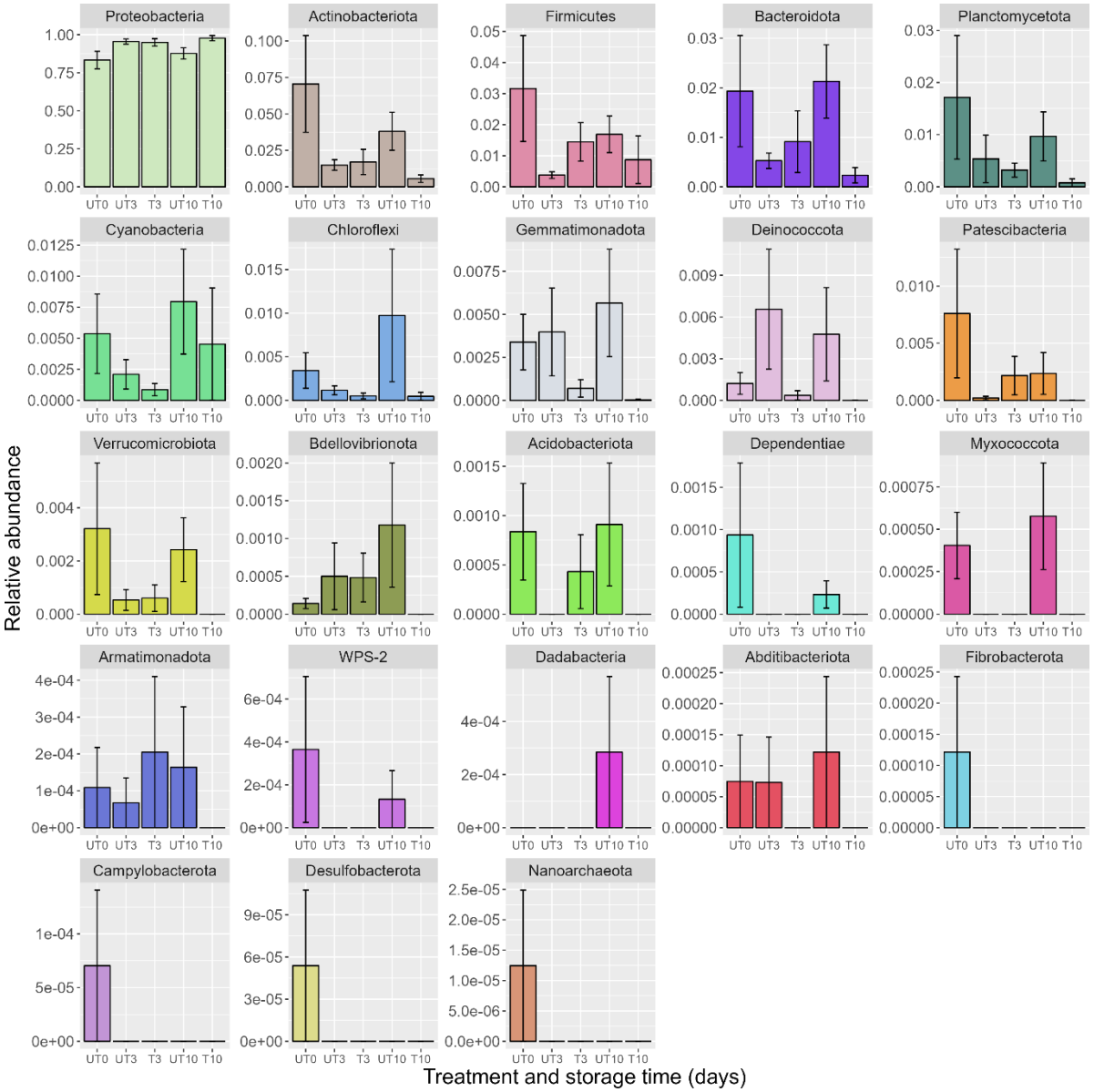
Appendix 2: The addition of chloroplast and mitochondria rRNA blockers visibly reduced amplification of 16S rRNA DNA from tomato calyxes and pedicels. V4 of the 16S rRNA gene was PCR-amplified with Invitrogen Platinum SuperFI DNA Polymerase, using primers 515F (Parada) and 806R (Apprill) from 15 ng genomic DNA extracted from tomato calyxes and pedicels. The expected amplicon size was ~397 bp. Sample 1 is B4-T10 and sample 2 is B5-UT0, which were used in the 16S rRNA microbiome experiment. 5 µM chloroplast and mitochondria rRNA blockers were either added to PCR reactions (to prevent amplification of plant DNA) or not. PCR negative controls (NCs) were collected by amplifying PCR mastermix only. PCR reactions were loaded onto a 1% agarose gel, which underwent gel electrophoresis before being visualised. Lane contents are labelled and the red arrow indicates a 400 bp band.

Appendix 3

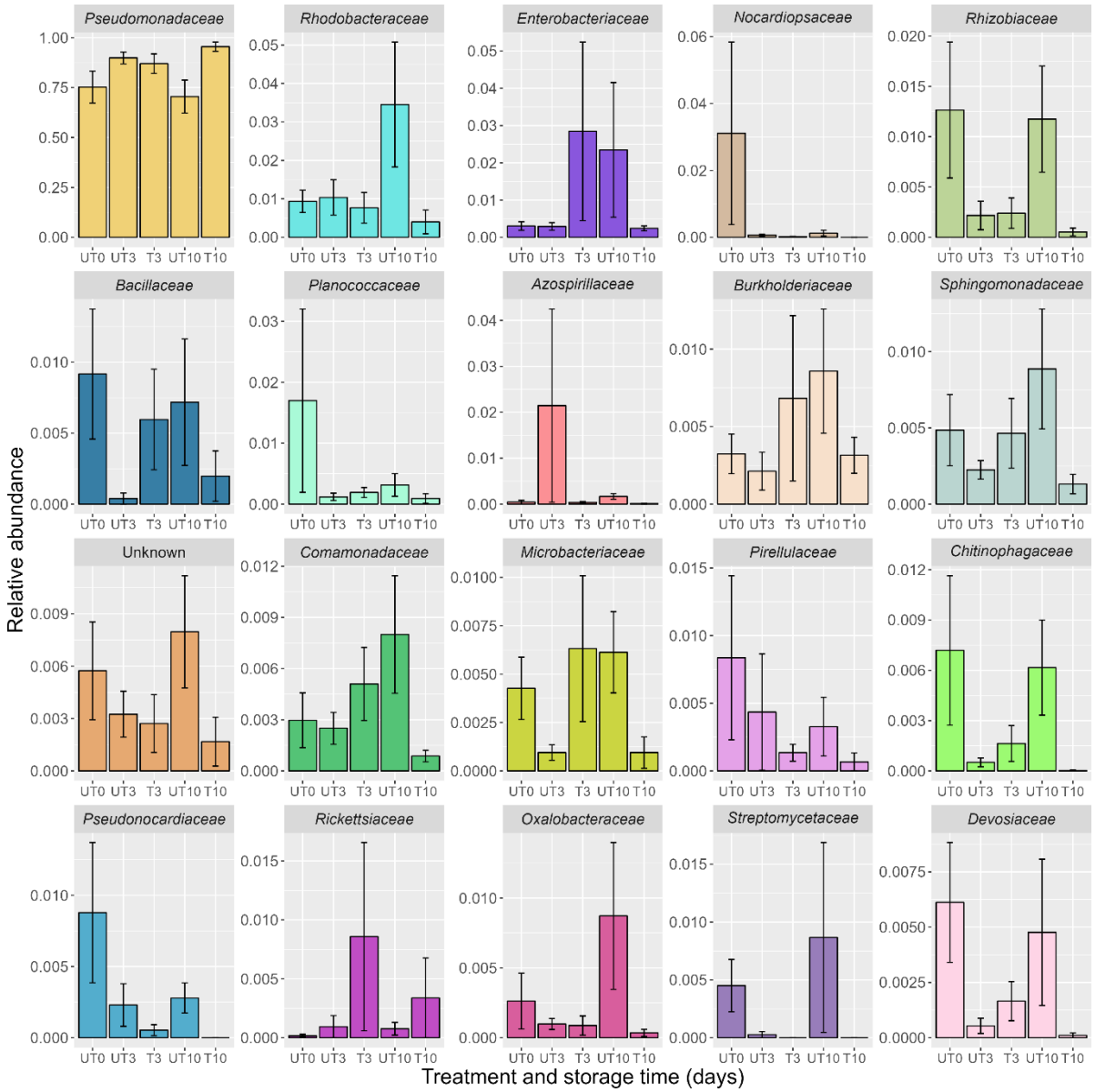
	Untreated	Treated
***E. coli* JHI-5025**		
Pst DC3000		
Pst T1		

Appendix 3: After ozone exposure, *E. coli* and *P. syringae* colonies presented different morphologies in comparison to the controls. Bacteria at OD_{600nm} 0.35 were spread onto LB agar and subjected to an ozone treatment (3 second ozone generation, ~350 - 700 peak ppm). LB agar plates were incubated at 28°C. *E. coli* was incubated for 18 hours whereas *P. syringae* was incubated for 48 hours before colonies were counted.

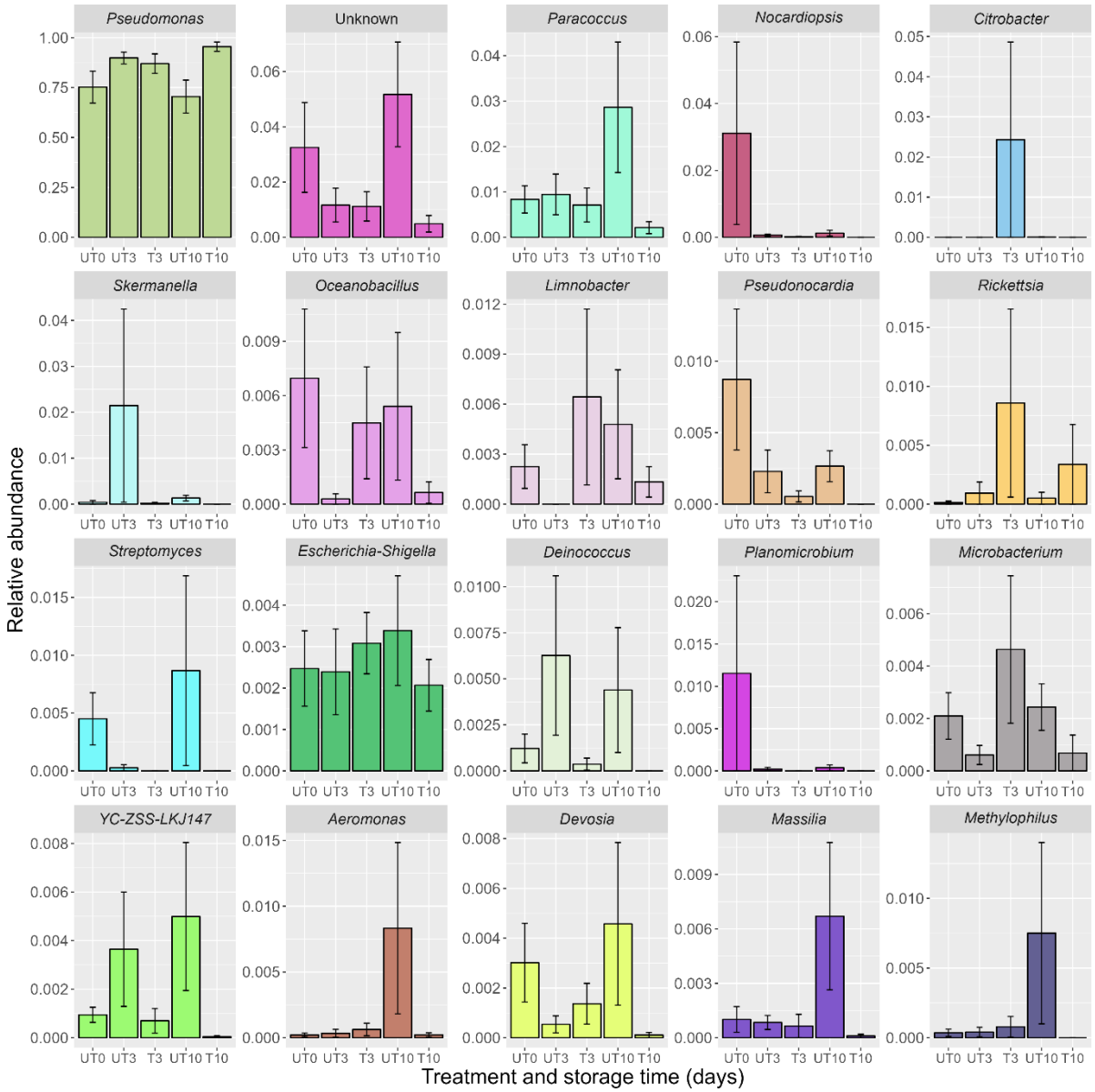
Appendix 4



Appendix 4.1: The relative abundance of bacterial phyla in the tomato calyx and pedicel changed over time and with ozone treatment. Tomatoes were subjected to either one of five conditions; either an ozone treatment (3 second ozone generation, ~350 - 700 peak ppm) or not and stored at 18ºC for 3 or 10 days (there was also an untreated day 0 control). DNA was extracted from tomato calyxes and pedicels, and 16S rRNA gene amplicons were sequenced. The relative abundance of each phylum (that was detected in the complete dataset) in each sample group is displayed. On the x-axis, UT or T represent untreated or treated and 0, 3 or 10 represent storage time (days). Mean and standard error are shown (n = 10).

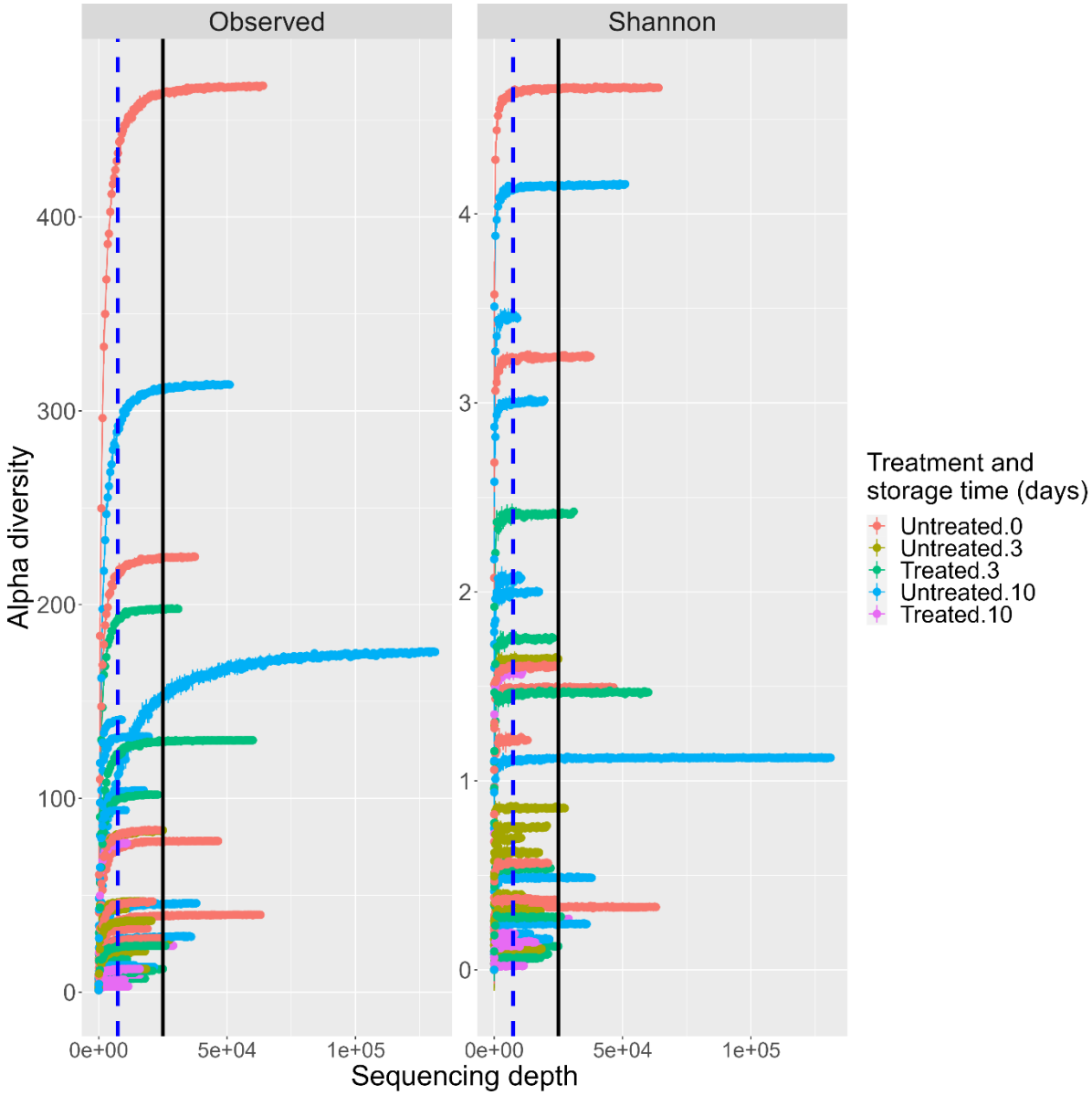


Appendix 4.2: The relative abundance of bacterial families in the tomato calyx and pedicel changed over time and with ozone treatment. Tomatoes were subjected to either one of five conditions; either an ozone treatment (3 second ozone generation, ~350 - 700 peak ppm) or not and stored at 18ºC for 3 or 10 days (there was also an untreated day 0 control). DNA was extracted from tomato calyxes and pedicels, and 16S rRNA gene amplicons were sequenced. The relative abundance of the top 20 families (which were detected across all samples) in each sample group is displayed. On the x-axis, UT or T represent untreated or treated and 0, 3 or 10 represent storage time (days). Mean and standard error are shown (n = 10).



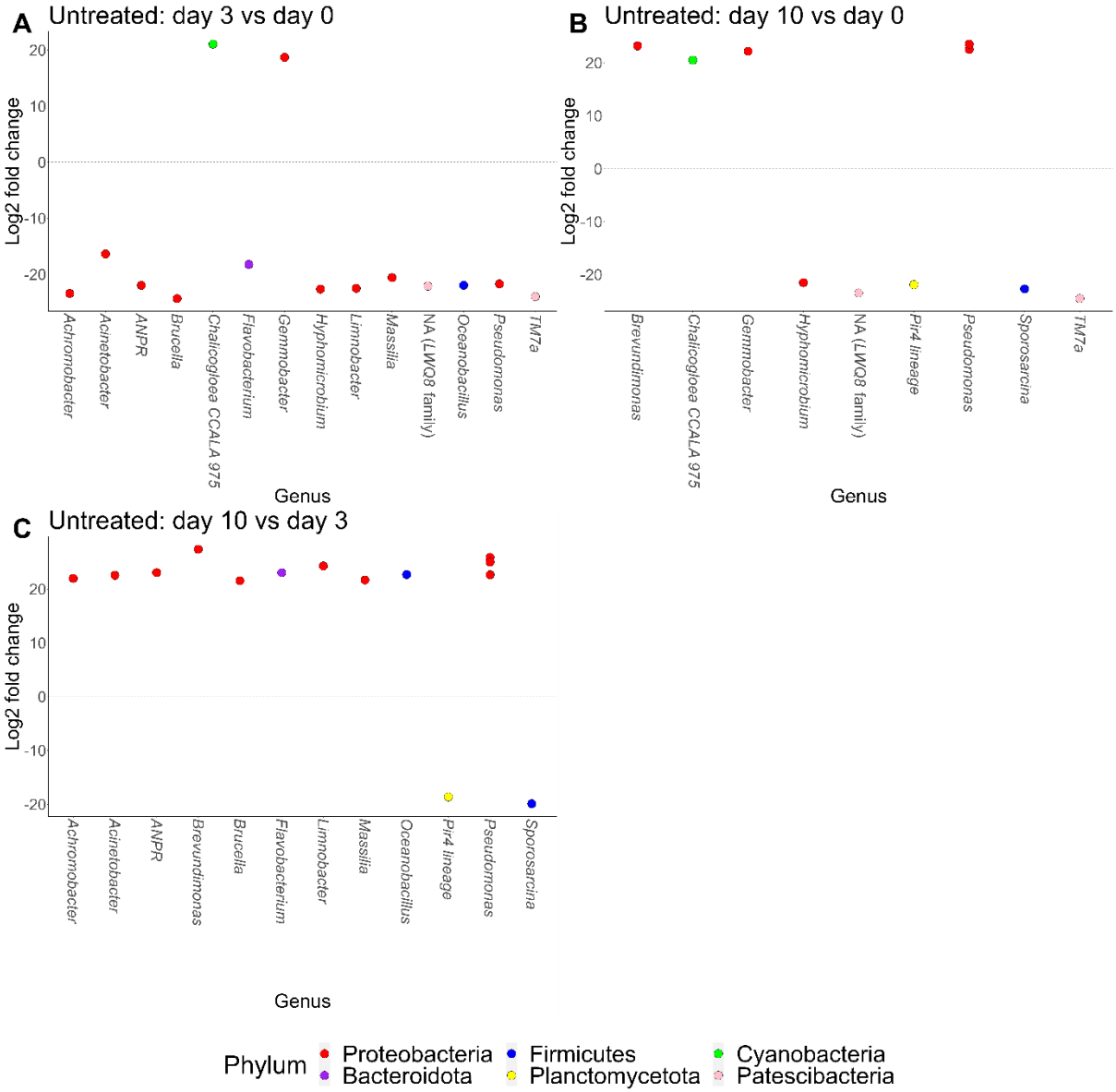
Appendix 4.3: The relative abundance of bacterial genera in the tomato calyx and pedicel changed over time and with ozone treatment. Tomatoes were subjected to either one of five conditions; either an ozone treatment (3 second ozone generation, ~350 - 700 peak ppm) or not and stored at 18ºC for 3 or 10 days (there was also an untreated day 0 control). DNA was extracted from tomato calyxes and pedicels, and 16S rRNA gene amplicons were sequenced. The relative abundance of the top 20 genera (which were detected across all samples) in each sample group is displayed. On the x-axis, UT or T represent untreated or treated and 0, 3 or 10 represent storage time (days). Mean and standard error are shown (n = 10).

Appendix 5

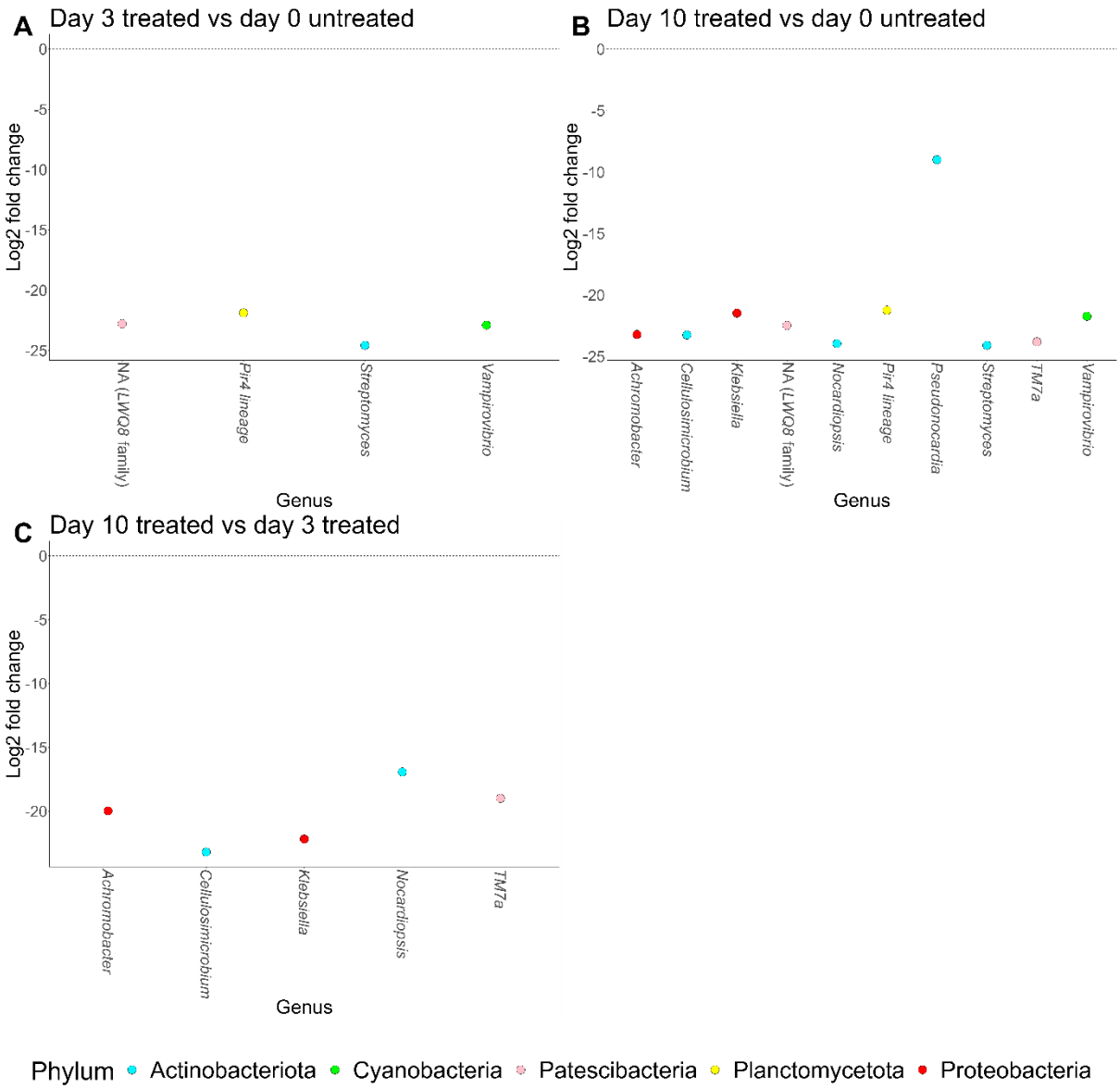


Appendix 5: Rarefaction curves for samples with >25,000 reads had mostly plateaued by 25,000 reads. Tomatoes were subjected to either one of five conditions; either an ozone treatment (3 second ozone generation, ~350 - 700 peak ppm) or not and stored at 18^{o}C for 3 or 10 days (there was also an untreated day 0 control). DNA was extracted from tomato calyxes and pedicels, and 16S rRNA gene amplicons were sequenced. The charts show the observed and Shannon's diversity for all samples, when an increasing number of sequences from each sample were randomly selected and measured. The mean observed or Shannon's diversity metric (from 10 groups of randomly selected reads) was calculated at the following sequencing depths for each sample: 1, 10, 100, and then at 500 intervals from 500 reads. A blue dashed line was added at a sequencing depth of 7400 because all samples were rarefied at 7400 reads. A black line was added at a sequencing depth of 25,000 because this is where the x-axis was constrained to present the rarefaction curve in figure 2.13.

Appendix 6



Appendix 6.1: ASVs significantly increased and decreased on the tomato calyx and pedicel over time. Tomatoes were subjected to either one of five conditions; either an ozone treatment (3 second ozone generation, ~350 - 700 peak ppm) or not and stored at 18°C for 3 or 10 days (there was also an untreated day 0 control). DNA was extracted from tomato calyxes and pedicels, and 16S rRNA gene amplicons were sequenced. Significant differences in the number of every type of ASV between all untreated samples at each time point were tested for with DeSeq2, so that significant differences detected were relative to the longer time point: **(A)** day 3 vs day 0, **(B)** day 10 vs day 0 and **(C)** day 10 vs day 3. ASVs which significantly increased or decreased over time were presented on the x-axis of charts as their genus but have been coloured according to their phylum. The log2 fold change is presented on the y-axis which shows the quantitative change in abundance of each organism. *ANPR = Allorhizobium-Neorhizobium-Pararhizobium-Rhizobium*.



Appendix 6.2: ASVs significantly increased and decreased on the tomato calyx and pedicel over time after ozone treatment. Tomatoes were subjected to either one of five conditions; either an ozone treatment (3 second ozone generation, ~350 - 700 peak ppm) or not and stored at 18ºC for 3 or 10 days (there was also an untreated day 0 control). DNA was extracted from tomato calyxes and pedicels, and 16S rRNA gene amplicons were sequenced. Significant differences in the number of every type of ASV between all treated samples at each time point (with inclusion of the untreated day 0 control) were tested for with DeSeq2, so that significant differences detected were relative to the longer time point: **(A)** day 3 vs day 0, **(B)** day 10 vs day 0 and **(C)** day 10 vs day 3. ASVs which significantly increased or decreased over time were presented on the x-axis of charts as their genus but have been coloured according to their phylum. The log2 fold change is presented on the y-axis which shows the quantitative change in abundance of each organism.

Appendix 7

Appendix 7.1: The genera of the ASVs which underwent significant changes in abundance over time on the tomato calyx and pedicel (with no treatment)

Group (figure 2.16: A)	Genus	Gram -stain	Reported doubling times	Reported disease in humans or plants by pathogenic isolates	Other information	Source
Early decrease, late increase	*Achromobacter*	-	*A. xylosoxidans*: 66 - 267 mins in ABTGC minimal media at 37ºC, *A. xylosoxidans*: 3 hours in mineral salts media supplemented with iminodisuccinate at 30ºC	It can be an opportunistic pathogen in humans, primarily causing pneumonia and bacteraemia	Obligate aerobe, catalase and oxidase positive, non-spore forming, can be found in soil and water	(Reinecke *et al.*, 2000; Isler *et al.*, 2020; Khademi *et al.*, 2021)
	Acinetobacter	-	*A. baumannii*: 40 - 100 mins in trypticase soy broth dialysate at 37ºC	It can be an opportunistic pathogen in humans, causing pneumonia, urinary tract, bloodstream and skin infections	Aerobe, catalase positive, oxidase negative, free-living saprophytes, non-spore forming, can be found in soil, water, sewage, food, on human specimens	(Antunes *et al.*, 2011; Bergogne-Bérézin, 2014; Kämpfer, 2014)
	Allorhizobium-Neorhizobium-Pararhizobium-Rhizobium	-	NA	NA	The genus is poorly characterised. It includes symbiotic soil microorganisms that form rhizospheres to promote nitrogen absorption and stimulate plant growth	(Syromyatnikov *et al.*, 2022)
	Brucella	-	*B. abortus*: 2.5 to 3 hours in varying growth conditions	It can cause brucellosis in humans, for example via the consumption of raw milk and dairy products	Aerobe, catalase positive, usually oxidase positive, non-spore-forming	(Rest and Robertson, 1975; López-Goñi *et al.*, 1992; Alton, 1996; Pappas, 2014; Rowe, 2014)
	Flavobacterium	-	*F. johnsoniae:* 69 mins in casitone-	Soft rot in fruits and vegetables	Obligate aerobe, a	(Braun *et al.*, 2005; Bernardet

			yeast extract medium at 30^{o}C	have been attributed to this genus, but it is mostly considered to be an opportunistic plant pathogen	physiologically diverse genus, non-spore-forming, widely distributed in soil and fresh water habitats	and Bowman, 2006; Waśkiewicz and Irzykowska, 2014)
	Limnobacter	-	NA	No evidence of pathogenicity	Obligate aerobe, chemolitho-heterotroph, has been isolated from lakes and volcanic deposits	(Duan *et al.*, 2020)
	Massilia	-	Growth was reported as slow on various agars	Human infections have rarely been reported but have included bacteraemia, CNS infections and septic abortion (not limited to immuno-compromised hosts)	Obligate aerobe, catalase positive, oxidase negative, non-spore forming, have been isolated from various environments including air, drinking water, rock surface, ice-core, glacier permafrost and human clinical samples	(La Scola *et al.*, 1998; Dahal *et al.*, 2021; Ali *et al.*, 2022)
	Oceanobacillus	+	NA	No evidence of pathogenicity	Obligate aerobe or facultative anaerobe, catalase positive, oxidase variable, obligately or facultatively alkaliphilic, can be found in deep sea sediments, salt fields, freshwater fish or insects, algal mat	(Roux *et al.*, 2013; Liu and Yang, 2014)
	Pseudomonas	-	*P. aeruginosa*: 1 - 1.5 hours in minimal media, 25 - 35 minutes in LB at 37^{o}C, *P. syringae* pv. glycinea: 1.5 - 2.5 hours in LB at varying temperatures	Some are plant pathogens which attack a variety of plants. Symptoms can include cankers, leaf and stem spots, blight,	Aerobe, catalase positive, usually oxidase positive, metabolically diverse, ubiquitous in the environment and are mainly	(Iglewski, 1996; Cousin, 1999; Keith *et al.*, 1999; Höfte and De Vos, 2006; LaBauve and

				soft rot and galls. Most that cause disease in humans are associated with opportunistic infections, but two species are known to cause glanders and melioidosis, which are specific human diseases	found in soil, water and vegetation but have also been isolated from healthy human hosts	Wargo, 2012; Dodd, 2014)
Early decrease	*Hyphomicrobium*	-	*Hyphomicrobium* strain M3: 9.1 hours on methanol at 30°C	No evidence of pathogenicity	Non-spore forming, typically isolated from industrial sewage, facultatively methylotrophic	(Urakami *et al.*, 1995; Layton *et al.*, 2000)
	TM7a	NA	NA	NA	The genus is poorly characterised. TM7 is found in diverse environments including soil, sea water, underground water and mammals. TM7 could be auxotrophic and metabolically dependent on other organisms.	(Bor *et al.*, 2019)
	LWQ8 family	NA	NA	NA	This family has not been characterised.	NA
Early increase	*Chalicogloea CCALA 975*	NA	NA	NA	This genus is poorly characterised. It includes cyanobacteria that form irregular packets in aerophytic and subaerophytic communities on stony and rocky substrates.	(Roldán *et al.*, 2013)
	Gemmobacter	-	NA	No evidence of pathogenicity	Aerobe or anaerobe, catalase positive, oxidase positive,	(Jin *et al.*, 2021)

					non-spore forming, widely distributed in natural and artificial environments	
Late decrease	*Pir4 lineage*	-	NA	NA	Aerobe or facultative anaerobe, chemo-organotrophs, mainly retrieved from a variety of low-oxygen habitats, main habitats are marine and freshwater environments	(Dedysh *et al.*, 2020)
	Sporosarcina	+	*S. pasteurii*: 14 - 17 hours in laboratory-grade yeast extract and food-grade yeast extract at 30^{o}C	NA	Obligate or facultative aerobe, catalase positive, most species are oxidase positive, forms endospores, has been isolated from soil and water	(Vos *et al.*, 2009; Omoregie *et al.*, 2019)
Late increase	*Brevundimonas*	-	Various strains: 75 - 135 mins in blood agar medium at 35^{o}C	It can be an opportunistic human pathogen which can cause bacteraemia in patients with underlying medical conditions	Aerobe, catalase positive, oxidase positive, have been isolated from multiple environments including soils, sea, sludge and sand	(Ryan and Pembroke, 2018; Huang *et al.*, 2022)
	Pseudomonas	See above				

NA values indicate that the information could not be sourced.

Appendix 7.2: The genera of the ASVs which underwent significant changes in abundance over time on the tomato calyx and pedicel after ozone treatment

Group (figure 2.16: B)	Genus	Gram -stain	Reported doubling times	Reported disease in humans or plants by pathogenic isolates	Other information	Source
Early decrease	*Pir4 lineage*	-	NA	NA	Aerobes and facultative anaerobes, chemo-organotrophs, mainly retrieved from a variety of low-oxygen habitats, main habitats are marine and fresh water environments	(Dedysh *et al.*, 2020)
	Streptomyces	+	It has been reported that *Streptomyces* doubling time requires 4 - 6 hours	Can cause disease in underground structures of plants, has previously been reported to cause mycetoma in immuno-compromised patients but cases are rare	Obligate aerobe, forms spores, soil bacteria, species are highly diverse in their carbon source utilisation	(Loria *et al.*, 1997; van Keulen *et al.*, 2007; Shepherd *et al.*, 2010; Riviere *et al.*, 2012)
	Vampirovibrio	NA	NA	No pathogenic activity against humans or plants has been reported	The genus is poorly characterised and only *V. chlorellavorus* has been described. It is a Gram-negative, aerobic, non-photosynthetic cyanobacterium which has a predatory lifestyle associated with *Chlorella* (an algae)	(Soo *et al.*, 2015)
	LWQ8 family	NA	NA	NA	This family has not been characterised.	NA
Late decrease	*Achromobacter*	-	*A. xylosoxidans*: 66 - 267 mins in ABTGC minimal media at 37^{o}C, *A. xylosoxidans*: 3 hours in mineral salts	It can be an opportunistic pathogen in humans, primarily causing pneumonia and bacteraemia	Obligate aerobe, catalase and oxidase positive, non-spore forming, can be found in soil and water	(Reinecke *et al.*, 2000; Isler *et al.*, 2020; Khademi *et al.*, 2021)

			media supplemented with imino-disuccinate at 30^{o}C			
	Cellulosimicrobium	+	NA	Rarely causes human infection but has infected immuno-compromised patients to primarily cause bacteraemia	Aerobe or facultative anaerobe, catalase positive, widely distributed in the environment and have mainly been isolated from soil, water and grass cuttings	(Rowlinson *et al.*, 2006; Delport *et al.*, 2014)
	Klebsiella	-	*K. pneumoniae*: 38 minutes in LB	Can be opportunistic pathogens which can cause a range of infections in human hosts including pneumonia, wound infections and urinary tract infections	Aerobe or facultative anaerobe, oxidase negative, encapsulated, can be found in soils, water, vegetation and humans.	(Bagley, 1985; Regué *et al.*, 2004; Dong *et al.*, 2022)
	Nocardiopsis	+	NA	Some are opportunistic human pathogens which can cause mycetoma, suppurative infections and abscesses	Aerobe, catalase positive, prevalent in terrestrial and marine environments	(Bennur *et al.*, 2015)
	TM7a	NA	NA	NA	The genus is poorly characterised. TM7 is found in diverse environments including soil, sea water, underground water and mammals. TM7 could be auxotrophic and metabolically dependent on other organisms.	(Bor *et al.*, 2019)
Decrease over time	*Pseudonocardia*	+	NA	Human infections have rarely been reported but have included opportunistic infection into cerebrospinal fluid of a brain injured patient	Aerobe, catalase positive, commonly found in soil and plants	(Riahi *et al.*, 2022)

NA values indicate that the information could not be sourced.

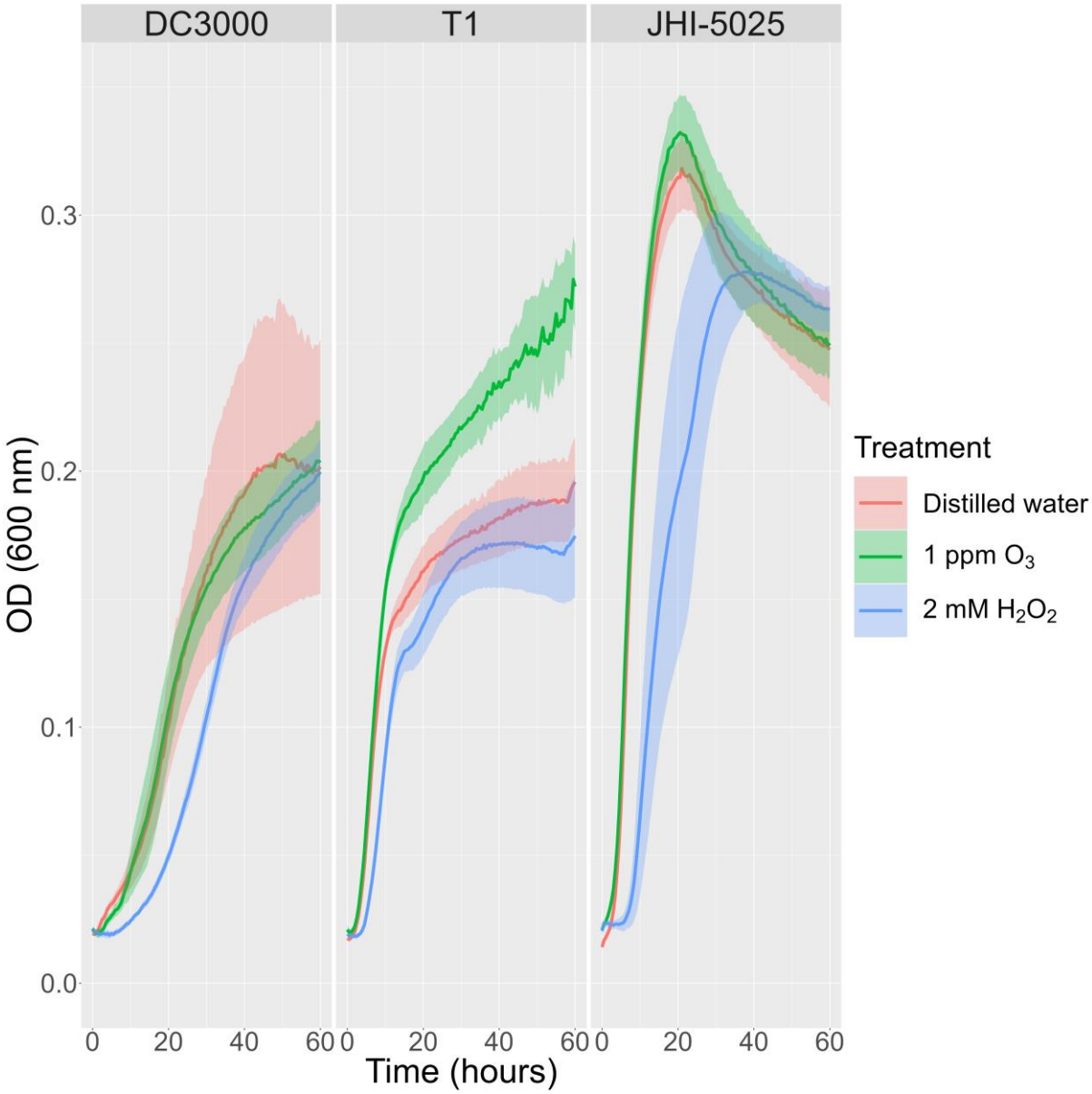
Appendix 7.3: The genera of the ASVs which were significantly increased or decreased on the tomato calyx and pedicel after ozone treatment (in comparison to non-treated samples) at 3 and 10 days post-harvest

Day post-harvest	Increase/ decrease relative to the ozone-treated sample	Genus	Gram -stain	Reported doubling times	Reported disease in humans or plants by pathogenic isolates	Other information	Source
3	Increase	*Limnobacter*	-	NA	No evidence of pathogenicity	Obligate aerobe, chemolitho-heterotrophic, has been isolated from lakes and volcanic deposits	(Duan *et al.*, 2020)
10	Decrease	*Cellvibrio*	-	NA	Can cause plant cell wall degradation which can allow for the colonisation of opportunistic plant pathogens	Aerobe, most can degrade cellulose, chitin, starch, xylan and dextran	(Wu and He, 2015)
10	Decrease	*Deinococcus*	Most +, some -	*D. radioduran*s: 130 mins in tryptone-glucose-yeast extract 2x medium at 30°C	No evidence of pathogenicity	Aerobe, heterotrophic, non-sporulating, found in diverse environments including plants, oceans, air and deserts	(Floc'h *et al.*, 2019; Jin *et al.*, 2019)
10	Decrease	*Limnobacter*	See above				
10	Decrease	*Pseudomonas*	-	*P. aeruginosa*: 1 - 1.5 hours in minimal media, 25 - 35 minutes in LB at 37ºC, *P. syringae* pv. glycinea: 1.5 - 2.5 hours in LB at varying temps	Some are plant pathogens which attack a variety of plants. Symptoms can include cankers, leaf and stem spots, blight, soft rot and galls. Most that cause disease in humans are associated with opportunistic infections, but two species are known to	Aerobe, catalase positive, usually oxidase positive, metabolically diverse, ubiquitous in the environment and are mainly found in soil, water and vegetation but have also been isolated from healthy human hosts	(Iglewski, 1996; Cousin, 1999; Keith *et al*., 1999; Höfte and De Vos, 2006; LaBauve and Wargo, 2012; Dodd, 2014)

					cause glanders and melioidosis, which are specific human diseases		
10	Decrease	*Pseudonocardia*	+	NA	Human infections have rarely been reported but have included opportunistic infection into cerebrospinal fluid of a brain injured patient	Aerobe, catalase positive, commonly found in soil and plants	(Riahi *et al*., 2022)
10	Decrease	*Stenotrophomonas*	-	*S. maltophilia:* 1 - 1.3 hours in In LB at 37ºC, 97 mins in LB on stationary microtiter plate at 37ºC	*S. maltophilia* can cause infections in wounds and the respiratory tract in immuno-compromised human hosts	Aerobe, metabolically diverse, commonly found throughout the environment, particularly in close association with plants	(Brooke *et al.*, 2008; Ryan *et al.*, 2009; Ferrer-Navarro *et al.*, 2013)

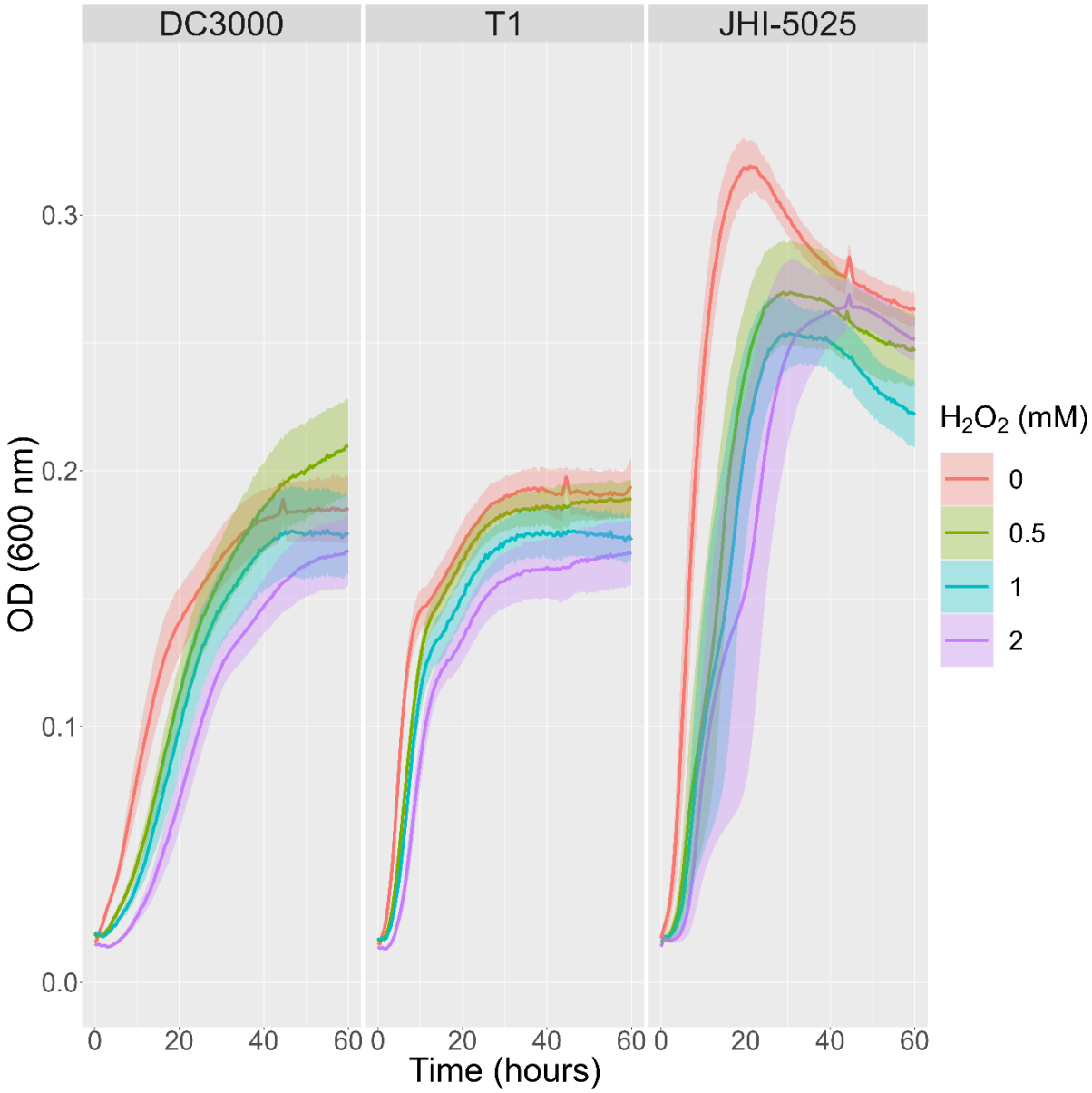
NA values indicate that the information could not be sourced.

Appendix 8

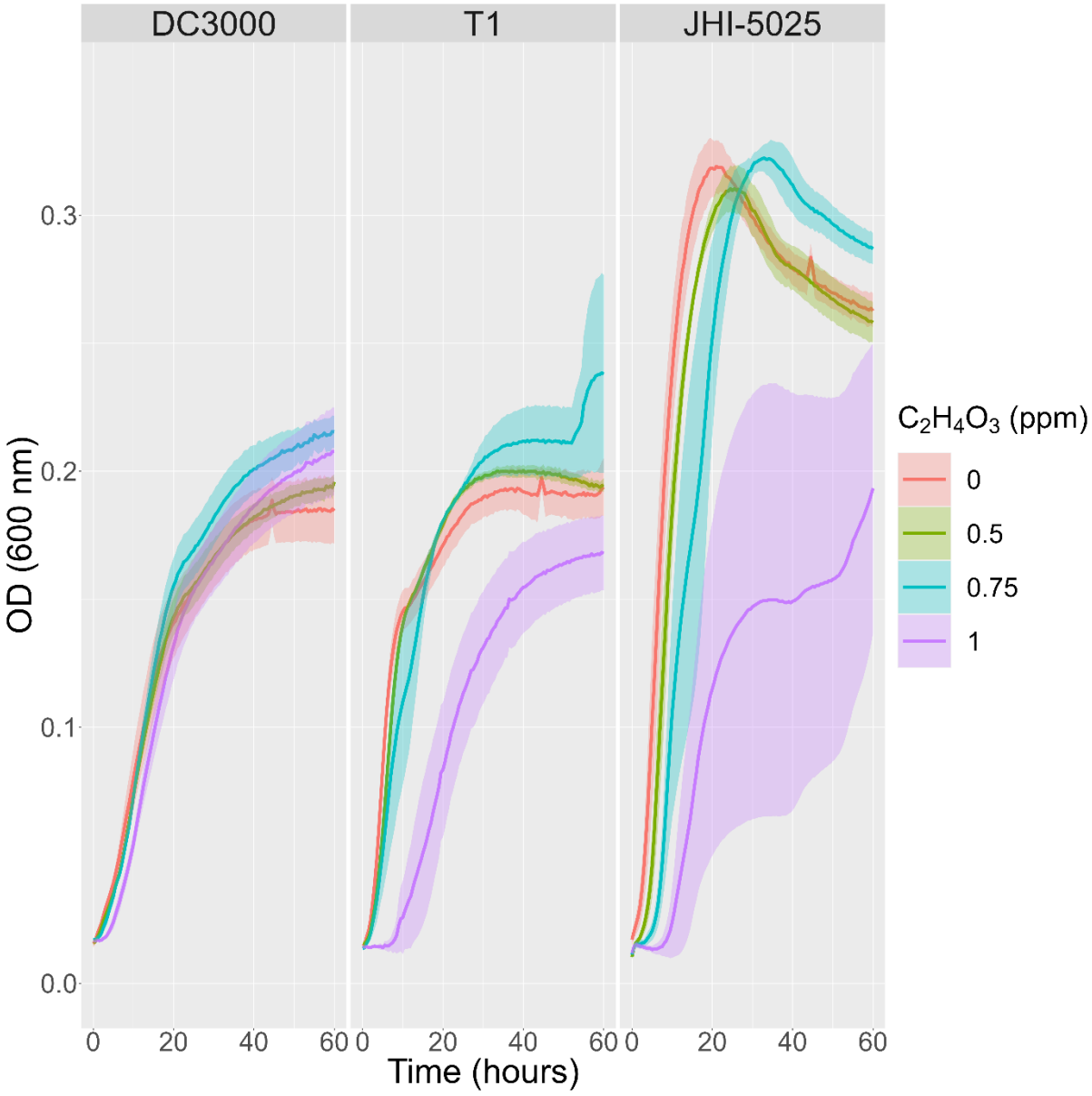


Appendix 8: Aqueous ozone did not extend the 'apparent' lag growth phase of bacteria, whereas hydrogen peroxide did. Bacteria (*P. syringae* pv. tomato DC3000, *P. syringae* pv. tomato T1, *E. coli* JHI-5025) which had grown to early exponential phase were added into M9 with distilled water, 1 ppm ozone (O_3) or 2 mM hydrogen peroxide (H_2O_2) in a glass bottle (final OD_{600nm} = 0.1). After 30 minutes, bacterial growth (OD_{600nm}) was monitored in a 96-well plate at 28°C with shaking. Mean and standard error are shown (n = 4).

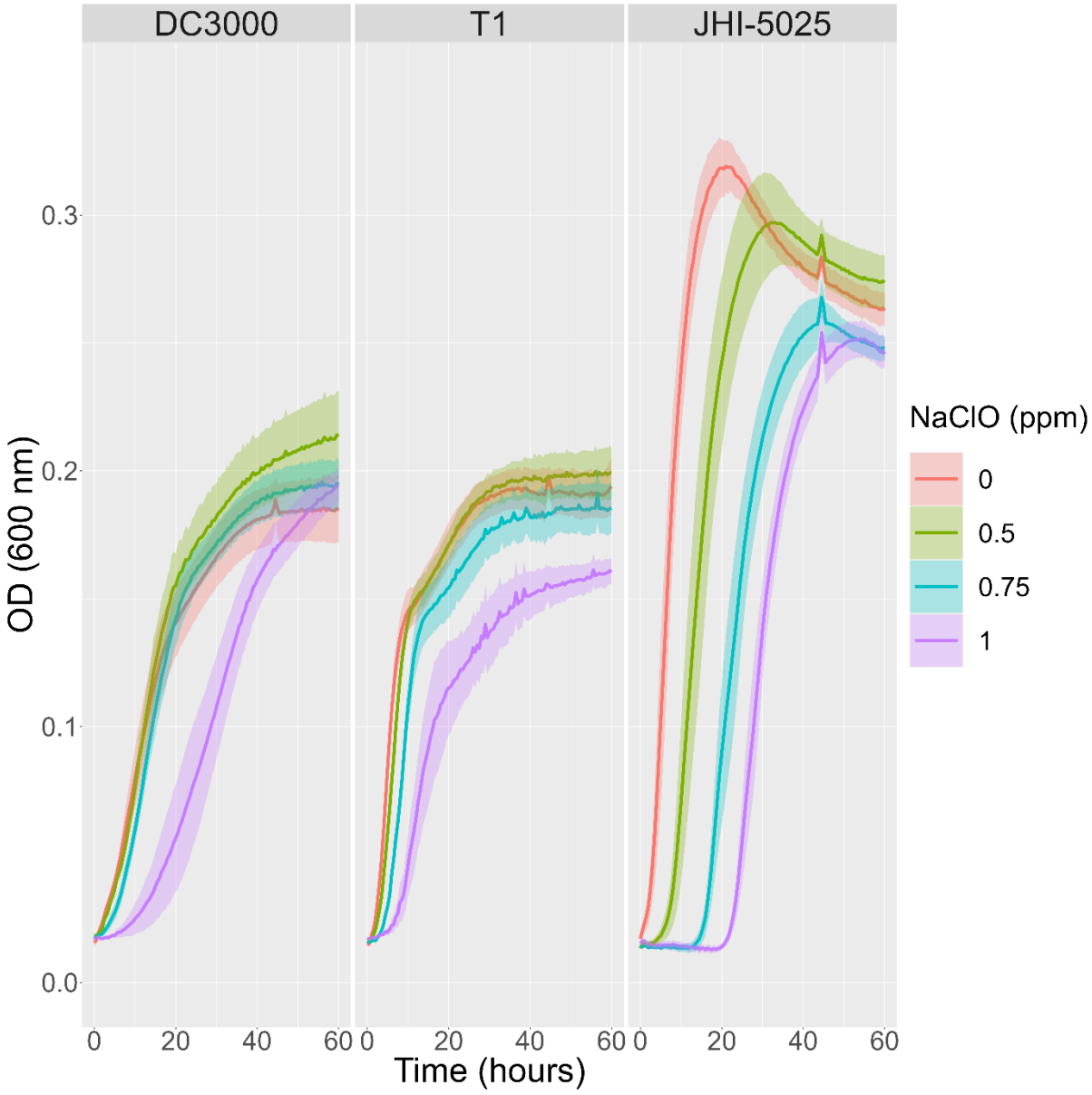
Appendix 9



Appendix 9.1: Increasing concentrations of hydrogen peroxide caused an extended 'apparent' lag growth phase. Bacteria (*P. syringae* pv. tomato DC3000, *P. syringae* pv. tomato T1, *E. coli* JHI-5025) which had grown to early exponential phase were added into M9 with hydrogen peroxide (H_2O_2) in a glass bottle (final OD_{600nm} = 0.1). Bacterial growth (OD_{600nm}) was immediately monitored in a 96-well plate at 28°C with shaking. Mean and standard error are shown (n = 4).

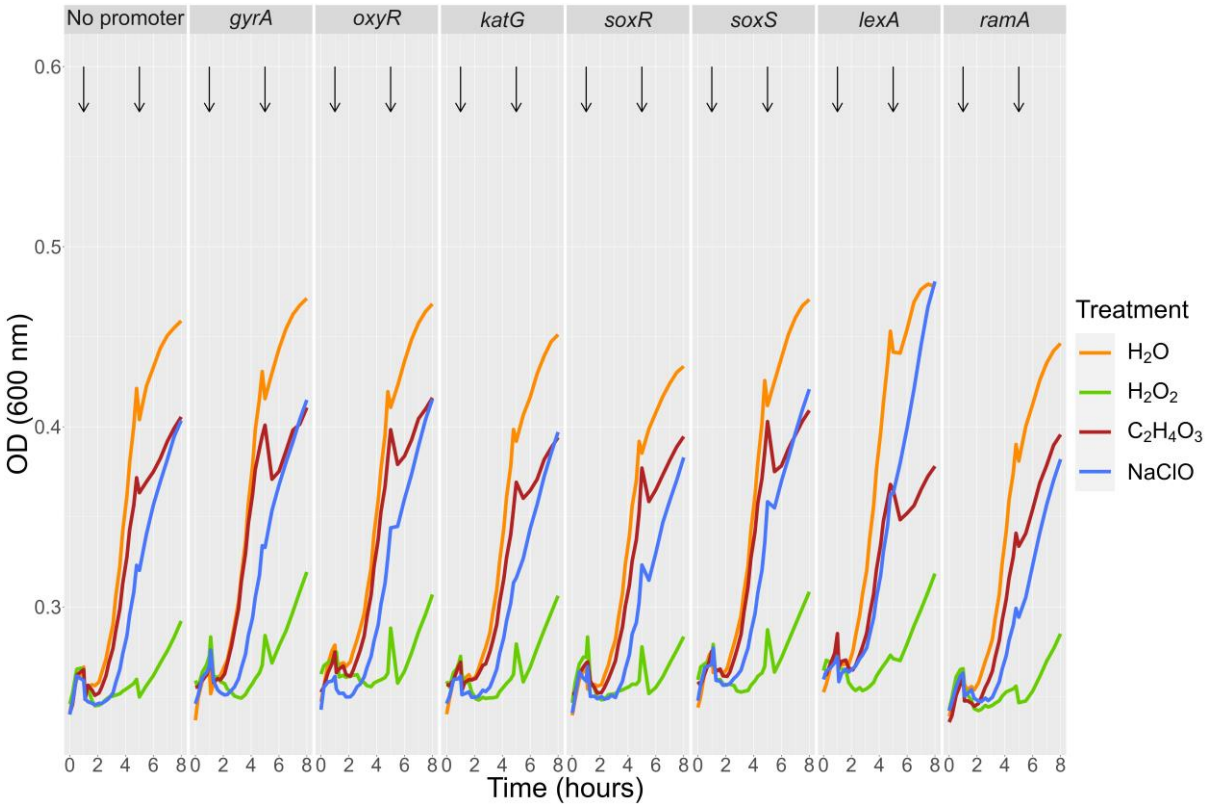


Appendix 9.2: Increasing concentrations of peracetic acid caused an extended 'apparent' lag growth phase. Bacteria (*P. syringae* pv. tomato DC3000, *P. syringae* pv. tomato T1, *E. coli* JHI-5025) which had grown to early exponential phase were added into M9 with peracetic acid ($C_2H_4O_3$) in a glass bottle (final OD_{600nm} = 0.1). Bacterial growth (OD_{600nm}) was immediately monitored in a 96-well plate at 28°C with shaking. Mean and standard error are shown (n = 3 - 4).



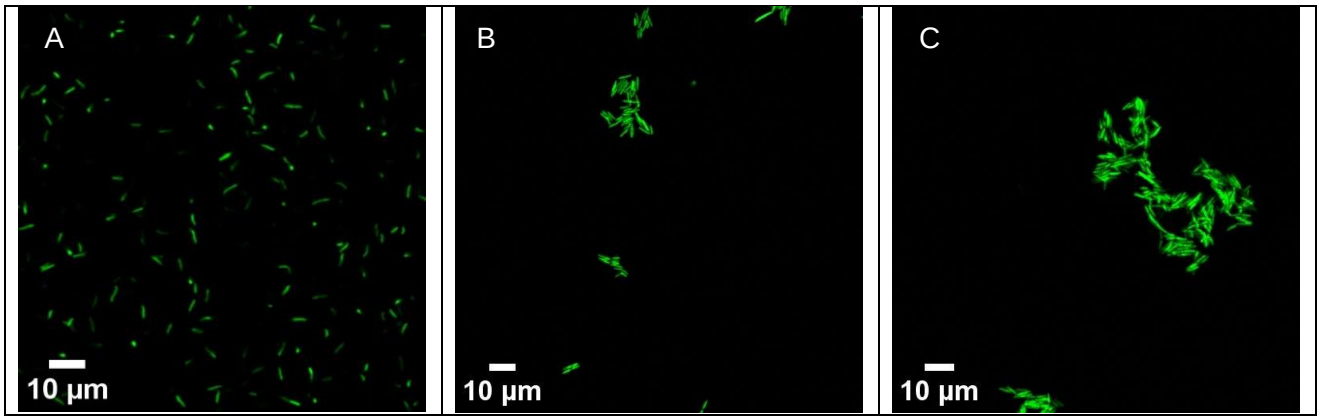
Appendix 9.3: Increasing concentrations of sodium hypochlorite caused an extended 'apparent' lag growth phase. Bacteria (*P. syringae* pv. tomato DC3000, *P. syringae* pv. tomato T1, *E. coli* JHI-5025) which had grown to early exponential phase were added into M9 with sodium hypochlorite (NaClO) in a glass bottle (final OD_{600nm} = 0.1). Bacterial growth (OD_{600nm}) was immediately monitored in a 96-well plate at 28ºC with shaking. Mean and standard error are shown (n = 3 - 4).

Appendix 10



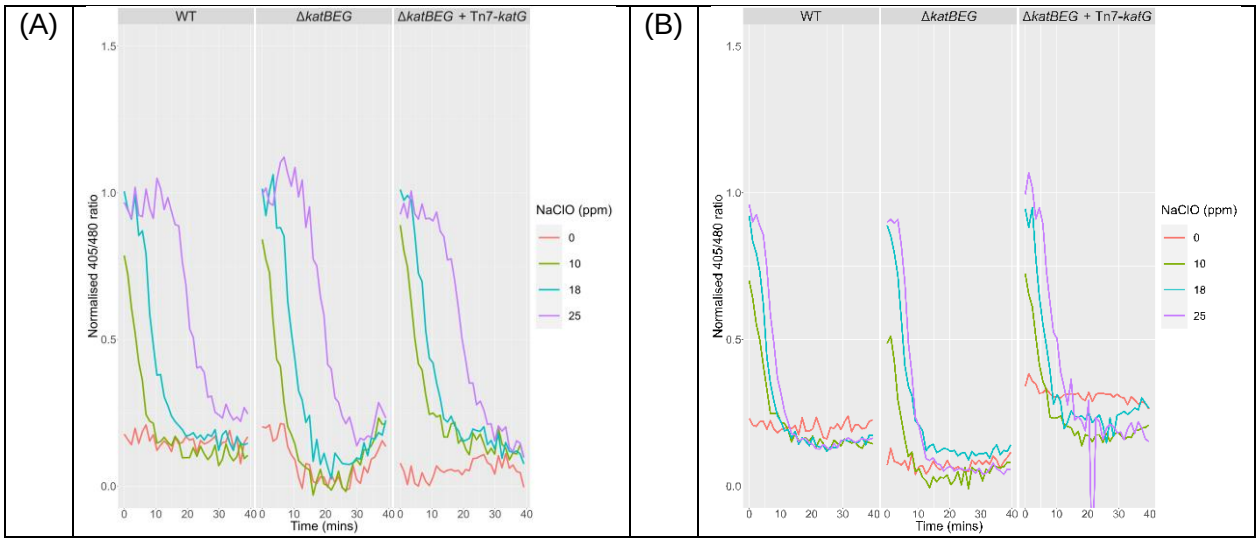
Appendix 10: Treatments caused different levels of stress to *E. coli* transcriptional fusion reporter strains. mCherry *E. coli* JHI-5025, which had been transformed with a GFP+ transcriptional fusion reporter for a selected gene (named in the figure), was grown to early exponential phase and added into M9 with either water, 5 mM hydrogen peroxide (H_2O_2), 1.040 ppm peracetic acid ($C_2H_4O_3$) or 2.5 ppm sodium hypochlorite (NaClO) in a glass bottle (final OD_{600nm} = 1). The reporter strains were then dispensed into a 96-well plate (incubated at 28^{o}C with intermittent shaking) for growth (OD_{600nm}) measurements over time. The figure displays the first 8 hours of the growth curves presented in figure 3.18: B, to better demonstrate differences in 'apparent' lag growth phase lengths.

Appendix 11



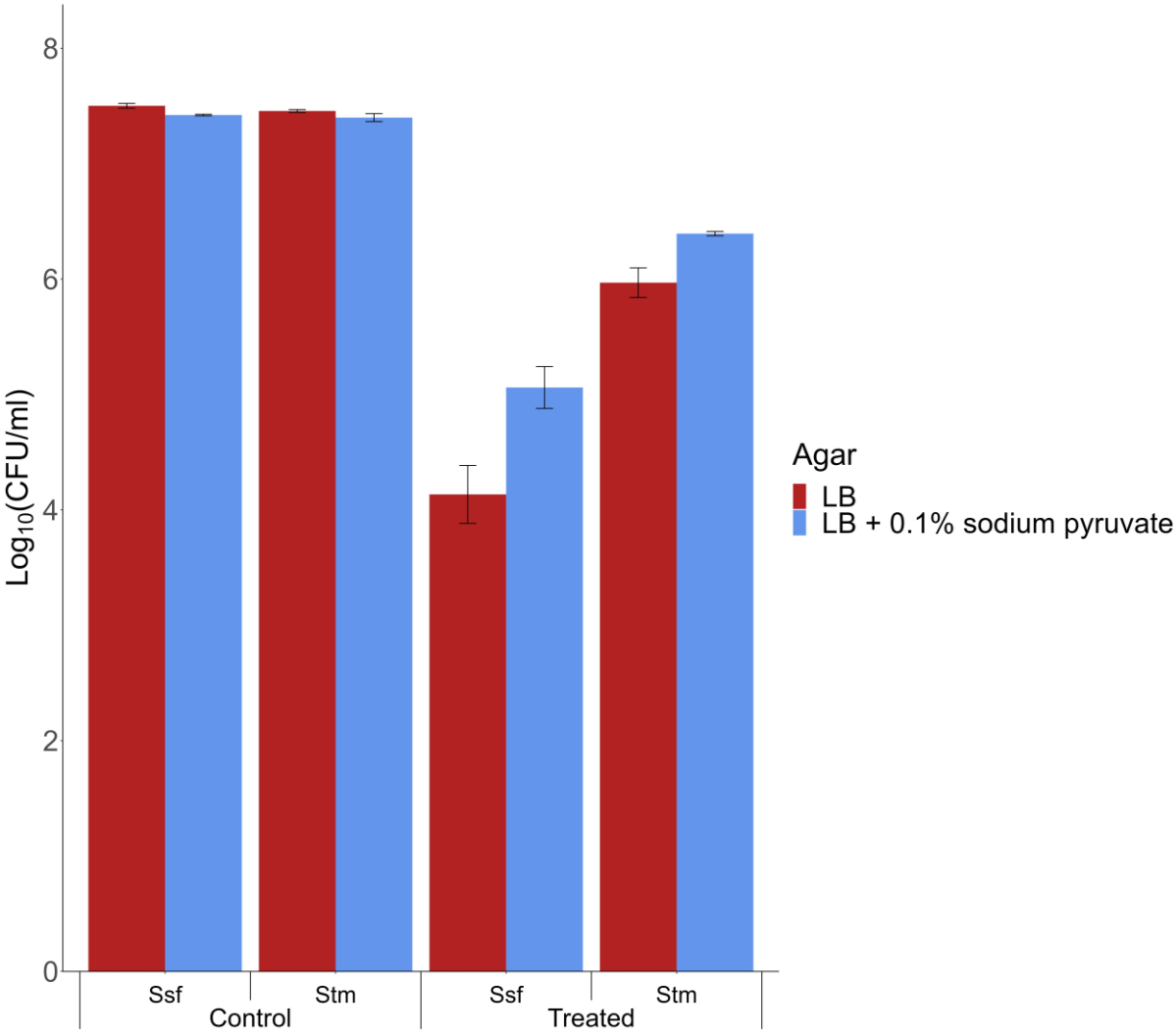
Appendix 11: (A) Pst DC3000 (pDSK-roGFP) did not form clusters in liquid medium whereas (B) Pst DC3000 Δ*katBEG* (pDSK-roGFP) and (C) Pst DC3000 Δ*katBEG* + Tn7_*katG* (pDSK-roGFP) did. Bacteria had been grown to early exponential phase in KB. Confocal microscope images were taken by William Kay with a TCS Leica SP5 confocal microscope (objective used: HC PL APO CS2 63.0x1.20 WATER UV). roGFP was excited with an argon laser (power = 20%) at 488 nm and emission was detected at 505 - 515 nm.

Appendix 12



Appendix 12: Catalases are not required for sodium hypochlorite tolerance. The results of the two independent replicates which were used to present the results in figure 3.24 are displayed in (**A**) and (**B**) respectively. Bacteria (*P. syringae* pv. tomato DC3000, *P. syringae* pv. tomato DC3000 Δ*katBEG*, *P. syringae* pv. tomato DC3000 Δ*katBEG* + Tn7_*katG*) which had been tagged with pDSK-roGFP were grown to early exponential phase and exposed to sodium hypochlorite (NaClO) in M9 (final OD_{600nm} = 1). Treatments were added to each bacterium at the same time. Data points represent the intracellular redox state of bacteria, which is a ratio of the fluorescence intensity measured at 405 nm (400 - 410 nm bandwidth) and 480 nm (475 - 485 nm bandwidth) excitation, 500 - 520 nm emission, at 28ºC with intermittent shaking. The data was normalised using measurements from the same bacterial strain, in a maximum oxidised and maximum reduced state, so that a normalised 405/480 ratio of 1 was equal to the maximum oxidised signal and 0.1 was equal to the maximum reduced signal.

Appendix 13



Appendix 13: The addition of 0.1% sodium pyruvate to LB agar caused resuscitation of viable but non-culturable *S. enterica* (which was evident by a higher culturability of heat-treated cells on LB agar + sodium pyruvate, in comparison to LB agar alone). *S. enterica* serovar Typhimurium (Stm) SL1344 and *S. enterica* serovar Senftenberg (Ssf) 20070885 (OD_{600nm} 0.02 in PBS) were incubated at 70°C for 3.25 minutes and then on ice for 10 minutes. They were serially diluted and then plated onto LB agar or LB agar + 0.1% sodium pyruvate before being incubated at 37°C for 24 hours. Colony forming units (CFU)/ml were calculated. Error bars represent the standard deviation between triplicate plates for a single biological replicate.

Appendix 14

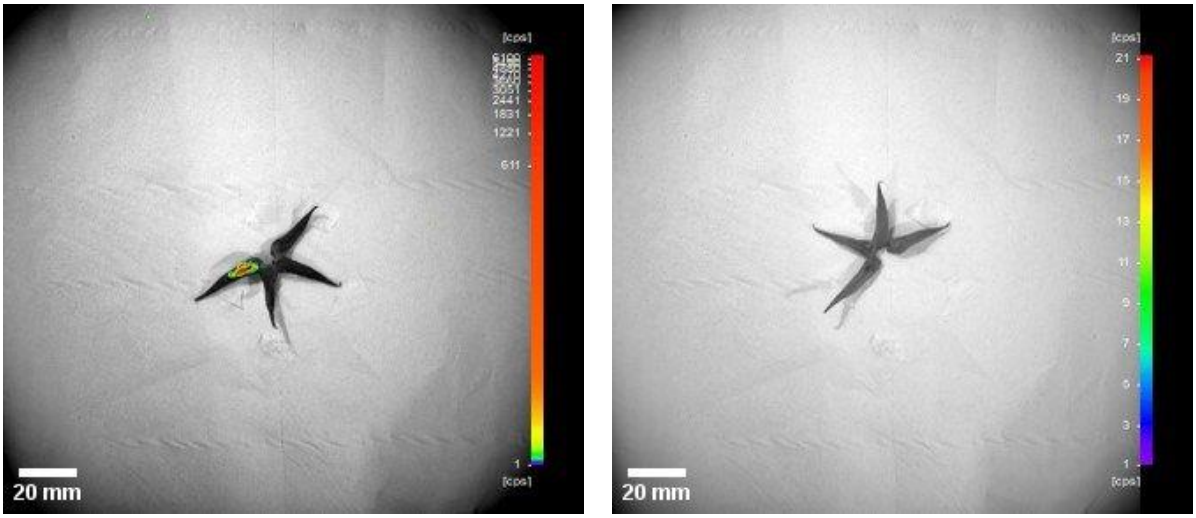
Water Supply Zone: 0205		CENTRAL OXFORD				Population: 70,923		
Time Period: 1 Jan 2022 to 31 Dec 2022			Concentration or Value (all samples)			No. of Samples		% of Samples
Parameter	Units	Regulatory Limit	Min.	Mean	Max.	Total	Contravening	Contravening
Clostridium perfringens	no./100ml	0	0	n/a	0	24	0	0
Coliform bacteria	no./100ml	0	0	n/a	19	130	1	1
Colony count 22°C	no./ml	-	0	n/a	1	46	0	0
E. coli	no./100ml	0	0	n/a	0	130	0	0
Enterococci	no./100ml	0	0	n/a	0	8	0	0
Colour (Pt/Co scale)	mg/l	20.0	<2.0	<2.0	<2.0	46	0	0
Conductivity at 20°C	µS/cm	2500	527	567	631	46	0	0
Hydrogen Ion	pH	6.50-9.50	7.40	7.49	7.70	46	0	0
Turbidity	FTU	4.00	<0.12	<0.12	0.29	46	0	0
Odour (quantatative)	dilution no.	0	0	0	0	46	0	0
Taste (quantatative)	dilution no.	0	0	0	0	46	0	0
Ammonium as NH4	mg/l	0.50	<0.02	<0.02	<0.02	8	0	0
Chloride as Cl	mg/l	250.0	29.4	37.1	51.3	8	0	0
Chlorine (Residual)	mg/l	-	0.13	0.50	0.75	130	0	0
Cyanide as CN	µg/l	50.0	<1.4	<1.4	<1.4	25	0	0
Fluoride as F	mg/l	1.50	0.10	0.11	0.12	8	0	0
Nitrate as NO3	mg/l	50.0	17.2	22.2	25.0	8	0	0
Nitrate/Nitrite calculation	mg/l	1.00	0.34	0.44	0.50	8	0	0
Nitrite as NO2	mg/l	0.500	<0.016	<0.016	<0.016	8	0	0
Sulphate as SO4	mg/l	250.0	65.0	75.7	92.0	8	0	0
Hardness (Total) as CaCO3	mg/l	-	252	266	283	4	0	
Alkalinity as CaCO3	mg/l	-	167	180	195	4	0	0
Aluminium as Al	µg/l	200.0	<10.5	16.4	28.8	46	0	0
Antimony as Sb	µg/l	5.00	0.30	0.34	0.50	8	0	0
Arsenic as As	µg/l	10.00	0.40	0.53	0.80	8	0	0
Boron as B	mg/l	1.00	0.04	0.05	0.05	8	0	0
Cadmium as Cd	µg/l	5.00	<0.40	<0.40	<0.40	8	0	0
Chromium as Cr	µg/l	50.0	<2.0	<2.0	<2.0	8	0	0
Copper as Cu	mg/l	2.000	0.004	0.005	0.010	8	0	0
Iron as Fe	µg/l	200.0	<3.4	5.4	24.7	46	0	0
Lead as Pb	µg/l	10.0	<0.9	2.0	6.3	8	0	0
Magnesium	mg/l	-	5.1	5.3	5.6	4	0	
Manganese as Mn	µg/l	50.0	<0.6	0.6	1.7	46	0	0
Mercury as Hg	µg/l	1.000	<0.070	<0.070	<0.070	25	0	0
Nickel as Ni	µg/l	20.0	<2.5	2.6	3.5	8	0	0
Selenium as Se	µg/l	10.0	<0.4	<0.4	<0.4	8	0	0
Sodium as Na	mg/l	200.0	22.1	29.4	44.0	8	0	0
Benzo (a) pyrene	µg/l	0.010	<0.004	<0.004	<0.004	8	0	0
PAHs (Sum of 4 substances)	µg/l	0.100	0	0	0	8	0	0
1,2 dichloroethane	µg/l	3.00	<0.10	<0.10	<0.10	8	0	0
Benzene	µg/l	1.00	<0.10	<0.10	<0.10	8	0	0
Tetra- & Trichloroethene calc	µg/l	10.00	0.00	0.00	0.00	8	0	0
Tetrachloromethane	µg/l	3.00	<0.10	<0.10	<0.10	8	0	0

Water Supply Zone: 0205		CENTRAL OXFORD				Population: 70,923		
Time Period: 1 Jan 2022 to 31 Dec 2022			Concentration or Value (all samples)			No. of Samples		% of Samples
Parameter	Units	Regulatory Limit	Min.	Mean	Max.	Total	Contravening	Contravening
Trihalomethanes	µg/l	100.0	9.6	14.1	16.6	8	0	0
Gross alpha activity	Bq/l	0.10	<0.05	<0.05	<0.05	13	0	0
Gross beta activity	Bq/l	1.00	0.10	0.18	<0.28	13	0	0
Bromate as BrO3	µg/l	10.0	<0.8	1.1	2.6	25	0	0
Total Organic Carbon as C	mg/l	-	0.9	1.3	1.9	25	0	0
2,4-D	µg/l	0.100	<0.017	<0.017	<0.017	25	0	0
2,4-DB	µg/l	0.100	<0.016	<0.016	<0.016	25	0	0
Atrazine	µg/l	0.100	<0.005	<0.005	<0.005	25	0	0
Bentazone	µg/l	0.100	<0.012	<0.012	<0.012	25	0	0
Bromoxynil	µg/l	0.100	<0.019	<0.019	<0.019	25	0	0
Carbendazim	µg/l	0.100	<0.020	<0.020	<0.020	25	0	0
Carbetamide	µg/l	0.100	<0.007	<0.007	<0.007	25	0	0
Chlortoluron	µg/l	0.100	<0.006	<0.006	<0.006	25	0	0
Clopyralid	µg/l	0.100	<0.022	<0.022	<0.022	25	0	0
Dicamba	µg/l	0.100	<0.022	<0.022	<0.022	25	0	0
Dichlorprop	µg/l	0.100	<0.012	<0.012	<0.012	25	0	0
Diuron	µg/l	0.100	<0.006	<0.006	<0.006	25	0	0
Flufenacet	µg/l	0.100	<0.005	<0.005	<0.005	25	0	0
Fluroxypyr	µg/l	0.100	<0.015	<0.015	<0.015	25	0	0
Isoproturon	µg/l	0.100	<0.005	<0.005	<0.005	25	0	0
Linuron	µg/l	0.100	<0.005	<0.005	<0.005	25	0	0
MCPA	µg/l	0.100	<0.020	<0.020	<0.020	25	0	0
Mecoprop	µg/l	0.100	<0.014	<0.014	<0.014	25	0	0
Metaldehyde	µg/l	0.100	<0.014	<0.014	<0.014	25	0	0
Metazachlor	µg/l	0.100	<0.006	<0.006	<0.006	24	0	0
Monuron	µg/l	0.100	<0.005	<0.005	<0.005	25	0	0
Pentachlorophenol	µg/l	0.100	<0.008	<0.008	<0.008	25	0	0
Picloram	µg/l	0.100	<0.021	<0.021	<0.021	25	0	0
Propyzamide	µg/l	0.100	<0.006	<0.006	<0.006	25	0	0
Quinmerac	µg/l	0.100	<0.017	<0.017	<0.017	25	0	0
Simazine	µg/l	0.100	<0.009	<0.009	<0.009	25	0	0
Triclopyr	µg/l	0.100	<0.016	<0.016	<0.016	25	0	0
Total Pesticides	µg/l	0.500	0.000	0.000	0.000	25	0	0

Appendix 14 taken from Thames Water Utilities Limited, 2023: The tap water used for experiments contained different constituents. Parameter (organism, substance or physical property) levels in tap water in central Oxford, 2022 is displayed.

Appendix 15

A. B.



Appendix 15: Luminescence on the underside of a calyx being imaged was not captured. (**A)** *E. coli* JHI-5025 (pIJ11282) was scraped from a LB agar plate with carbenicillin and smeared onto one side of a tomato calyx, which was subsequently imaged for luminescence with a NightOWL LB 983 NC100 *in vivo* imaging system with a 20 minute exposure time. (**B)** The calyx was then flipped over and imaged again with the same settings. This experiment was completed twice.